Ian Manners

Synthetic Metal-Containing Polymers

Synthetic Metal-Containing Polymers. Ian Manners

ISBN: 3-527-29463-5

Related Titles from WILEY-VCH

S. Farikov (Ed.)

Handbook of Thermoplastic Polyesters

2000
ISBN 3-527-30113-5

S. Farikov (Ed.)

Transreactions in Condensation Polymers

1999
ISBN 3-527-29790-1

H.-G. Elias

An Introduction to Polymer Science

1997
ISBN 3-527-28790-6

G. Hadziioannou, P. F. Van Hutten (Eds.)

Semiconducting Polymers

1999
ISBN 3-527-29507-0

E. S. Wilks (Ed.)

Industrial Polymers Handbook

2001
ISBN 3-527-30260-3

Ian Manners

Synthetic Metal-Containing Polymers

WILEY-VCH Verlag GmbH & Co. KGaA

Author

Prof. Dr. Ian Manners
University of Toronto
Department of Chemistry
80 St. George Street
Toronto
Ontario M5S 1A1
Canada

Cover Picture A depiction of the structure of metallated (Zn) DNA (see Chapter 7, section 7.6) superimposed on a polarizing optical micrograph that shows a lyotropic liquid crystalline mesophase formed by a Pt polyyne (see Chapter 5, section 5.2.3.2.)

Library of Congress Card No.: applied for

British Library Cataloguing-in-Publication Data
A catalogue record for this book is available from the British Library.

Bibliographic information published by Die Deutsche Bibliothek
Die Deutsche Bibliothek lists this publication in the Deutsche Nationalbibliografie; detailed bibliographic data is available in the Internet at <http://dnb.ddb.de>

Printed in the Federal Republic of Germany
Printed on acid-free paper

Composition K+V Fotosatz GmbH, Beerfelden
Printing strauss offsetdruck GmbH, Mörlenbach
Bookbinding Litges & Dopf Buchbinderei GmbH, Heppenheim

ISBN 3-527-29463-5

Preface

Polymer science has developed rapidly over the last few decades of the 20th century into an exciting area of high-tech materials research. A major contribution to this transformation has been provided by the infusion of creative ideas from synthetic organic chemists. Until recently, the impact of inorganic chemistry on polymer science has been much more limited in scope and has been primarily restricted to the discovery of highly active olefin polymerization catalysts. This is mainly a result of the challenging synthetic problems concerning the formation of long polymer chains containing elements other than carbon. These hurdles are now being overcome and the tantalizing possibility of exploiting the rich diversity of structures, properties, and function provided by inorganic elements in the development of new macromolecular and supramolecular polymeric materials is being productively realized. The new hybrid materials being created represent a welcome addition to the materials science toolbox, and impressively complement those now accessible using organic chemistry.

This book focuses on the area of metal-containing polymers which, based on the unique properties of transition elements and main group metals, exhibit particular promise. The work is organized to provide interested researchers in Universities and Industry with a critical review of the state of the art, and to help stimulate fundamental and applied research in the future. An overview of key concepts in polymer science and background to the challenges and motivations for the development of metal-containing polymers is provided in the introductory Chapter 1. Chapters 2–8 cover the different structural types of metallopolymer currently available with an emphasis on well-characterized materials, properties, and applications. Chapter 2 focuses on polymers with metals in the side group structure. Chapters 3–7 discuss the various classes of metallopolymer with transition or main group metals in the main chain. Dendritic and hyperbranched metallopolymers are described in Chapter 8. The structural diversity of the materials now available is impressive, as is the range of function. The extensive list of uses includes applications as catalysts, electrode mediators, sensors, and as stimuli responsive gels; as photonic, conductive, photoconductive, and luminescent materials; as precursors to magnetic ceramics and nanopatterned surfaces; and as bioactive materials and metalloenzyme models.

The creation of this book has been accomplished with the help of many other individuals. I would like to express my deep appreciation to a number of my grad-

uate students and postdocs who generously volunteered their talents and help with various aspects of this work. I would like to thank in particular Sara C. Bourke who provided exceptional help and valuable critique throughout the various stages of putting the manuscript together. I also wish to acknowledge the efforts of Katie Porter, Dr. Paul Cyr, Alex Bartole-Scott, Dr. Zhuo Wang, Dr. Xiaosong Wang, Sebastien Fournier, Keith Huynh and Fabio di Lena who helped with the correction and proof-reading of the various chapters. I would also like to thank my wife Deborah O'Hanlon-Manners for helpful comments, proof-reading, and very useful advice.

Finally, I would like to dedicate this book to the people from my personal life whose encouragement over the years has always been essential – my wife Deborah and children Hayley and Chris, my mother Jean D. Manners and late father Derek S. Manners, and my late grandmother Daisy M. Manners.

Ian Manners
Toronto, November 2003

Contents

Preface *V*

Abbreviations *XI*

1 Introduction *1*
1.1 Metal-containing Polymers *1*
1.2 Fundamental Characteristics of Polymeric Materials *3*
1.2.1 Polymer Molecular Weights *3*
1.2.2 Amorphous, Crystalline, and Liquid-crystalline Polymers: Thermal Transitions *5*
1.2.3 Polymers versus Oligomers: Why are High Molecular Weights Desirable? *9*
1.2.4 Polymer Solubility *10*
1.2.5 Block Copolymers *11*
1.2.6 Dendrimers and Hyperbranched Polymers *14*
1.2.7 Electrically Conducting Polymers *14*
1.3 Motivations for the Incorporation of Metals into Polymer Structures *16*
1.3.1 Conformational, Mechanical, and Morphological Characteristics *18*
1.3.2 Precursors to Ceramics *18*
1.3.3 Magnetic, Redox, Electronic, and Optical Properties *19*
1.3.4 Catalysis and Bioactivity *20*
1.3.5 Supramolecular Chemistry and the Development of Hierarchical Structures *21*
1.4 Historical Development of Metal-based Polymer Science *22*
1.5 Synthetic Routes to Metal-containing Polymers *25*
1.5.1 The Synthesis of Side-chain Metal-containing Polymers *25*
1.5.2 Main-chain Metal-containing Polymers *27*
1.5.2.1 Why are Transition Metals in the Polymer Main Chain Desirable? *27*
1.5.2.2 The Synthesis of Main-chain Metal-containing Polymers *28*
1.5.2.2.1 Addition Polymerization *28*
1.5.2.2.2 Polycondensations *29*
1.5.2.2.3 Ring-opening Polymerization (ROP) *33*
1.6 References *34*

2 Side-Chain Metal-Containing Polymers *39*
2.1 Introduction *39*
2.2 Side-chain Polymetallocene Homopolymers and Block Copolymers *39*
2.2.1 Organic Polymers with Metallocene Side Groups 9
2.2.1.1 Poly(vinylferrocene) *39*
2.2.1.2 Other Organic Polymers with Metallocene-containing Side Groups *43*
2.2.2 Inorganic Polymers with Metallocene Side Groups *49*
2.2.2.1 Polyphosphazenes with Ferrocene- or Ruthenocene-containing Side Groups *49*
2.2.2.2 Polysilanes, Polysiloxanes, and Polycarbosilanes with Metallocene Side Groups *50*
2.3 Other Side-chain Metallopolymers *54*
2.3.1 Polymers with π-Coordinated Metals *54*
2.3.2 Polymers with Pendant Polypyridyl Complexes *55*
2.3.3 Polymers with Other Pendant Metal-containing Units, Including the Area of Polymer-supported Catalysts *60*
2.3.4 Block Copolymers with Pendant Metal-containing Groups *62*
2.3.4.1 Approaches using Ring-opening Metathesis Polymerization (ROMP) *63*
2.3.4.2 Coordination to Pyridyl Substituents in Preformed Blocks *64*
2.3.4.3 Coordination to Other Substituents in Preformed Blocks *66*
2.4 References *67*

3 Main-Chain Polymetallocenes with Short Spacer Groups *71*
3.1 Introduction *71*
3.2 Polymetallocenylenes and Polymetallocenes with Short Spacers Obtained by Condensation Routes *73*
3.2.1 Polymetallocenylenes *73*
3.2.2 Other Polymetallocenes with Short Spacers Obtained by Polycondensation Routes *78*
3.3 Ring-opening Polymerization (ROP) of Strained Metallocenophanes *82*
3.3.1 Thermal ROP of Silicon-bridged [1]Ferrocenophanes *82*
3.3.2 Thermal ROP of Other Strained Metallocenophanes *84*
3.3.3 Living Anionic ROP of Strained Metallocenophanes *87*
3.3.4 Transition Metal-catalyzed ROP of Strained Metallocenophanes *89*
3.3.5 Other ROP Methods for Strained Metallocenophanes *91*
3.3.6 Properties of Polyferrocenylsilanes *91*
3.3.6.1 Polyferrocenylsilanes in Solution *92*
3.3.6.2 Polyferrocenylsilanes in the Solid State: Thermal Transition Behavior, Morphology, and Conformational Properties *93*
3.3.6.3 Electrochemistry, Metal-Metal Interactions, Charge-transport, and Magnetic Properties of Oxidized Materials *96*
3.3.6.4 Redox-Active Polyferrocenylsilane Gels *100*

3.3.6.5 Thermal Stability and Conversion to Nanostructured Magnetic Ceramics *101*
3.3.6.6 Charge-tunable and Preceramic Microspheres *103*
3.3.6.7 Water-Soluble Polyferrocenylsilanes: Layer-by-layer Assembly Applications *105*
3.3.6.8 Applications as Variable Refractive Index Sensors and as Nonlinear Optical Materials *106*
3.3.7 Properties of Other Ring-opened Polymetallocenes and Related Materials *106*
3.3.8 Polyferrocenylsilane Block Copolymers *108*
3.3.8.1 Synthetic Scope *108*
3.3.8.2 Self-assembly in Block-selective Solvents *109*
3.3.8.3 Self-assembly in the Solid State *112*
3.3.9 Polyferrocenylphosphine Block Copolymers *115*
3.4 Transition Metal-catalyzed Ring-opening Metathesis Polymerization (ROMP) of Metallocenophanes *116*
3.5 Atom Abstraction-induced Ring-opening Polymerization of Chalcogenido-bridged Metallocenophanes *117*
3.6 Face-to-face and Multidecker Polymetallocenes Obtained by Condensation Routes *118*
3.7 References *122*

4 Main-Chain Metallopolymers Containing π-Coordinated Metals and Long Spacer Groups *129*
4.1 Introduction *129*
4.2 Polymetallocenes with Long Insulating Spacer Groups *129*
4.2.1 Organic Spacers *129*
4.2.2 Organosilicon Spacers *135*
4.2.3 Siloxane Spacers *137*
4.3 Polymetallocenes with Long Conjugated Spacer Groups *138*
4.4 Other Metal-containing Polymers with π-Coordinated Metals and Long Spacer Groups *142*
4.4.1 π-Cyclobutadiene Ligands *142*
4.4.2 π-Cyclopentadienyl Ligands *146*
4.4.3 π-Arene Ligands *147*
4.4.4 π-Alkyne Ligands *149*
4.5 References *150*

5 Metallopolymers with Metal-Carbon σ-Bonds in the Main Chain *153*
5.1 Introduction *153*
5.2 Rigid-rod Transition Metal Acetylide Polymers *154*
5.2.1 Polymer Synthesis *154*
5.2.2 Structural and Theoretical Studies of Polymers and Model Oligomers *162*
5.2.3 Polymer Properties *164*

5.2.3.1 Thermal and Environmental Stability *165*
5.2.3.2 Solution Properties *165*
5.2.3.3 Optical Properties *167*
5.2.3.4 Nonlinear Optical Properties *170*
5.2.3.5 Electrical and Photoconductive Properties *171*
5.3 Polymers with Skeletal Metallocyclopentadiene Units *172*
5.4 Other Polymers with M–C σ-Bonds in the Main Chain *174*
5.5 References *176*

6 Polymers with Metal-Metal Bonds in the Main Chain *181*
6.1 Introduction *181*
6.2 Polystannanes *182*
6.2.1 Oligostannanes *182*
6.2.2 Polystannane High Polymers *184*
6.3 Polymers Containing Main-chain Metal-Metal Bonds that Involve Transition Elements *189*
6.4 Polymers that Contain Metal Clusters in the Main Chain *196*
6.5 Supramolecular Polymers that Contain Metal-Metal Interactions *199*
6.6 References *201*

7 Main-Chain Coordination Polymers *203*
7.1 Introduction *203*
7.2 Polypyridyl Coordination Polymers *204*
7.2.1 Homopolymers with Octahedral Metals *204*
7.2.2 Homopolymers with Tetrahedral Metals *213*
7.2.3 Stars and Block Copolymers *216*
7.3 Coordination Polymers Based on Schiff-base Ligands *221*
7.4 Coordination Polymers Based on Phthalocyanine Ligands and Related Macrocycles *226*
7.5 Miscellaneous Coordination Polymers Based on Electropolymerized Thiophene Ligands *228*
7.6 Coordination Polymers Based on DNA *229*
7.7 Coordination Polymers Based on Other Lewis Acid/Lewis Base Interactions *231*
7.8 References *233*

8 Metallodendrimers *237*
8.1 Introduction *237*
8.2 Metallodendrimers with Metals in the Core *238*
8.3 Metallodendrimers with Metals at the Surface *243*
8.4 Metallodendrimers with Metals at Interior Sites *256*
8.5 References *267*

Subject Index *271*

Abbreviations

A-*b*-B	diblock copolymer
A-*r*-B	random copolymer
Ac	acetyl group
ADIMET	acyclic diyne metathesis
ADMET	acyclic diene metathesis
AFM	atomic force microscopy
AIBN	azobisisobutyronitrile
Ar	aryl group
bipy or bpy	2,2′-bipyridine
cod	cyclooctadiene
Cp	cyclopentadienyl
DCC	dicyclohexylcarbodiimide
depe	bis(diethylphosphino)ethane
DMA	dynamic mechanical analysis
DME	1,2-dimethoxyethane
DMF	dimethylformamide
dmpe	bis(dimethylphosphino)ethane
DMSO	dimethylsulfoxide
DP_n	number-average degree of polymerization
DP_w	weight-average degree of polymerization
dppe	bis(diphenylphosphino)ethane
dppm	bis(diphenylphosphino)methane
DSC	differential scanning calorimetry
E_g	band gap energy
$\Delta E_{1/2}$	redox coupling
ESR	electron spin resonance
Fc	ferrocenyl group -(η^5-C_5H_4)Fe(η^5-C_5H_5)
fc	ferrocenylene group -(η^5-C_5H_4)Fe(η^5-C_5H_4)-
FESEM	field emission scanning electron microscopy
GPC	gel permeation chromatography
$[\eta]$	intrinsic viscosity
η_{sp}	specific viscosity
ΔH_{cryst}	lattice enthalpy

Hex	hexyl group
HOCO	highest occupied crystal orbital
HOMO	highest occupied molecular orbital
IR	infrared
ITO	indium tin oxide
IVCT	intervalence charge transfer
IVET	intervalence electron transfer
K_c	comproportionation constant
λ	wavelength
L	neutral 2-electron donor ligand
LED	light emitting diode
LMCT	ligand to metal charge transfer
LUCO	lowest unoccupied crystal orbital
LUMO	lowest unoccupied molecular orbital
MALDI-TOF	matrix-assisted laser desorption ionization – time of flight
M_n	number-average molecular weight
M_w	weight-average molecular weight
Mes	mesityl (2,4,6-trimethylphenyl) group
MLCT	metal to ligand charge transfer
NBE	norbornene
NIR	near infrared
NLO	non-linear optical
NMP	*N*-methylpyrrolidin-2-one
NMR	nuclear magnetic resonance
OBDD	ordered bicontinuous double-diamond
Oct	octyl group
OTf	triflate (trifluoromethylsulfonate) group
OTTLE	optically transparent thin-layer electrochemistry
PB	polybutadiene
PDI	polydispersity index
PDMS	poly(dimethylsiloxane)
Pen	pentyl group
PEO	poly(ethylene oxide)
PFP	polyferrocenylphosphine
PFS	polyferrocenylsilane
phen	1,10-phenanthroline
PI	polyisoprene
PMMA	poly(methylmethacrylate)
PPV	poly(phenylenevinylene)
PS	polystyrene
PSS	poly(styrene sulfonate)
PVFc	poly(vinylferrocene)
PVP	poly(vinylpyridine)
P2VP	poly(2-vinylpyridine)
P4VP	poly(4-vinylpyridine)

PVTPP	poly(vinyltriphenylphosphine)
PXRD	powder X-ray diffraction
py or pyr	pyridine
RIE	reactive ion etching
ROMP	ring-opening metathesis polymerization
ROP	ring-opening polymerization
σ (in Scm^{-1})	electrical conductivity
ΔS_{diss}	entropy of dissolution
SAXS	small-angle X-ray scattering
SBP	soybean peroxidase
SCE	saturated calomel electrode
SEC	size exclusion chromatography
SEM	scanning electron microscopy
SHG	second harmonic generation
SPM	scanning probe microscopy
STM	scanning tunnelling microscopy
T_c	crystallization temperature
T_{cl}	clearing temperature
T_g	glass transition temperature
T_{lc}	melting temperature to give a mesophase
T_m	melting temperature
TCNE	tetracyanoethylene
TCNQ	7,7,8,8-tetracyanoquinodimethane
TEM	transmission electron microscopy
terpy	terpyridyl
TGA	thermogravimetric analysis
THF	tetrahydrofuran
TMEDA	*N*,*N*,*N*′,*N*′-tetramethylethylenediamine
TMS	trimethylsilyl group
Tol	toluene
tppz	tetrapyridylphenazine
UPS	ultraviolet photoelectron spectroscopy
UV	ultraviolet
VFc	vinylferrocene
vis	visible
VPO	vapour pressure osmometry
WAXS	wide angle X-ray scattering
XPS	X-ray photoelectron spectroscopy
$Z_{c,w}$	weight-average critical entanglement chain length

1
Introduction

1.1
Metal-Containing Polymers

Carbon is not a particularly abundant terrestrial element, ranking 14th among those in the Earth's crust, oceans, and atmosphere. Nevertheless, carbon-based or organic macromolecules form the basis of life on our planet, and both natural and synthetic macromolecules based on carbon chains are ubiquitous in the world around us. Organic polymers are used as plastics, elastomers, films, and fibers in areas as diverse as clothing, food utensils, car tires, compact discs, packaging materials, and prostheses [1]. Moreover, with the additional impetus provided by the Nobel prize winning discovery of electrical conductivity in doped polyacetylene in the mid-1970s, exciting new applications in electroluminescent and integrated optical devices and sensors are also now under development [2–6]. The remarkable growth in the applications of organic polymeric materials in the latter half of the 20th century can mainly be attributed to their ease of preparation, and the useful mechanical properties and unique propensity for fabrication that are characteristic of long-chain macromolecules. Their ease of preparation is a consequence of the highly developed nature of organic synthesis, which, with its logical functional group chemistry and ready arsenal of metal-catalyzed reactions, allows a diverse range of carbon-based polymers to be prepared from what are currently plentifully available and cheap petroleum-derived monomers [7, 8]. In the late 20th century, organic polymer science has been further advanced by the creation of remarkable polymer architectures such as block copolymers, star polymers, and tree-like molecules or *dendrimers*, which are attracting intense attention.

In contrast to the situation in organic chemistry, the ability to chemically manipulate atoms of inorganic elements is generally at a much more primitive stage of development. Even seemingly simple small inorganic molecules can still be surprisingly elusive, and the formation of bonds between inorganic elements is still often limited to salt metathesis processes. Inorganic analogues of readily available multiply-bonded organic monomers such as olefins and acetylenes, for example, are generally rather difficult to prepare. The development of routes to polymer chains of substantial length constructed mainly or entirely from inorganic elements has therefore been a challenge. Indeed, apart from the cases of polysiloxanes (**1.1**) [9, 10], poly-

Synthetic Metal-Containing Polymers. Ian Manners

ISBN: 3-527-29463-5

phosphazenes (**1.2**) [9, 11–13], and polysilanes (**1.3**) [9, 14, 15], this area has only been significantly expanded since the 1980s and 1990s [8].

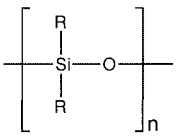

1.1

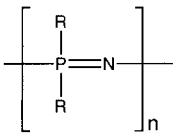

1.2

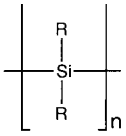

1.3

In the case of polymers based on non-metallic main group elements, the development of novel thermal, Lewis acid or base promoted, or transition metal-catalyzed polycondensation strategies that proceed with the elimination of small molecules such as $Me_3SiOCH_2CF_3$, Me_3SiCl, H_2, H_2O, and CH_4, as well as the discovery of ring-opening polymerization (ROP) and related processes, has permitted improved approaches to existing polymer systems (e.g. **1.2** and **1.3**) [16–25] and access to new materials. Examples of the latter include polyoxothiazenes (**1.4**) [26], polythionylphosphazenes (**1.5** and **1.6**) [27–29], polyphosphinoboranes (**1.7**) [30], polyborazylenes (**1.8**) [31], and other systems that contain boron-nitrogen rings such as polycyclodiborazanes (**1.9**) [32].

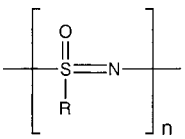

1.4

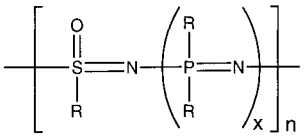

1.5 x = 2
1.6 x = 1

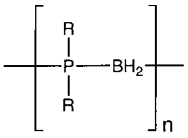

1.7

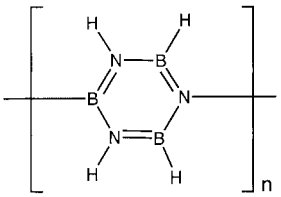

1.8

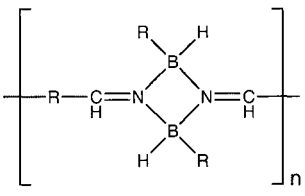

1.9

Many similar synthetic challenges exist in the area of polymers based on metallic elements. At the molecular level, metal chemistry is well developed. For example, the preparation of carefully designed, single-site transition metal catalysts has already had a dramatic impact on polymer science, particularly for the polymerization

of alkenes [33]. Inorganic solid-state materials chemistry has also now been developed to the extent that scientists are able to exploit the vast range of possibilities arising from the chemical diversity made available throughout the Periodic Table [34–36]. The creation of high-temperature ceramic superconductors, state-of-the-art magnetic, electrochromic, or electrooptical materials, and unprecedented catalysts with controlled porosity, are all consequences of chemists' now highly impressive ability to organize atoms of inorganic elements in two and three dimensions. In contrast, the elaboration of efficient synthetic routes to metal-containing polymers has been the real roadblock to the development of 1-D analogues of the well-established 2-D layered and 3-D metal-containing solid-state materials. This is particularly the case if the metal atoms are located directly in the main chain, where they are most likely to exhibit the most profound influence on the properties of the macromolecular material. Over the last decade of the 20th century, there have been clear indications that this synthetic problem is being productively tackled and a wide variety of intriguing new polymer systems have emerged. These developments are the subject of this book, which is written both to review the state-of-the-art and also to further help stimulate both fundamental and applied research in this exciting area that is ripe for exploitation and full of future potential.

1.2 Fundamental Characteristics of Polymeric Materials

Polymers exhibit a range of architectures and unique properties, the study of which represents a major core area of polymer science. Although this book assumes that the reader is familiar with some of the basic concepts of polymer science, such as the structures of common macromolecular materials (polystyrene, polyisoprene, etc.), additional knowledge is certainly desirable for an appreciation of much of the research described and the challenges for the future. In this section, we briefly cover some key points for the benefit of readers unfamiliar with the areas that are relevant to the discussions in subsequent chapters. For detailed background material the reader is referred to the many excellent introductory and advanced books on polymer science and the recent literature cited in this section [7, 37–42].

1.2.1 Polymer Molecular Weights

Samples of synthetic polymers are generally formed by reactions where both the start and end of the growth of the macromolecular chain are uncontrolled and are relatively random events. Even chain-transfer reactions, where, for example, one polymer chain stops growing and in the process induces another to begin, are prevalent in many systems. Synthetic polymer samples, therefore, contain molecules with a variety of different chain lengths and are termed *polydisperse*. For this reason, the resulting molecular weight distribution is characterized by an *average molec-*

ular weight. The two most common are the *weight-average molecular weight*, M_w, and the *number-average molecular weight*, M_n. The quantity M_w/M_n is termed the *polydispersity index* (PDI), which measures the breadth of the molecular weight distribution and is ≥ 1. In the case where the polymer chains are of the same length $M_w = M_n$ (i.e. PDI = 1), the sample is termed *monodisperse*. Such situations are rare, except in the case of biological macromolecules, but essentially monodisperse systems also occur with synthetic polymers where the polymerization by which they are prepared is termed *living*. In such cases, initiation is rapid and no termination or chain-transfer reactions occur; under such conditions, the polymer chains initiate at the same instant and grow until the monomer is completely consumed, resulting in macromolecular chains of the same length [7]. In practice, living systems are not perfect; for example, very slow termination reactions generally occur. This leads to polymer samples which are of narrow polydispersity ($1.0 < PDI < 1.2$) rather than perfectly monodisperse (PDI = 1.0). Living systems are of particular interest because they allow the formation of controlled polymer architectures. For example, unterminated chains can be subsequently reacted with a different monomer to form block copolymers.

A variety of different experimental techniques exist for the measurement of M_w and M_n [38–41]. Some afford absolute values, while others give estimates that are relative to standard polymers, such as polystyrene, which are used as references. One of the simplest techniques for obtaining a measurement of the molecular weight of a polymer is Gel Permeation Chromatography (GPC) (also known as Size Exclusion Chromatography, SEC). This method affords information on the complete molecular weight distribution as well as values of M_w and M_n (and hence the PDI). Unfortunately, the molecular weights obtained are relative to that of the polymer standard used to calibrate the instrument unless special adaptations of the experiment are made or standard monodisperse samples of the polymer under study are also available as references. Light-scattering measurements are generally time consuming but permit absolute values of M_w to be obtained and also yield a wealth of other information concerning the effective radii of polymer coils in the solvent used, polymer-solvent interactions, and polymer diffusion coefficients. The introduction of light-scattering detectors for GPC instruments has now made it possible for both absolute molecular weights and molecular weight distributions to be determined routinely. It should also be noted that mass spectrometry techniques such as Matrix-Assisted Laser Desorption Ionization – Time of Flight (MALDI-TOF) have now been developed to the stage where they are extremely useful for analysis of the molecular weights of polymers and can give molecular ions for macromolecules with molecular weights substantially greater than 100,000.

Although most polymer samples possess a single molecular weight distribution by GPC and are termed *monomodal*, for some the molecular weight distribution actually consists of several individual, resolvable distributions. In such cases, the molecular weight distribution is referred to as *multimodal*. For example, if a high and a low molecular weight fraction can be distinguished then the distribution is termed *bimodal* (Fig. 1.1 a). Examples of broad and narrow monomodal molecular weight distributions are shown in Fig. 1.1 b and 1.1 c, respectively.

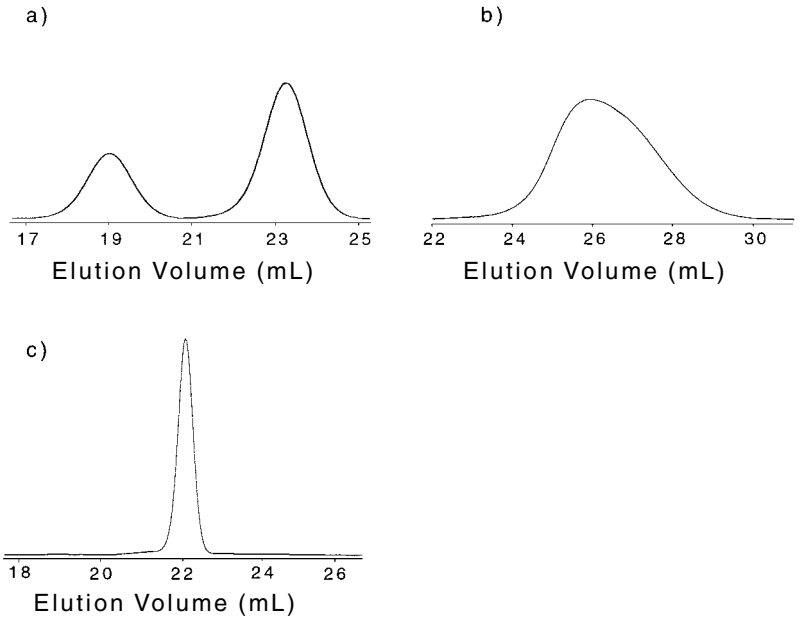

Fig. 1.1 Typical GPC traces showing (**a**) a bimodal molecular weight distribution, (**b**) a broad monomodal molecular weight distribution (PDI = 2.3), and (**c**) a narrow monomodal molecular weight distribution (PDI = 1.05). The *x*-axis shows the elution volume for the GPC instrument with molecular weight increasing from right to left.

1.2.2

Amorphous, Crystalline, and Liquid-Crystalline Polymers: Thermal Transitions

As polymer chains are usually long and flexible, they would be expected to pack randomly in the solid state to give an amorphous material. This is true for many polymers, particularly those with an irregular chemical structure. Examples are the stereoirregular materials *atactic* polystyrene (**1.10**) and *atactic* polypropylene (**1.11**), in which the Ph and the Me substituents, respectively, are randomly oriented.

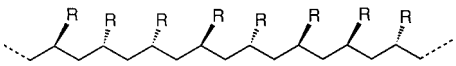

1.10 R = Ph
1.11 R = Me

However, polymer chains that have regular structures can pack together in an ordered manner to give crystallites. In general, perfect single crystals are not formed by long polymer chains for entropic reasons, and such materials are therefore often more correctly referred to as *semicrystalline*, as amorphous regions are

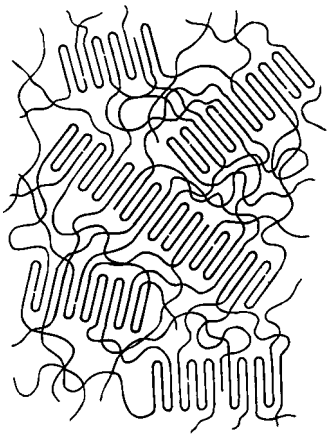

Fig. 1.2 Model of a semicrystalline polymer showing chain-folded crystallites embedded in an amorphous matrix (Reproduced from [37a]).

also present [43]. At the edges of the crystallites, the macromolecular chains fold and re-enter the crystal. The manner in which this occurs has been a subject of much debate in the polymer science community, but a reasonable picture of the amorphous and crystalline regions of a semicrystalline polymer is shown in Fig. 1.2. Information on the morphology of polymers is revealed by techniques such as powder X-ray diffraction (PXRD), which is often called wide-angle X-ray scattering (WAXS) by polymer scientists, and small-angle X-ray scattering (SAXS). The crystallites exist in a polymer sample below the *melting temperature* (T_m), an order-disorder transition, above which a viscous melt is formed.

The presence of crystallites can lead to profound changes in the properties of a polymeric material. For example, crystallites are often of the appropriate size to scatter visible light and thereby cause the material to appear opaque. They often lead to an increase in mechanical strength, but also to brittleness. Gas permeability generally decreases, as does solubility in organic solvents as an additional lattice energy term must be overcome for dissolution to occur. Examples of crystalline polymers are the stereoregular materials *syndiotactic* polystyrene (**1.12**), in which the orientation of the Ph groups alternates in a regular manner, and *isotactic* polypropylene (**1.13**), in which the Me groups have the same orientation. This structural regularity allows the polymer chains to pack together in a regular manner as crystallites.

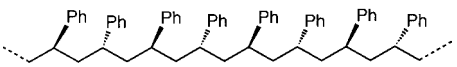

1.12

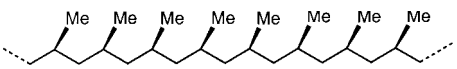

1.13

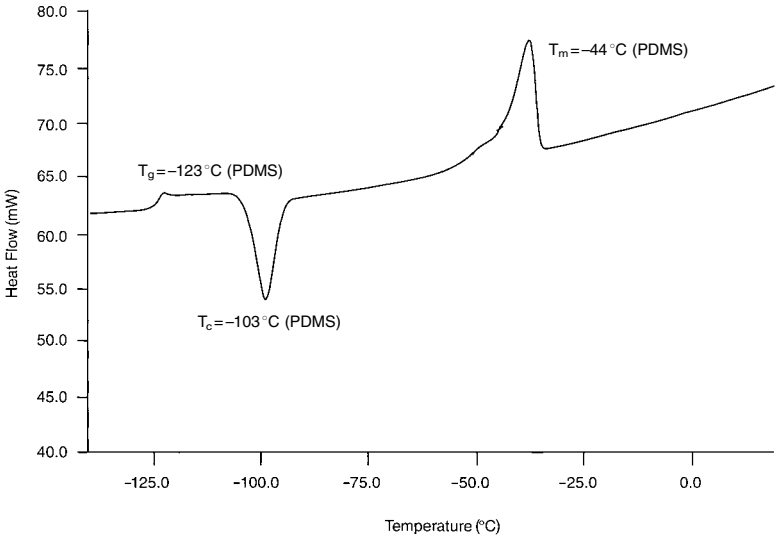

Fig. 1.3 A DSC trace showing a series of idealized thermal transitions (i.e. T_g, T_m, and T_c) for poly(dimethylsiloxane) (PDMS).

In addition to the melting temperature (T_m), which arises from the order-disorder transition for crystallites in a polymer sample, amorphous regions of a polymer show a *glass transition* (T_g). This second-order thermodynamic transition is not characterized by an exotherm or endotherm, but rather by a change in heat capacity, and is related to the onset of large-scale conformational motions of the polymer main chain. Generally, stiff polymer chains and large, rigid side groups generate high T_g values. Below the T_g an amorphous polymer is a glassy material, whereas above the T_g it behaves like a viscous gum, because the polymer chains can move past one another. By linking the polymer chains together through cross-linking reactions, rubbery elastomers can be generated from low T_g polymers. Purely amorphous polymers such as atactic polystyrene show only a glass transition ($T_g \approx 100\,^{\circ}C$), whereas semicrystalline polymers show both a T_m and a T_g. Semicrystalline polymeric materials are rigid plastics below the T_g and become more flexible above the T_g. Above the T_m, a viscous melt is formed.

It is noteworthy that the rate of polymer crystallization can be extremely slow and polymers that can potentially crystallize are often isolated in a kinetically stable, amorphous state. The polyester poly(ethylene terephthalate) (**1.14**) provides a good example. This material has a T_g of 69 °C and a T_m of 270 °C, but crystallization only becomes rapid well above the T_g. Rapid cooling from the melt yields an amorphous material, whereas slow cooling or annealing above the T_g can yield percentage crystallinities up to 55% [38]. A potentially crystallizable polymer that is in an amorphous state can show an exothermic *crystallization transition* (T_c) at elevated temperatures. The thermal transitions of a polymer are commonly investigated by the technique of differential scanning calorimetry (DSC). A typical DSC trace showing a T_g, a T_c, and a T_m is shown in Fig. 1.3.

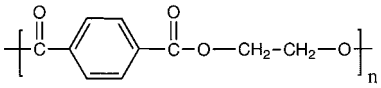

1.14

Polymers can also exhibit *liquid crystallinity*, a fluid state in which some long-range positional or orientational order, or a *mesophase*, exists [43, 44]. This arises when significant shape anisotropy is present in the polymer main chain or side-group structure. Liquid crystallinity can exist in the bulk material, where the mesophase is formed over a certain temperature range (*thermotropic*), or as a consequence of a preferred arrangement of polymer molecules in solution above a certain concentration (*lyotropic*). Thermotropic liquid-crystalline materials show a mesophase between a *melting temperature for the crystalline phase* (T_{lc}) and the *clearing temperature* (T_{cl}), above which an isotropic melt is formed. The order present in liquid-crystalline polymers can be used to broadly classify the materials as *nematic* (order in only one dimension) or *smectic* (weakly layered), as illustrated for the case of a main-chain liquid-crystalline polymer that consists of rigid and flexible segments (Fig. 1.4a and b, respectively). Many permutations on this theme are possible, as illustrated in Fig. 1.4c to g [43, 44]. Liquid-crystalline polymers can be analyzed by polarizing optical microscopy, where the ability of mesophases to influence the plane of polarized light yields various textures, which are used to characterize the materials. Liquid-crystalline polymers are of considerable interest as high-performance materials and have potential uses in photonics and data storage.

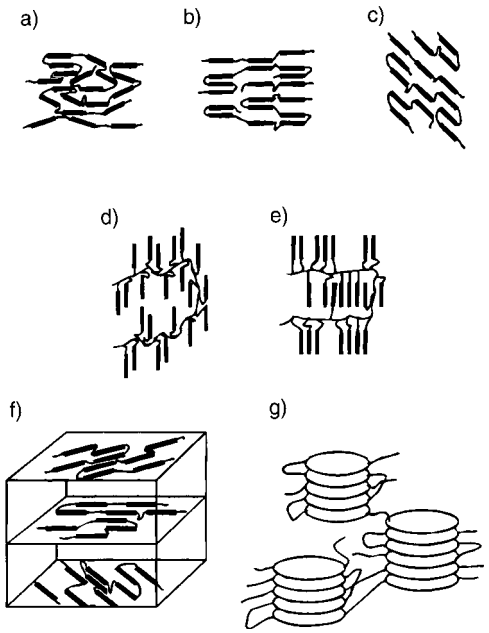

Fig. 1.4 Nematic and smectic main-chain liquid-crystalline polymers: (**a**) main-chain nematic, (**b**) main-chain smectic A, (**c**) main-chain smectic C, (**d**) side-chain nematic, (**e**) side-chain smectic A, (**f**) main-chain cholesteric, (**g**) main-chain discotic (Reproduced from [43]).

1.2.3
Polymers versus Oligomers: Why are High Molecular Weights Desirable?

Two related questions that are often asked are the following: "How long does a molecule have to be in order for it to be called a polymer rather than an oligomer?" and "Why are high molecular weights desirable?" Indeed, the electronic and optical properties of extended conjugated molecular structures are often maximized at chain lengths of 30 chain atoms or so. So why are longer chains needed? The main reasons for the widespread use of polymers are their excellent mechanical properties such as strength, deformability, and elasticity. Simple considerations allow a rough estimation of the substantial chain lengths necessary to obtain these properties.

In crystalline polymers, the need is for polymer molecules that function as "tie molecules" which are long enough to connect individual crystallites (see Fig. 1.2). This leads to strong covalent bond connections both within the crystallites and also between them, and thereby enhances mechanical strength. Typically, chains must consist of at least 100 chain atoms for such connections to be possible. For a monomer of molecular weight 100, this corresponds to $M_n \approx 10{,}000$. In amorphous polymers, the chains need to be long enough for entanglement to take place (Fig. 1.5). Chain entanglements help the material to maintain structural integrity under stress. The onset of significant chain entanglement, the *weight-average critical entanglement chain length* $Z_{c,w}$, can be determined from melt viscosity measurements and generally corresponds to ca. 600 chain atoms. For poly(dimethylsiloxane), $Z_{c,w} = 630$, which corresponds to $M_w \approx 23{,}000$, whereas for polystyrene $Z_{c,w} = 600$, which corresponds to $M_w \approx 31{,}000$. These molecular weights therefore represent the low end for the useful mechanical properties of these polymers [39]. Clearly, the molecular weight required for useful mechanical properties depends on the particular polymer being considered.

The need for high molecular weights in order to obtain useful mechanical properties is neatly illustrated by a comparison of straight-chain hydrocarbons. It is easy to appreciate the difference between a birthday candle (a mixture of C_{25}–C_{50} alkanes, i.e. $M_n \approx 500$), which is a brittle material and breaks easily, and a polyethylene wash bottle tip (chains of >1000 carbon atoms, i.e. $M_n > 15{,}000$), which can be repeatedly bent [39].

It is obvious, then, that high molecular weight polymers have major advantages over low molecular weight analogues for most applications. However, it is important to note that exceptions to this rule exist. For example, in applications as toner particles in laser printing and xerography, where low melting points are impor-

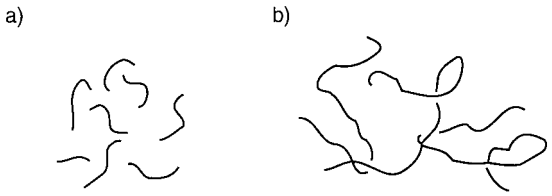

Fig. 1.5 (**a**) Oligomers, which do not entangle due to their short chains, and (**b**) chain entanglements in an amorphous high molecular weight polymer.

tant, low molecular weight materials are actually desirable. In addition, for certain electronics applications, well-defined monodisperse oligomers (e.g. the linear hexamer sexithiophene) can have better defined and more predictable electronic and optical properties. In such cases, the lower processability of the oligomer can be circumvented by the use of vacuum deposition to form high quality films. Relatively low molecular weight polymers are also useful as precursors to ceramic materials. For example, after fabrication into fibers, pyrolysis can yield a ceramic product in high yield. In such applications, sufficient viscosity for spinning into fibers and high ceramic yield are of great importance. Nevertheless, in the vast majority of cases, high molecular weights allow more desirable material properties. In this book, then, we will make a broad generalization and use the term "polymer" to refer to materials with $M_n > 10{,}000$, and will use the term oligomer to refer to materials of lower molecular weight.

1.2.4 Polymer Solubility

Films of polymeric materials are readily fabricated from solution by evaporation- or dip-casting and by spin-coating techniques. However, polymers generally show a lower tendency to dissolve in solvents compared to molecular compounds for thermodynamic reasons. This is a consequence of the fact that the *entropy of dissolution*, ΔS_{diss}, is substantially reduced for a macromolecular material relative to that for a small molecule compound. In solution, the additional disorder for a polymer chain compared to that present in an amorphous polymeric solid is very small, especially if the main chain is rigid (i.e. the T_g is high). The polymer segments in solution are still constrained to one dimension and so the amount of "disorder" is not vastly different from the situation in the solid state. By contrast, small molecules possess considerably more translational freedom in solution compared to the solid state, as motion in three different dimensions is possible. The thermodynamic polymer solubility problem becomes particularly acute if the polymer is crystalline, as an unfavorable lattice enthalpy term ΔH_{cryst} must also be overcome for dissolution to occur. Thus, the choice of a solvent that has favorable interactions with a polymer becomes critical when dissolution of the polymer is desired. The attachment of long flexible organic substituents (e.g. *n*-alkyl or *n*-alkoxy groups) to a polymer with a rigid backbone is a common and important strategy for generating solubility in organic solvents. In addition, the introduction of polar groups or ionic sites can allow dissolution in hydrophilic solvents and in water. Thus, by a consideration of these factors and logical synthetic manipulations of polymer structures, the dissolution of virtually all uncrosslinked polymeric materials can, in fact, be achieved. It should also be noted, however, that dissolution of polymers in solvents can still be slow for kinetic reasons, even when the process is thermodynamically favorable. When a solid sample of a polymer dissolves, permeation of solvent into the solid from the solid/solvent interface can be slow, as long polymer chains must be completely solvated before diffusion into the bulk solvent is possible. Such a process is generally much more rapid for molecular compounds with smaller dimensions. Finally, it

should be noted that crosslinked polymers swell but do not dissolve in solvents which otherwise dissolve the analogous uncrosslinked material. The degree of swelling is inversely dependent on the degree of crosslinking. This generates gels, which have a wide variety of uses. For example, hydrogels made from crosslinked hydrophilic polymers are used as contact lenses.

1.2.5 Block Copolymers

The polymers discussed in the previous section are derived from a single monomer, and are termed *homopolymers*. Physical mixtures of two or more polymers are termed *blends*, and these hybrid materials have useful combinations of properties derived from the constituent homopolymers. Generally, for reasons analogous to those leading to a low entropy of dissolution in solvents (Sect. 1.2.4), and in dramatic contrast to the situation for small molecule compounds, the entropy of mixing of two homopolymers ΔS_{mix} is very small. As this is usually insufficient to overcome the unfavourable and positive value of the enthalpy of mixing ΔH_{mix} the material will phase-separate into regions of immiscible homopolymers at the microscopic level [39]. It is difficult to overemphasize the tendency of two polymers to phase-separate even if the difference in chemical structure is small. For example, even high molecular weight polyethylene and deuterated polyethylene are not miscible in all proportions!

Copolymers contain repeat units derived from different monomers chemically bound in the main chain. Considering two different monomers A and B, it is possible to envisage random copolymer structures (e.g. ...ABBABAABA...), alternating structures (...ABABAB...), and many others such as graft structures, where, for example, side chains formed from B are attached to a main chain derived from A. *Block copolymers* (...AAAAAABBBBBB..., or A-*b*-B) are a particularly interesting example of a copolymer architecture and these materials possess a range of remarkable and useful properties [45]. For example, diblock copolymers form colloidal dispersions in solvents that are selective for one of the blocks, where supramolecular micellar aggregates are formed, with the insoluble block forming the *core* and the soluble block forming the *corona* [45, 46]. These micelles are generally much more stable than those formed by small molecule surfactants and are usually spherical in nature (Fig. 1.6), although a range of remarkable architectures including cylinders, vesicles, and even onion-like structures have now been generated [47–49].

Micellar structures can be visualized after solvent evaporation by techniques such as transmission electron microscopy (TEM) or atomic force microscopy (AFM). The micellar aggregates can be studied in solution by static and dynamic light-scattering, which can give micelle sizes and aggregation numbers as well as information on the shape of the micelles formed. Crosslinking of either the core or corona has been studied as a means of making the micellar structures permanent in the sense that they do not dissociate into individual block copolymer molecules in the presence of a good solvent for both blocks [50–55].

In the solid state, phase-separation of immiscible blocks generally occurs to give nanodomains that can be ordered. For example, the diblock copolymer polysty-

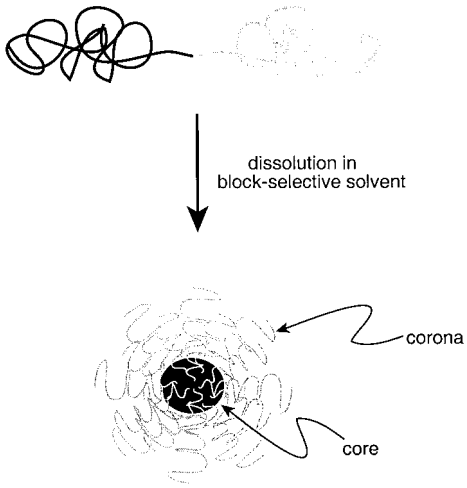

Fig. 1.6 Formation of spherical micelles from a block copolymer in a block-selective solvent.

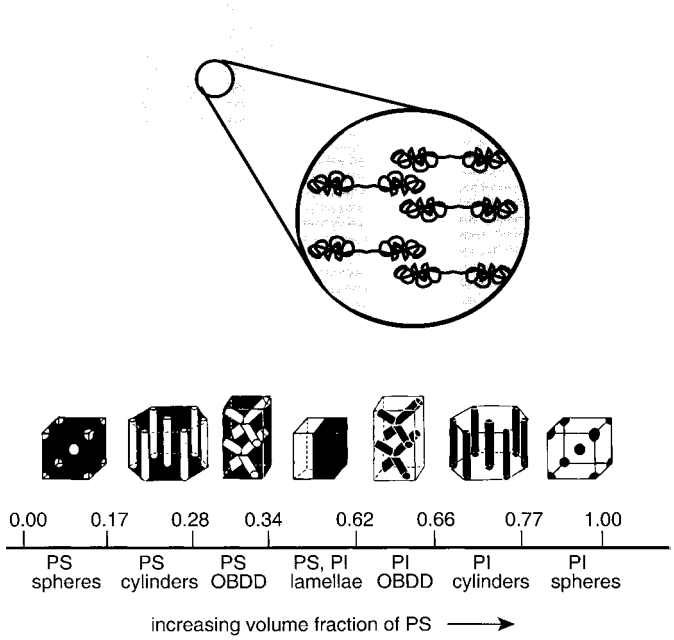

Fig. 1.7 Polystyrene-*b*-polyisoprene (PS-*b*-PI) solid-state morphologies as a function of increasing volume fraction of the polystyrene block (Adapted from [56]).

rene-*b*-polyisoprene (PS-*b*-PI) has been particularly well-studied, and ordered arrays of spheres, cylinders, bicontinuous double-diamonds (OBDD), and lamellae are formed as the relative block lengths (and hence block volume fractions) are altered from highly asymmetric through to a similar value (Fig. 1.7) [45, 56]. More complex structures, such as gyroids, are formed within a relatively restricted range of block lengths. The structures can be imaged by techniques such as TEM and AFM, and further information on the order present in such systems can be revealed by techniques such as SAXS [43, 56].

The micellar structures and phase-separated domains have dimensions on the nanometer scale and are of considerable interest for a wide range of applications. These include uses as micellar drug delivery agents and catalysts, as nanoscopic etching resists for creating patterned surfaces in nanolithography, and for the generation of structures with periodic changes in refractive index for applications in photonics [45, 46, 57–61].

An elegant example that illustrates the enormous potential of this area is that provided by the use of the hydrophilic polyether domains of phase-separated polyisoprene-*b*-poly(ethylene oxide) (PI-*b*-PEO) as a reaction medium for the sol-gel hydrolysis of silicon and aluminum alkoxides [62]. The resulting structures can, for example, be subsequently dispersed in a solvent and consist of crosslinked silica/alumina/PEO nano-objects solubilized by the polyisoprene chains (Fig. 1.8).

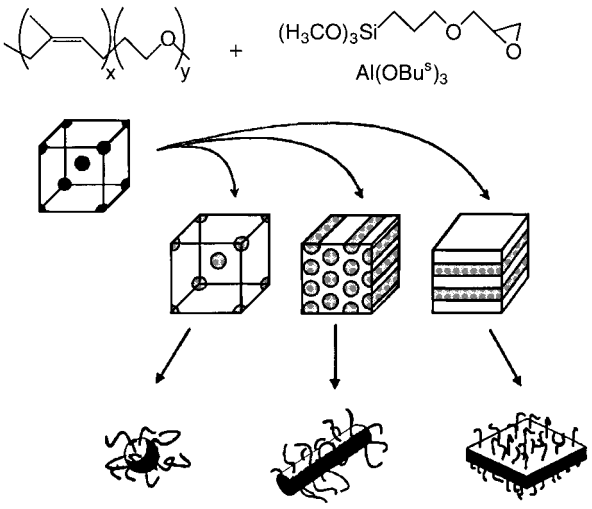

Fig. 1.8 Nano-objects with controlled shape and size from block copolymer mesophases: At the top left, phase-separated PI-*b*-PEO is shown, where the spheres consist of the PEO block. Subsequent dispersion and sol-gel hydrolysis of silicon and aluminum alkoxides in the PEO block leads to swelling of this block and, if desired, morphological transitions. Dissolution of the PI block in a selective solvent leads to "hairy" nano-objects consisting of crosslinked silica/alumina/PEO (Adapted from [62]).

Important commercial uses of block copolymers depend on phase separation in the solid state. For example, triblock copolymers PS-*b*-PB-*b*-PS (PB = polybutadiene) that contain a long PB block form glassy domains of PS ($T_g = 100\,^{\circ}C$) within a matrix of low T_g PB ($T_g \approx -100\,^{\circ}C$). The glassy PS domains function as physical crosslinks, which prevent the PB chains from slipping past one another under deformation. This generates elastomeric properties but, unlike normal elastomers which are permanently chemically crosslinked, heating above the T_g of the PS block allows the material to be reprocessed. This reversibility has led to the term *thermoplastic elastomer* for these materials, which are known as Kratons and are sold commercially [39].

1.2.6 Dendrimers and Hyperbranched Polymers

The area of tree-like polymer architectures was pioneered by the Tomalia, Newkome, and Vögtle groups in the late 1970s and 1980s [63–66]. The original syntheses of dendritic structures involved a *divergent* approach, where the structures were assembled by starting at a core and working outwards. Additional impetus to the area was subsequently provided by the demonstration of a new conceptual approach to dendrimers, which involved *convergent* synthesis, as reported almost simultaneously by the groups of Neenan and Miller, and by Hawker and Fréchet in 1990 [67, 68]. Here, the dendrimer was synthetically assembled by the reaction of a series of arms at a core. These two different methods are illustrated in Fig. 1.9.

The general area of dendritic and hyperbranched polymers has received remarkable attention over the past decade. New properties not available with linear polymers have been demonstrated. For example, evidence has been provided that supports the existence of considerable space for the encapsulation of small molecules, and this has led to the idea of a "dendritic box" [69]. A severe problem with dendrimers is their time-consuming synthesis and, recently, facile synthetic methods that form hyperbranched materials that may exhibit many of the advantageous properties of dendritic macromolecules have been receiving significant attention [70].

1.2.7 Electrically Conducting Polymers

Most polymers (typified by polystyrene and polyethylene) are electrically insulating and have conductivities $\sigma < 10^{-14}$ S cm^{-1}. The observation that polyacetylene could be oxidatively doped with iodine to become electrically conducting (values have now been reported up to $\sigma > 10^5$ S cm^{-1}) represented a pivotal discovery in polymer science that ultimately resulted in the award of the Nobel Prize for Chemistry in 2000 [4]. The study of electrically conducting polymers is now well advanced and two extremes in the continuum of transport mechanisms exist. If the charge carriers are present in delocalized orbitals that form a band structure along the polymer backbone, they conduct by a *delocalization* mechanism. In contrast, isolated groups in a polymer can function as acceptors or donors of electrons and can permit

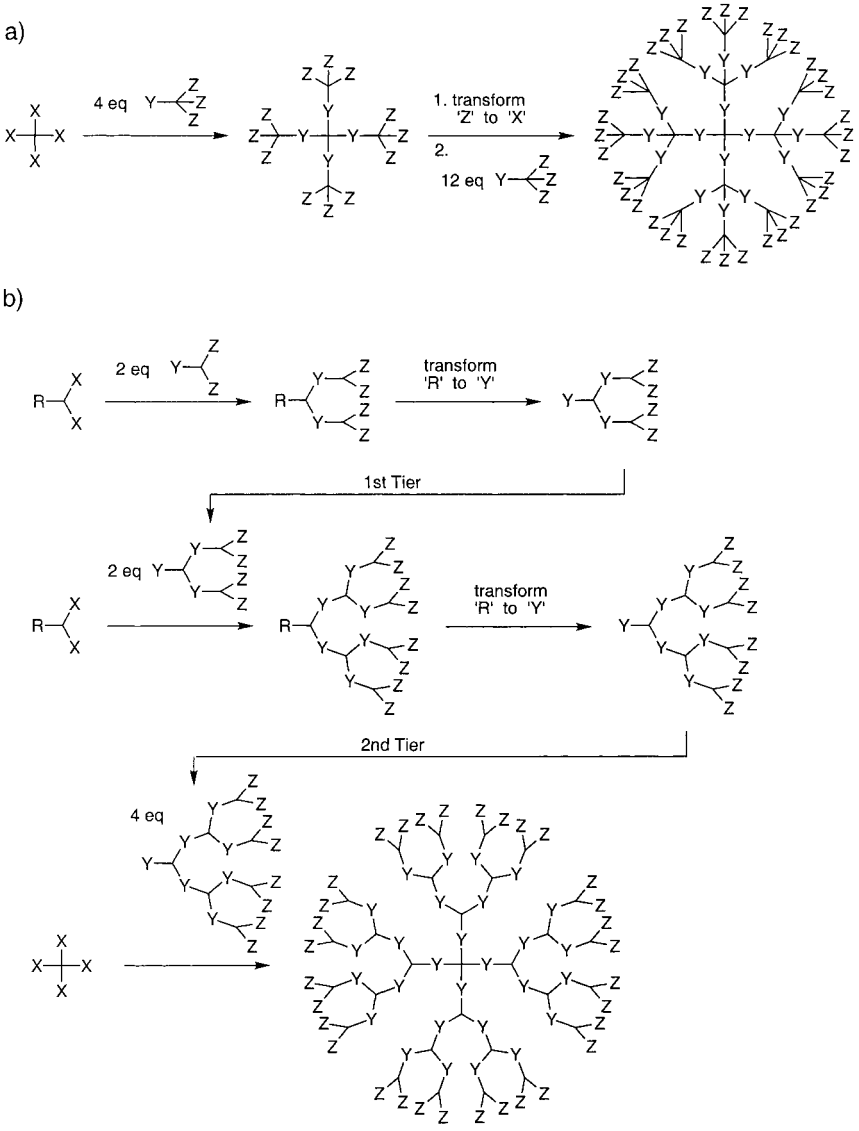

Fig. 1.9 Syntheses of dendrimers: (**a**) Divergent method, (**b**) convergent method.

charge transport of electrons or holes by a *redox conduction* or *hopping* mechanism. Although the conductivities observed in the former case are generally appreciably higher, both types of system are of considerable interest depending upon the conductivity desired for a particular application. High conductivities are desirable for many device applications, and materials such as polythiophene (**1.15**), polyaniline (**1.16**), and polypyrrole (**1.17**) have attracted much attention [6, 71]. On the other

hand, the semiconductivity of poly(vinyl carbazole) (**1.18**) ($10^{-7} < \sigma < 10^{-5}$ cm^{-1}) has led to interest in its use as a hole-transport material in xerography.

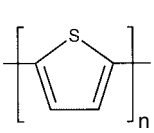

1.15

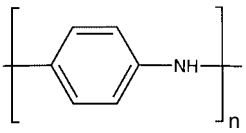

1.16

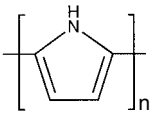

1.17

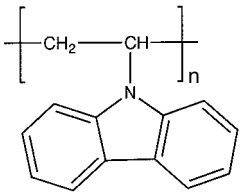

1.18

It should be noted that, in addition to their use as electronic conductors, polymers can also function as ionic conductors. Materials such as poly(ethylene oxide) and certain oligoethyleneoxy-substituted polyphosphazenes and polysiloxanes, which conduct Li^+ ions, are used in this regard as polymeric electrolytes for battery applications [9].

1.3 Motivations for the Incorporation of Metals into Polymer Structures

As mentioned earlier (Sect. 1.1), transition metal complexes and metal-containing solid-state materials are well-studied, and the presence of metal centers has been shown to give rise to a diverse range of interesting and often useful redox, magnetic, optical, electrical, and catalytic properties. In addition, metal centers have been shown to play a pivotal role with respect to both the structure and function of many biopolymers such as metalloproteins. The incorporation of transition metals into the structure of synthetic polymers, therefore, clearly offers considerable potential for the preparation of processable materials with properties that differ significantly from those of conventional organic polymers. For this reason, the development of metal-containing polymers should create exciting new dimensions for polymer materials science and, from an applied angle, significant applications for some of these unique new materials are also to be expected.

Several different possible types of metal-containing polymer structures exist, depending on where the metal atoms are incorporated and the nature of the linkages between them. A major subdivision of linear polymers involves a considera-

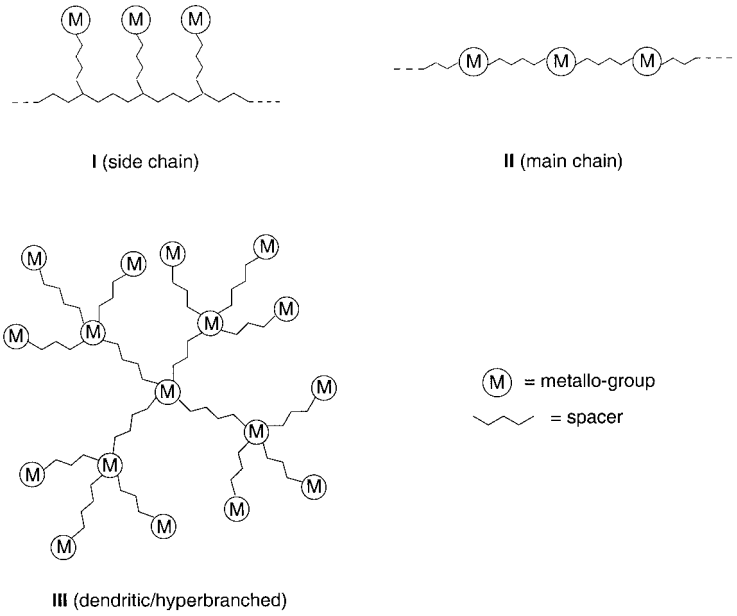

Fig. 1.10 Structural classes of metal-containing polymers.

tion of the location of the metallo-centers. These can be either in the side-group structure (**I**) or directly in the main chain (**II**) (see Fig. 1.10). We will use this general subdivision, although we note that these situations represent extremes. For example, a situation that lies in between these two cases is one in which the metal-containing moiety can be removed from, but is electronically coupled to, the polymer backbone. In addition, it is possible to prepare materials with metals in both the side-group structure and the main chain. Dendrimers and hyperbranched polymers (**III**) (Fig. 1.10) represent another structural class of growing interest. In this case, the metallo-centers can be located throughout the structure or, alternatively, in the core or at the periphery.

The linkages or "spacers" between the metallo-centers can either possess conjugated structures (involving delocalization of σ- or π-electrons) or essentially localized electrons. Again, these situations represent extremes, and partial conjugation is often possible. Studies of how the electronic structure of the linker can be changed to control interactions between the metals is an important area of research and has important implications for the physical properties (e.g. conductivity, magnetic properties) and applications of the materials.

It is useful to consider the types of characteristics expected for metal-containing polymers that provide a key motivation for making the materials. Some of the main reasons for the incorporation of metals into polymer structures are now outlined.

1.3.1 Conformational, Mechanical, and Morphological Characteristics

A carbon atom is small and is usually limited to coordination numbers ≤4, and is generally restricted to three geometries – linear, trigonal planar, and tetrahedral. The properties of organic polymers depend acutely on the nature of the polymer chain and the side groups. By contrast, metal atoms cover an enormous range of sizes and can exhibit a broad array of coordination numbers; values of up to 12 are well known and of up to 8 are common [72]. In addition, a wealth of geometries is known for metal centers. For example, in contrast to carbon, four-coordinate metal complexes can possess either tetrahedral or square-planar geometries. The flexible bonding characteristics of transition metals can also give rise to structures that are completely unprecedented in carbon chemistry. For example, metal-metal quadruple bonds are well-known, and metallocenes and cyclobutadiene complexes exhibit a totally different type of geometry to that found in organic molecules. In ferrocene, the prototypical metallocene, rotation about the iron-cyclopentadienyl bond is virtually unhindered. It is interesting to think about the influence that these novel structural features might have on the conformational, mechanical, and morphological properties of a polymer. Bearing in mind the immense structural diversity possible with metal complexes, this would clearly be expected to be a fascinating area. In addition, the diverse range of coordination numbers and geometries available for transition elements offers the possibility of accessing interesting liquid-crystalline materials [36].

1.3.2 Precursors to Ceramics

The possibility of using polymers, which can be easily processed into shapes, films or fibers, as precursors to ceramics has attracted intense recent interest [73–78]. Ceramics generally possess many desirable physical properties, such as hardness and useful electronic or magnetic properties, but their processability is generally poor. Polycarbosilanes have been successfully used to prepare silicon carbide monoliths and fibers by a pyrolysis technique, and a similar process that utilizes polyacrylonitrile has been used to make carbon fibers. For example, polycarbosilane **1.19** (Eq. 1.1) can be spun into fibers, which can then be heated in air to create a coating of SiO_2 that prevents melting. Subsequent thermal treatment at 800 °C yields amorphous SiC fibers, and at higher temperatures these are increasingly reinforced and strengthened by the presence of β-SiC crystallites [77]. The key to the success of this process is to use a polymer that, when pyrolyzed, forms the desired ceramic product in high yield, and allows the shape of the precursor polymer to be retained.

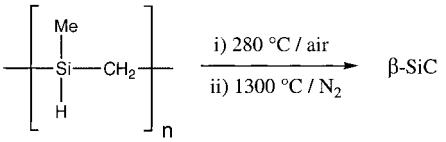

(1.1)

1.19

Transition metal-based polymers might also be expected to function as convenient precursors to metal-containing ceramic films, fibers, and coatings that would have high stability, and desirable/useful electronic or magnetic properties following thermal or photochemical treatment or exposure to ionizing radiation or plasmas. This provides a further motivation for making and studying metal-containing polymeric materials.

1.3.3 Magnetic, Redox, Electronic, and Optical Properties

Carbon atoms strongly prefer a spin-paired, singlet ground state and, as a consequence, the vast majority of organic compounds are diamagnetic. In contrast, transition metals routinely form stable ions in which unpaired electrons are present. Indeed, the existence of cooperative interactions, which allow the alignment of the magnetic moments of transition metal ions in the solid state, forms the basis of the vast array of magnetic materials in applications from computer discs to video tapes. The possibility of accessing polymers that possess magnetic moment alignment, and consequently ferromagnetic, ferrimagnetic, or superparamagnetic properties in the solid state, provides an additional reason for interest in metal-based polymers [36, 79]. Clearly, processable materials of this type would be of considerable interest for many applications. However, the design would have to be intricate. In addition to the presence of cooperative interactions along a linear polymer chain, 3-D cooperative intermolecular interactions between the chains would also need to be present. In the absence of an ordering mechanism, the materials would be paramagnetic and of less interest. Moreover, if the alignment were antiparallel, even less useful antiferromagnetic materials would result [36].

As a consequence of their electronic structure, metal atoms (especially those of transition elements) generally exist in a variety of oxidation states. This can be expected to facilitate access to redox-active materials. In addition, the low electronegativity of transition metal atoms should promote electron mobility and access to interesting charge-transport properties. This is apparent when a metalloid such as silicon or germanium is used to form polymer chains. Thus, whereas polyethylene possesses an essentially localized backbone, polysilanes (**1.3**) and polygermanes (**1.20**) possess σ-delocalized electronic structures, and doping with oxidants allows semiconducting materials ($\sigma > 10^{-5}$ S cm^{-1}) to be obtained, in which holes are the charge carriers [9]. Such unusual characteristics are expected to be further enhanced if even more electropositive metallic elements are used to construct polymer chains. The presence of transition metal centers can also impart interest-

ing photophysical properties [80]. Due to spin-orbit coupling effects, long-lived triplet excited states are often readily accessible and phosphorescence is a well-established and useful phenomenon. Photoinduced charge transfer processes have been well-studied and form the basis for many explorations of the photocatalytic properties of transition metal complexes. Areas such as nonlinear optics and photonics, which require access to processable materials with electron delocalization and polarizability or high refractive indices, may also benefit from the incorporation of metals into polymer structures [80].

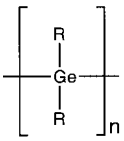

1.20

1.3.4 Catalysis and Bioactivity

The ability of transition metals to bind and activate organic molecules, and to release the transformed organic product with turnover, forms the basis of the vast catalytic chemistry of transition metal complexes [81]. In addition, metal atoms play a key role at the catalytic centers of many enzymes [82]. For example, metalloenzymes participate in hydrolysis, oxidation, reduction, electron-transfer chemistry, and many other remarkable processes such as nitrogen fixation. The long-term development of synthetic polymers that perform catalytic chemistry in a manner analogous to enzymes is a goal of profound interest. The use of a polymer would facilitate product separation and catalyst recycling, particularly if the material were crosslinked and therefore insoluble in the reaction medium. To date, most work has focused on the use of an organic polymer backbone with catalytically active metals bound to ligands in the side-group structure. Problems with this approach have arisen due to leaching of the catalytically active transition metal from the polymer. In addition, in contrast to the situation with enzymes, relatively low activities have often been reported due to the difficulty associated with substrates accessing the catalytic centers. However, recent results have appeared much more promising and improvements in polymer design and synthetic control over the polymer structure offer hope that these deficiencies will be overcome in the future.

Many metal complexes have been shown to possess bioactivity and several drugs based on metal complexes have been developed. These include platinum, gold, and bismuth compounds used in the treatment of certain kinds of cancer, arthritis, and stomach ailments, respectively [82]. The development of analogous polymeric chemotherapeutic materials, that would less easily diffuse through membranes, is also an important objective.

1.3.5
Supramolecular Chemistry and the Development of Hierarchical Structures

Studies of biological systems have revealed that functional structures in Nature generally display hierarchical order in that they are organized over a variety of length scales [46, 82]. For example, hemoglobin, the oxygen-transporting metalloprotein in blood, is a superstructure made up of four subunits, two α- and two β-polypeptide chains, each with an oxygen-binding iron porphyrin group [82]. The overall superstructure, which is illustrated for the carbon monoxide complex carboxyhemoglobin, in which CO is coordinated to iron (Fig. 1.11), can be analyzed in terms of quaternary, tertiary, secondary, and primary structures, which together provide the optimal functioning of the material [83].

A challenge of considerable interest for the future is to learn how to apply self-assembly principles that involve the use of non-covalent interactions, to the generation of new synthetic materials with hierarchical order [46]. To take an illustrative, previously discussed example, monomer molecules can be converted into block copolymer macromolecules (Sect. 1.2.5). These subsequently self-assemble into structures with higher degrees of order, as illustrated by the formation of the various morphologies of phase-separated block copolymers in the solid state (Fig. 1.7) [45, 56]. Exciting general progress is now being made in the synthesis of hierarchical structures. An elegant example is provided by the use of hydrogen-bonding and van der Waals interactions to assemble individual flat poly(benzyl ether) dendrimer arms or "dendrons" into cylindrical columnar assemblies that self-organize into a 2-D hexagonal lattice (Fig. 1.12) [84].

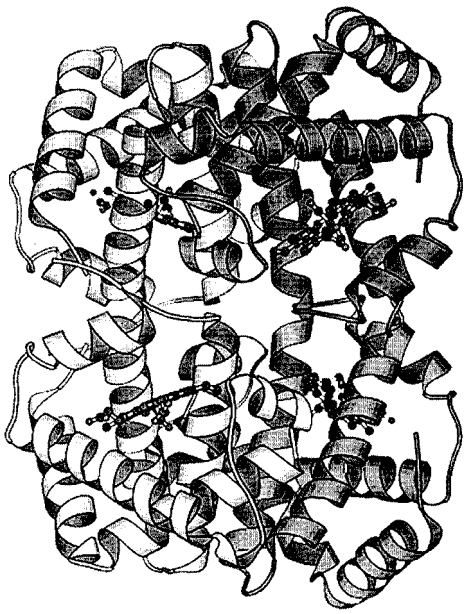

Fig. 1.11 The structure of carboxyhemoglobin (Reproduced from [83]). 4 iron porphyrin centers are present.

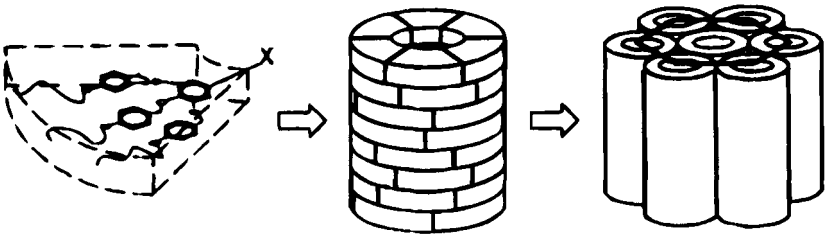

Fig. 1.12 Hierarchical self-assembly of flat monodendrons into cylindrical columnar assemblies that self-organize into a 2-D hexagonal lattice (Reproduced from [84]).

Significantly, the incorporation of transition elements into self-organizing motifs provides additional possibilities for supramolecular chemistry and the properties of the resulting assemblies. For example, as mentioned above, the coordination numbers and geometries accessible with transition metals vary much more widely than with carbon. Applications in the area of liquid-crystalline materials are particularly promising, as an almost unlimited diversity of structure appears possible with metallomesogens [36]. In addition, metallic elements provide new types of "weak" interaction that supplement the well-known hydrogen bonds, which play such a key role in the determination of the 3-D conformational structures of biopolymers such as nucleic acids. For example, unconventional hydrogen (or "hydride-proton") bonds ($H^{\delta-}\cdots H^{\delta+}$) involving electron-rich (e.g. metal hydride) and electron-poor hydrogen substituents have been used to generate novel materials with extended structures in the solid state [85]. Interactions between gold atoms (Au···Au) or "aurophilic bonds" have approximately the same strength as conventional hydrogen bonds, and are a consequence of the relativistic effects that are significant for heavy metal elements. These have also been used to facilitate the formation of remarkable chain and catenane structures [86–88]. In addition, weak coordination bonds between vanadyl groups (V=O···V=O) have been used to generate liquid-crystalline ordering [89]. The exploitation of such interactions at the polymer level, and the development of metallopolymers (e.g. block copolymers) that undergo self-assembly to form metal-containing structures that are ordered on the nanometer scale, is of intense interest. The creation of new types of supramolecular functional materials with a wealth of attractive properties and potential applications that complement those accessible with organic materials is a logical consequence [90].

1.4 Historical Development of Metal-Based Polymer Science

It is both interesting and informative to briefly consider the historical development of the metal-containing polymer field. Without attempting to be exhaustive, a selection of some of the key breakthroughs, with an important influence on the development of the area (see Fig. 1.13), are discussed below.

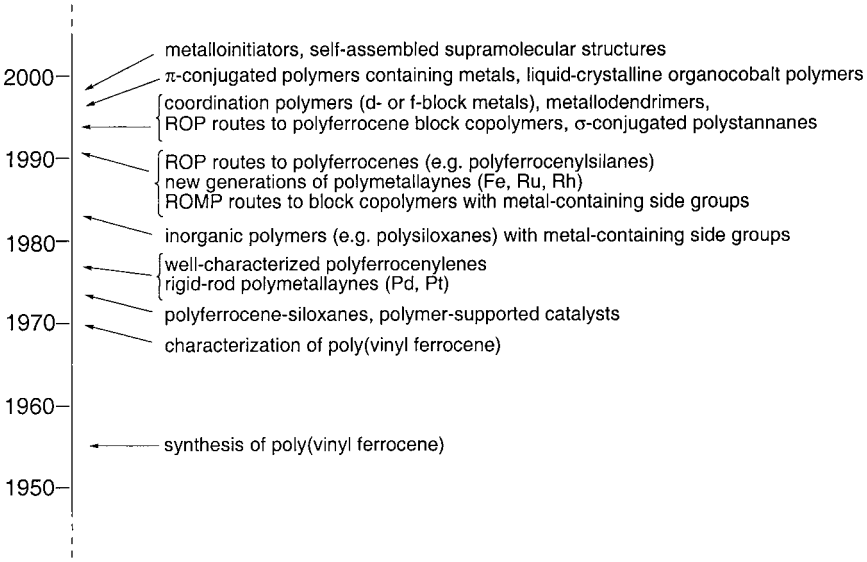

Fig. 1.13 Some key breakthroughs in the field of metal-containing macromolecules.

The birth of polymer science can be traced to the acceptance of Staudinger's hypothesis, that polymeric materials are comprised of long chain macromolecules, in the early 1930s. This led to the rapid subsequent synthetic development of organic polymers and parallel studies of their physical properties. The first soluble metal-containing polymer, poly(vinyl ferrocene) (**1.21**), was prepared by radical polymerization in 1955. With the growing interest in new polymeric materials with novel properties, the 1960s and early 1970s was a time of much activity in the area of metal-containing polymer science. However, few, if any, well-characterized, soluble, high molecular weight materials were actually reported during this period. The first well-characterized polymer of appreciable molecular weight with metal atoms in the main chain, a polyferrocene-siloxane material (**1.22**), was prepared by Pittmann in 1974 by a polycondensation strategy. Noteworthy work by Neuse later in the same decade led to well-characterized but rather low molecular weight polyferrocenylenes (**1.23**). Also in the late 1970s, the first reports of members of the important class of rigid-rod polymetallayne polymers containing Pd and Pt (**1.24**) were made by Hagihara, Takahashi, and Sonogashira [91].

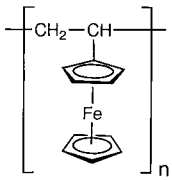

1.21

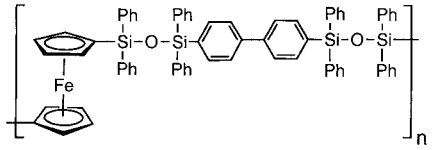

1.22

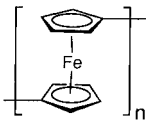

1.23

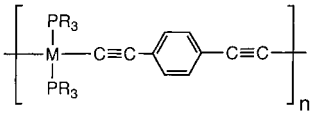

1.24 M = Pd or Pt

A series of important developments in the area of metal-containing polymers occurred in the 1990s as a consequence of a range of key synthetic breakthroughs. For example, ROP routes and ROP-related processes have provided access to polymetallocenes such as polyferrocenylsilanes (**1.25**) and analogues with, for example, disulfido spacers (**1.26**). Also included are main-chain metal-containing polymeric materials with controlled architectures, such as block copolymers [90, 91]. In the early 1990s, homopolymers and block copolymers with metal-containing side groups were also made available by the technique of ring-opening metathesis polymerization (ROMP) [92]. In 1993, transition metal-catalyzed polycondensation strategies yielded the first polystannanes (**1.27**), with main chains consisting of tin atoms, and well-defined organocobalt polymers and coordination polymers (e.g. **1.28**) incorporating a variety of transition metal elements or lanthanide metals were described [90, 91, 93]. Star and dendritic materials containing metal atoms either in the core, at the periphery, or distributed throughout the structure were also described around the same time [94, 95]. An exciting development from the late 1990s involves the creation of metallo-initiators for controlled polymerization reactions that have considerable synthetic potential [96]. An interesting feature of many of the polymers prepared in the late 1990s is the presence of metal atoms as an integral part of the main chains of heteroaromatic π-conjugated polymeric frameworks. These materials (e.g. **1.29**) are the focus of growing interest [97, 98]. Self-assembled and hierarchical structures based on metal-containing polymers, such as liquid crystals, self-assembled block copolymer micelles and superlattices, are also starting to attract intense attention, and this area is set to expand rapidly during the 21st century [90, 99–102].

Full details of these contributions, together with many others of arguably comparable significance, can be found in the subsequent chapters. In the final section of this Introduction, the currently available range of synthetic routes for making polymers with metals in the side-group structure or main chain are reviewed.

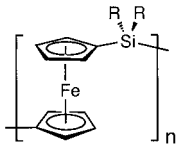

1.25

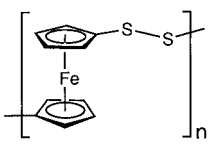

1.26

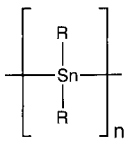

1.27

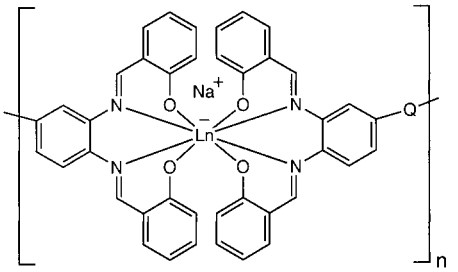

Ln = Eu, La, Gd, Y, Yb

Q = —, CH_2, SO_2

1.28

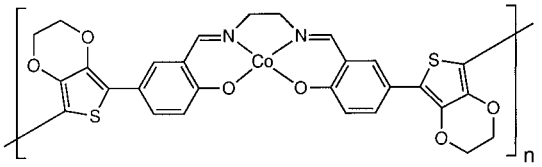

1.29

1.5
Synthetic Routes to Metal-Containing Polymers

1.5.1
The Synthesis of Side-Chain Metal-Containing Polymers

The incorporation of metallic elements into the side-group structure of high molecular weight organic and inorganic polymers has, in general, been well-developed. Such materials are generally accessible by subtle variations of the synthetic methods used to prepare the metal-free materials and can often take advantage of well-established organic functional group chemistry. Representative examples of typical syntheses include the free radical polymerization of vinylcymantrene to yield poly(vinylcymantrene) (**1.30**, Eq. 1.2) [103, 104], and the formation of polysilanes (**1.31**, Eq. 1.3) and polyphosphazenes (**1.32**, Eq. 1.4) with metallocene side groups, by condensation and ring-opening polymerization, respectively [105, 106]. The attachment of organometallic moieties to phosphinated polystyrene (to give **1.33**, Eq. 1.5) and to poly(propyleneimine) dendrimers (to afford **1.34**, Eq. 1.6) provide further examples of successful synthetic strategies [107, 108].

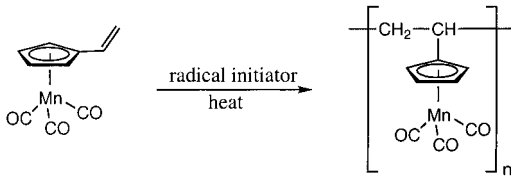

(1.2)

1.30

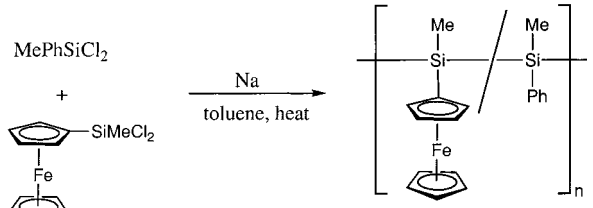

(1.3)

1.31

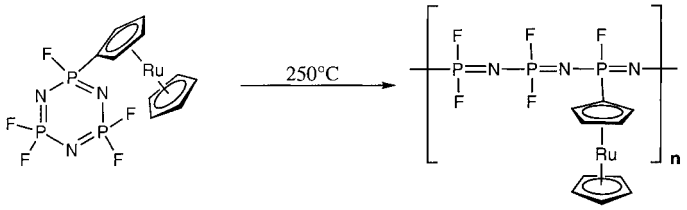

(1.4)

1.32

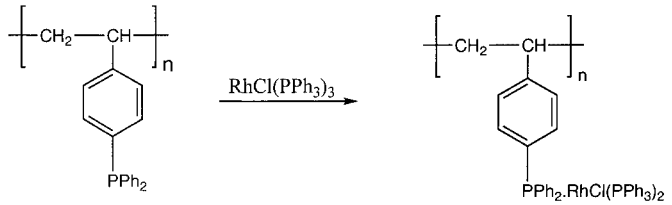

(1.5)

1.33

In certain cases, the presence of the metal-containing moiety can lead to significant restrictions upon the methods of polymerization that can be used. For example, in the case of polysilanes with ferrocene side groups (**1.31**) prepared by Wurtz coupling, it was found that attempts to introduce high loadings of ferrocene were unsuccessful and only relatively low loadings of the organometallic moiety were found to be achievable [105].

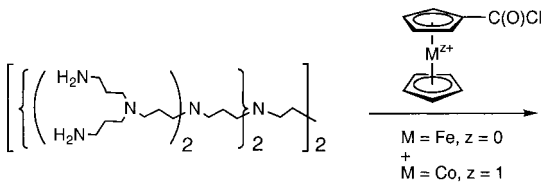

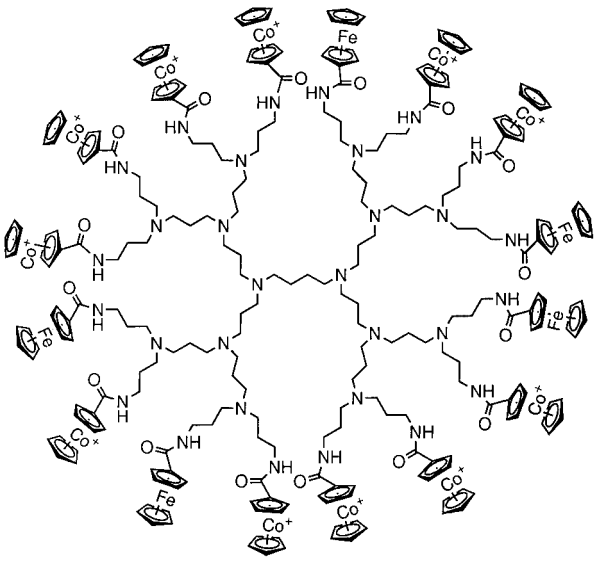

1.34

(1.6)

1.5.2
Main-Chain Metal-Containing Polymers

1.5.2.1 **Why are Transition Metals in the Polymer Main Chain Desirable?**

For many applications, side-chain metal-containing polymers are sufficient. However, to access the most profound alterations in polymer properties that arise from the presence of metal atoms in a polymer structure, incorporation in the main chain is required. Potential advantages of including metals in the backbone of a polymer rather than in the side-group structure include the following:

1. The influence of the varied geometries of transition metal centers on the conformational and thermophysical properties would be more significant.
2. The development of materials with properties that depend on the ability of the metal atoms to interact with one another in a controlled manner would be facilitated, as smaller changes in M · · · M distance accompany backbone motions compared to those of side groups.

3. Access to interesting charge-transport properties and other characteristics that depend on delocalization effects would be favored as the metal could potentially be placed directly in the conjugation pathway.
4. Leaching of the metal from the polymer would be expected to be less problematic and this might be significant for catalytic or preceramic applications.

Unfortunately, compared to side-chain metallopolymers, the synthesis of main-chain metal-containing polymers is much less developed, although significant progress has been made over the last two decades of the 20th century. In short, the construction of long chains containing metal atoms represents a challenging synthetic problem. Moreover, very significantly, the synthetic problem becomes ever more challenging as the distance between the metal atoms in the backbone of the prospective polymeric material decreases and, consequently, the degree of "metallization" becomes more substantial and the possibility for interesting metal-metal interactions is enhanced.

1.5.2.2 **The Synthesis of Main-Chain Metal-Containing Polymers**

Consideration of the main synthetic routes to organic polymers illustrates the problems associated with the synthesis of main-chain metal-containing polymers (see Scheme 1.1). There are two main methods of polymer synthesis – *chain-growth polymerizations* and *step-growth polymerizations* [7]. Chain-growth processes involve initiation, propagation and, usually, termination and chain-transfer steps. Very significantly, the presence of reactive intermediates (radicals, cations, anions, organometallic species, etc.) that react rapidly with monomer molecules in an efficient propagation step, generally allows the facile formation of high molecular weight polymeric materials. Indeed, a usual characteristic of this type of polymerization is that a high molecular weight polymer is formed even at low monomer conversion. In contrast, in step-growth polymerizations, the reaction intermediates are of comparable reactivity to the monomers, and the generation of high molecular weight materials requires stringently accurate reaction stoichiometry and ca. 100% monomer conversion [7].

1.5.2.2.1 **Addition Polymerization**

Addition polymerization of unsaturated organic molecules (α-alkenes, acetylenes, isonitriles, etc.) provides a versatile and industrially important route to many organic polymers. Such processes have as their thermodynamic driving force the conversion of π-bonds into new and more stable σ-bonds and proceed by a chain-growth mechanism that involves radicals, anions, cations or other reactive species as intermediates. However, analogous polymerizations are very difficult to use for the synthesis of metal-containing polymers, as suitably reactive but stable multiple bonds involving metallic elements are relatively difficult to prepare. In contrast to the situation for organic molecules, the isolation of stable species with multiple bonds that involve metallic elements usually requires the presence of sterically demanding, oligomerization-inhibiting ancillary ligation. Although the

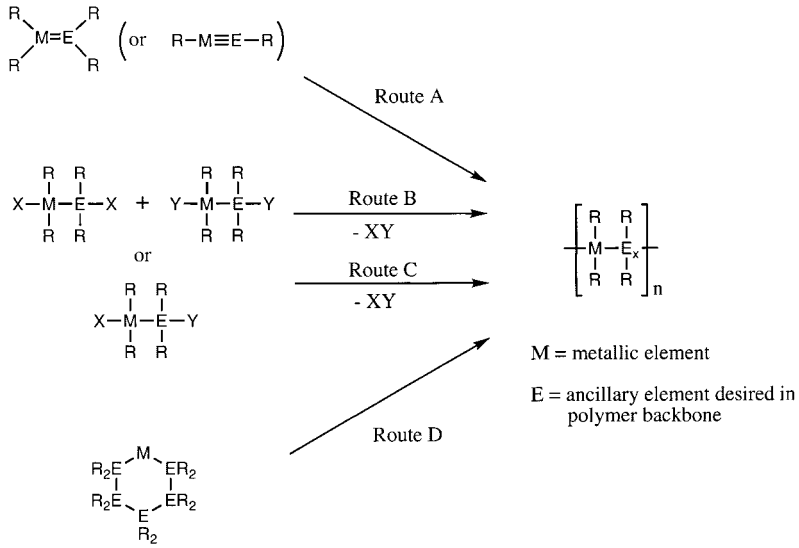

Scheme 1.1

addition polymerization of examples of these materials is of great potential interest (Scheme 1.1, Route A), such chemistry is virtually unexplored and very few studies have been reported. In the case of species such as $[Cl_3M \equiv N]_\infty$ (M = Mo or W), with metal-nitrogen multiple bonds, individual monomers (**1.35**) seem to be preferred, as attempted dissolution of solid-state materials (**1.36**) that contain extended M–N chains leads to depolymerization (Eq. 1.7). The structures of the latter materials have been analyzed by single-crystal X-ray diffraction and show the presence of alternating strong (effectively triple) and very weak (< single) bonds in the metal-containing chains [109, 110]. Similar features have been observed for analogous vanadium systems $[Cl_2L_2V \equiv N]_\infty$ (L_2 = diimine) [111].

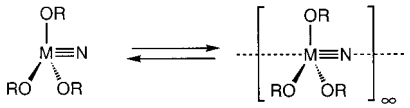

1.35 solution ⇌ **1.36** solid state (1.7)

1.5.2.2.2 **Polycondensations**

Early attempts to prepare main-chain metal-containing polymers mainly focused on the use of step-growth polycondensation processes (Scheme 1.1, Route B). These routes work well for the synthesis of carbon-based polymers when difunctional organic monomers are used because the latter are generally easily accessible in a high degree of purity. This allows the stringent stoichiometry and conver-

sion requirements that need to be fulfilled for the formation of high molecular weight polymers by step-growth polycondensation reactions to be satisfied. This type of methodology also works reasonably well if the metal atoms desired in the polymer backbone are well-spaced. In such cases, organic functional group chemistry can be used to successfully couple the monomers, provided that the synthetic transformations are compatible with the stability of the metal center. However, severe problems arise when polymeric materials with main-chain metal atoms in close proximity are desired. In these cases, the functional group chemistry needed for efficient monomer coupling is poorly developed and difunctional metal-containing monomers (dilithiated species, for example) are often so reactive that they are difficult to prepare and purify. Thus, in many cases, exact reactant stoichiometries for polycondensation reactions cannot be achieved. This generally results in the formation of low molecular weight oligomeric products that are well below the critical entanglement molecular weight necessary for the formation of fabricated materials (e.g. free-standing films, fibers, etc.) with reasonable mechanical strengths (see Sect. 1.2.3).

To appreciate the requirements for accessing high molecular weight polymers by step-growth polycondensation reactions, a more detailed discussion is desirable. To access substantial molecular weights (M_n > ca. 10,000) using a polycondensation of two difunctional monomers (Eq. 1.8), two stringent criteria need to be satisfied. First, exact reaction stoichiometries are required (i.e. the functional groups must be present in equal amounts) and second, high conversions are necessary (i.e. the extent of reaction must be virtually 100%).

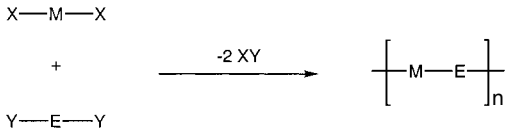

(1.8)

The dramatic influence that these two "stoichiometry" and "conversion" factors can have on molecular weight cannot be overemphasized, and can be explained in terms of the classic theory of polycondensation reactions developed by Carothers [7, 40]. Based on this theory, the *number average degree of polymerization* DP_n (i.e. the value of M_n divided by the molecular weight of a repeat unit) is given by the expression in Eq. 1.9.

$$DP_n = \frac{1 + r}{1 + r - 2rp} \tag{1.9}$$

DP_n = number average degree of polymerization
r = stoichiometric ratio of functional groups X and Y present
p = extent of reaction (the fraction of functional groups that have reacted)

Thus, high values of DP_n (i.e. high molecular weights) result when the stoichiometric ratio r and extent of reaction p have values close to unity. The "stoichiom-

etry" criterion is not normally a problem in organic polycondensation reactions as the difunctional monomers are usually easy to prepare and purify. However, the "conversion" criterion often presents a challenge and reactions must be driven to completion by, for example, the removal of a volatile small molecule product if high molecular weight polymers are to be generated. For metal-containing monomers the opposite is usually true. Reactions generally proceed to close to 100% completion (i.e., $p=1$) but, as mentioned above, difunctional, metal-containing (and, in general, inorganic) monomers are often highly reactive, and are therefore difficult to purify completely, or have poorly defined structures. This makes it very difficult to achieve values of the stoichiometric ratio r close to unity. This can be appreciated by a consideration of the limiting case of Eq. 1.9 when $p=1$ (Eq. 1.10).

$$\text{If} \quad p = 1 \qquad DP_n = \frac{(1+r)}{(1-r)} \tag{1.10}$$

The equation indicates that even if a reaction proceeds to 100% completion (i.e. if the conversion criterion is satisfied perfectly and $p=1$), the ratio of the pure difunctional monomers must still be 0.98 : 1.00 or better (i.e. $r>0.98$) if values of M_n of 10,000 or greater are to be obtained. This calculation assumes that a monomer unit has a molecular weight of 100. Values of DP_n as a function of r for cases where $p=1$ are shown in Table 1.1 and illustrate the dramatic tail-off in DP_n and M_n as the stoichiometric ratio r deviates further from unity.

Although the above considerations help to explain many of the failures to prepare high molecular weight metal-containing polymers by condensation routes in the 1960s and 1970s, highly efficient coupling procedures have been developed more recently, and these have contributed significantly to the renaissance of metal-based polymer science. An early example of the progress in this area is provided by the synthesis of rigid-rod organometallic polymers in the late 1970's; these fascinating polymers are discussed in detail in Chapter 5. Well-defined and efficient routes have also been used to prepare coordination polymers (e.g. **1.37**, Eq. 1.11). Metal-catalyzed coupling procedures of high efficiency have also been utilized to prepare polymers containing cyclobutadiene cobalt units (e.g. **1.38**, Eq. 1.12) [112, 113].

Table 1.1 Values of DP_n and M_n corresponding to different values of r in Eq. 1.10 for a hypothetical monomer of molecular weight 100

r	DP_n	M_n
1.00	∞	∞
0.99	199	19,900
0.98	99	9,900
0.97	66	6,600
0.96	49	4,900
0.95	39	3,900
0.90	19	1,900

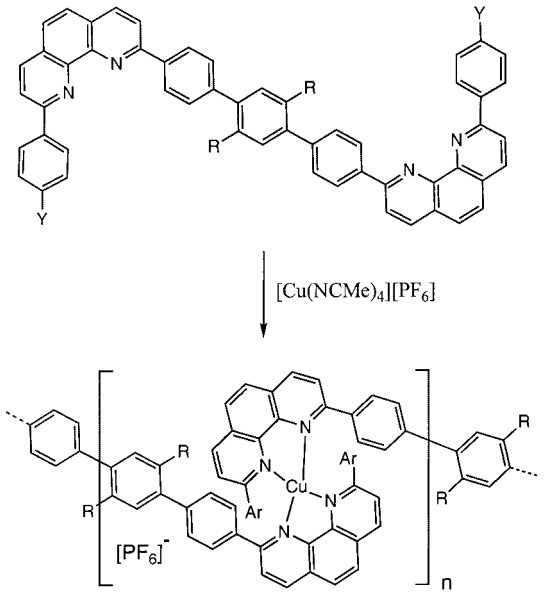

(1.11)

1.37

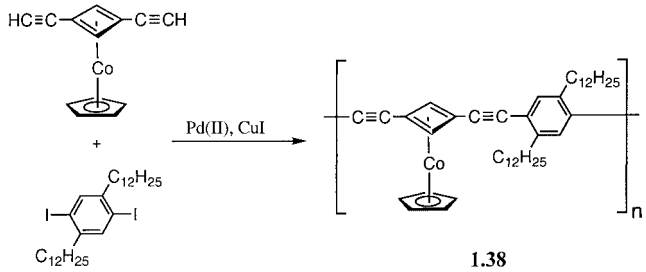

(1.12)

1.38

A very promising variant on this type of condensation polymerization involves the use of monomers that possess groups X and Y, which can be eliminated from the same molecule. This circumvents the need for careful control of reaction stoichiometry. Moreover, in certain cases, polymerization of monomers of this type can follow a chain-growth type of mechanism that leads to high molecular weights much more easily. Such processes (Scheme 1.1, Route C) have not yet been explored for the formation of metal-containing polymers, but are well-established for the synthesis of certain classes of polymers based on main-group elements such as polyphosphazenes (**1.2**) and polyoxothiazenes (**1.4**) [12, 16, 26].

1.5.2.2.3 **Ring-Opening Polymerization (ROP)**

A further common and important route to organic polymers involves ROP, and this methodology is used industrially to prepare nylon-6 and poly(ethylene oxide). In the vast majority of cases, the presence of ring strain provides the thermodynamic driving force for the ROP process [7]. Most examples of ROP proceed by a chain-growth route. Indeed, the discovery of ROP routes to polycarbonates and other materials has the advantage of providing access to polymers of more substantial molecular weights than those typically available by polycondensation [7].

Metal-containing rings are relatively well-known, but few have been studied with respect to their polymerization behavior. Nevertheless, in the last decade, a range of examples of successful ROP processes (Scheme 1.1, Route D) have been described for ferrocenophanes and related derivatives, and this has provided access to high molecular weight main-chain polymetallocenes. Thermal and transition metal-catalyzed ROP and metal-catalyzed ring-opening metathesis polymerization (ROMP) processes have been reported for metallocenophanes and yield ring-opened polymers (e.g. **1.39**, Eq. 1.13 and **1.40**, Eq. 1.14) [114, 115]. Several examples of living polymerizations have been achieved by the treatment of [1]ferrocenophanes with anionic initiators. No appreciable termination or chain transfer is observed and the resulting polymer chains have a very narrow molecular weight distribution ($M_w/M_n \approx 1$) [7]. The living nature of the ROP process allows the sequential polymerization of different monomers, and thereby provides access to block copolymers and other controlled architectures. For example, treatment of phosphorus-bridged [1]ferrocenophane **1.41** with BuLi yields the living anionic polymer **1.42**, which reacts with silicon-bridged [1]ferrocenophane **1.43** to yield the living block copolymer **1.44** and the polyferrocenylphosphine-*b*-polyferrocenylsilane block copolymer **1.45**, with a narrow polydispersity, upon hydrolytic work-up (Eq. 1.15) [116].

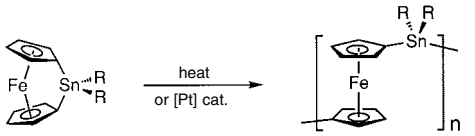

(1.13)

1.39

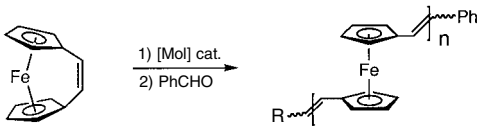

(1.14)

1.40

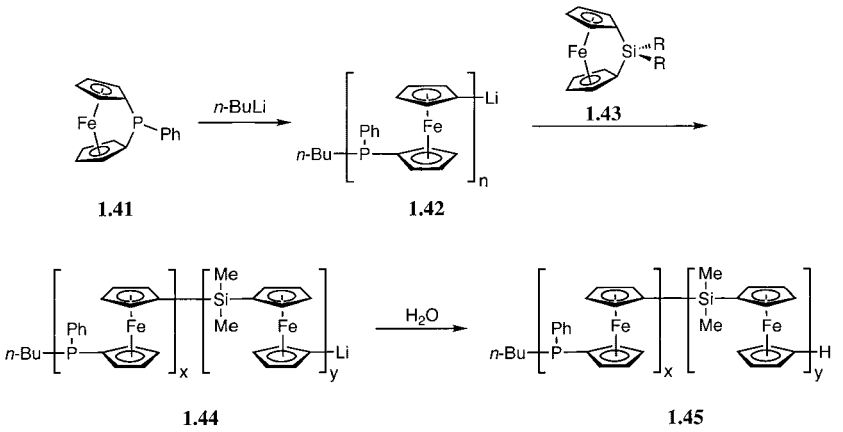

(1.15)

This survey of synthetic routes to metallopolymers completes the discussion of introductory topics in this chapter. In the following chapters, the main classes of metal-containing polymers will be discussed, with emphasis not only on synthetic details, but also on their properties and applications. The general philosophy will be to focus on well-characterized and well-studied materials which are truly polymeric in nature ($M_n > 10{,}000$, see section 1.2.3) rather than to exhaustively discuss every metallopolymer mentioned in the literature. Particular attention is given to examples where studies of properties and potential functions have been performed.

1.6 References

1 J. Alper, G.L. Nelson, *Polymeric Materials: Chemistry for the Future*, ACS, Washington DC, **1989**.

2 *Polymer Science and Engineering: The Shifting Research Frontiers*, National Research Council, National Academy Press, **1994**.

3 J.H. Burroughes, D.D.C. Bradley, A.R. Brown, R.N. Marks, K. Mackay, R.H. Friend, P.L. Burns, A.B. Holmes, *Nature* **1990**, *347*, 539.

4 See reviews reproduced from Nobel Lectures: (a) H. Shirakawa, *Angew. Chem. Int. Ed.* **2001**, *40*, 2574; (b) A.G. MacDiarmid, *Angew. Chem. Int. Ed.* **2001**, *40*, 2581; (c) A.J. Heeger, *Angew. Chem. Int. Ed.* **2001**, *40*, 2591.

5 Review: A. Kraft, A.C. Grimsdale, A.B. Holmes, *Angew. Chem. Int. Ed.* **1998**, *37*, 402.

6 Review: J. Roncali, *Chem. Rev.* **1997**, 97, 173.

7 G. Odian, *Principles of Polymerization, 3rd ed.*, Wiley-Interscience, New York, **1991**.

8 Review: I. Manners, *Angew. Chem. Int. Ed. Engl.* **1996**, *35*, 1602.

9 J.E. Mark, H.R. Allcock, R. West, *Inorganic Polymers*, Prentice Hall, Englewood Cliffs, NJ, **1992**.

10 *Siloxane Polymers* (Eds.: S.J. Clarson, J.A. Semlyen), Prentice Hall, Englewood Cliffs, NJ, **1993**.

11 Review: H.R. Allcock, *Adv. Mater.* **1994**, *6*, 106.

12 Review: R.H. Neilson, P. Wisian-Neilson, *Chem. Rev.* **1988**, *88*, 541.

13 Review: R. De Jaeger, M. Gleria, *Prog. Polym. Sci.* **1998**, *23*, 179.

14 Review: R. West, *J. Organomet. Chem.* **1986**, *300*, 327.

15 Review: R. D. Miller, J. Michl, *Chem. Rev.* **1989**, *89*, 1359.
16 C. H. Honeyman, I. Manners, C. T. Morrissey, H. R. Allcock, *J. Am. Chem. Soc.* **1995**, *117*, 7035.
17 R. A. Montague, K. Matyjaszewski, *J. Am. Chem. Soc.* **1990**, *112*, 6721.
18 C. T. Aitken, J. F. Harrod, E. Samuel, *J. Am. Chem. Soc.* **1986**, *108*, 4059.
19 T. D. Tilley, *Acc. Chem. Res.* **1993**, *26*, 22.
20 M. Cypryk, Y. Gupta, K. Matyjaszewski, *J. Am. Chem. Soc.* **1991**, *113*, 1046.
21 K. Sakamoto, K. Obata, H. Hirata, M. Nakajima, H. Sakurai, *J. Am. Chem. Soc.* **1989**, *111*, 7641.
22 Y. Li, Y. Kawakami, *Macromolecules* **1999**, *32*, 6871.
23 R. Zhang, J. E. Mark, A. R. Pinhas, *Macromolecules* **2000**, *33*, 3508.
24 S. M. Katz, J. A. Reichl, D. H. Berry, *J. Am. Chem. Soc.* **1998**, *120*, 9844.
25 P. A. Bianconi, T. W. Weidman, *J. Am. Chem. Soc.* **1988**, *110*, 2342.
26 A. K. Roy, G. T. Burns, G. C. Lie, S. Grigoras, *J. Am. Chem. Soc.* **1993**, *115*, 2604.
27 M. Liang, I. Manners, *J. Am. Chem. Soc.* **1991**, *113*, 4044.
28 A. R. McWilliams, D. P. Gates, M. Edwards, L. M. Liable-Sands, I. Guzei, A. L. Rheingold, I. Manners, *J. Am. Chem. Soc.* **2000**, *122*, 8848.
29 V. Chunechom, T. E. Vidal, H. Adams, M. L. Turner, *Angew. Chem. Int. Ed.* **1998**, *37*, 1928.
30 H. Dorn, R. A. Singh, J. A. Massey, J. M. Nelson, C. A. Jaska, A. J. Lough, I. Manners, *J. Am. Chem. Soc.* **2000**, *122*, 6669.
31 P. J. Fazen, J. S. Beck, A. T. Lynch, E. E. Remsen, L. G. Sneddon, *Chem. Mater.* **1990**, *2*, 96.
32 N. Matsumi, T. Umeyama, Y. Chujo, *Macromolecules* **2001**, *34*, 3510.
33 Review: H. H. Brintzinger, D. Fischer, R. Mülhaupt, B. Rieger, R. M. Waymouth, *Angew. Chem. Int. Ed. Engl.* **1995**, *34*, 1143.
34 L. Smart, E. Moore, *Solid State Chemistry, An Introduction*, Chapman Hall, London, **1995**.
35 P. A. Cox, *Electronic Structure and Chemistry of Solids*, Oxford University Press, Oxford, **1987**.
36 *Inorganic Materials, 2nd ed.*, (Eds.: D. W. Bruce, D. O'Hare), John Wiley & Sons, Toronto, **1996**.
37 (a) S. L. Rosen, *Fundamental Principles of Polymeric Materials, 2nd ed.*, Wiley Interscience, New York, **1993**.
(b) P. C. Painter, M. M. Coleman, *Fundamentals of Polymer Science, 2nd ed.*, Technomic, Lancaster, PA, **1997**.
38 B. M. Novak, *Organic Polymer Chemistry: A Primer*, Saunders, New York, **1995**.
39 L. H. Sperling, *Introduction to Physical Polymer Science*, John Wiley & Sons, New York, **2001**.
40 R. J. Young, P. A. Lovell, *Introduction to Polymers, 2nd ed.*, Chapman & Hall, New York, **1991**.
41 H. R. Allcock, F. W. Lampe, J. E. Mark, *Contemporary Polymer Chemistry*, Prentice Hall, Englewood Cliffs, NJ, **2003**.
42 I. M. Campbell, *Introduction to Synthetic Polymers, 2nd ed.*, Oxford Science University Press, New York, **2000**.
43 A. E. Woodward, *Understanding Polymer Morphology*, Hanser, New York, **1995**.
44 H. Finkelmann, *Angew. Chem. Int. Ed. Engl.* **1987**, *26*, 816.
45 I. W. Hamley, *The Physics of Block Copolymers*, Oxford University Press, New York, **1998**.
46 (a) M. Antonietti, C. Göltner, *Angew. Chem. Int. Ed. Engl.* **1997**, *36*, 910; (b) S. Förster, M. Antonietti, *Adv. Mater.* **1998**, *10*, 195.
47 L. Zhang, A. Eisenberg, *Science* **1995**, *268*, 1728.
48 L. Zhang, A. Eisenberg, *J. Am. Chem. Soc.* **1996**, *118*, 3168.
49 J. P. Spatz, S. Mössmer, M. Möller, *Angew. Chem. Int. Ed. Engl.* **1996**, *35*, 1510.
50 G. Liu, *Adv. Mater.* **1997**, *9*, 437.
51 G. Liu, J. Ding, *Adv. Mater.* **1998**, *10*, 69.
52 K. L. Wooley, *Chem. Eur. J.* **1997**, *3*, 1397.
53 Y.-Y. Won, H. T. Davis, F. S. Bates, *Science* **1999**, *283*, 960.
54 V. Bütün, A. B. Lowe, N. C. Billingham, S. P. Armes, *J. Am. Chem. Soc.* **1999**, *121*, 4288.
55 R. Erhardt, A. Böker, H. Zettl, H. Kaya, W. Pyckhout-Hintzen, G. Krausch, V. Abetz, A. H. E. Müller, *Macromolecules* **2001**, *34*, 1069.
56 F. S. Bates, *Science* **1991**, *251*, 898.

57 M. Park, C. Harrison, P.M. Chaikin, R.A. Register, D.H. Adamson, *Science* **1997**, *276*, 1401.

58 J.P. Spatz, P. Eibeck, S. Mössmer, M. Möller, T. Herzog, P. Ziemann, *Adv. Mater.* **1998**, *10*, 849.

59 V.Z.-H. Chan, J. Hoffman, V.Y. Lee, H. Iatrou, A. Avgeropoulos, N. Hadjichristidis, R.D. Miller, E.L. Thomas, *Science* **1999**, *286*, 1716.

60 T. Thurn-Albrecht, R. Steiner, J. DeRouchey, C.M. Stafford, E. Huang, M. Bal, M. Tuominen, C.J. Hawker, T.P. Russell, *Adv. Mater.* **2000**, *12*, 787.

61 A.C. Edrington, A.M. Urbas, P. DeRege, C.X. Chen, T.M. Swager, N. Hadjichristidis, M. Xenidou, L.J. Fetters, J.D. Joannopoulos, Y. Fink, E.L. Thomas, *Adv. Mater.* **2001**, *13*, 421.

62 R. Ulrich, A. Du Chesne, M. Templin, U. Wiesner, *Adv. Mater.* **1999**, *11*, 141.

63 D.A. Tomalia, A.M. Naylor, W.A. Goddard III, *Angew. Chem. Int. Ed. Engl.* **1990**, *29*, 138.

64 D.A. Tomalia, *Sci. Am.* **1995**, *272*, 62.

65 M. Fischer, F. Vögtle, *Angew. Chem. Int. Ed.* **1999**, *38*, 884.

66 G.R. Newkome, C.N. Moorefield, F. Vögtle, *Dendritic Molecules: Concepts, Synthesis, Perspectives*, VCH, Weinheim, **1996**.

67 T.M. Miller, T.X. Neenan, *Chem. Mater.* **1990**, *2*, 346.

68 C.J. Hawker, J.M.J. Fréchet, *J. Am. Chem. Soc.* **1990**, *112*, 7638.

69 J.F.G.A. Jansen, E.M.M. de Brabander-van den Berg, E.W. Meijer, *Science* **1994**, *266*, 1226.

70 A. Sunder, J. Heinemann, H. Frey, *Chem. Eur. J.* **2000**, *6*, 2499.

71 Q.T. Zhang, J.M. Tour, *J. Am. Chem. Soc.* **1998**, *120*, 5355.

72 F.A. Cotton, G. Wilkinson, C.A. Murillo, M. Bochman, *Advanced Inorganic Chemistry*, 6th ed., Wiley Interscience, Toronto, **1999**.

73 Review: H.-P. Baldus, M. Jansen, *Angew. Chem. Int. Ed. Engl.* **1997**, *36*, 328.

74 Review: J. Bill, F. Aldinger, *Adv. Mater.* **1995**, *7*, 775.

75 D. Segal, *Chemical Synthesis of Advanced Ceramic Materials*, Cambridge University Press, New York, **1991**.

76 Review: M. Peuckert, T. Vaahs, M. Brück, *Adv. Mater.* **1990**, *2*, 398.

77 Review: R.M. Laine, F. Babonneau, *Chem. Mater.* **1993**, *5*, 260.

78 Q. Liu, W. Shi, F. Babonneau, L.V. Interrante, *Chem. Mater.* **1997**, *9*, 2434.

79 Review: D.L. Leslie-Pelecky, R.D. Rieke, *Chem.* Mater. **1996**, *8*, 1770.

80 Reviews: (a) N.J. Long, *Angew. Chem. Int. Ed. Engl.* **1995**, *34*, 21; (b) I.R. Whittall, A.M. McDonagh, M.G. Humphrey, M. Samoc, *Adv. Organomet. Chem.* **1998**, *42*, 291; (c) I.R. Whittall, A.M. McDonagh, M.G. Humphrey, M. Samoc, *Adv. Organomet. Chem.* **1998**, *43*, 349; (d) J.R. Lakowicz, *Principles of Fluorescence Spectroscopy, 2nd ed.*, Kluwer, London, **1999**, p 573–594.

81 R.H. Crabtree, *The Organometallic Chemistry of the Transition Metals*, 3rd ed., Wiley and Sons, New York, **2001**.

82 S.J. Lippard, J.M. Berg, *Principles of Bioinorganic Chemistry*, University Science, Mill Valley, **1994**.

83 http://metallo.scripps.edu/PROMISE/MAIN.html

84 V. Percec, W.-D. Cho, P.E. Mosier, G. Ungar, D.J.P. Yeardley, *J. Am. Chem. Soc.* **1998**, *120*, 11061.

85 (a) K. Abdur-Rashid, D.G. Gusev, S.E. Landau, A.J. Lough, R.H. Morris, *J. Am. Chem. Soc.* **1998**, *120*, 11826. (b) R.H. Crabtree, P.E.M. Siegbahn, O. Eisenstein, A.L. Rheingold, T.F. Koetzle, *Acc. Chem. Res.* **1996**, *29*, 348.

86 C.P. McArdle, J.J. Vittal, R.J. Puddephatt, *Angew. Chem. Int. Ed.* **2000**, *39*, 3819.

87 R.E. Bachman, M.S. Fioritto, S.K. Fetics, T.M. Cocker, *J. Am. Chem. Soc.* **2001**, *123*, 5376.

88 M.M. Olmstead, F. Jiang, S. Attar, A.L. Balch, *J. Am. Chem. Soc.* **2001**, *123*, 3260.

89 H. Zheng, C.K. Lai, T.M. Swager, *Chem. Mater.* **1995**, *7*, 2067.

90 I. Manners, *Science* **2001**, *294*, 1664.

91 Review: P. Nguyen, P. Gómez-Elipe, I. Manners, *Chem. Rev.* **1999**, *99*, 1515.

92 V. Sankaran, J. Yue, R.E. Cohen, R.R. Schrock, R.J. Silbey, *Chem. Mater.* **1993**, *5*, 1133.

2
Side-Chain Metal-Containing Polymers

2.1
Introduction

Polymers with metal-containing groups in the side-chain structure have the longest history of any of the various classes of metal-containing macromolecules. The first example, poly(vinylferrocene), was briefly described in 1955 [1]. Since that time, a variety of side-chain polymeric materials have been prepared, containing either main group metals or transition elements. This chapter surveys the synthesis and properties of some of the most interesting, well-characterized materials. In addition, possible applications of the side-chain metal-containing polymers as electrode mediators, liquid-crystalline materials, charge-transport materials, and as components of electronic devices such as diodes and sensors, in luminescent devices, and as catalytic and bioactive materials, are discussed.

2.2
Side-Chain Polymetallocene Homopolymers and Block Copolymers

2.2.1
Organic Polymers with Metallocene Side Groups

2.2.1.1 Poly(vinylferrocene)

Since the discovery and elucidation of the structure of ferrocene **2.1** in the early 1950s [2], this fascinating species has been a continual source of intrigue for chemists [3, 4]. In addition to possessing a vast organic chemistry (involving, e.g., electrophilic substitution reactions), this prototypical, amber-colored 18-electron metallocene also undergoes reversible one-electron oxidation to the 17-electron blue ferrocenium ion **2.2** (Eq. 2.1). Importantly, ferrocene is easy to prepare, cheap, commercially available, and air-, moisture-, and thermally stable [3]. Based on these considerations it is not surprising that the possibility of obtaining ferrocene-based polymeric materials, whereby the unique physical and chemical features of this organometallic species are combined with the facile processability of high molecular weight polymers, has attracted intense interest [5, 6].

Synthetic Metal-Containing Polymers. Ian Manners

ISBN: 3-527-29463-5

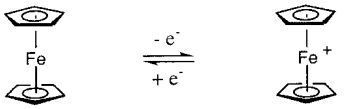

2.1 2.2 (2.1)

Radical-initiated polymerization of vinylferrocene [1] (**2.3**) to give poly(vinylferrocene) (**2.4**) was first conducted shortly after the discovery of ferrocene, and this method has been reinvestigated many times in subsequent years (Eq. 2.2) [7–12]. Detailed characterization of this polymeric organometallic material was first reported in 1970 [13]. The initiator normally used to prepare poly(vinylferrocene) is azobis(isobutyronitrile) (AIBN), as peroxide initiators tend to oxidize the Fe center in the monomer. Molecular weights are typically less than 10,000, but the synthesis of polymers with $M_w > 10^5$ (PDI > 1.3) using this route has been reported. However, these higher molecular weight samples often possess a multimodal weight distribution [10]. It has been reported that the molecular weight of poly(vinylferrocene) does not increase with a decrease in initiator concentration [10]. This was attributed to the high tendency for chain transfer with vinylferrocene in comparison to other vinyl monomers such as styrene [10]. Vinylferrocene can be copolymerized with other vinyl monomers such as styrene, methyl methacrylate, and acrylonitrile, and the relative reactivity ratios for the monomers in these systems have been determined [7–9].

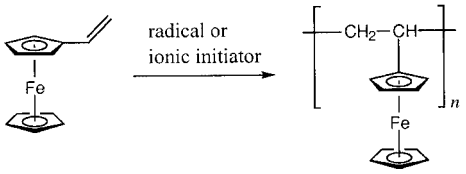

2.3 2.4 (2.2)

Cationic initiation and Ziegler-Natta methods have also been employed successfully in order to obtain poly(vinylferrocene) [14]. Due to the electron-donating nature of a ferrocene substituent, it was initially believed that anionic initiators would not be able to induce the polymerization of vinylferrocene. However, in the early 1990s, living anionic polymerization of vinylferrocene in solution was achieved at low temperatures (–70 °C to –30 °C) in THF using alkyllithium initiators [15]. Block copolymers of poly(vinylferrocene) with poly(methyl methacrylate), PVFc-*b*-PMMA (**2.5**) or polystyrene, PVFc-*b*-PS, as coblocks were also reported (Scheme 2.1) [15].

Considerable effort has been invested in studies of the properties of poly(vinylferrocene), a yellow powder that is stable in air in the solid state. The material is also soluble in most common, moderately polar, organic solvents and the resulting solutions are usually stable to air. Poly(vinylferrocene) has been studied in solution, and THF was found to be a good solvent for this material and

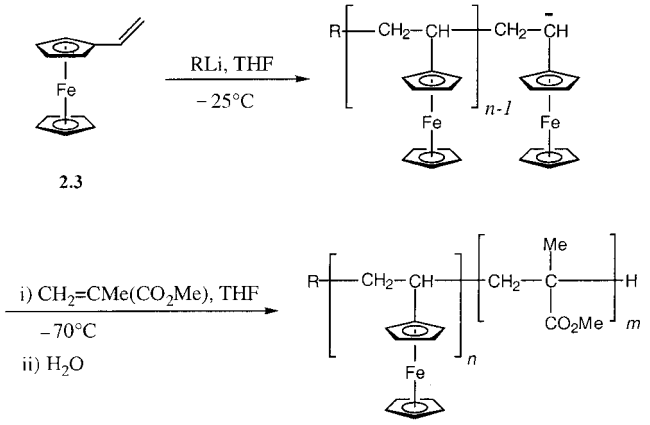

2.3

PVFc-*b*-PMMA

2.5 **Scheme 2.1**

diethyl ether a marginal one [10]. However, in chlorinated solvents, the polymer is reported to be unstable, and a green precipitate is formed after a few weeks in air. The precipitate is believed to be ionic in nature and to contain ferrocenium units. Of probable relevance to this observation is a report that photolysis of a solution of poly(vinylferrocene) in CCl_4 leads to oxidation of the ferrocene groups, as shown in Eq. 2.3 [10].

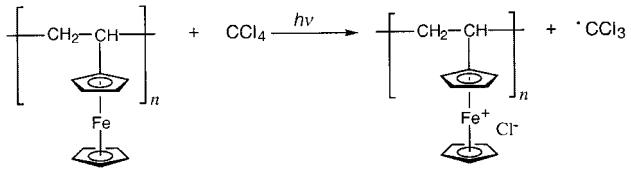

2.4 (2.3)

The λ_{max} for the low-energy d-d transition in poly(vinylferrocene) in the visible region (in CH_2Cl_2) occurs at 440 nm, as determined by UV/vis spectroscopy, a wavelength similar to that observed for unsubstituted ferrocene itself. The IR spectrum of poly(vinylferrocene) shows peaks consistent with a monoalkyl ferrocene, and the ^{57}Fe Mössbauer spectrum exhibits a doublet with an isomer shift of 0.78 mm s^{-1} and a quadrupole splitting of 2.44 mm s^{-1} [10, 13]. The glass transition temperature has been assigned as 190 °C by DSC [10, 13] and a melting point of ca. 280 °C has been reported [1], but other studies of the microstructure and morphology of this material indicate that the polymer is amorphous [16]. More extensive investigations of the physical properties of poly(vinylferrocene) have indicated a T_g of 222 °C for higher molecular weight samples [12, 15].

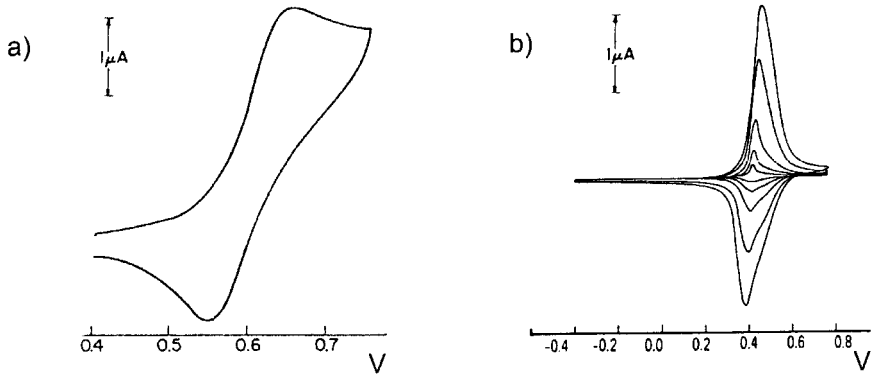

Fig. 2.1 Cyclic voltammograms for poly(vinylferrocene): (**a**) in hexamethylphosphoramide/0.1 M $[Et_4N][BF_4]$, (**b**) as a thin film on Pt (various scan rates). Potentials are *vs.* standard calomel electrode. (Adapted from (**a**) [17] and (**b**) [18b])

Much of the interest in poly(vinylferrocene) arises from the presence of redox-active iron sites attached to the polymer chain. Cyclic voltammetry experiments [17, 18] have revealed that the iron sites are non-interacting, as a single reversible oxidation wave is observed as the iron centers interconvert between Fe^{II} and Fe^{III} states (Fig. 2.1). The intensity of the current per molecule is directly proportional to the molecular weight of the polymer sample [18]. The observation of a single cyclic voltammetric wave in solvents of low dielectric constant is in contrast to the situation for polymers in which the ferrocene units are in close proximity in the polymer backbone, such as polyferrocenylsilanes (see Chapter 3, Section 3.3.6.3). For the latter materials, evidence for communication between iron centers is provided by the presence of *two* reversible oxidation waves. This has been explained in terms of oxidation of one Fe center making the neighboring Fe centers more difficult to oxidize.

Poly(vinylferrocene) is an insulator in its pristine state (i.e. when all iron centers are present as Fe^{II}) with a conductivity in the region of 10^{-14}–10^{-12} S cm^{-1} [19, 20]. Oxidation with, for example, I_2, quinones, or TCNQ, yields mixed-valent systems in which both Fe^{II} and Fe^{III} sites are present. These materials display much higher conductivities with values in the semiconductor range (10^{-8}–10^{-6} S cm^{-1}) that were found to be relatively independent of the counteranion present [20]. The maximum conductivities were reached at ca. 50% oxidation of the ferrocene sites, as would be expected for a hole-hopping model. Photoconductivity was not detected for the partially oxidized materials [20]. Based on studies of ferrocenium and mixed-valent biferrocene compounds [21, 22], as well as on Mössbauer spectroscopic analyses of vinylferrocene-containing copolymers [13, 23], charge has been found to be localized mainly on iron. An electron-hopping (or, more accurately, hole-hopping) model has been suggested as the mode for electron transfer, as the all-carbon backbone of the polymer is insulating [20].

The redox behavior of poly(vinylferrocene) $(VFc^{0/+})_n$ has been utilized in the construction of a microelectrochemical diode along with a redox-active viologen-

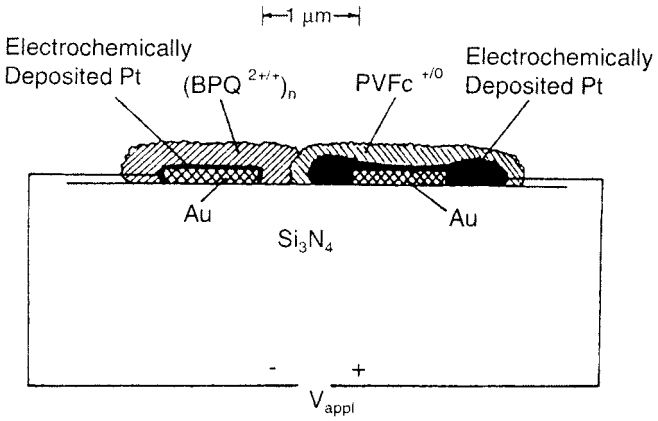

Fig. 2.2 A cross-sectional view of a microelectrochemical diode fabricated using poly(vinylferrocene). (Adapted from [24])

based *N,N'*-dibenzyl-4,4'-bipyridinium-based polymer $(BPQ^{2+/+})_n$ (see Fig. 2.2; Fc = pendant ferrocenyl group) [24]. The polymers were coated upon microelectrodes and current was found to pass when the negative lead was attached to the $(BPQ^{2+/+})_n$ electrode and the positive lead was connected to the $(VFc^{+/0})_n$ electrode. Thus, as the applied potential approaches the difference in redox potentials of the two polymers, current flows as a result of the redox reaction in Eq. 2.4a, which is favorable by ca. 0.9 V. However, current does not flow if the applied potential is in the opposite sense as the process shown in Eq. 2.4b is disfavored by ca. 0.9 V. The switching time of this diode, which is controlled by the time required to oxidize or reduce the polymers, was found to be long in comparison with that of solid-state diodes [24].

$$BPQ^{+} + Fc^{+} \longrightarrow BPQ^{2+} + Fc^{0} \qquad (2.4a)$$

$$BPQ^{2+} + Fc^{0} \longrightarrow BPQ^{+} + Fc^{+} \qquad (2.4b)$$

2.2.1.2 Other Organic Polymers with Metallocene-Containing Side Groups

A variety of other organic polymers with metallocene-containing side groups have been synthesized. However, very few of the materials have been as well-studied as poly(vinylferrocene). Crystalline organometallic complexes that contain ferrocene have been shown to possess interesting nonlinear optical (NLO) properties [25] and this has led to interest in the preparation of processable polymeric analogues. For example, a random copolymer (**2.6**) of methyl methacrylate (95 mol%) and a ferrocene-containing methacrylate (5 mol%) has been synthesized using free radical polymerization in order to evaluate the second-order NLO properties of the material [26]. The molecular weight of **2.6** was found to be $M_n = 3.0 \times 10^4$ by GPC relative to polystyrene standards, and the thermal behavior of the material was nearly identical

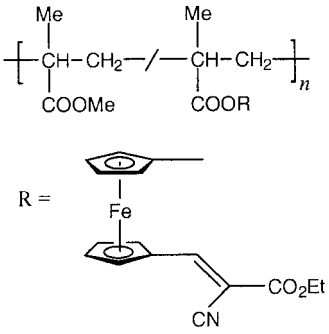

2.6

to that of poly(methyl methacrylate). After poling, the material was analyzed for second-order nonlinear optical properties and was found to possess a second harmonic generation efficiency approximately four times that of a quartz standard [26].

A series of very well-characterized polyacrylates, polymethacrylates, and related materials bearing ferrocene side groups ultimately derived from ferrocenylethanol as starting material has been prepared by AIBN-initiated radical polymerization [27]. The absolute molecular weights were found to be in the range $M_w = 2.9 \times 10^4$–8.7×10^5 by light-scattering measurements.

Ring-opening metathesis polymerization (ROMP) of norbornenes with ferrocene side groups using molybdenum alkylidene initiators has provided a controlled route to polymers with organic backbones and metallocene-containing side groups such as **2.7** (Eq. 2.5). Molecular weights for homopolymer **2.7** were in the range $M_n = 5090$–9030, with PDI values of 1.2 or less. Due to the living nature of the polymerization using the Mo catalysts, block copolymers could also be prepared (Scheme 2.2) [28, 29]. For example, ROMP of norbornene to afford the living polynorbornene **2.8** followed by addition of the ferrocenylnorbornene monomer yielded the living diblock copolymer **2.9**. Subsequent end-capping with an aldehyde led to the isolated block copolymers **2.10** with $M_n = 10{,}460$–$16{,}190$ and PDI values of 1.05–1.07.

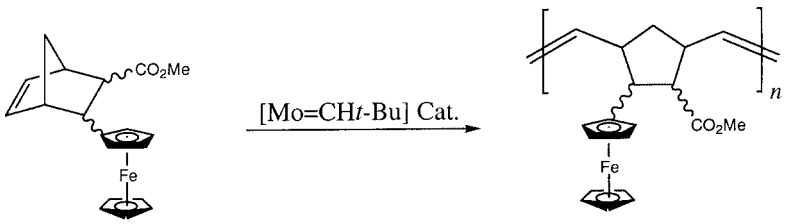

2.7

(2.5)

DSC measurements on the block copolymers revealed two T_gs with values close to those of the individual homopolymers. This thermal behavior is consistent with a

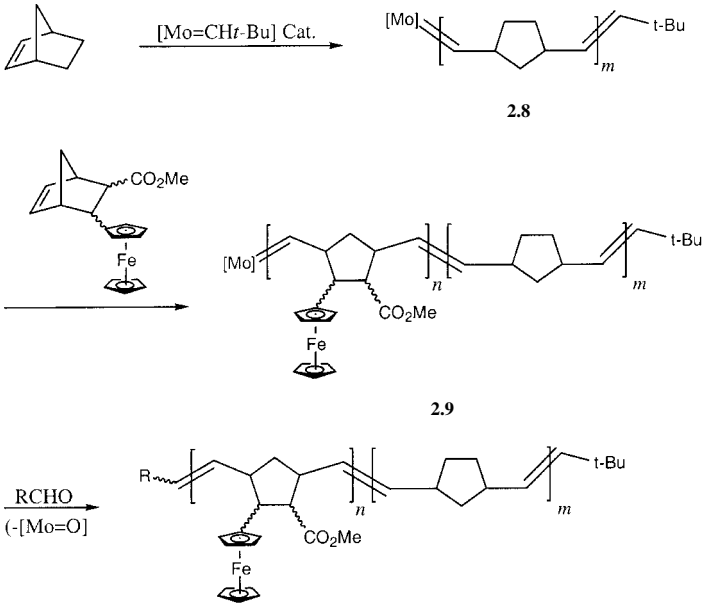

Scheme 2.2

block rather than a random copolymer structure. As was found for poly(vinylferrocene), cyclic voltammetry measurements showed the presence of one reversible oxidation wave, consistent with the existence of non-interacting redox sites. The living chain end of the polyferrocenylnorbornenes could also be capped with pyrene. The presence of the neighboring ferrocene moieties led to the emission of the pyrene unit being quenched by a factor of ca. 30 compared to emission from 1-vinylpyrene [29]. The quenching mechanism might involve electron transfer from the ferrocene group, or energy transfer as the ferrocene d-d absorption band and the pyrene emission spectrum partially overlap.

The synthesis of poly(ethynylferrocene) (**2.11**, M = Fe) has been studied by a number of different research groups [30–33]. In 1995, well-defined materials with controlled molecular weights up to 1.8×10^4 (M_w) with fairly narrow polydispersities (<1.3) (values determined by GPC using a light-scattering detector) were prepared by living polymerization using a Mo alkylidene initiator. In addition, examples of the analogous poly(ethynylruthenocene) (**2.11**, M = Ru) ($M_w = 7.6\times10^3$–1.9×10^4, PDI = 1.14–1.24) were also prepared [34]. The living polymers could be terminated with pyridinecarboxaldehyde and the tertiary nitrogen subsequently quaternized with methyl iodide. The charged systems were found to exhibit a more intense, red-shifted absorption in their UV/vis spectra than the corresponding uncharged systems.

Polypyrrole and polythiophene derivatives with pendant ferrocene groups (e.g. **2.12**) have also been prepared using electropolymerization techniques [35]. Studies of these materials by means of *in situ* conductivity measurements revealed that the redox conduction, due to hole hopping between the ferrocene units, was en-

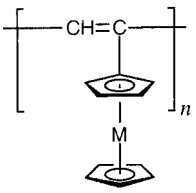

M = Fe or Ru

2.11

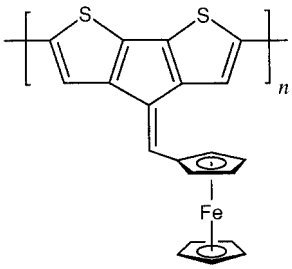

2.12

hanced by a decrease of the Fc-backbone distance and by conjugation of the organometallic group with the polymer backbone (as in polymer **2.12**, which possesses a redox conductivity of ca. 8×10^{-3} S cm^{-1}).

Ferrocene side groups have also been introduced at low loadings into side-chain liquid-crystalline polymers, with the aim of exploring the effect of redox activity on the properties of the materials. For example, the redox-active copolymers **2.13** undergo reversible oxidation with Cu^{II} salts or *p*-benzoquinone to generate the liquid-crystalline ionomers **2.14** (Eq. 2.6) [36]. Introduction of the neutral ferrocene moiety has only a minor influence on the liquid-crystalline properties. However, after oxidation, significant effects on mesophase stability were noted. Thus, small-angle X-ray scattering and dynamic mechanical analysis showed that the ferrocenium groups and counteranions form ionic clusters, which physically crosslink the material and give rise to elastomeric properties.

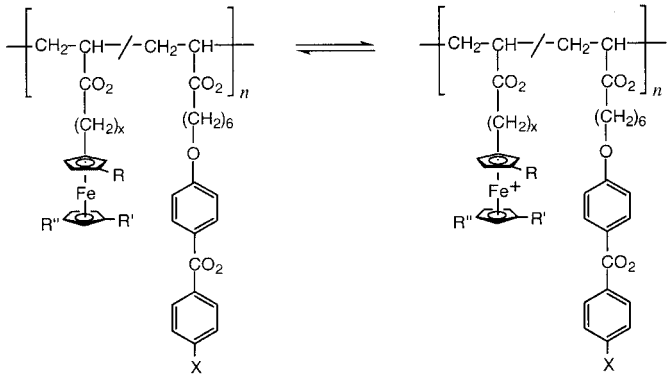

(2.6)

X = CN or OMe

2.13

2.14

This type of approach has been extended to main-chain liquid-crystalline polymers **2.15** with low loadings of ferrocene groups in the side-group structure. In some cases, changes in liquid-crystalline morphology from nematic to smectic have been observed upon oxidation, as the formation of ionic domains facilitates the generation of layered structures (Fig. 2.3) [37].

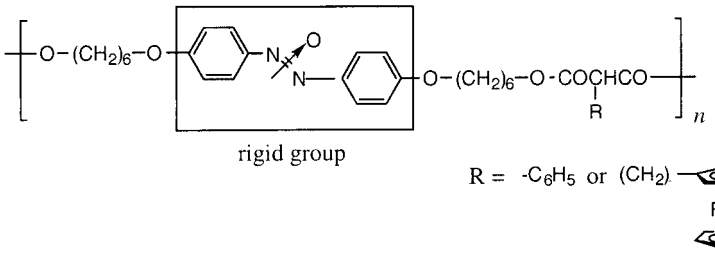

2.15

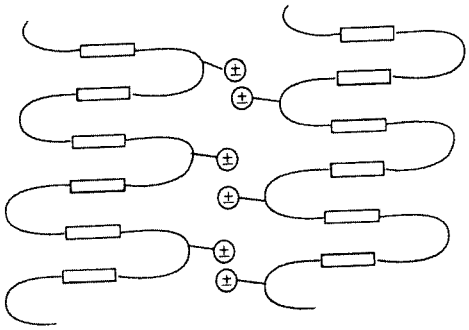

Fig. 2.3 Formation of layered structures induced by oxidation of ferrocene groups in polymers **2.15** and the consequent formation of ionic clusters of cations and counteranions. The rigid group consists of a mixture of nitroxide isomers. (Reproduced from [37a])

Ferrocene-containing polymers are also of interest for biomedical applications. For example, polypeptides with ferrocene side groups have attracted attention since a range of water-soluble ferrocenium salts have been found to possess significant antiproliferative activity against various tumors. The water-soluble polymers **2.16** and analogues thereof also show similar activity [38]. In addition, the cationic ferrocene polymers **2.17**, derived from a poly(allylamine), have been used in multilayer biosensor devices [39]. Sequential layer-by-layer deposition of **2.17** and anionic glucose oxidase can be used to prepare alternating cationic-anionic polymer multilayer structures on alkanethiol-modified gold electrodes. Catalysis of the oxidation of glucose was detected, thus indicating that the ferrocene groups mediate electron transfer between reduced glucose oxidase and the gold electrode. In the absence of such electrode mediators, electron transfer is extremely slow as an insulating protein sheath surrounds the redox center in the enzyme. Analogous results have been reported for related systems based on ferrocene-modified organic polymers (e.g. the conjugated ferrocenyl-substituted polyaniline **2.18**) [40, 41]. Several examples of other redox metallopolymers which function in this manner will be discussed elsewhere in this chapter (Section 2.3.2).

In general, much less work has been reported on side-chain polymers containing metallocenes other than ferrocene. For example, ruthenium and osmium analogues of poly(vinylferrocene) have been described, but their characterization has been fairly limited [16, 42, 43]. Poly(vinylruthenocene) is reported to be a light-yellow solid with a $T_g > 250\,^{\circ}C$, and the preparation of samples with molecular weights of up to

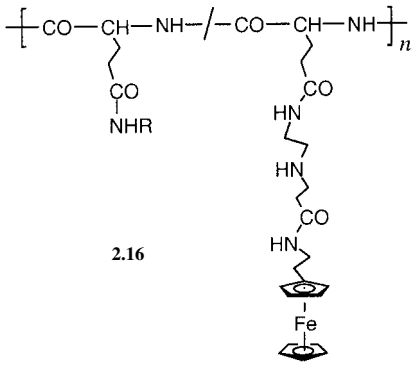

2.16

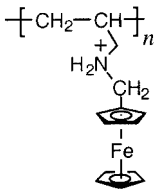

2.17

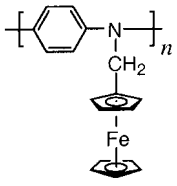

2.18

$M_w = 1.2 \times 10^5$ with broad molecular weight distributions (PDI $\approx$ 6) has been reported by the free radical polymerization of vinylruthenocene in benzene with AIBN as the initiator [43]. The polymers were proposed to possess a branched structure as a result of chain-transfer steps. Copolymers with other organic vinyl monomers have also been prepared [43]. Poly(vinylruthenocene) and poly(vinylosmocene) have been tested as preheat shields for targets in inertial-confinement nuclear fusion [42].

Organic polymers have also been used as supports for catalytically-active early transition metal metallocenes as well as a broad range of other metal-based catalytic species (see Section 2.3.3). Macroporous polystyrene beads cross-linked with 1 or 2% divinylbenzene have been particularly popular as a support. Generally, the beads are used in a swollen state, which is achieved by immersion in a suitable solvent, so that substrates can access the reactive sites. As an example, beads containing the organotitanium units **2.19**, derived from poly(chloromethylstyrene) (Eq. 2.7), were studied in the 1970s, and excellent activity for the hydrogenation of 1-hexene was demonstrated [44–46]. Analogous systems containing zirconocene and hafnocene units have also been studied for the polymerization of alkenes and exhibit significant promise [47, 48].

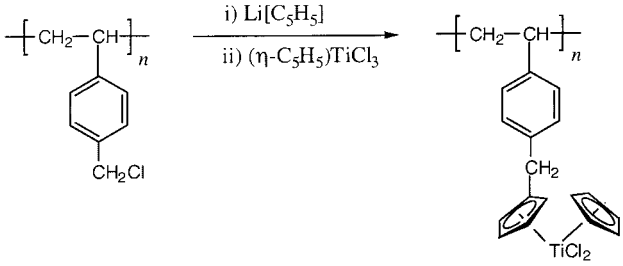

(2.7)

2.19

2.2.2 Inorganic Polymers with Metallocene Side Groups

Many examples of *inorganic* polymers with metallocene–containing side groups also exist. Most of the polymers prepared have been based on main chains of polyphosphazenes, polysilanes, polysiloxanes, and polycarbosilanes. These materials are surveyed in the following sections.

2.2.2.1 Polyphosphazenes with Ferrocene- or Ruthenocene-Containing Side Groups

The earliest and most well-developed route to polyphosphazenes involves the thermal ring-opening polymerization of cyclic phosphazenes bearing halogen substituents at phosphorus. Use of this method and subsequent halogen replacement with alkoxides has led to the synthesis of ferrocene- and ruthenocene-containing polyphosphazenes (**2.20** and **2.21**) with molecular weights (M_w) in excess of 2×10^6 [49, 50].

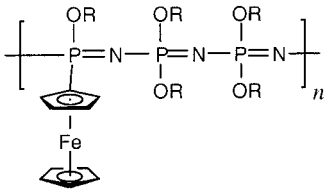

2.20

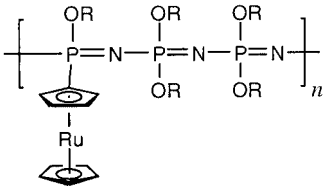

2.21

In general, cyclotriphosphazenes with less than three halogen substituents do not undergo thermal ring-opening polymerization. However, a range of cyclic phosphazenes without any halogen side groups (**2.22**) have been found to polymerize, provided that transannular ferrocenyl substituents are present. ROP of **2.22** yields polymer **2.23** (Eq. 2.8) with molecular weights as high as $M_w = 1.8 \times 10^6$ (PDI = 6.2) [51, 52]. In most cases, the presence of a small amount of an initiator such as $[NPCl_2]_3$ is necessary for polymerization to occur. X-Ray crystallographic studies of several of these strained ferrocenylorganocyclotriphosphazene monomers **2.22** have shown that the phosphazene ring is forced into a high energy, non-planar conformation [53]. By contrast, in most cyclotriphosphazenes the phosphorus-nitrogen ring is essentially planar.

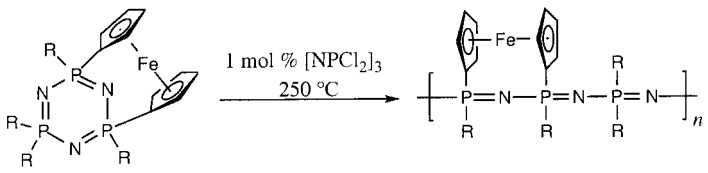

(2.8)

2.22 **2.23**

R = non-halogen substituent

Polymers **2.20** and **2.23** (as well as copolymers bearing both ferrocene and ruthenocene moieties) have been partially oxidized with iodine, resulting in weakly semiconducting materials. These materials have also been deposited on electrode surfaces, where the polymers act as electrode mediator coatings that aid electron transfer between the electrode and redox-active species in solution [54].

Polyphosphazenes with ferrocenyl substituents (**2.24**) have also been synthesized by the functionalization of poly(methylphenylphosphazene) and related polymers by means of a deprotonation-electrophilic addition strategy (see, e.g., Eq. 2.9) [55, 56]. This versatile reaction sequence has yielded materials with, for example, degrees of substitution of 45% and 36% for polymers **2.24** (R = H) and **2.24** (R = Me), respectively. The molecular weights of the polymers were $M_w = 2.0 \times 10^5$ and 1.5×10^5 for **2.24** (R = H) and **2.24** (R = Me), respectively (with PDI values of 1.4–2.0). The glass transition temperatures increased in comparison with the unsubstituted polymer ($T_g = 37\,^\circ C$) with values of 92 °C for **2.24** (R = H) and 87 °C for **2.24** (R = Me), respectively.

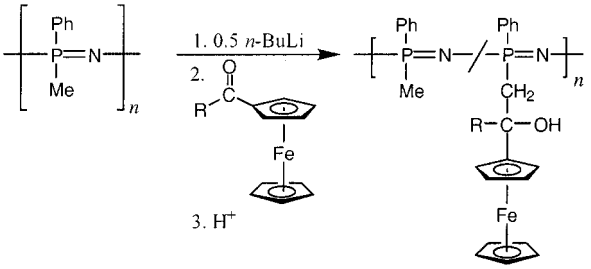

(2.9)

2.24 (R = H or Me)

2.2.2.2 Polysilanes, Polysiloxanes, and Polycarbosilanes with Metallocene Side Groups

The synthesis of interesting polysilanes that bear low loadings of ferrocene substituents (**2.25**) by Wurtz coupling has been reported (Eq. 2.10) [57]. Random copolymers with weights (M_w) up to 3.9×10^5 were isolated from mixtures of high and low molecular weight fractions. The ratio of methylphenylsilane to methylferrocenylsilane segments ranged from 6:1 to 27:1. In common with other polysilanes, these materials were found to be photosensitive and depolymerized upon exposure to UV light. However, the copolymers displayed significantly greater photostability than a corresponding sample of poly(methylphenylsilane), indicating that ferrocene moieties bound to the polymer chain provided a degree of stabilization for the polysilane backbone towards photodegradation. Cyclic voltammetry experiments [58] revealed two oxidation waves for the copolymers. The first wave, due to oxidation of iron sites, was reversible, whereas the second, irreversible oxidation at higher potential was assigned to oxidation of the polysilane backbone. No appreciable electrochemical interaction was observed between neighboring iron sites or between iron sites and the polymer backbone.

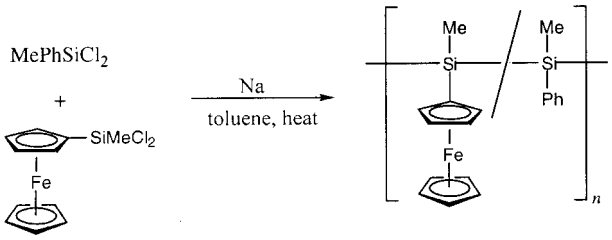

(2.10)

2.25

Polysiloxane random copolymers (with molecular weights of 5000 to 10,000) with pendant ferrocene groups have been synthesized (**2.26**) by hydrosilylation of vinylferrocene or 9-ferrocenyl-1-nonene with a poly(methylhydrosiloxane)-*r*-poly(dimethylsiloxane) random copolymer (Eq. 2.11). These materials were used as amperometric biosensors for the detection of glucose [59]. In this application, the polymers effectively mediated electron transfer between reduced glucose oxidase and a conventional carbon paste electrode. The response of the sensor to glucose was dependent upon the nature of the polymeric backbone. The optimal response was achieved by finding a compromise between increased polymer flexibility and decreased spacing between individual relay (i.e. ferrocene) sites.

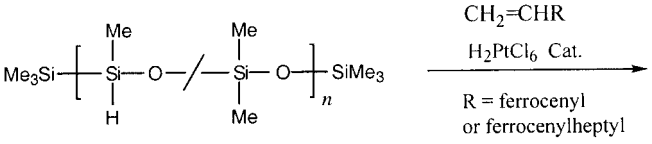

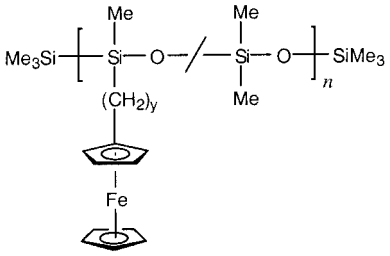

(2.11)

2.26

(y = 2 or 9)

The hydrosilylation strategy has also been used to prepare well-characterized side-chain liquid-crystalline polymers containing ferrocene [60]. Grafting of vinyl-terminated mesogens onto poly(methylhydrosiloxane-*r*-dimethylsiloxane) yielded materials with 1,1′- (**2.27a**) and 1,3-disubstituted (**2.27b**) ferrocene units

(Eq. 2.12). The molecular weights were in the range $M_w = 2.5–3.1 \times 10^4$ and the PDI values were 1.4–1.6. The liquid-crystalline nature of the resulting polymers was investigated by polarizing optical microscopy, DSC, and X-ray diffraction. The materials were found to display "layered"-type smectic A and/or smectic A and smectic C phases, depending specifically on the length of the flexible chains connected to the ferrocene unit [60]. For example, polysiloxane **2.27a** with $m = 9$ and $n = 18$ showed a T_{lc} of 136 °C, at which the material melted to form a smectic C phase. At 140 °C, this transformed into a smectic A phase, and at the clearing temperature $T_{cl} = 183$ °C an isotropic melt was formed. The proposed supramolecular organization of the smectic A phases is shown in Fig. 2.4.

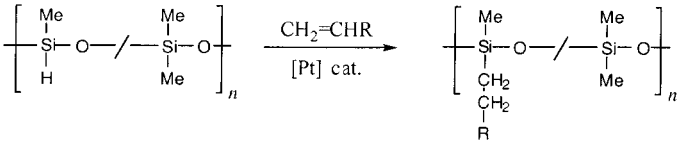

2.27

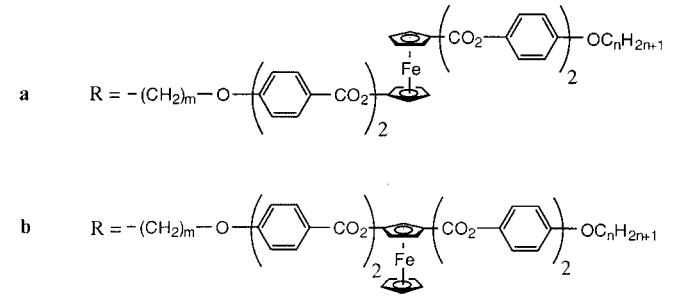

(2.12)

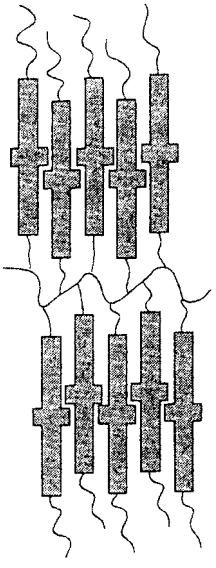

Fig. 2.4 The proposed supramolecular organization of the ferrocene-containing side groups in the smectic A phases of polymers **2.27**. (Reproduced from [60a])

Polysiloxanes with pendant zirconocene units have also been explored as alkene polymerization catalysts. For example, polysiloxanes **2.28** containing indenyl groups have been synthesized by hydrolytic condensation of the corresponding dichloroorganosilanes [61]. Treatment with BuLi followed by the metal halide was claimed to yield materials with idealized structure **2.29** (Scheme 2.3). However, no structural characterization of the products was reported, apart from their low molecular weights according to GPC measurements (M_w = 700–3600). It seems likely that chain cleavage reactions occur in the BuLi deprotonation step, and crosslinking processes upon addition of the Zr halide are highly likely. Nevertheless, appreciable activities for the polymerization of ethene and propene were detected for **2.29** and analogous species in the presence of methylalumoxane [61].

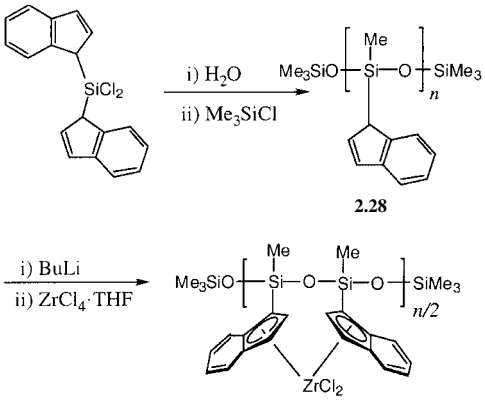

Scheme 2.3

As an alternative approach, polycarbosilanes **2.31** bearing pendant zirconocene moieties have also been prepared by ring-opening polymerization of the spirocyclic monomer **2.30** (Eq. 2.13) [62]. In this case, the materials were structurally characterized, but the soluble fraction was of low molecular weight (M_w < ca. 3000) and the high molecular weight fraction was insoluble in organic solvents. In the presence of activators, both fractions functioned as ethene polymerization catalysts with moderate activity [62].

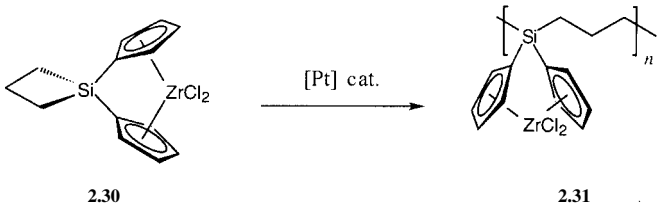

(2.13)

2.3
Other Side-Chain Metallopolymers

2.3.1
Polymers with π-Coordinated Metals

The radical polymerization of various other organometallic vinyl monomers has been well-studied. For example, in 1978 it was shown that vinylcymantrene **2.32** undergoes radical homopolymerization in the presence of AIBN as initiator at 50–80 °C in organic solvents such as benzene to yield poly(vinyl cymantrene) **2.33** (Eq. 2.14) [63]. Molecular weights varied from $M_w = 5 \times 10^3$ to 3.6×10^5, with broad PDI values in the range 3.2–8.9.

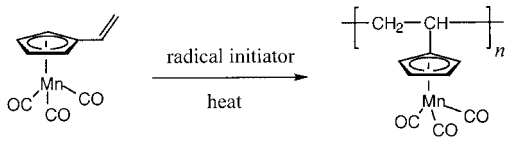

(2.14)

2.32 **2.33**

On photolysis, copolymers of vinyl(methylcymantrene) and octyl methacrylate have been shown to lose CO and thereby generate polymers **2.34** possessing 16-electron Mn centers, which coordinate to N_2 to yield **2.35** (Eq. 2.15). The coordination is reversible and can be used to prepare membranes which exhibit facilitated transport of this gas [64]. Comparison of the diffusion coefficients for normal "Henry-mode" diffusion and the facilitated "Langmuir-mode" diffusion due to the mediation of the manganese centers which function as N_2 carriers showed that the latter mechanism contributes substantially. Moreover, as expected for this interpretation, the contribution from the facilitated transport mode increased as the loading of the Mn sites became higher.

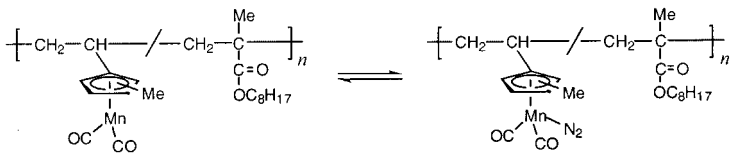

2.34 **2.35**

(2.15)

The attachment of cymantrene groups to polymers has attracted interest for other reasons. Studies have shown, for example, that adherent, abrasion-resistant

coatings are formed on metals when thin films of the Mn-containing polymer are subjected to irradiation with UV light [65]. The polymerization of styrenetricarbonylchromium **2.36** has also been studied [66]. This species is available from the reaction of styrene with $Cr(CO)_3(NH_3)_3$. Although the Cr monomer **2.36** resisted attempts at homopolymerization, copolymerizations with styrene, methyl acrylate, as well as with **2.32** to yield bimetallic polymers **2.37** (Eq. 2.16) were possible. In addition, copolymerization with vinylferrocene afforded copolymers of low molecular weight ($M_n \approx$ ca. 4000). A variety of other organometallic vinyl monomers **2.38** have been successfully polymerized to yield polymers **2.39** that contain pendant Cr, W, and Ir carbonyl moieties (Eq. 2.17) [67].

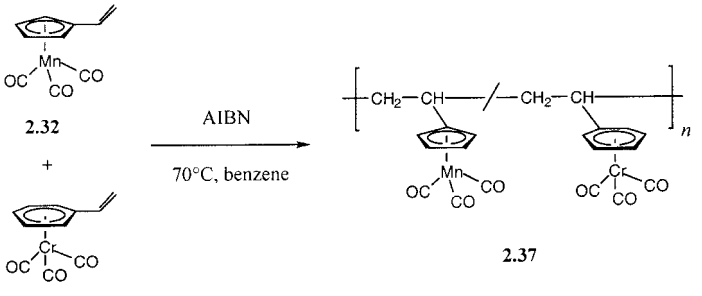

(2.16)

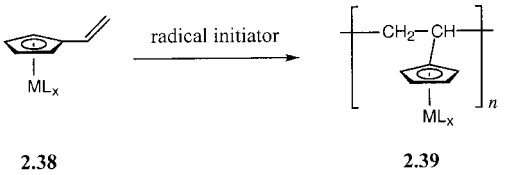

(2.17)

ML_x = $Cr(NO)(CO)_2$, $W(CO)_3Me$, or $Ir(CO)_2$

2.3.2
Polymers with Pendant Polypyridyl Complexes

The octahedral Ru^{II} complex $[Ru(bipy)_3]^{2+}$ (bipy = 2,2′-bipyridyl) exhibits efficient photoluminescence, electroluminescence, and also electrochemically-generated chemiluminescence (quantum yields up to 5–7%) through the reactions shown in Eqs. 2.18a and 2.18b, respectively (excited states are labelled *) [68–70]. These properties have led to a range of studies on polymers with appended polypyridyl and related complexes.

$$[Ru(bipy)_3]^{2+} \xrightarrow{h\nu} [Ru(bipy)_3]^{2+*} \xrightarrow{-h\nu'} [Ru(bipy)_3]^{2+} \qquad (2.18a)$$

$$\begin{array}{ccccc} [Ru(bipy)_3]^{3+} & & [Ru(bipy)_3]^{2+*} & & 2\,[Ru(bipy)_3]^{2+} \\ + & \longrightarrow & + & \longrightarrow & + \\ [Ru(bipy)_3]^{+} & & [Ru(bipy)_3]^{2+} & & h\nu \end{array} \qquad (2.18b)$$

The first examples in which an Ru complex was attached to a polystyrene backbone through a bromination, lithiation, bipyridylation, and metal complexation reaction sequence were reported in 1980. Related materials have been prepared using other synthetic approaches, and their photochemical properties have been studied in some detail [71, 72]. More recently, Ru^{II} polypyridyl complexes have been attached as pendant groups to conjugated polymers such as poly(*p*-phenylene vinylene) (PPV), which themselves exhibit electroluminescence and photoluminescence. For example, the Ru bipyridyl polymer **2.40** has been prepared by a Pd-catalyzed Heck-type coupling reaction (Eq. 2.19) and single-layered light-emitting devices have been fabricated by sandwiching 70 nm films of **2.40** between a hole-injecting indium tin oxide (ITO) electrode and an electron-injecting Al electrode [73]. At high loadings of the Ru polypyridyl substituents, only red light emission from the Ru complex was observed as the emission from the PPV backbone was quenched by energy transfer from the Ru complex. However, at low loadings of the complex, quenching was inefficient and the green PPV emission

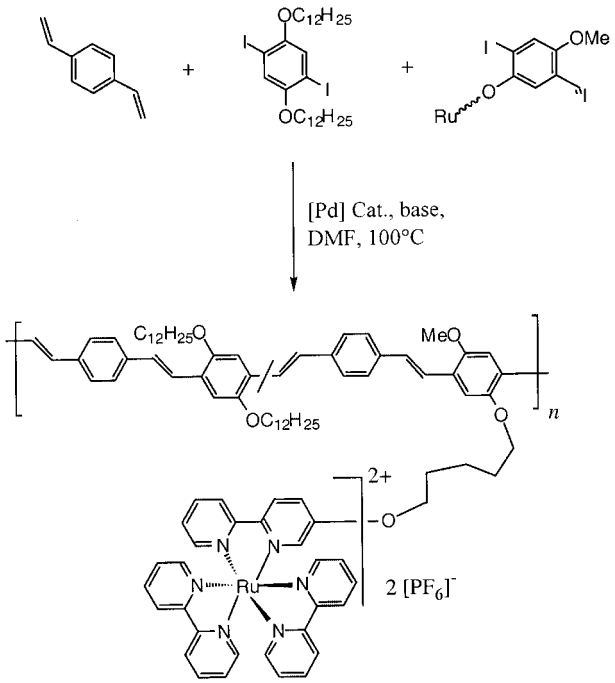

(2.19)

2.40

was observed as well, resulting overall in the emission of yellow light. This led to interesting color tuning effects, which may prove useful in light-emitting devices. Polymers analogous to **2.40** based on terpyridyl ligands were similarly synthesized and studied, and were found to exhibit similar behavior. A range of interesting materials similar in structure to **2.40**, in which the metal is actually incorporated as part of the π-conjugated polymer backbone, have also been prepared. These materials are discussed in Chapter 7.

The lifetime of the excited state formed by photoirradiation of $[Ru(phen)_3]^{2+}$ (phen = 1,10-phenanthroline) is substantially longer than that of $[Ru(bipy)_3]^{2+}$, and this results in long-lived phosphorescence. Moreover, the long-lived excited state is effectively quenched by oxygen over a useful pressure range, which has led to interest in the use of this complex as a sensor for oxygen or for monitoring air pressure variations [74, 75]. Polymers **2.41** have recently been developed, which provide thin films comprised of a highly permeable polythionylphosphazene matrix incorporating the phosphorescent Ru-phen sensor [76]. Problems associated with the facile aggregation of the cationic Ru-phen complex that occur in simple dispersions of the complex in most permeable polymers would be expected to be reduced by covalent attachment. Possible applications include uses as thin polymer films that monitor air-pressure distributions over aircraft and automobile design models in wind tunnels through phosphorescence imaging, or that measure the dissolved oxygen concentration in water for environmental purposes [76].

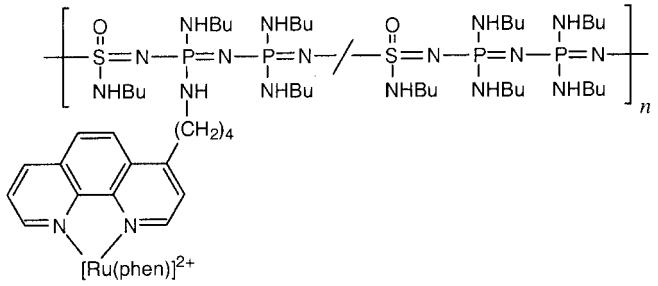

phen = 1,10-phenanthroline

2.41

Ru polypyridyl complexes have also been used to create self-oscillating gels [77]. In contrast to conventional stimuli-responsive gels, these swell and contract periodically at a constant temperature like a "beating heart" without the need for external stimuli. The gels were constructed from a copolymer **2.42** of *N*-isopropylacrylamide and a vinyl Ru bipy monomer together with a crosslinker. Immersion in a solution of Ce^{IV}/Ce^{III} induced the oscillatory Belousov-Zhabotinsky reaction, which led to oxidation and reduction of the Ru^{II} complex and self-oscillation of the gel (Fig. 2.5) [77]. A related approach has been used to prepare analogous Ru-containing polymers that alternate between being soluble and insoluble in a solvent [78].

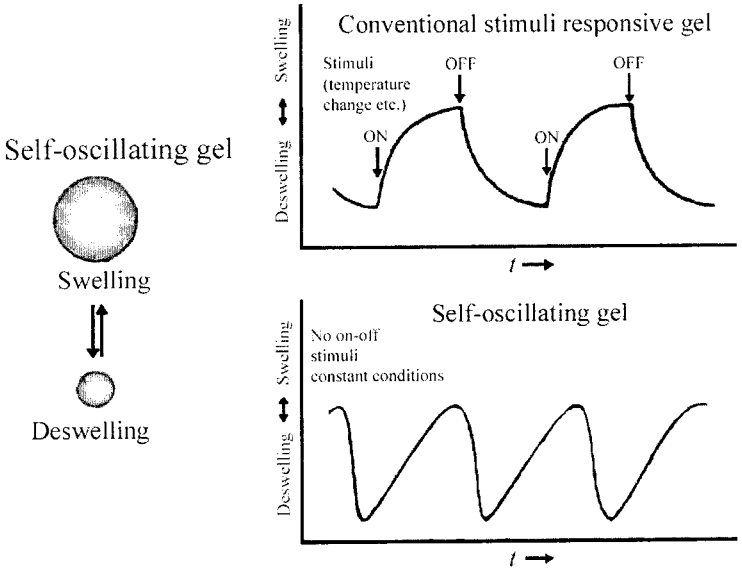

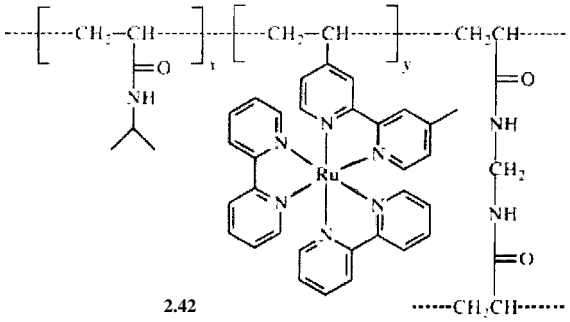

2.42

Fig. 2.5 Self-oscillating gels based on Ru bipy polymers. (Adapted from [77b])

Side-chain redox polymers derived from poly(vinylpyridine) have also received significant attention. For example, the Os^{II} polycation **2.43** has been used as an electrode mediator for electron transfer between an electrode and the redox centers of several enzymes [79–81]. Polycation **2.43** ($M_w \approx 6 \times 10^4$) forms an electrostatic complex with the polyanionic enzyme glucose oxidase at low ionic strengths, which brings the Os^{II}/Os^{III} redox center and enzyme redox centers within range for electron transfer [79]. Interestingly, covalent attachment of the redox polymer to the enzyme was found to be necessary for complex formation at high ionic strengths. In the absence of complexation, a negligibly slow electron-transfer rate was observed. Adsorption of the polycationic redox polymer **2.43** on an electrode thereby offers the possibility of creating a device that functions as a glucose sensor [79]. In a further development, the use of the same Os-containing

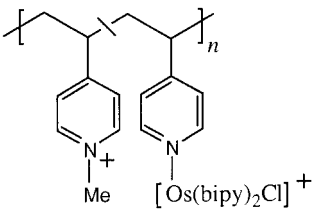

bipy = 2,2'-bipyridine

2.43

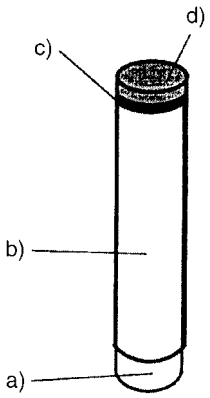

Fig. 2.6 Schematic of a microsensor; (**a**) gold wire (diameter 0.25 mm), (**b**) polyimide cladding (5 μm thick), (**c**) platinum black with adsorbed enzyme (5 μm thick), (**d**) Os-based redox hydrogel (50 μm thick). (Reproduced from [80])

polymer in combination with pyruvate oxidase allows the construction of an amperometric sensor utilizing a gold electrode to detect pyruvate in biological fluids [80]. This is shown schematically in Fig. 2.6.

The use of another Os^{II}-containing polymer analogous to **2.43**, in combination with the enzyme soybean peroxidase (SBP), has made it possible to detect a single base pair mismatch in an 18-base oligonucleotide [81]. This was achieved by covalent attachment of a single-stranded 18-base probe oligonucleotide to the Os redox polymer film on a microelectrode and attachment of target single-stranded 18-base oligonucleotides to the enzyme. Hybridization of the probe and target oligonucleotides led to an increase in current, which was larger in the case of a complementary 18-base target oligonucleotide attached to SBP than for analogs with single or multiple base mismatches (see Fig. 2.7). The current detected resulted from the electrocatalytic reduction of H_2O_2 to water. These studies suggest that such devices may ultimately be used in gene detection arrays.

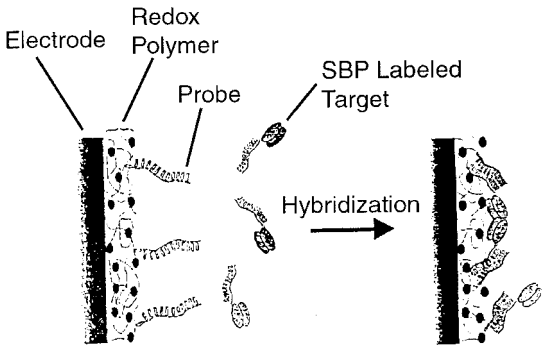

Fig. 2.7 Schematic of the DNA base-pair mismatch detection system based on an Os redox polymer. (Adapted from [81])

2.3.3
Polymers with Other Pendant Metal-Containing Units, Including the Area of Polymer-Supported Catalysts

Many other metal-containing groups have been attached to organic polymers. Polymers **2.44** containing Pd–C σ-bond linkages have been successfully prepared by the radical polymerization of *p*-substituted styrene derivatives (Eq. 2.20) [82]. Substituents bearing main group metals have been appended to vinyl polymer backbones. For example, polymethacrylates with $SnBu_3$ substituents can be prepared by free radical copolymerization of the respective monomers or by treatment of poly(methyl methacrylate)-*r*-poly(methacrylic acid) with $(Bu_3Sn)_2O$ [83]. These materials have been explored as antifouling paints on ships and offshore oil platforms. Oxotitanium clusters have been similarly incorporated to generate novel inorganic-organic hybrid polymers [84]. Polyaminophosphazenes with coordinated $PtCl_2$ units are of interest as tumor-inhibiting materials [85]. In addition, ROMP of norbornenes bearing pendant cationic organoiron substituents bound through arene-metal bonds has yielded redox-active organoiron polymers such as **2.45** (Eq. 2.21). These materials show reversible one-electron reduction waves at –50 °C by cyclic voltammetry, whereas the electron-transfer process to generate 19-electron neutral iron sites is irreversible at room temperature [86].

Of particular significance is the large number of catalytically active metal complexes that have been bound to polymer supports (such as cross-linked polystyrene) by various methods [87]. Much of the work has been stimulated by the discovery of solid-phase peptide synthesis that was introduced by Merrifield in 1963 and culminated in his award of the Nobel Prize for Chemistry in 1984. This area is of intense interest for the preparation of polymers and also, more generally, in organic synthesis as separation of the products from the catalyst is, in principle, achieved cleanly and easily. Such systems are of particular significance for combinatorial chemistry as they generally offer the possibility of rapid screening of libraries of catalysts. However, it should be noted that in certain cases polymer-supported organic reactions can show significant differences from standard reactions with respect to substrate selectivity, rate, product distribution, and product stereo-

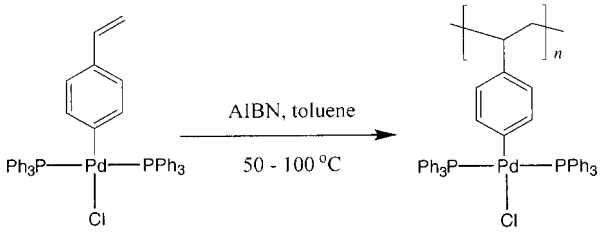

(2.20)

2.44

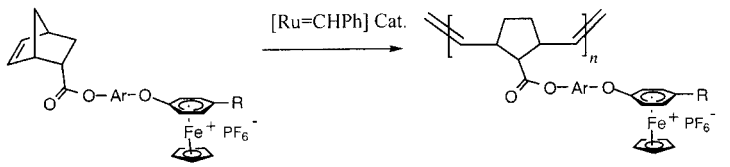

(2.21)

Ar = p-C_6H_4, R = Me

2.45

chemistry [87]. In addition, leaching of the metal complex from the polymeric support over time is a common problem.

The vast area of polymer-supported catalysts is too broad to cover systematically in this monograph. In addition, as the loadings of metal ions on the polymers are generally very low, the cited reviews are a more appropriate source of information [87]. We have already discussed supported catalytically active metallocene complexes in earlier sections (2.2.1.2 and 2.2.2.2). Some illustrative examples of the types of transformations that have been achieved are shown in Table 2.1.

Here, we discuss a typical example that involves the use of rhodium-containing, polymeric water-soluble hydroformylation catalysts, which clearly demonstrates the exciting potential of this area [88]. Rhodium polymers of proposed structure **2.46** were prepared from poly(pentenoic) acid ($M_w \approx 5000$) by acylation of the amine $HN(CH_2CH_2PPh_2)_2$ using dicyclohexylcarbodiimide (DCC) as the coupling agent, followed by metallization with $[Rh(1,5\text{-cod})Cl_2]_2$ (Scheme 2.4). The Rh-containing material proved to be water-soluble and was isolated as a yellow powder. It was characterized by means of NMR spectroscopy, although the exact identity of the coordination environment at Rh remained unclear. The loading of Rh complexes per side group was ca. 10%, and the polymer possessed a molecular weight (M_w) of 7700 with a PDI of 3.1 by GPC in THF (versus polystyrene standards). The Rh polymer was found to be an excellent catalyst for the hydroformylation of alkenes and represents the first polymeric metal complex capable of converting vinylarenes to 2-arylpropanals in a highly chemoselective and regioselective manner [88].

Table 2.1 Representative reactions with polymer-supported catalysts

Catalytic metal	*Polymer support*	*Catalytic reaction*	*Reference*
Ru, Rh	Phosphinated polystyrene	Alkene isomerization	89
Rh	Phosphinated polystyrene	Alkene hydroformylation	90
Rh	Cyclopentadienyl ligand on polystyrene	Pyridine synthesis	91
Pd	Cyanomethylated polybenzimidazole	Alkene oxidation	92
Ni	P/O ligand on polystyrene	Ethene polymerization	93
Cu	Nitroxide-functionalized polystyrene	Oxidation of alcohols	94

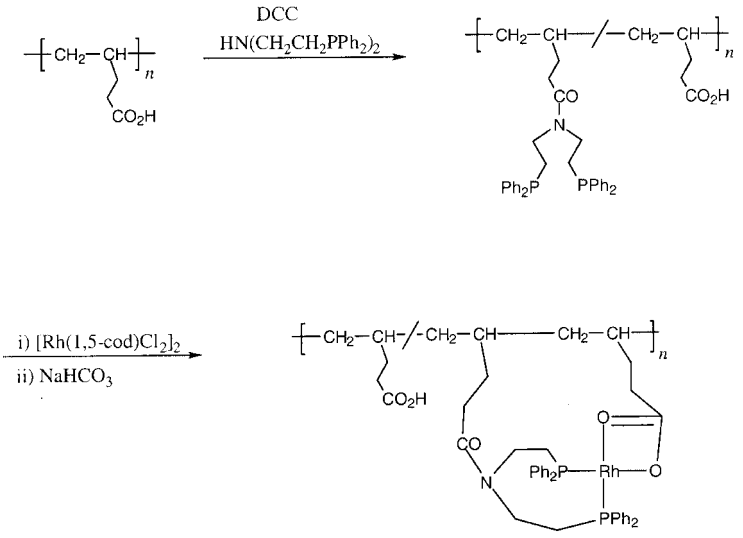

Scheme 2.4

2.46

2.3.4

Block Copolymers with Pendant Metal-Containing Groups

Block copolymers exhibit outstanding potential for a variety of applications as a result of their self-assembly into supramolecular structures (see Chapter 1, Section 1.2.5). However, the exploration of metal-containing multiblock materials was only begun in the early 1990s. Block copolymers derived from the living anionic polymerization of vinylferrocene were already mentioned in Section 2.2.1.1. In this section, side-chain metal-containing block copolymers are surveyed. Examples of block copolymers with metals in the main chain will be discussed in Chapter 3 (Section 3.3.8) and Chapter 7 (Section 7.2.3).

2.3.4.1 Approaches using Ring-Opening Metathesis Polymerization (ROMP)

ROMP provided the first examples of block copolymers with pendant metal-containing groups. As discussed earlier, ROMP of substituted norbornenes has been used to prepare block copolymers with ferrocene side groups (see Section 2.2.1.2). The technique of using norbornenes with pendant metal-containing groups is very versatile and also allows the preparation of block copolymers which contain Sn, Pb, Zn, Pd or Pt in the side-group structure [95–97]. The procedure in the case of Sn is illustrated in Scheme 2.5 [95]. Addition of the Sn-containing norbornene derivative to living polynorbornene generated with a tungsten alkylidene catalyst, followed by capping with 1,3-pentadiene, which is unreactive towards the Sn sites but reactive with the chain end, afforded diblock copolymer **2.47**. Thin films of the air-sensitive, metal-containing block copolymers were characterized by TEM, which showed the presence of phase-separated microdomains in which the metal was confined to the domains derived from the metal-containing block.

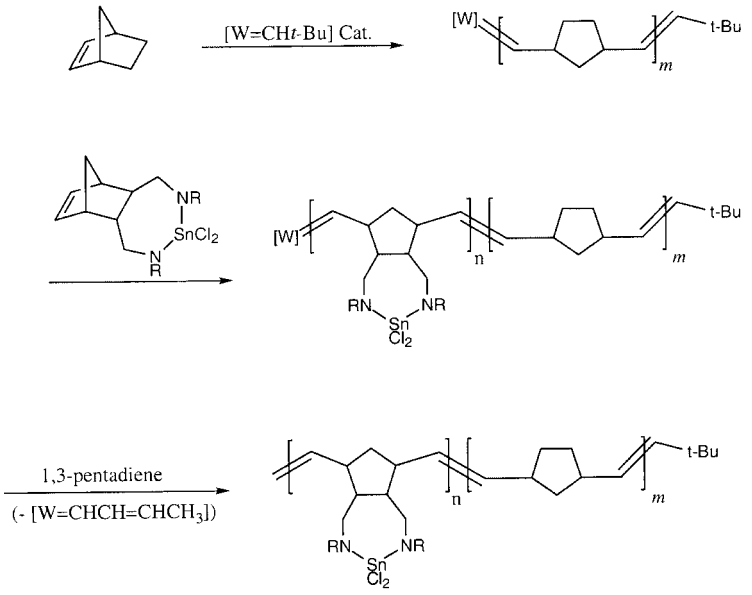

2.47 **Scheme 2.5**

Phase-separated, metal-containing block copolymers formed by ROMP offer interesting possibilities for the controlled formation of semiconductor and metal nanoclusters, which are of intense interest as a result of their size-dependent electronic and optical properties, as well as their catalytic behavior. Zinc-containing block copolymers generated by ROMP have been shown to form ZnS nanoclusters within the phase-separated organozinc domains upon treatment with gaseous H_2S [96]. The cluster sizes generated were up to 30 Å, and their small size led to quantum size effects. For example, a band gap of 5.7 eV was measured for the

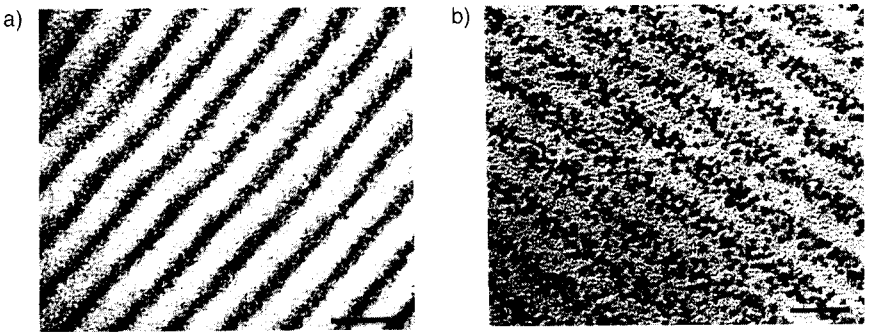

Fig. 2.8 TEM images of thin films of a block copolymer **2.48** (M = Pd) showing a lamellar morphology (**a**) before and (**b**) after treatment with H_2, showing the growth of Pd nanoclusters in the phase-separated Pd-containing domains. Regions containing Pd are dark as a result of the efficient electron scattering by this element (scale bar represents 25 nm) (Reproduced from [97])

roughly spherical 30 Å clusters, which is substantially larger than that for bulk ZnS (3.5 eV). Similarly, the Pd- or Pt-containing materials **2.48** were prepared by sequential ROMP of a metal-containing norbornene and methyltetracyclodecene [97]. Subsequent treatment of the Pd- or Pt-containing materials with molecular H_2 led to the formation of metallic nanoclusters within the microphase-separated domains. TEM images of the Pd-containing materials, which possess a lamellar morphology, before and after H_2 treatment, are shown in Fig. 2.8.

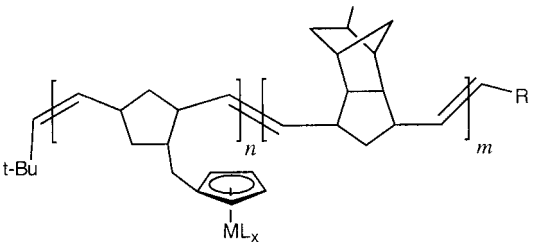

M = Pd or Pt

2.48

2.3.4.2 **Coordination to Pyridyl Substituents in Preformed Blocks**

Vinylpyridine undergoes living anionic polymerization, which allows the preparation of block copolymers containing coordinating pyridine units. Such systems have attracted significant attention. For example, polystyrene-*b*-poly(4-vinylpyridine) (PS-*b*-P4VP) has been used to coordinate a variety of transition metals. Reaction with $ReCl(CO)_3(bipy)$ in the presence of $Ag[ClO_4]$ yielded the Re-substituted block copolymer **2.49** with an ionic Re-containing block [98]. The loading of Re in the PVP block was relatively low (10–20%). In solvents that are selective for the Re-coordinated PVP block, a variety of morphologies were observed by TEM after

solvent evaporation. These included spheres and cylinders with cores of PS and coronas of the Re-containing PVP block. The morphologies observed were dependent on the relative block lengths and the polarities of the chosen solvents. The pendant Re groups are luminescent and further studies of these systems should be of clear interest.

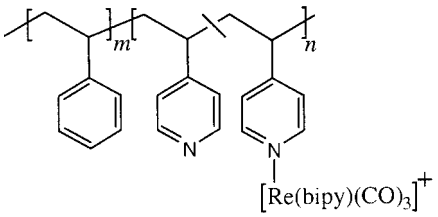

2.49

The attachment of Au units to the P2VP units of similar block copolymers has been explored as a means of accessing nanolithographic templates [99, 100]. Dissolution of polystyrene-*b*-poly(2-vinylpyridine) in toluene leads to spherical micelles with a core of P2VP and a corona of PS. Treatment of such solutions with $HAuCl_4$ leads to protonation to afford **2.50** with electrostatically bound $[AuCl_4]^-$ anions.

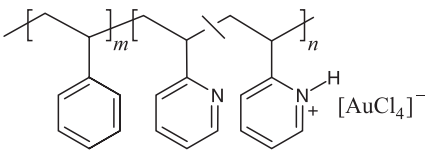

2.50

Films of densely packed spherical micelles can be prepared by dipping substrates such as GaAs wafers into the solutions, and these can be utilized in nanolithography to create islands or holes in substrates. The use of an Ar^+ beam resulted in slower etching of the PS-covered Au-containing micellar cores relative to the GaAs substrate and islands of diameter 20 nm were created (Fig. 2.9). On the other hand, Au-loaded block copolymer micelles in which prior reduction of Au^{III} to a single particle of elemental Au in the core had taken place gave different results. In films of these micelles, the cores were selectively etched *faster* than the PS corona by an Ar^+ beam as the sputtering probability is proportional to the square of the mass number of the element, and polymer-Au interactions are reduced in this case. This generated 10 nm diameter holes in substrates such as GaAs, which were rapidly etched relative to PS (Fig. 2.10) [99].

Similar synthetic strategies involving the attachment of Pd complexes to the PVP block, followed by reduction to yield catalytically-active metal nanoparticles in

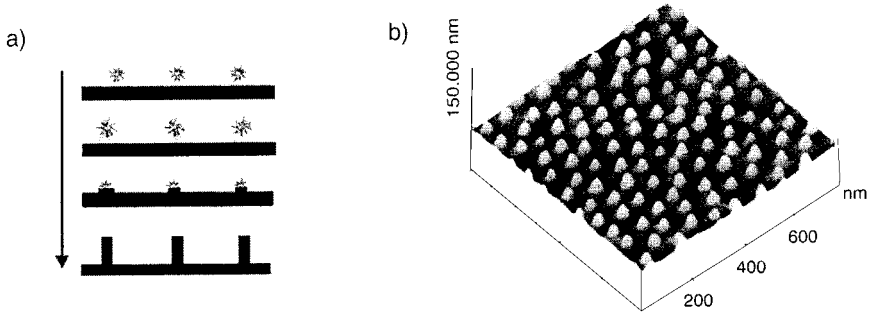

Fig. 2.9 (**a**) Schematic and (**b**) scanning force microscope image showing the formation of islands using a nanolithographic micellar mask based on Au-containing block copolymer **2.50**. Relative etch rates: substrate GaAs 30, PS 15, P2VP 15, P2VP/$HAuCl_4$ 36 Å min^{-1} (Ar^+ beam normal to substrate, 1.1 keV energy, 12 μA/cm^2 current density). (Adapted from [99])

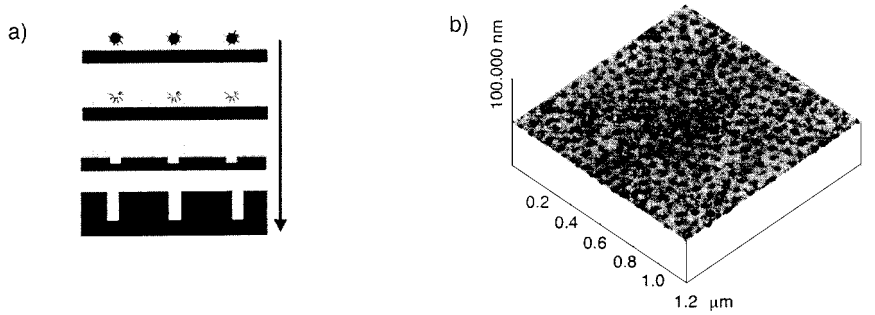

Fig. 2.10 (**a**) Schematic and (**b**) scanning force microscope images showing the formation of holes using a nanolithographic micellar mask based on Au-containing block copolymer **2.50** containing a single gold particle due to reduction prior to film formation. Relative etch rates: substrate GaAs 30, PS 15, P2VP 15, Au 360 Å min^{-1} (Ar^+ beam normal to substrate, 1.1 keV energy, 12 μA/cm^2 current density). (Adapted from [99])

the micellar core, have also been explored by several groups. Applications in the Heck reaction have been studied in detail and advantages over the use of low molecular weight Pd catalysts in terms of stability and ease of use have been demonstrated [101].

2.3.4.3 Coordination to Other Substituents in Preformed Blocks

The coordination of metals to various other pendant sites present in block copolymers has also been explored. For example, metal coordination to the olefinic groups present in the polybutadiene blocks of polystyrene-*b*-polybutadiene (PS-*b*-PB) diblock and PS-*b*-PB-*b*-PS triblock copolymers has been reported [102]. This was achieved by the reaction of the block copolymers with various metal complexes such as $Fe_3(CO)_{12}$, $[Rh(\mu\text{-}Cl)(CO)_2]_2$, $PdCl_2(NCMe)_2$, and $PtCl_2(NCMe)_2$ to

afford materials with Fe-, Rh-, Pd-, and Pt-containing blocks. Intermolecular cross-linking was possible, but solubility in organic solvents was maintained and micellization was observed in most cases. However, on solvent removal and drying, many of the polymers became insoluble.

The pendant phosphino groups of polystyrene-*b*-poly(vinyltriphenylphosphine) (PS-*b*-PVTPP) have also been used to coordinate Pd salts [103]. Complex aggregation phenomena were observed in solution due to the possibility of intermolecular cross-linking reactions, and reduction with hydrazine or other reductants was shown to yield Pd nanoparticles.

As a final example, the anionic sites generated from polyacrylic acid core-forming blocks within cross-linked micelles of triblock copolymers in water have also been used to bind Pd^{2+} ions [104]. In this case, subsequent reduction with hydrazine yielded Pd nanoparticles, which were shown to catalyze the hydrogenation of alkenes.

2.4 References

1 F. S. Arimoto, A. C. Haven, Jr., *J. Am. Chem. Soc.* **1955**, *77*, 6295.

2 G. Wilkinson, *J. Organomet. Chem.* **1975**, *100*, 273.

3 (a) *Ferrocenes* (Eds.: A. Togni, T. Hayashi), VCH Publishers, New York, **1995**. (b) N. J. Long, *Metallocenes*, Blackwell Science, Oxford, **1998**.

4 Inorganic Materials, 2nd ed. (Eds.: D. W. Bruce, D. O'Hare), John Wiley & Sons, Toronto, **1996**.

5 E. W. Neuse, H. Rosenberg, *J. Macromol. Sci. – Rev. Macromol. Chem.* **1970**, *C4*, 1.

6 I. Manners, *Angew. Chem. Int. Ed. Engl.* **1996**, *35*, 1602.

7 C. U. Pittmann, Jr., R. L. Voges, J. Elder, *Polym. Lett.* **1971**, *9*, 191.

8 C. U. Pittmann, Jr., P. L. Grube, *J. Polym. Sci. Part A-1* **1971**, *9*, 3175.

9 J. C. Lai, T. Rounsfell, C. U. Pittmann, Jr., *J. Polym. Sci. Part A-1* **1971**, *9*, 651.

10 Y. Sasaki, L. L. Walker, E. L. Hurst, C. U. Pittmann, Jr., *J. Polym. Sci. Polym. Chem. Ed.* **1973**, *11*, 1213.

11 M. H. George, G. F. Hayes, *J. Polym. Sci. Polym. Chem. Ed.* **1975**, *13*, 1049.

12 M. H. George, G. F. Hayes, *J. Polym. Sci. Polym. Chem. Ed.* **1976**, *14*, 475.

13 C. U. Pittmann, Jr., J. C. Lai, D. P. Vanderpool, M. Good, R. Prados, *Macromolecules* **1970**, *3*, 746.

14 C. Aso, T. Kunitake, T. Nakashima, *Makromol. Chem.* **1969**, *124*, 232.

15 (a) O. Nuyken, V. Burkhardt, T. Pöhlmann, M. Herberhold, *Makromol. Chem., Macromol. Symp.* **1991**, *44*, 195. (b) O. Nuyken, V. Burkhardt, C. Hübsch, *Macromol. Chem. Phys.* **1997**, *198*, 3353; (c) O. Nuyken, V. Burkhardt, T. Pöhlmann, M. Herberhold, F. J. Litterst, C. Hübsch, in: *Macromolecular Systems: Microscopic Interactions and Macroscopic Properties* (Eds.: H. Hoffmann, M. Schwoerer, T. Vogtmann), Wiley-VCH, Weinheim, **2000**, pp. 305–324.

16 S. Swarup, A. N. Nigam, *Polym. Commun.* **1989**, *30*, 190.

17 T. W. Smith, J. E. Kuder, D. Wychick, *J. Polym. Sci. Polym. Chem. Ed.* **1976**, *14*, 2433.

18 (a) J. B. Flanagan, S. Margel, A. J. Bard, F. C. Anson, *J. Am. Chem. Soc.* **1978**, *100*, 4248; (b) A. Diaz, M. Seymour, K. H. Pannell, J. M. Rozell, *J. Electrochem. Soc.* **1990**, *137*, 503.

19 D. O. Cowan, J. Park, C. U. Pittmann, Jr., Y. Sasaki, T. K. Mukherjee, N. A. Diamond, *J. Am. Chem. Soc.* **1972**, *94*, 5110.

20 C. U. Pittmann, Jr., B. Surynarayanan, Y. Sasaki, in: *Inorganic Compounds with*

Unusual Properties, American Chemical Society, Adv. Chem Ser. **1976**, *150*, 46.
21 D. O. Cowan, F. Kaufman, *J. Am. Chem. Soc.* **1970**, *92*, 219.
22 D. O. Cowan, F. Kaufman, *J. Am. Chem. Soc.* **1970**, *92*, 6198.
23 C. U. Pittmann, Jr., J. C. Lai, D. P. Vanderpool, M. Good, R. Prados, in: *Polymer Characterization: Interdisciplinary Approaches* (Ed.: C. D. Craver), Plenum Publishing Corp., New York, **1971**; pp. 97–124.
24 G. P. Kittlesen, H. S. White, M. S. Wrighton, *J. Am. Chem. Soc.* **1985**, *107*, 7373.
25 M. L. H. Green, S. R. Marder, M. E. Thompson, J. A. Bandy, D. Bloor, P. V. Kolinsky, R. J. Jones, *Nature* **1987**, *330*, 360.
26 M. E. Wright, E. G. Toplikar, R. F. Kubin, M. D. Seltzer, *Macromolecules* **1992**, *25*, 1838.
27 Y. Yang, Z. Xie, C. Wu, *Macromolecules* **2002**, *35*, 3426.
28 D. Albagli, G. Bazan, M. S. Wrighton, R. R. Schrock, *J. Am. Chem. Soc.* **1992**, *114*, 4150.
29 D. Albagli, G. C. Bazan, R. R. Schrock, M. S. Wrighton, *J. Phys. Chem.* **1993**, *97*, 10211.
30 T. Nakashima, T. Kunitake, *Makromol. Chem.* **1972**, *157*, 73.
31 C. U. Pittmann, Jr., Y. Sasaki, P. L. Grube, *J. Macromol. Sci., Chem.* **1974**, *A8 (5)*, 923.
32 C. Simionescu, T. Lixandru, I. Negulescu, I. Mazilu, L. Tataru, *Makromol. Chem.* **1973**, *163*, 59.
33 C. Simionescu, T. Lixandru, I. Mazilu, L. Tataru, *Makromol. Chem.* **1971**, *147*, 69.
34 M. Buchmeiser, R. R. Schrock, *Macromolecules* **1995**, *28*, 6642.
35 G. Zotti, S. Zecchin, G. Schiavon, A. Berlin, G. Pagani, A. Canavesi, *Chem. Mater.* **1995**, *7*, 2309.
36 A. Weisemann, R. Zentel, G. Lieser, *Acta Polym.* **1995**, *46*, 25.
37 (a) G. Wilbert, S. Traud, R. Zentel, *Macromol. Chem. Phys.* **1997**, *198*, 3769; (b) for related work see F. Turpin, D. Guillon, R. Deschenaux, *Mol. Cryst. Liq. Cryst.*, **2001**, *362*, 171.
38 G. Caldwell, M. G. Meirim, E. W. Neuse, C. E. J. van Rensburg, *Appl. Organomet. Chem.* **1998**, *12*, 793.
39 J. Hodak, R. Etchenique, E. J. Calvo, K. Singhal, P. N. Bartlett, *Langmuir* **1997**, *13*, 2708.
40 C.-L. Wang, A. Mulcandani, *Anal. Chem.* **1995**, *67*, 1109.
41 S.-F. Hou, H.-Q. Fang, H.-Y. Chen, *Anal. Lett.* **1997**, *30*, 1631.
42 J. E. Sheats, F. Hessel, L. Tsarouhas, K. G. Podejko, T. Porter, L. B. Kool, R. L. Nolan, Jr., in: *Metal-containing Polymer Systems* (Eds.: J. E. Sheats, C. E. Carraher, Jr., C. U. Pittmann, Jr.), Plenum Publishing Corp., New York, **1985**, pp. 83–98.
43 C. T. Willis, J. E. Sheats, *J. Polym. Sci. Polym. Chem.* **1984**, *22*, 1077.
44 R. H. Grubbs, C. Gibbons, L. C. Kroll, W. D. Bonds, C. H. Brubaker, *J. Am. Chem. Soc.* **1973**, *95*, 2373.
45 W. D. Bonds, C. H. Brubaker, E. S. Chandrasekaran, C. Gibbons, R. H. Grubbs, L. C. Kroll, *J. Am. Chem. Soc.* **1975**, *97*, 2128.
46 R. Grubbs, C. P. Lau, R. Cukier, C. H. Brubaker, *J. Am. Chem. Soc.* **1977**, *99*, 4517.
47 A. G. M. Barrett, Y. R. de Miguel, *Chem. Commun.* **1998**, 2079.
48 S. B. Roscoe, J. M. J. Fréchet, J. F. Walzer, A. J. Dias, *Science* **1998**, *280*, 270.
49 H. R. Allcock, K. D. Lavin, G. H. Riding, *Macromolecules* **1985**, *18*, 1340.
50 H. R. Allcock, G. H. Riding, K. D. Lavin, *Macromolecules* **1987**, *20*, 6.
51 I. Manners, G. H. Riding, J. A. Dodge, H. R. Allcock, *J. Am. Chem. Soc.* **1989**, *111*, 3067.
52 H. R. Allcock, J. A. Dodge, I. Manners, G. H. Riding, *J. Am. Chem Soc.* **1991**, *113*, 9596.
53 H. R. Allcock, J. A. Dodge, I. Manners, M. Parvez, G. H. Riding, K. B. Visscher, *Organometallics* **1991**, *10*, 3098.
54 R. A. Saraceno, G. H. Riding, H. R. Allcock, A. G. Ewing, *J. Am. Chem. Soc.* **1988**, *110*, 7254.
55 P. Wisian-Neilson, R. R. Ford, *Macromolecules* **1989**, *22*, 72.
56 P. Wisian-Neilson, C. Zhang, K. A. Koch, *Macromolecules* **1998**, *31*, 1808.

57 K. H. Pannell, J. M. Rozell, J. M. Ziegler, *Macromolecules* **1988**, *21*, 276.

58 A. Diaz, M. Seymour, K. H. Pannell, J. M. Rozell, *J. Electrochem. Soc.* **1990**, *137*, 503.

59 P. D. Hale, L. I. Boguslavsky, T. Inagaki, H. I. Karan, H. S. Lee, T. A. Skotheim, Y. Okamoto, *Anal. Chem.* **1991**, *63*, 677.

60 R. Deschenaux, I. Jauslin, U. Scholten, F. Turpin, D. Guillon, B. Heinrich, *Macromolecules* **1998**, *31*, 5647.

61 T. Arai, H. T. Ban, T. Uozumi, K. Soga, *J. Polym. Sci. Polym. Chem.* **1998**, *36*, 421.

62 T. J. Peckham, P. Nguyen, S. C. Bourke, Q. Wang, D. G. Harrison, P. Zoricak, C. Russell, L. M. Liable-Sands, A. Rheingold, A. J. Lough, I. Manners, *Organometallics* **2001**, *20*, 3035.

63 C. U. Pittmann, Jr., C.-C. Lin, T. D. Rounsefell, *Macromolecules* **1978**, *11*, 1022.

64 H. Nishide, H. Kawakami, Y. Kurimura, E. Tsuchida, *J. Am. Chem. Soc.* **1989**, *111*, 7175.

65 F. B. McCormick, B. B. Wright, J. W. Williams, in: *Metal-Containing Polymeric Materials* (Eds.: C. U. Pittmann, Jr., C. E. Carraher, Jr., M. Zeldin, J. E. Sheats, B. M. Culbertson), Plenum Publishing Corp., New York, **1996**, p. 177.

66 C. U. Pittmann, Jr., P. L. Grube, O. E. Ayers, S. P. McManus, M. D. Rausch, G. A. Moser, *J. Polym. Sci. Part A-1* **1972**, *10*, *379*.

67 C. U. Pittmann, Jr., C. E. Carraher, Jr., J. R. Reynolds, in: *Encycl. Polym. Sci. Eng.* (Ed.: J. I. Kroschwitz) Wiley-Interscience, New York, **1987**, *10*, p 564–578.

68 A. Juris, V. Balzani, F. Barigelletti, S. Campagna, P. Belser, A. von Zelewsky, *Coord. Chem. Rev.* **1988**, *84*, 85.

69 W. L. Wallace, A. J. Bard, *J. Phys. Chem.* **1979**, *83*, 1350.

70 R. S. Glass, L. R. Faulkner, *J. Phys. Chem.* **1981**, *85*, 1160.

71 M. Kaneko, S. Nemoto, A. Yamada, Y. Kurimura, *Inorg. Chim. Acta* **1980**, *44*, L289.

72 F. Zhao, J. Zhang, X. Hou, T. Abe, M. Kaneko, *J. Chem. Soc., Faraday Trans.* **1998**, *94*, 277.

73 C. T. Wong, W. K. Chan, *Adv. Mater.* **1999**, *11*, 455.

74 (a) J. N. Demas, B. A. DeGraff, *J. Chem. Educ.* **1997**, *74*, 690. (b) M. Gouterman, *J. Chem. Educ.* **1997**, *74*, 697.

75 (a) C. Preininger, I. Klimant, O. S. Wolfbeis, *Anal. Chem.* **1994**, *66*, 1841. (b) G. Di Marco, M. Lanza, S. Campagna, *Adv. Mater.* **1995**, *7*, 468. (c) M. C. Moreno-Bondi, O. S. Wolfbeis, M. J. P. Leiner, B. P. H. Schaffar, *Anal. Chem.* **1990**, *62*, 2377.

76 Z. Wang, A. R. McWilliams, C. E. B. Evans, X. Lu, S. Chung, M. A. Winnik, I. Manners, *Adv. Func. Mater.* **2002**, *12*, 415.

77 (a) R. Yoshida, T. Takahashi, T. Yamaguchi, H. Ichijo, *J. Am. Chem. Soc.* **1996**, *118*, 5134. (b) R. Yoshida, T. Takahashi, T. Yamaguchi, H. Ichijo, *Adv. Mater.* **1997**, *9*, 175.

78 R. Yoshida, T. Sakai, S. Ito, T. Yamaguchi, *J. Am. Chem. Soc.* **2002**, *124*, 8095.

79 N. Gajovicm, G. Binyamin, A. Warsinke, F. W. Scheller, A. Heller, *Anal. Chem.* **1998**, *70*, 2149.

80 D. W. Schmidtke, A. Heller, *Anal. Chem.* **2000**, *72*, 2963.

81 D. J. Caruana, A. Heller, *J. Am. Chem. Soc.* **1999**, *121*, 769.

82 N. Fujita, K. Sonogashira, *J. Polym. Sci. Polym. Chem.* **1974**, *12*, 2845.

83 J. M. Bellama, W. F. Manders, in: *Inorganic and Organometallic Polymers* (Eds.: M. Zeldin, K. J. Wynne, H. R. Allcock), ACS Symposium Series, vol. 360, American Chemical Society, Washington D.C., **1988**, p. 483.

84 B. Moraru, N. Hüsing, G. Kickelbick, U. Schubert, P. Fratzl, H. Peterlik, *Chem. Mater.* **2002**, *14*, 2732.

85 H. R. Allcock, R. W. Allen, J. P. O'Brien, *J. Am. Chem. Soc.* **1977**, *99*, 3984.

86 A. S. Abd-El-Aziz, L. J. May, J. A. Hurd, R. M. Okasha, *J. Polym. Sci. A Polym. Chem.* **2001**, *39*, 2716.

87 (a) P. Hodge, *Chem. Soc. Rev.* **1997**, *26*, 417; (b) C. U. Pittmann, Jr., in: *Comprehensive Organometallic Chemistry* (Eds.: G. Wilkinson, F. G. A. Stone, E. W. Abel), Vol. 8, Pergamon Press, Oxford, **1982**; p 553; (c) B. C. Gates, J. Lieto, in: *Encycl.*

Polym. Sci. Eng. (Ed.: J.I. Kroschwitz) **1987**, *2*, 708; (d) *Catalysis by Polymer-Immobilized Metal Complexes* A.D. Pomogailo, Gordon and Breach, **1998**.

88 A.N. Ajjou, H. Alper, *J. Am. Chem. Soc.* **1998**, *120*, 1466.

89 C. Carlini, G. Braca, F. Ciadelli, G. Sbrana, *J. Mol. Catal.* **1977**, *2*, 379.

90 P. Terreros, E. Pastor, J.L.G. Fierro, *J. Mol. Catal.* **1989**, *53*, 359.

91 P. Diversi, G. Ingrosso, A. Lucherini, A. Minutillo, *J. Mol. Catal.* **1987**, *40*, 359.

92 H.G. Tang, D.C. Sherrington, *J. Mol. Catal.* **1994**, *94*, 7.

93 G. Braca, M. Di Girolamo, A.M. Raspolli-Galletti, G. Sbrana, M. Brunelli, G. Bertolini, *J. Mol. Catal.* **1992**, *74*, 421.

94 T. Miyazawa, T. Endo, *J. Mol. Catal.* **1988**, *49*, L31.

95 C.C. Cummins, M.D. Beachy, R.R. Schrock, M.G. Vale, V. Sankaran, R. E. Cohen, *Chem. Mater.* **1991**, *3*, 1153.

96 V. Sankaran, J. Yue, R.E. Cohen, R.R. Schrock, R.J. Silbey, *Chem. Mater.* **1993**, *5*, 1133.

97 Y.N.C. Chan, G.S.W. Craig, R.R. Schrock, R.E. Cohen, *Chem. Mater.* **1992**, *4*, 885.

98 S. Hou, W.K. Chan, *Macromol. Rapid Commun.* **1999**, *20*, 440.

99 J.P. Spatz, T. Herzog, S. Mössmer, P. Ziemann, M. Möller, *Adv. Mater.* **1999**, *11*, 149.

100 J.P. Spatz, S. Mössmer, C. Hartmann, M. Möller, T. Herzog, M. Kreger, H.-G. Boyen, P. Ziemann, B. Kabius, *Langmuir* **2000**, *16*, 407.

101 S. Klingelhöfer, W. Heitz, A. Greiner, S. Oestreich, S. Förster, M. Antonietti, *J. Am. Chem. Soc.* **1997**, *119*, 10116.

102 L.D. Bronstein, M.V. Seregina, O.A. Platonova, Y.A. Kabachii, D.M. Chernyshov, M.G. Ezernitskaya, L.V. Dubrovina, T.P. Bragina, P.M. Valetsky, *Macromol. Chem. Phys.* **1998**, *199*, 1357.

103 D.M. Chernyshov, L.D. Bronstein, H. Börner, B. Berton, M. Antonietti, *Chem. Mater.* **2000**, *12*, 114.

104 R.S. Underhill, G. Liu, *Chem. Mater.* **2000**, *12*, 3633.

3
Main-Chain Polymetallocenes with Short Spacer Groups

3.1
Introduction

Although the first polymers with metals in the side chains were prepared as early as the mid-1950s, the development of main-chain metal-containing polymers has been much slower. This is particularly the case when the metal atoms are linked together by short spacers and their close spatial proximity might be expected to give rise to interesting properties due to the presence of metal-metal interactions. This chapter focuses on materials of this type which contain metallocene units in the main chain, as polymers possessing these organometallic moieties dominate this particular area. Analogous materials with longer spacers, defined as those having more than three atoms between the π-coordinated metal centers, are structurally much more diverse but, in general, less well-studied. These polymers will be discussed in Chapter 4.

As in the case of side-chain metal-containing polymers (Chapter 2), the development of main-chain polymers that incorporate metallocene units has represented a major area of research. Since the discovery and structural elucidation of ferrocene, the prototypical metallocene, a vast organic chemistry has been demonstrated for this species, and the reversible one-electron oxidation to the blue ferrocenium ion has been much exploited [1–3]. The exciting possibilities for polyferrocenes with short spacers between the metal-containing units are illustrated by the results of detailed studies of dimeric species. Thus, oxidation of biferrocenes and biferrocenylenes has provided access to mixed-valent species such as **3.1** and **3.2**, respectively, in which the unpaired electrons are delocalized on a variety of time scales depending on substituent, counterion, and solid-state environmental effects [4, 5]. Many of the other properties of molecular ferrocenes also make their incorporation into polymer structures highly desirable. For example, liquid-crystalline ferrocenes have been prepared and ferrocene-based charge-transfer materials such as **3.3** have attracted considerable attention with respect to their cooperative magnetic properties [6, 7]. Equally encouraging are the facts that ferrocene is easy to prepare, cheap and commercially available, and air-, moisture-, and thermally-stable.

As described in Chapter 2, attempts to incorporate ferrocene into the side-chain structure of polymers have been very successful. In this case, a variety of high

Synthetic Metal-Containing Polymers. Ian Manners

ISBN: 3-527-29463-5

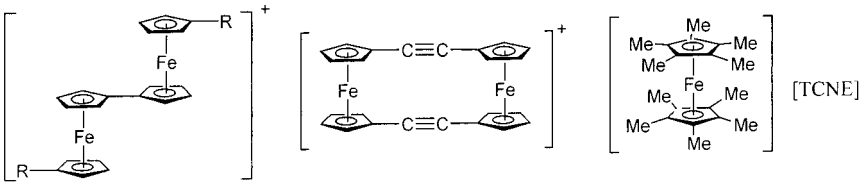

3.1 3.2 3.3

molecular weight materials have been prepared with either organic or inorganic main chains by means of subtle modifications of existing synthetic methodologies. The incorporation of ferrocene into the main chain of polymers, where the organometallic groups are joined by long spacers (i.e. with three or more atoms) has also been productive, as discussed in Chapter 4. In such cases, advantage can be taken of the facile derivatization of ferrocene to access well-defined difunctional monomers, which can then be productively used in step-growth polycondensation reactions. High molecular weight polymeric materials result, provided that the coupling methodology is compatible with the presence of the organometallic nucleus. In contrast to the situation with side-chain polymers and main-chain materials with long spacer groups, until the early 1990s the synthesis of main-chain polymers containing ferrocene units in close proximity to one another had met with very limited success. The problem regarding the synthesis of such materials arises from the fact that suitable, well-defined difunctional monomers are difficult to prepare in a high degree of purity. Under such conditions, step-growth polycondensation reactions are prone to yield low molecular weight oligomeric products. The discovery of ring-opening polymerization (ROP) routes to such materials in 1992 represented a key solution to this problem (see Sections 3.3 and 3.4) [8]. As discussed earlier (Chapter 1, Section 1.5.2.2.3), such polymerizations proceed by a chain-growth route, which tends to yield high molecular weight polymers without the stringent stoichiometry and conversion requirements characteristic of step-growth polycondensations.

Nevertheless, despite these breakthroughs, it is very apparent that the incorporation of metallocenes other than ferrocene into polymer structures has been developed to a much lesser extent, and for the 21st century, this still remains a substantial synthetic challenge. This is despite the fact that many other metallocenes are readily accessible, stable, and also exhibit interesting physical, redox, and catalytic properties [2, 4, 9]. The lower ease of derivatization of most other metallocenes compared to ferrocene and, in some cases (e.g. that of ruthenocene), the problem of relative expense, have clearly been important factors which have held back synthetic developments in this area. Nevertheless, it is anticipated that the development of main-chain polymers based on other metallocenes is likely to be very fertile ground for future research.

Excellent, critical reviews of the general field of main-chain metallocene-based polymers were published as early as 1970 [10]. At this time, the authors were more than aware of the limitations in the characterization of the vast majority of

the materials being reported. Indeed, the authors stated that many of the structures assigned to the polymers in the article were "hypothetical and need rigorous analytical verification" and added that "the description of experimental procedures and polymer properties more often than not has been superficial or has been lacking altogether" [11]. Although the earlier, pioneering work in the area will be mentioned, this chapter will focus on the more recent developments, as many of the materials reported earlier were of very low molecular weight, showed poor solubility, and were inadequately characterized.

3.2 Polymetallocenylenes and Polymetallocenes with Short Spacers Obtained by Condensation Routes

3.2.1 Polymetallocenylenes

The earliest routes to polyferrocenylene involved poorly defined free-radical recombination processes (Eq. 3.1). In 1960, the polymerization of molten ferrocene at 200 °C in the presence of approximately stoichiometric amounts of *t*-butyl peroxide, *t*-BuO*O*t-Bu, as the radical source was described [12–14]. The yields of soluble material of idealized structure **3.4** were low (ca. 5–15%), as were the molecular weights (<7000).

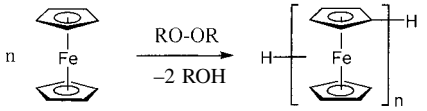

(3.1)

3.4

A later reinvestigation of the original work that used elemental analysis, IR and NMR spectroscopy, and thermogravimetric analysis to characterize the products confirmed the uncontrolled nature of the polymerization [15, 16]. It is presumed that ferrocene radicals **3.5** are generated by hydrogen abstraction from the cyclopentadienyl rings by *t*-BuO$^{\bullet}$ species formed upon initiator thermolysis. Although the former can subsequently recombine to form ferrocenylene oligomers, the soluble polymer product of idealized structure **3.4** was found to contain both homoannular (1,2- and 1,3-) and heteroannular (1,1′-) ferrocene units. This is attributed to the presence of the multiple C–H sites on the metallocene that can participate in radical generation. Moreover, the reinvestigation also provided evidence for the presence of alkoxy substituents derived from the recombination of ferrocene-based radicals with *t*-BuO$^{\bullet}$ species (Scheme 3.1) [15, 16].

Subsequently, a series of different radical reactions were reported, such as mixed Ullmann reactions of halo- and 1,1′-dihaloferrocene with copper bronze [17, 18], coupling reactions of lithio- and 1,1′-dilithioferrocene with cobalt chloride in the pres-

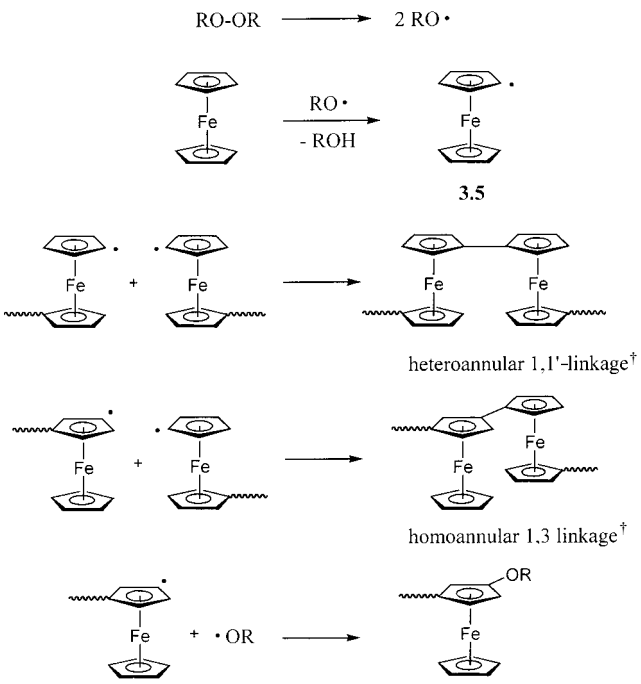

Scheme 3.1 † note that the annularity is specified for the ferrocene unit on the left side of the structure

ence of organic halides [19–21], and the treatment of poly(mercuriferrocenylene) with metallic silver [22], or heating in molten ferrocene [23], or the use of glow-discharge polymerization [24]. All routes led to oligomers with molecular weights in the range $M_n = 1000–3500$, with poorly defined structures and paramagnetic behavior. The latter property may arise from the presence of impurities or oxidized iron sites within the oligomer chain [10]. In the case of glow-discharge polymerization, cross-linked polyferrocenylene was produced. Other reported methods, such as polyrecombination processes involving chloromercuri- and bis(chloromercuri)ferrocene assisted by palladium salts [25], or the direct reaction of dilithioferrocene · TMEDA with cobalt chloride [26], resulted in the formation of paramagnetic oligomers in low yields together with biferrocenylene resulting from internal cyclization processes.

The conductivity of unoxidized oligo(1,1′-ferrocenylene), prepared by the radical recombination of ferrocene, was studied, and this led to the conclusion that the material was an insulator [27–29]. However, upon partial oxidation with iodine or quinones, the presence of mixed-valence states led to a dramatic increase in conductivity from a value of 10^{-14} Scm^{-1} for the pristine material to a maximum of 10^{-6}–10^{-8} Scm^{-1} at room temperature. Similar values have been determined for biferrocenylene and biferrocene salts [30–32].

Arguably the most impressive early results on polyferrocenylenes in terms of product yield, molecular weight, and purity were obtained in 1979 using the step-

growth polycondensation reaction of equimolecular amounts of dilithioferrocene · TMEDA with diiodoferrocene at temperatures not exceeding 25 °C (Eq. 3.2) [33]. Using this method, a yield of 85% of light-tan, soluble, spectroscopically well-defined (all heteroannular), amorphous and diamagnetic polyferrocenylene (**3.6**) was produced with $M_n < 4000$ (determined by vapor-pressure osmometry, VPO). Subsequent fractionation yielded small quantities of samples with M_n values of up to ca. 1×10^4.

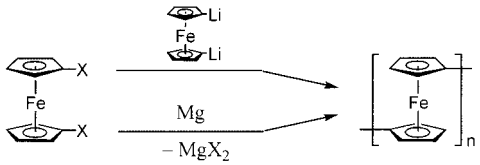

X = Br, I **3.6** (3.2)

Following this development, dehalogenation of dihaloferrocenes with magnesium was shown to produce semicrystalline polyferrocenylene **3.6** in good yield (Eq. 3.2) [34, 35]. When a benzene-insoluble fraction of the product ($M_n = 4600$) was partially oxidized with 7,7,8,8-tetracyanoquinodimethane (TCNQ), the electrical conductivity of the resulting material ($\sigma \approx 10^{-2}$ Scm^{-1}) was found to be higher than that observed previously for the amorphous polyferrocenylene [35], presumably as a consequence of an appreciable degree of crystallinity detected in the former [36]. Rapid electron transfer between the Fe^{II} and Fe^{III} sites was also detected for these TCNQ-doped crystalline materials on the Mössbauer spectroscopic time scale (ca. 10^{-7} s) at room temperature [35]. This is illustrated in Fig. 3.1, in which the individual quadrupolar doublets for the Fe^{II} and the Fe^{III} environments, which are still resolved at –196 °C, are seen to merge at 28 °C. On the other hand, analogous studies of I_2-oxidized materials indicated hole localization on the Mössbauer time scale and lower conductivities ($\sigma \approx 10^{-4}$ Scm^{-1}). This was attributed to the amorphous nature of the materials, as indicated by powder X-ray diffraction (PXRD) studies. These observations were supported by electrochemical studies of polyferrocenylene-modified electrodes, in which the presence of multiple or broad peaks was interpreted in terms of some degree of hole delocalization among the iron atoms on the cyclic voltammetric time scale [37]. Further detailed studies on the electronic structure of polyferrocenylene **3.6** by UV photoelectron spectroscopy suggested that the appreciable rather than high conductivity of these polymers is a consequence of limited hole mobility [38]. The occupied orbitals for **3.6**, based on this work, are shown in Fig. 3.2. As expected, the doping of polyferrocenylene was predicted to be facile, based on the low ionization threshold energies. However, the band dispersion (or bandwidth) was only estimated to be roughly 0.6 eV. This value is rather small compared to the 2–4 eV typical of conjugated organic polymers such as poly(*p*-phenylene) and polyacetylene. Thus, the narrow bands would be expected to result in a relatively limited degree of hole delocalization, and this led to the description of the system as having intermediate delocalization between that of π-conjugated conducting polymers such as polyacetylene and σ-localized insulating polymers such as polyethy-

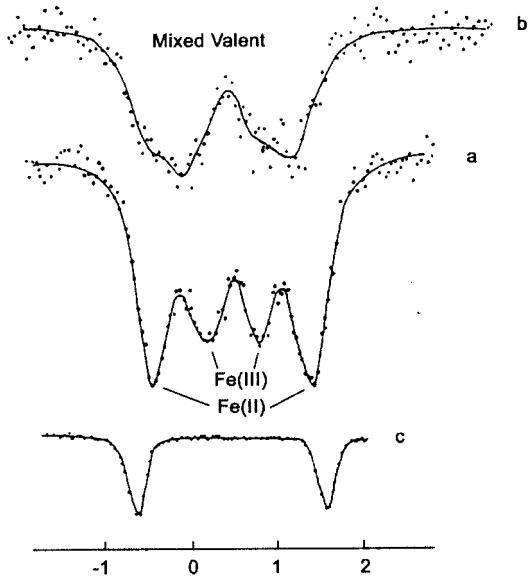

Fig. 3.1 Mössbauer spectra of the adduct of polyferrocenylene (**3.6**) with 0.81 equivalents of TCNQ, showing that the quadrupolar doublets for the Fe^{II} and Fe^{III} environments, which (**a**) are still resolved at –196 °C, (**b**) merge at 28 °C due to hole delocalization on the timescale of the experiment (ca. 10^{-7} s). (**c**) The Mössbauer spectrum of polyferrocenylene at room temperature is shown for comparison and features a single Fe^{II} quadrupolar doublet. (Adapted from [35])

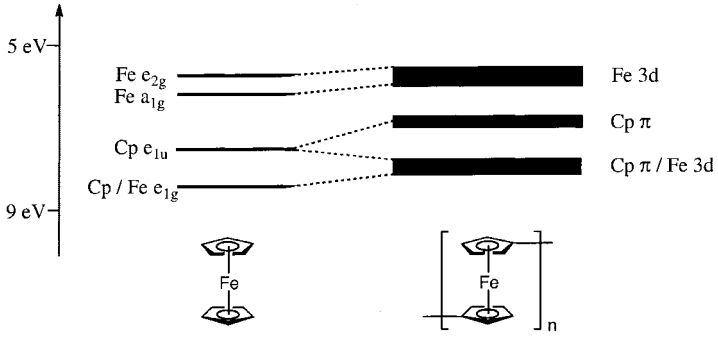

Fig. 3.2 Qualitative representation of the occupied orbitals of polyferrocenylene (**3.6**) and ferrocene based on ultraviolet photoelectron spectroscopic data, assuming a staggered conformation of the metallocene units. (Adapted from [38])

lene. It should be noted that, although the hole delocalization is limited in polyferrocenylene **3.6**, as discussed above, it can become apparent using "slow" techniques with relatively long time scales, such as Mössbauer spectroscopy (ca. 10^{-7} s).

In 1996, an alternative synthetic methodology was developed, which permits the synthesis of more soluble *n*-hexyl-substituted polyferrocenylenes. This involved the reaction of the dihexylfulvalene dianion with $[FeCl_2(THF)_2]$ (Eq. 3.3) [39]. Although this step-growth polycondensation method does not generate high molecular weight materials in large quantities, a fraction of poly(1,1′-dihexylferrocenylene) (**3.7**) with $M_n \approx 5000$ and PDI = 1.2 was isolated in very low yield. In addition, when oxidized with TCNQ or tetracyanoethylene (TCNE), this material exhib-

ited photoconductivity and acted as a p-type semiconductor. The electrochemistry of both the polymer and individual oligomers is consistent with the presence of substantial metal-metal interactions [39].

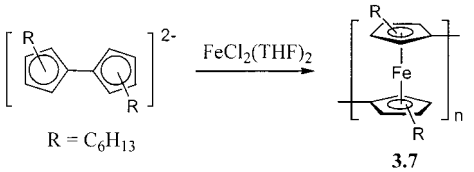

3.7 (3.3)

Copper-mediated polycondensations of diiodoferrocenes and bis(stannyl)ferrocenes at 150–180 °C have also been used to prepare fairly low molecular weight, well-characterized polyferrocenylenes with substituents on the Cp rings (Eq. 3.4) [40]. Yellow-orange to tan-colored polyferrocenylenes **3.8** with solubilizing groups such as methyl or trimethylsilyl substituents were prepared. These polymers possess molecular weights in the range of $M_n \approx 1500–3600$ (PDI ≈ 1.5–3.0). Cyclic voltammetric studies showed two waves with a very large redox-coupling (0.46–0.485 V) indicative of the presence of substantial metal-metal interactions (Fig. 3.3), with the first wave representing initial oxidation at alternating iron sites (see Section 3.3.6.3 for a more detailed discussion on related systems). However, although the TCNE adducts of **3.8** showed broad intervalence electron-transfer bands in the near-IR region, their Mössbauer spectra were consistent with a trapped valence state (i.e. discrete Fe^{II} and Fe^{III} sites) on the time scale for this technique (ca. 10^{-7} s) [40].

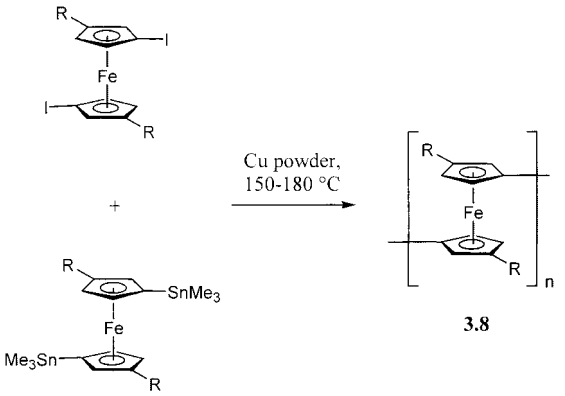

3.8 (3.4)

Apart from the case of polyferrocenylenes, very little work has been reported on analogous materials containing directly linked metallocene units. The synthesis of very low molecular weight polyruthenocenylenes **3.9** ($M_n \approx 1400$) using, for example, Ullmann coupling has been briefly described (Eq. 3.5). The few results on oli-

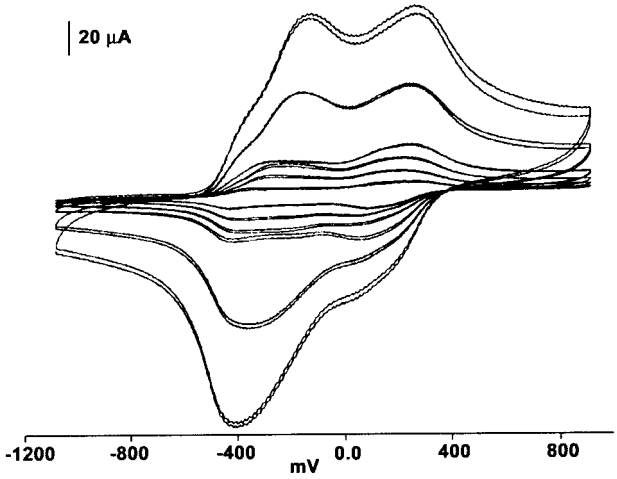

Fig. 3.3 Cyclic voltammograms of polyferrocenylene **3.8** (R = Me) at various scan rates (0.1 M $[Bu_4N][PF_6]$ in CH_2Cl_2) showing two reversible oxidation waves separated by a redox coupling $\Delta E_{1/2}$ of ca. 0.47 V. (Adapted from [40])

gomeric materials in this area are summarized in an excellent review that covers work on polymetallocenylenes prior to 1981 [41].

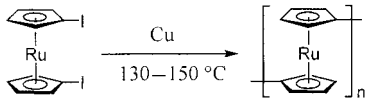

(3.5)

3.9

3.2.2

Other Polymetallocenes with Short Spacers Obtained by Polycondensation Routes

Polymetallocenes with single-carbon spacers (i.e. **3.10**) have been the focus of numerous investigations. Polycondensation routes developed in the 1960s involved the reaction of aldehydes with the corresponding metallocenes (M = Fe, Ru), as well as the cationic polymerization of carbinols. These and related routes have been critically reviewed in detail [10]. Both methods were carried out using Lewis- or protic-acid catalysts and yielded similar products. The materials obtained were oligomeric and consisted of a mixture of heteroannular (1,1′-) and homoannular (1,2- and 1,3-) metallocene units. Crosslinking was also noted at high temperatures and resulted in an increase in the number of methylene bridges per repeat unit.

A similar route was reported in the mid-1960s for the synthesis of polyferrocenes with phosphorus spacers (**3.11**, **3.12**) [42, 43]. Reaction of ferrocene with $PPhCl_2$, $P(O)PhCl_2$ or $P(S)PhCl_2$ in the presence of a Lewis acid catalyst such as $ZnCl_2$ in the melt or in solution at 80–170 °C yielded low molecular weight materials

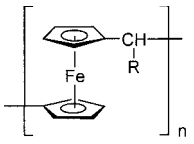

3.10

R = H, CH_3, C_6H_5

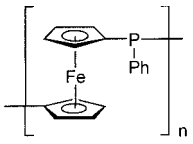

3.11

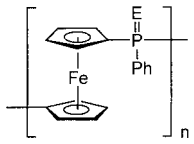

3.12

E = O, S

(M_n < 6000 by VPO and generally < 3500). The composition of the materials depended on the reaction conditions. Again, this work has been reviewed in detail [10].

In 1982, well-defined materials of structure **3.11** were obtained from the reported polycondensation reaction of 1,1′-dilithioferrocene · TMEDA with $PPhCl_2$ [44]. The molecular weights of the polyferrocenylphosphine products were found to depend on the reaction conditions. For example, products with M_w = 8900 (by light-scattering) were reported when the reaction was performed in dimethoxyethane at 25 °C, while high molecular weights (M_w = 131,000–161,000) were obtained in diethyl ether at 25 °C or in dimethoxyethane at –40 °C. The high molecular weights in the latter cases are highly unexpected as dilithioferrocene is extremely reactive and difficult to purify, and polycondensation reactions require exact reaction stoichiometries in order to achieve appreciable chain lengths (see Chapter 1, Section 1.5.2.2.2). Significantly, more recent work in the mid-1990s has shown that these high molecular weight products probably arise from a chain-growth reaction, rather than from a polycondensation, which involves the anionic ring-opening polymerization of a phosphorus-bridged [1]ferrocenophane generated *in situ* (see Section 3.3.3) [45].

The air- and thermally stable (to > 350 °C) polyferrocenylphenylphosphine **3.11** was shown to react with low concentrations of $Co_2(CO)_8$, leading to products containing chelated cobalt centers [46]. According to IR and ^{31}P NMR data, three Co–P bonds were present per metal atom, and the cobalt environments possessed a pseudo-trigonal bipyramidal geometry. The catalytic potential of the materials in the hydroformylation of 1-hexene was studied and was shown to be similar to that of the complex $HCo(CO)_3PPh_3$.

Polyferrocenylsilanes (**3.13**) of very low molecular weight were first described in two patents in the 1960s [47, 48]. The polymers were prepared from dilithioferrocene by a reported polycondensation reaction with the appropriate dihaloorganosilanes (Me_2SiCl_2 or Ph_2SiCl_2) in polar solvent mixtures at 0–25 °C. The resulting materials were described as black or chocolate-brown in color. Although clearly impure, the partially soluble polymers were reported to be reasonably thermally stable (to > 250 °C). VPO gave molecular weights M_n of 1700–3400 (R = Me) and 2400–7000 (R = Ph), which correspond to ca. 5–19 repeat units [48].

This work was preceded by an investigation of an alternative route involving the condensation of $FeCl_2$ with $Li_2[(C_5H_4)_2SiMe_2]$, which afforded even lower molecular weight samples of **3.13** (R = Me) that should be termed oligo(ferrocenyldimethylsilane)s [47]. Recently, slightly higher molecular weight materials with M_n up to

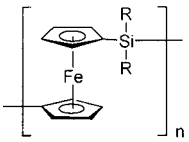

3.13

R = Me, Ph

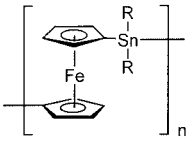

3.14

R = Me, Et, *n*-Bu, Ph

4100 have been reported using this route [49]. The low values of M_n obtained are to be expected for step-growth polycondensation processes involving dilithio reagents, which are difficult to obtain in a high degree of purity (see Chapter 1, Section 1.5.2.2.2). The synthesis of low molecular weight polyferrocenylstannanes (**3.14**) with M_w up to 4600 has also been reported using an analogous polycondensation pathway involving dilithioferrocene [50, 51].

Poly(ferrocenylenevinylene) derivatives (**3.15**) with M_n values of 3000–10,000 and polydispersities of ca. 2.2–2.8 (determined by GPC) were synthesized in 1995 in high yields by a titanium-induced McMurry coupling reaction of the corresponding alkylferrocenyl carbaldehyde monomers (Eq. 3.6) [52]. Characterization of these soluble polymers by NMR and IR revealed the presence of *trans*-vinylene units. The UV/vis spectra of the polymers are similar to those of the monomers and this indicates a fairly localized electronic structure in the former. The relatively limited electron delocalization is also reflected in the electrical and optical properties. For example, the values for iodine-doped conductivity ($\sigma = 10^{-2}$ S cm^{-1}) and nonlinear third-order optical susceptibility ($\chi^{(3)} = 1\text{–}4\times10^{-12}$ esu) are lower than those of linear conjugated polymers such as poly(1,4-phenylenevinylene) ($\sigma = 2.5\times10^{3}$ S cm^{-1}, $\chi^{(3)} = 8\times10^{-12}$ esu).

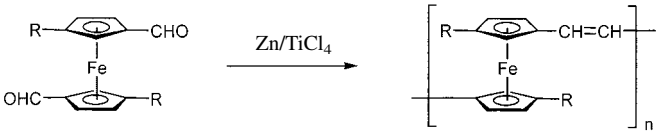

(3.6)

3.15

R = C_2H_5, C_6H_{13}, $C_{12}H_{25}$

Ferrocene-acetylene polymers **3.16** with the metallocene units linked through their 1,3-positions have been prepared by a Pd-catalyzed polycondensation process (Eq. 3.7) and their properties have been investigated in some detail [53, 54]. Fractions of **3.16** (R = CH_2NMe_2) with molecular weights of up to $M_n \approx 4300$ and PDI ≈ 1.7 were successfully prepared, and UV/vis spectroscopy provided evidence for significant electron delocalization in these interesting 1,3-substituted materials. More detailed studies were conducted on polymers **3.16** (R = CH_2OMe) with proposed molecular weights of ca. 10,000. The relationship between λ_{max} for the ferrocene d–d band transition versus $1/n$ (n = number of ferrocene-acetylene repeat

units) was found to be linear, with a limiting value of $\lambda_{max}=472$ nm for $n=\infty$. In addition, electrochemical studies indicated the presence of redox couplings (ca. 0.15 V) that provided further evidence for substantial electronic communication between the metallocene units [54].

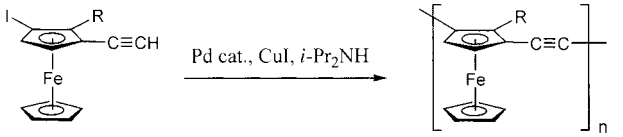

(3.7)

3.16

R = CH_2OMe or CH_2NMe_2

Disulfide-bridged oligoferrocenes **3.18** ($M_w < 3500$) were prepared in an attempt to copolymerize ferrocenedithiol with norbornadiene in the presence of AIBN in toluene [55, 56]. Rather than the expected radical-induced polyaddition [57] to give **3.17** (Eq. 3.8), condensation of the ferrocene monomer was observed with norbornene and nortricyclane units as end-groups (Eq. 3.9). The isolated oligomers (**3.18**) were characterized by NMR spectroscopy and field-desorption mass spectrometry, and possessed a chain length of 2–12 repeat units as determined by GPC.

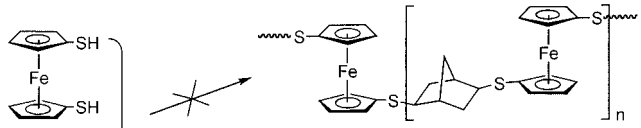

(3.8)

3.17

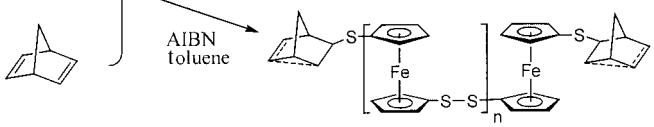

(3.9)

3.18

n = 1- 11

Another group of polymers to consider at this point are polymetallocenes in which metallocene fragments are connected through the metal via spacers involving oxygen or other elements. Most of the research in this area has involved titanium derivatives and was carried out with the ultimate aim of exploiting the catalytic properties that the $TiCp_2$ unit can introduce to the polymer. For example, several attempts have been made to synthesize polytitanoxane **3.19**, but with very limited success. Thus, the synthesis of **3.19** has been claimed by means of the sequential reduction (with zinc) and oxidation (with oxygen) of titanocene dichloride in organic solvents, since the use of basic aqueous conditions leads to facile metal-ring bond cleavage [58]. The yellow solid obtained, however, was an insoluble

crosslinked material with poor thermal and hydrolytic stability, from which some of the cyclopentadienyl substituents had still been eliminated. The characterization was limited and the structure (**3.20**) was postulated mainly on the basis of elemental analysis. A linear polymer product was postulated when $[Cp_2Ti]_2$ or $Cp_2Ti(CO)_2$ was used in a reaction with oxygen, but in these cases insoluble materials were also obtained and a peroxo-bridged structure was suggested [59].

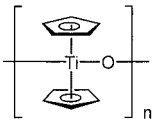

3.19

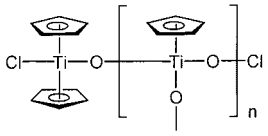

3.20

3.3 Ring-Opening Polymerization (ROP) of Strained Metallocenophanes

3.3.1 Thermal ROP of Silicon-Bridged [1]Ferrocenophanes

ROP reactions generally occur by a chain-growth mechanism (Chapter 1, Section 1.5.2.2.3) and therefore represent a particularly desirable route for the preparation of high molecular weight polyferrocenes. As is clear from the polymers described so far in Sections 3.1 and 3.2, such materials are rare if the ferrocene groups are in close proximity to one another so as to permit substantial metal-metal interactions. The first syntheses of polymetallocenes by ROP methods were reported in early 1992. A novel atom-abstraction-induced ROP process for [3]trithiaferrocenophanes was described early in that year and these results are discussed in Section 3.5 [60]. Thermal ROP of strained metallocenophanes, which is discussed in this section, was reported a few months thereafter [61].

A key general requirement for most ROP processes is a strained cyclic monomer. Ferrocenophanes, in which a single atom bridges the two cyclopentadienyl ligands (i.e. [1]ferrocenophanes), have been known since 1975 and fit this requirement [62]. In contrast to the situation in ferrocene, where the planes of the cyclopentadienyl (Cp) ligands are parallel to one another, in these species the Cp ligands are forced into a tilted higher-energy arrangement by the presence of a single bridging atom. However, although stoichiometric ring-opening reactions were described for silicon-bridged [1]ferrocenophanes in the late 1970s [63], no successful ROP reactions for these species were reported until 1992.

The first examples of the use of ROP of strained metallocenophanes to prepare high molecular weight polymetallocenes ($M_n > 10^5$) involved silicon-bridged [1]ferrocenophane monomers **3.21** [61]. Specifically, polyferrocenylsilanes (PFSs) **3.22** (R,R′ = Me or Ph) were prepared by the thermal ROP of strained, ring-tilted silicon-bridged [1]ferrocenophanes **3.21** (R,R′ = Me or Ph) in the melt, at 130–

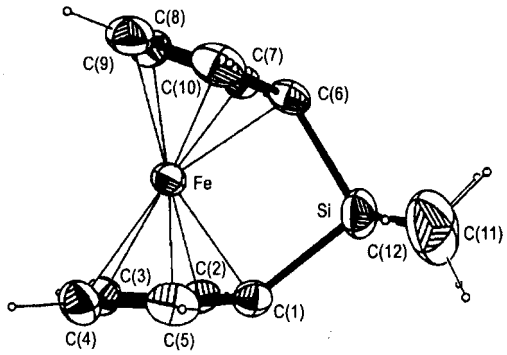

Fig. 3.4 Molecular structure of silicon-bridged [1]ferrocenophane **3.21** (R = R′ = Me) as determined by single-crystal X-ray diffraction; the planes of the Cp ligands are tilted by 20.8°. (Reproduced from [64])

220 °C in evacuated Pyrex glass tubes (Eq. 3.10). This type of monomer possesses tilt angles of 16–21° between the planes of the Cp ligands and strain energies of ca. 70–80 kJ mol^{-1} according to DSC measurements [64, 65]. The strain present is illustrated by the Cp ring-tilted molecular structure of **3.21** (R = R′ = Me) determined by single-crystal X-ray diffraction (Fig. 3.4) [64].

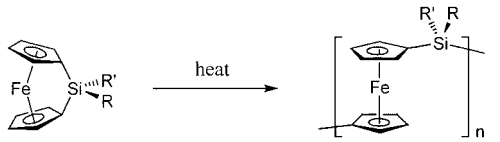

(3.10)

3.21 **3.22**

The thermal ROP route is very general and a wide range of semicrystalline and amorphous polyferrocenylsilanes **3.22** have thereby been prepared with different substituents at silicon and/or on the Cp rings [66]. These thermally ring-opened materials have been fully characterized using a wide range of spectroscopic and analytical methods. Also, their molecular weights have been established by absolute methods, such as static light scattering, to be in the range of $M_w = 10^5$–10^6. Detailed studies of the properties of these materials are described in a later section (3.3.6).

Spirocyclic [1]ferrocenophanes have also been shown to thermally polymerize and these species function as crosslinking agents that allow access to polyferrocenylsilanes with controlled crosslink densities [67]. Amber, solvent-swellable gels are available by this route (see Section 3.3.6.4). The [1]dichlorosilaferrocenophane **3.23** represents a very useful precursor to [1]ferrocenophanes **3.24** with alkoxy (or amino) substituents, and subsequent ROP allows access to, for example, polyferrocenylalkoxysilanes **3.25** (Eq. 3.11) [68]. In addition, polymers with Si-H or Si-Cl groups have been prepared, and these provide opportunities for post-polymerization modification by hydrosilylation and nucleophilic substitution, respectively [66].

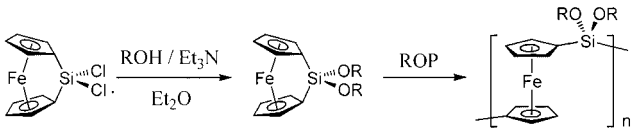

(3.11)

3.23 **3.24** **3.25**

The mechanism of the thermal ROP of silicon-bridged [1]ferrocenophanes is not yet known in definitive detail. However, studies of the polymerization of monomers with unsymmetrically substituted Cp ligands indicate that ROP proceeds with cleavage of the Cp–Si bond [69]. It is possible that traces of nucleophilic impurities initiate the polymerization, although a mechanistic process involving radicals cannot be completely ruled out [70].

The thermal ROP of silicon-bridged [1]ferrocenophanes requires moderately high temperatures (100–250 °C) and there is little or no molecular weight control. In addition, the molecular weight distributions are quite broad ($M_w/M_n \approx 1.5$–2.5). This polymerization method has now been superceded in many ways by ambient temperature ROP methods that involve the use of anionic initiators (see Section 3.3.3) or transition metal catalysts (see Section 3.3.4).

3.3.2
Thermal ROP of Other Strained Metallocenophanes

The thermal ROP methodology established for silicon-bridged [1]ferrocenophanes has been extended to many other strained metallocenophanes, which has allowed access to high molecular weight polyferrocenes with different spacer groups. As discussed later (see Section 3.3.7), this permits modification of the properties of the polymer, such as the extent of the metal-metal interactions.

Thermal ROP of germanium-bridged [1]ferrocenophanes **3.26** was reported shortly after that of the silicon-bridged analogues, and high molecular weight polyferrocenylgermanes **3.27** ($M_w = 10^5$–10^6) were obtained at ca. 120 °C or higher temperatures (Eq. 3.12) [71].

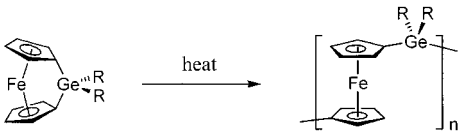

(3.12)

3.26 **3.27**

Polyferrocenylphenylphosphines **3.29**, analogous to those previously synthesized by polycondensation routes (Section 3.2.2), have also been prepared by thermal ROP of phosphorus-bridged [1]ferrocenophanes **3.28** (Eq. 3.13) [72]. The solubility of the materials was observed to increase when the cyclopentadienyl rings were substituted with *n*-butyl or trimethylsilyl groups. Sulfurization was carried out in order to facilitate their characterization by GPC, as the polyferrocenylphosphine

precursors **3.29** were found to adsorb to the porous material (styragel) generally used in GPC columns. Polymers with trimethylsilyl substituents on the cyclopentadienyl rings, however, could be analyzed by GPC without the need for sulfurization. A comparison between unsulfurized (**3.29**, R′ = $SiMe_3$, R = Ph) and sulfurized (**3.30**, R′ = $SiMe_3$, R = Ph) polymer samples from the same batch revealed that these materials possessed essentially the same molecular weight, which indicated that chain cleavage does not occur during the sulfurization step.

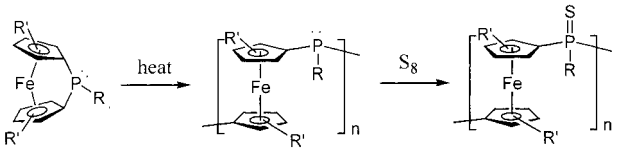

3.28 **3.29** **3.30** (3.13)

R' = H, *n*-Bu, $SiMe_3$

Thermal ROP of highly strained sulfur-bridged [1]ferrocenophanes (**3.31**), which possess tilt angles between the planes of the Cp rings of ca. 31°, has been shown to yield the polyferrocenylsulfides (**3.32**) [73]. The unsubstituted polymer **3.32** (R = H) is insoluble in organic solvents, but random methylation of the Cp rings affords soluble materials **3.32** (R = Me) [73]. First row element bridged [1]boraferrocenophanes (**3.33**) have also been reported. These highly strained species possess very large tilt angles (ca. 32°) and undergo ROP to give polyferrocenylboranes (**3.34**) [74]. The synthesis of [1]stannaferrocenophanes with bulky substituents at tin, followed by thermal ROP at 150 °C, has led to high molecular weight polyferrocenylstannanes **3.35** ($M_w > 10^5$, PDI ≈ 1.5), a new class of bimetallic polymers [75].

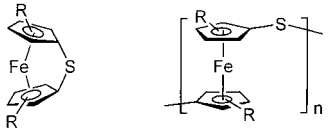

3.31 **3.32**

R = H or Me R = H or Me

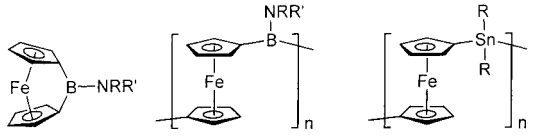

3.33 **3.34** **3.35**

NRR' = $N(SiMe_3)_2$, N(*t*-Bu)$SiMe_3$, or N(*i*-Pr)$_2$ R, R' = *t*-Bu, Mes

Strained [2]metallocenophanes can also function as ROP precursors. For example, hydrocarbon-bridged [2]ferrocenophanes **3.36** (M = Fe, $E_1 = E_2 = CH_2$) were found to undergo ROP at 300 °C, providing access to polyferrocenylethylenes **3.37** (M = Fe,

$E_1 = E_2 = CH_2$) (Eq. 3.14) [76]. The ferrocenylethylene polymers **3.37** were found to be insoluble when R = H, but were readily soluble when R = Me. In the latter case, a bimodal molecular weight distribution was detected, with both an oligomeric fraction ($M_w = 4800$) and a high molecular weight fraction ($M_w = 9.6 \times 10^4$) being present. Analogous strained monomers that contain ruthenium instead of iron, [2]ruthenocenophanes **3.36** (M = Ru, $E_1 = E_2 = CH_2$), possess ring-tilt angles of ca. 30°, significantly larger than that present in the [2]ferrocenophanes **3.36** (M = Fe, $E_1 = E_2 = CMe_2$) (23°). Not surprisingly, the Ru monomers have been found to undergo ROP at lower temperatures (220 °C) to yield polyruthenocenylethylenes **3.37** (M = Ru, $E_1 = E_2 = CH_2$, R = H or Me) [77]. The thermal ROP of [2]ferrocenophanes with C–P and C–S bridges has also been reported, but analogous monomers with C–Si bridges are resistant to thermal ROP due to insufficient ring strain [78].

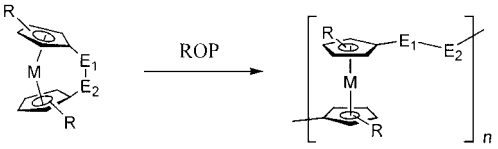

3.36 **3.37** (3.14)

M = Fe or Ru
R = H or Me
$E_1 = E_2 = CH_2$ or CMe_2

The use of thermal ROP also allows access to a range of random copolymers. For example, polyferrocenylsilane-*r*-polysilane materials (**3.38**) (Eq. 3.15) have been prepared by the thermal ring-opening copolymerization of silicon-bridged [1]ferrocenophanes with cyclic tetrasilanes [79]. These copolymers are particularly interesting since they contain ferrocene moieties linked by σ-delocalized oligosilane segments. It is noteworthy that these photosensitive materials are inaccessible by thermal ROP of ferrocenophanes with oligosilane bridges due to insufficient ring strain [64].

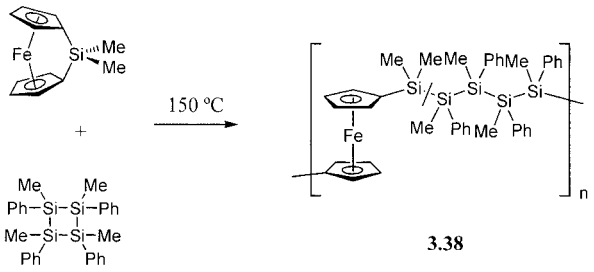

3.38 (3.15)

Thermal copolymerization of different [1]ferrocenophanes has also been reported to give polyferrocenylsilane random copolymers [80]. In addition, random copolymers **3.39** derived from [1]ferrocenophanes and silicon-bridged bis(benzene)chromium complexes have been synthesized (Eq. 3.16) [81].

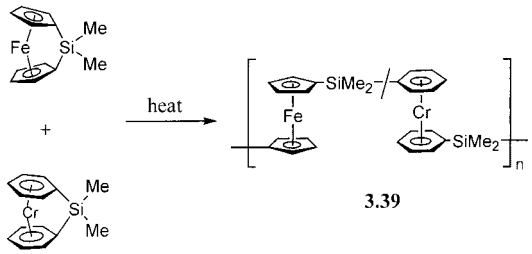

3.39

(3.16)

3.3.3 Living Anionic ROP of Strained Metallocenophanes

Anionic ROP reactions of metallocenophanes were first reported in 1994 [82]. Silicon-bridged [1]ferrocenophanes **3.21** (R = R′ = Me) were shown to undergo polymerization in the presence of an anionic initiator such as lithioferrocene or *n*-BuLi [82]. When extremely pure monomer and solvents were used, the living anionic ROP of **3.21** (R = R′ = Me) could be achieved [82, 83]. The reaction involves the formation of an anionic polymer **3.40**, the living end of which can be subsequently terminated with various capping agents to afford polyferrocenylsilanes **3.41** (Scheme 3.2). Since the initiation process is rapid and no chain transfer or uncontrolled termination occurs, polyferrocenylsilanes with very narrow polydispersities (PDI < 1.10) are accessible. The molecular weights of the resulting polymers (M_n

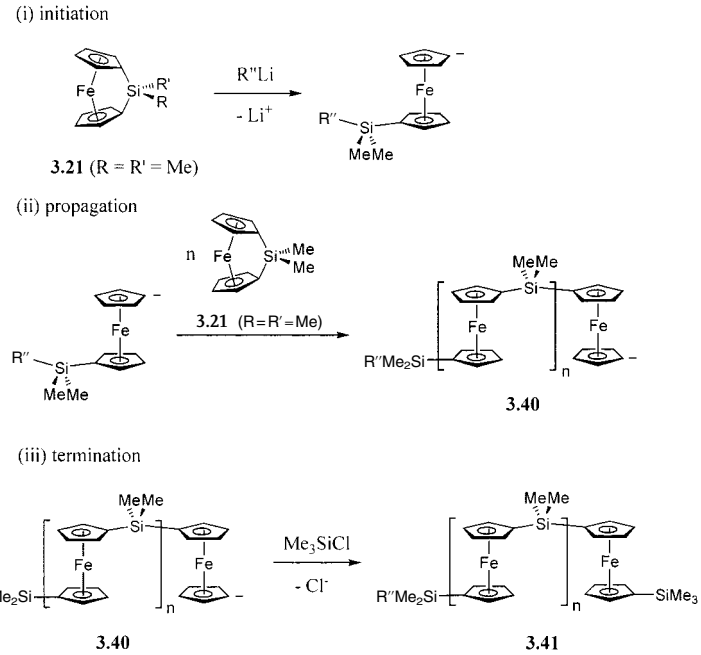

Scheme 3.2

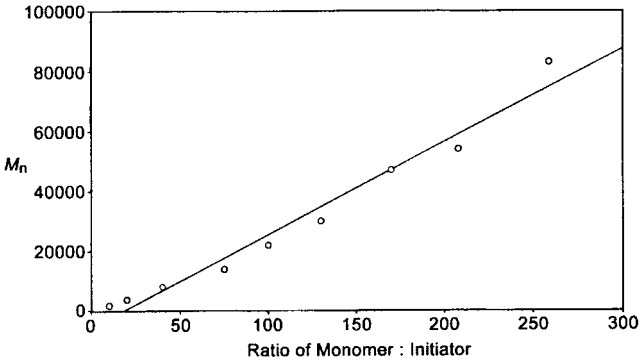

Fig. 3.5 Plot of M_n *vs.* monomer:initiator ratio for the living anionic ROP of silicon-bridged [1]ferrocenophane **3.21** (R = R′ = Me) with *n*-BuLi as initiator and H_2O as terminator. (Reproduced from [83])

up to ca. 120,000) depend on the monomer-to-initiator ratio, as this governs the number of chain propagating sites (Fig. 3.5) [82, 83]. The living anionic ROP process appears to be very general for silicon-bridged [1]ferrocenophanes and has been extended to a range of different monomers [84].

Although early attempts to induce the anionic ROP of phosphorus-bridged [1]ferrocenophanes only generated a mixture of oligomers [44], living anionic ROP has been achieved by the use of highly purified monomers [45]. Thus, polyferrocenylphosphines **3.11** with controlled molecular weights (up to $M_w \approx 36{,}000$) and narrow polydispersities (PDI = 1.08–1.25) have been prepared using organolithium initiators. It was reported in the early 1980s that high molecular weight polyferrocenylphosphines **3.11** were generated under certain conditions in a polycondensation reaction of dilithioferrocene · TMEDA with $PhPCl_2$ [44]. The results from studies of the anionic ROP of phosphorus-bridged [1]ferrocenophanes suggest, however, that the high polymers **3.11** generated in these cases were almost certainly formed via a chain-growth route, namely the anionic ROP of a [1]ferrocenophane generated *in situ* under the reaction conditions (Eq. 3.17) [45, 85]. It is plausible that similar anionic ROP reactions occur, at least to some extent, in the condensation routes to polyferrocenylsilanes described in patents in the 1960s [45, 85, 86].

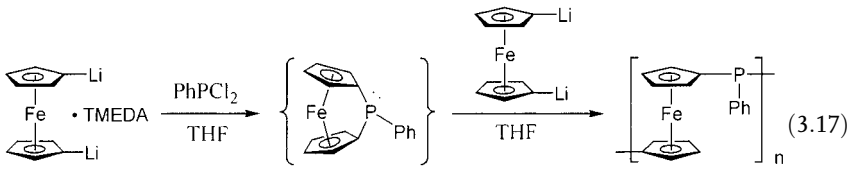

(3.17)

3.11

TMEDA = $Me_2NCH_2CH_2NMe_2$

Highly purified monomer and solvents are necessary for living anionic ROP since the concentration of highly reactive propagation sites is extremely low. However, living polymerizations are exceptionally useful as they allow the preparation of well-defined homopolymers with controlled molecular weights and narrow molecular weight distributions (PDI < 1.2). Even more significantly, they allow the synthesis of block copolymers by, for example, the addition of another monomer to the living anionic polyferrocene chain ends. The use of this technique to prepare polyferrocene block copolymers, and the properties of these materials, are discussed in Section 3.3.8.

3.3.4
Transition Metal-Catalyzed ROP of Strained Metallocenophanes

A very convenient, transition metal-catalyzed ROP route to polymetallocenes from strained metallocenophanes was reported in 1995 [87, 88]. Various Rh^{I}, Pd^{II}, Pd^{0}, Pt^{II}, and Pt^{0} complexes were found to catalyze the ROP of [1]silaferrocenophanes **3.21** in solution at room temperature to yield high molecular weight polyferrocenylsilanes **3.22** ($M_n \approx 10^5$) (Eq. 3.18). A major advantage of these transition metal-catalyzed processes is that, in contrast to anionic polymerization, ambient temperature polymerization can be achieved without the need for extremely pure monomers and solvents. Copolymerization of silicon-bridged [1]ferrocenophanes with other monomers is also possible. For example, transition metal-catalyzed ROP of silicon- and germanium-bridged [1]ferrocenophanes afforded random copolymers with both silicon and germanium atoms in the main chain [88, 89], whereas reactions of silicon-bridged [1]ferrocenophanes with cyclocarbosilanes yielded polyferrocenylsilane-*r*-polycarbosilane random copolymers [90]. The use of the mild, transition metal-catalyzed ROP route is especially advantageous in the case of [1]ferrocenophanes with halogen substituents at the bridging silicon. Unlike the alkyl- or aryl-substituted [1]ferrocenophanes, which typically undergo thermal ROP at 120–150 °C, the halogen-substituted analogues thermally polymerize at a much higher temperature (> 250 °C). However, in the presence of a transition metal catalyst, these monomers also undergo facile ROP at room temperature to give the corresponding polymers in high yields [91].

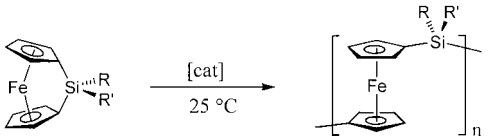

(3.18)

3.21 **3.22**

Studies have shown that unsymmetrical [1]ferrocenophanes, in which only one of the cyclopentadienyl rings is methyl-substituted, yield regioregular polyferrocenylsilanes upon transition metal-catalyzed ROP, whereas thermal ROP of the same monomers yields regioirregular materials [69, 90].

In the absence of additives, transition metal-catalyzed ROP of silicon-bridged [1]ferrocenophanes yields high molecular weight materials with no appreciable control of molecular weight. However, the addition of hydrosilanes such as Et_3SiH permits molecular weight control, and the polymers thus obtained (**3.42**) have been shown to possess an M_n value of ca. 10^3–10^4 with polydispersities typically in the range 1.3–1.6 (Fig. 3.6) [90]. Characterization of the low molecular weight polymers by NMR and IR spectroscopies confirmed the nature of the end groups. Similarly, the use of poly(methylhydrosiloxane) as the source of Si–H bonds yields novel graft copolymers **3.43** [90]. This methodology can also be extended to the preparation of star and block structures, including water-soluble materials [90, 92, 93].

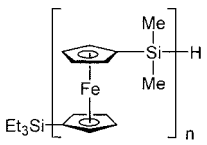

3.42

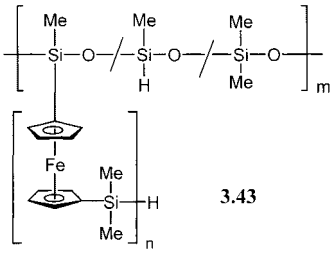

3.43

Research has also focused on understanding the mechanism of the transition metal-catalyzed ROP reactions of [1]ferrocenophanes. A logical first step in the polymerization is insertion of the transition metal into the strained Cp-carbon-bridging element bond in the ferrocenophane. Polymers **3.42** formed in the presence of hydrosilanes are believed to result from competitive oxidative-addition between the Si–H bond of the hydrosilane and the strained Cp–Si bond of the ferrocenophane at the catalytic center, followed by reductive elimination. Detailed work has indicated that colloidal metal is the likely catalyst in the ROP reactions [94].

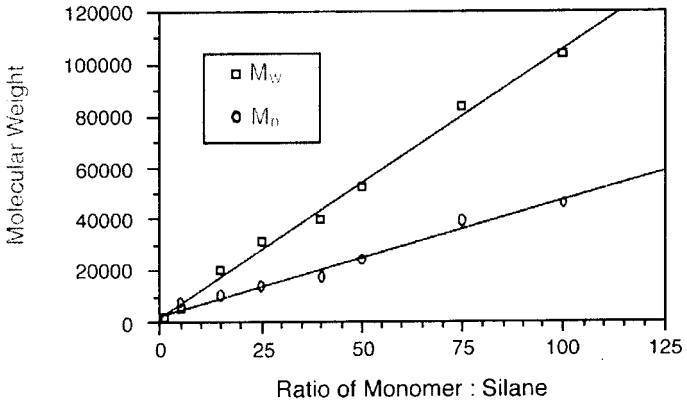

Fig. 3.6 Plot of molecular weight *vs.* the ratio of monomer: Et_3SiH for the Pt-catalyzed ROP of silicon-bridged [1]ferrocenophane **3.21** (R = R′ = Me) in the presence of Et_3SiH. (Reproduced from [90])

Metal-catalyzed ROP has also been reported for a [2]ferrocenophane with a Ge–Ge bridge, whereas the analogous species with an Si–Si bridge resists polymerization [95]. The presence of weak Cp–Ge bonds may be important in the successful ROP observed in the former case.

3.3.5
Other ROP Methods for Strained Metallocenophanes

Cationic ROP has been demonstrated for highly reactive [1]stannaferrocenophanes [96] and [2]ferrocenophanes with a C–S bridge [78]. [1]Stannaferrocenophanes have also been shown to undergo ROP in the presence of nucleophiles such as pyridine at room temperature [96]. Photochemically-induced ROP of phosphorus-bridged [1]ferrocenophane **3.28** (R = Ph, R′ = H) (see p. 85) has also been reported and, after subsequent sulfurization of the resulting polyferrocenylphosphine **3.29**, poly(ferrocenylphenylphosphinesulfide) **3.30** with $M_n = 1.9 \times 10^3$ and PDI = 1.72 was isolated [97]. In addition, this reaction has been reported to occur when transition metal fragments are coordinated to the bridging phosphorus atom. For the tungsten species **3.44** ($ML_x = W(CO)_5$, R = Ph), polymer **3.45** ($ML_x = W(CO)_5$, R = Ph) with $M_n = 1.8 \times 10^4$ and a PDI = 1.67 was isolated; for the manganese species **3.44** ($ML_x = Mn(CO)_2Cp$, R = Ph), polymer **3.45** ($ML_x = Mn(CO)_2Cp$, R = Ph) was obtained with $M_n = 1.1 \times 10^4$ and PDI = 2.0 (Eq. 3.19). Silicon-bridged [1]ferrocenophanes have been reported to undergo ^{60}Co γ-ray-induced ROP in the solid state, and this allows access to stereoregular polyferrocenylsilanes [98].

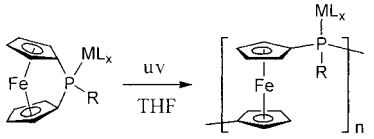

3.44 **3.45** (3.19)

3.3.6
Properties of Polyferrocenylsilanes

ROP methods have allowed access to a wide variety of high molecular weight polyferrocenes, of which the polyferrocenylsilanes are the prototypical example. Studies of the latter materials have provided an excellent opportunity for the systematic and detailed examination of a class of main-chain metal-containing macromolecules; representative examples are included in Table 3.1. This section surveys some of the properties of these interesting polymers.

Table 3.1 Thermal transition and GPC molecular weight data for selected polyferrocenylsilanes **3.22** [66, 68, 117]

R	*R′*	T_g (T_m) (°C) [b]	M_n [a]	PDI [c]
H	H	16 (165)	[e]	[e]
Me	Me	33 (122–145)	3.4×10^5	1.5
Et	Et	22 (108)	4.8×10^5	1.5
n-Pr	*n*-Pr	24 (98)	8.5×10^4	2.7
n-Bu	*n*-Bu	3 (116, 129)	3.4×10^5	2.6
n-Pen	*n*-Pen	–11 (80–105)	3.0×10^5	1.6
n-Hex	*n*-Hex	–26	7.6×10^4	1.6
Me	H	9 (87, 102)	4.2×10^5	2.0
Me	Et	15	3.0×10^4	1.3
Me	$CH_2CH_2CF_3$	59	8.1×10^5	3.3
Me	$CH=CH_2$	28	7.7×10^4	2.1
Me	*n*-$C_{18}H_{37}$	1 (16)	5.6×10^5	2.5
Me	Ph	90	1.5×10^5	2.0
Me	Fc [d]	99	7.1×10^4	2.3
Me	5-norbornyl	81	1.1×10^5	1.5
OMe	OMe	19 (80–103)	1.5×10^5	2.0
OEt	OEt	0	3.8×10^5	2.1
OCH_2CF_3	OCH_2CF_3	16	2.2×10^5	1.2
OBu	OBu	–43	3.9×10^5	2.1
OHex	OHex	–51	0.9×10^5	2.6
$O(CH_2)_{11}CH_3$	$O(CH_2)_{11}CH_3$	(–30)	1.9×10^5	2.5
$O(CH_2)_{17}CH_3$	$O(CH_2)_{17}CH_3$	(32)	2.3×10^5	2.1
OC_6H_5	OC_6H_5	54	2.3×10^5	2.0
OC_6H_4-*p*-^{t}Bu	OC_6H_4-*p*-^{t}Bu	89	1.9×10^5	1.9
OC_6H_4-*p*-Ph	OC_6H_4-*p*-Ph	97	5.4×10^4	2.0
Me [f]	Me [f]	93	2.8×10^5	1.5
Me [g]	Me [g]	116	2.3×10^5	1.4

a Obtained from analysis of polymer solutions in THF using polystyrene standards.
b DSC data collected at a heating rate of 10 °C/min.
c PDI = M_w/M_n.
d Fc = (η-C_5H_4)Fe(η-C_5H_5).
e Insoluble polymer.
f One Me group on each Cp ligand.
g One C_5Me_4 ligand and one C_5H_4 ligand.

3.3.6.1 **Polyferrocenylsilanes in Solution**

The vast majority of polyferrocenylsilanes are soluble in common organic solvents and GPC has proven useful in the determination of the molecular weights and molecular weight distributions of these metal-containing polymers. However, the determination of absolute values of M_w by static light-scattering methods has shown that the use of GPC with polystyrene calibration standards significantly underestimates the molecular weights of these materials. For example, detailed solution studies have been performed on a series of well-defined poly(ferrocenyldimethylsilane)s **3.22** (R = R′ = Me) with PDIs <1.2 that spans a molecular weight range of 10,000–

100,000 g mol^{-1} [99]. Using a gel-permeation chromatograph equipped with refractive index, viscometry, and light-scattering detectors, it was shown that, in THF, poly(ferrocenyldimethylsilane) possesses a more compact random-coil conformation than polystyrene of the same molecular weight in the same solvent. This explains the 30% underestimation of the true molecular weight of polyferrocenylsilanes by conventional GPC methods using polystyrene standards, as the latter technique separates molecules on the basis of hydrodynamic size. Thus, Mark-Houwink parameters were also established for PFS **3.22** (R = R′ = Me) in THF at 23 °C, and the *a* value of 0.62 is typical for flexible chains in a fairly poor solvent. In contrast, the value for polystyrene in THF is larger (0.72). In this study, a universal calibration curve in THF was also established [99].

Solution characterization by NMR has proved to be an invaluable tool as these polymers possess ^{1}H, ^{13}C, and ^{29}Si NMR-active nuclei in the polymer backbone. In several cases, high-resolution NMR has been used to investigate the tacticity of polyferrocenylsilanes [91].

3.3.6.2 Polyferrocenylsilanes in the Solid State: Thermal Transition Behavior, Morphology, and Conformational Properties

Glass transitions for poly(ferrocenylalkyl/arylsilanes) **3.22** determined by DSC cover a wide range of temperatures (ca. –51 to 150 °C) (Table 3.1). As expected, long flexible substituents on silicon lead to the lowest T_g values, whereas the replacement of hydrogen on the Cp ligands by groups such as Me or $SiMe_3$ leads to a very significant increase in T_g. Symmetrically substituted polyferrocenylsilanes **3.22** (R = R′) often show a propensity to crystallize, and several examples have been studied in detail by a range of techniques including DSC, WAXS, atomic force microscopy, and X-ray and electron diffraction analyses of fibers and films [66]. As for other semicrystalline polymers, the morphology of many of these materials shows a dependence on thermal history. Their crystallinity has been observed to increase over time, especially when samples are annealed above the T_g. On the other hand, polyferrocenylsilanes that are unsymmetrically substituted at silicon are generally amorphous, presumably as a consequence of their atactic stereostructure.

Polyferrocenylsilanes can be fabricated into films, shapes, and fibers using conventional polymer processing techniques. The dimethyl derivative **3.22** (R = R′ = Me), which has been studied in the most detail, is an amber, film-forming thermoplastic (Fig. 3.7a) which shows a T_g at 33 °C and melt transitions (T_m) in the range 122–145 °C. The multiple melt transitions arise from the presence of crystallites of different size, which melt at slightly different temperatures [65, 100]. Poly(ferrocenyldimethylsilane) **3.22** (R = R′ = Me) can be melt-processed above 150 °C (Fig. 3.7b) and can be used to prepare crystalline, nanoscale fibers (diameter 100 nm to 1 μm) by electrospinning. In this method, an electric potential is used to produce an ejected jet from a solution of the polymer in THF, which subsequently stretches, splays, and dries. The nanofibers of different thickness show different colors due to interference effects similar to those seen in soap bubbles

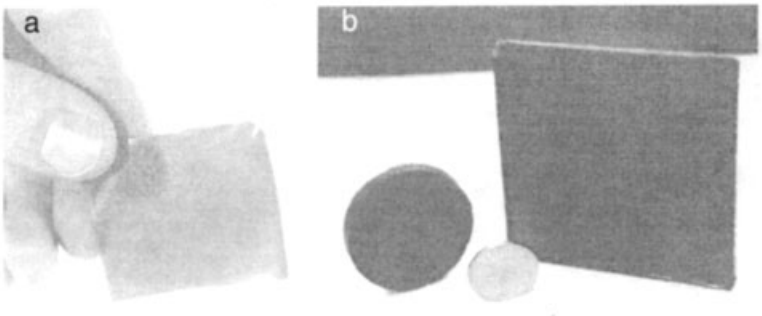

Fig. 3.7 Polyferrocenyldimethylsilane **3.22** (R = R′ = Me) as (**a**) a solvent cast film, and (**b**) melt-extruded shapes.

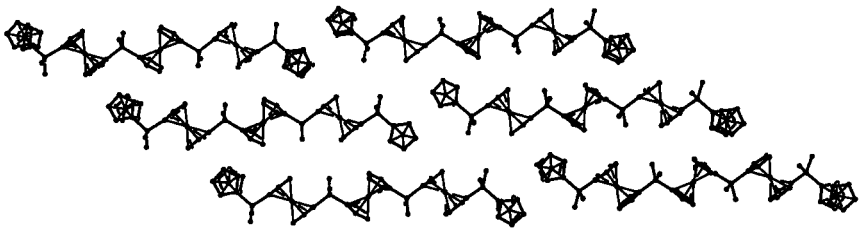

Fig. 3.8 View of the crystal-packing arrangement of pentamer molecules **3.46** parallel to the [011] planes showing three pairs of molecules. The terminal ferrocenyl groups are twisted in opposite directions perpendicular to the interior, *trans*-planar, zig-zag units. (Reproduced from [102 **a**])

[101]. As with the dimethyl material, other symmetrically substituted polyferrocenylsilanes **3.22** (R = R′) with short (C_2–C_5) alkyl chains at silicon also crystallize, and similar melting behavior is observed (Table 3.1) [66]. In contrast, the *n*-hexyl analogue **3.22** (R = R′ = *n*-hexyl) is an amber, amorphous gum with a T_g of –26 °C. Apparently, regular packing of polyferrocenylsilane chains is no longer possible once the length of the alkyl chains on silicon exceeds five carbon atoms.

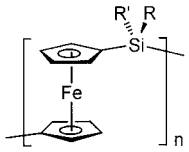

3.22

The possible conformations of PFS chains in the solid state have attracted significant interest from several research groups, and much work has also focused on the prototypical material, poly(ferrocenyldimethylsilane) **3.22** (R = R′ = Me). One contribution towards an understanding of the conformations adopted by

poly(ferrocenyldimethylsilane) chains involved X-ray structural studies of well-defined oligomers. In particular, a model pentamer **3.46** was successfully characterized by single-crystal X-ray diffraction [102]. The pentamer molecules possess a *trans*-planar zig-zag conformation, in which the end ferrocenes are twisted out of the plane (Fig. 3.8). Interestingly, the powder diffractogram of the pentamer is similar to that of the analogous high polymer, with an intense diffraction peak at $d = 6.37$ Å, and this suggests a similar structure in the crystalline domains in the solid state of the latter. The planes giving rise to this peak in the pentamer, the (011) planes, are shown in Fig. 3.8. Further important insight has been provided by means of a molecular mechanics study of oligomeric models of polyferrocenylsilanes [103]. The calculations showed that the molecules are conformationally flexible, and that in the lowest-energy conformations there is an electrostatic attraction between the positively charged iron atoms and the negatively charged Cp ligands that are in close proximity. As expected, for the isolated molecules the conformations were found to be governed by intramolecular interactions, whereas in the solid state intermolecular interactions were predicted to be more important. Significantly, although it was concluded that a *trans*-planar structure analogous to the central portion of the pentamer **3.46** is possible for the polyferrocenylsilanes (Fig. 3.8), twisting of some of the ferrocene units out of the plane in a manner similar to the end groups in the pentamer was also viewed as being favorable as a result of inter-chain iron-Cp interactions.

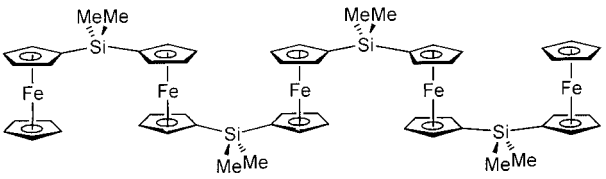

3.46

Detailed work on the morphology of polyferrocenylsilane **3.22** (R = R′ = Me) using X-ray diffraction techniques on films and fibers has revealed the coexistence of a 3-D monoclinic crystalline polymer phase and a 2-D mesophase with hexagonal or tetragonal packing of the macromolecules [104]. It is suggested that the coexistence of these phases is most likely a result of the close energies of the various conformations of the polymer backbone. The results for the 3-D monoclinic phase also support earlier suggestions that the linear polymer chains possess a *trans*-planar zig-zag conformation in the solid state, as found for the low molecular weight pentameric analogue **3.46** (see Fig. 3.8). Studies on electrospun nanofibers (diameter 100–1000 nm) of **3.22** (R = R′ = Me) using single-fiber electron-diffraction techniques were also consistent with the assignment of a monoclinic unit cell [101].

Alkoxy-substituted polyferrocenylsilanes (**3.25**) (see Eq. 3.11) are generally amorphous, and T_g values as low as –51 °C have been detected when OR = *n*-hexyloxy. Polyferrocenylsilanes symmetrically substituted with long alkoxy side chains (**3.25**,

OR = *n*-octadecyloxy) have been found to crystallize and to form lamellar structures with interdigitated side groups [68]. As noted above, polyferrocenylsilanes with unsymmetrical substitution on the bridging silicon (**3.22**, $R \neq R'$) possess tacticity and offer the possibility of forming stereoregular polymer structures. The materials prepared by either thermal or transition metal-catalyzed ROP that have been studied to date have, nevertheless, been atactic. Interestingly, however, ^{60}Co γ-irradiation of single crystals of the monomer **3.21** (R = Me, R′ = Ph) yields a poly(ferrocenylmethylphenylsilane) **3.22** (R = Me, R′ = Ph) which clearly exhibits appreciable stereoregularity by NMR and is probably syndiotactic [98].

Hydrosilylation reactions have been performed with polyferrocenylsilanes containing Si–H functionalities in order to attach mesogenic azobenzene groups. This has allowed the preparation of calamitic thermotropic side-chain liquid-crystalline materials that display a nematic mesophase between ca. 53 and 250 °C [105].

The T_g values of polyferrocenylsilanes, which can be as low as ca. –50 °C, are remarkable for a polymer structure with a bulky unit such as ferrocene in the main chain. Even when the influence of the side groups is small, the T_g values are still close to ambient temperature (e.g., for **3.22** (R = R′ = H), T_g = 16 °C). By contrast, the T_g of poly(vinylferrocene) is reported to be high (185 or 233 °C; Chapter 2, Section 2.2.1.1). The ability of the iron atom in each ferrocene unit to act as a freely rotating "molecular ball-bearing" [106] probably plays a key role in generating the observed conformational flexibility in polyferrocenylsilanes. This aspect has been explored by means of variable-temperature solid-state ^2H NMR studies on PFSs **3.22**, which were specifically deuterated either on the Cp rings or in the side groups [107].

3.3.6.3 Electrochemistry, Metal-Metal Interactions, Charge-Transport, and Magnetic Properties of Oxidized Materials

A key characteristic of polyferrocenylsilanes is the presence of *two* reversible oxidation waves due to Fe^{II}/Fe^{III} redox processes in the cyclic voltammograms of the materials in moderately polar organic solvents, as illustrated for the case of PFS **3.22** (R = R′ = Me) in Fig. 3.9 [61, 108, 109]. This is in contrast to the situation for ferrocene and side-chain polymers such as polyvinylferrocene, for which a single oxidation wave is detected (see Chapter 2, Fig. 2.1, Section 2.2.1.1). The proposed explanation for polyferrocenylsilanes invokes initial oxidation at alternating iron sites as a consequence of significant interactions between the iron atoms. Thus, as one iron center is oxidized at potential $E_{1/2}(1)$, the neighboring sites become more difficult to oxidize and therefore do so at a higher potential $E_{1/2}(2)$. As a consequence, two oxidation waves with a redox coupling $\Delta E_{1/2} = E_{1/2}(2) - E_{1/2}(1)$ result. This process is depicted in Scheme 3.3.

Detailed electrochemical studies on model oligoferrocenylsilanes that possess two to nine ferrocene units fully support this explanation [102]. The peak separations for the different polymers, which provide a useful estimate of the degree of interaction between the metal centers, are generally in the range $\Delta E_{1/2}$ = 0.20–0.25 V in CH_2Cl_2 with $[Bu_4N][PF_6]$ as supporting electrolyte, with some depen-

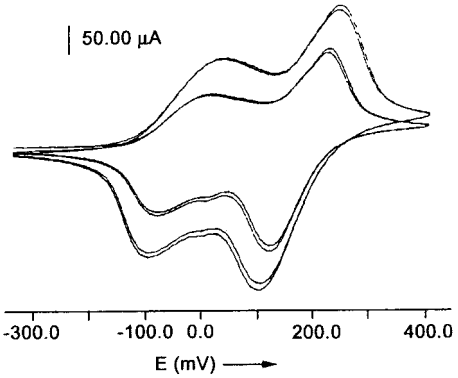

Fig. 3.9 Cyclic voltammogram of polyferrocenyldimethylsilane **3.22** (R=R′=Me) (0.1 M $[Bu_4N][PF_6]$ in CH_2Cl_2) at scan rates of 500 and 1000 mV s^{-1}, showing two reversible oxidation waves separated by a redox coupling $\Delta E_{1/2}$ of ca. 0.24 V. (Reproduced from [108])

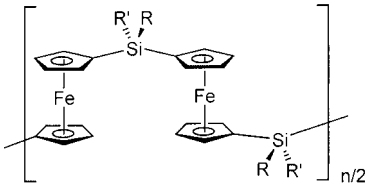

3.22

$E_{1/2}(1)$

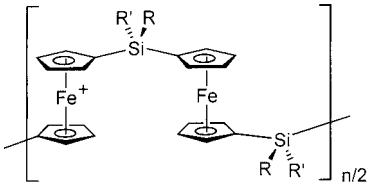

$E_{1/2}(2)$

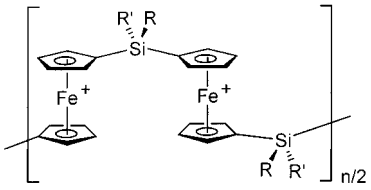

Scheme 3.3

dence on the substituents present at silicon. This corresponds to a comproportionation constant K_c of ca. 10^4, which is consistent with class II mixed-valence behavior. Class I materials have $K_c = 0$ and show no signs of electron transfer, whereas class III materials generally have $K_c > 10^5$ and the valence electrons are completely delocalized. Oxidation of oligo- and polyferrocenylsilanes yields mixed-valence materials, which display an intervalence electron-transfer band of significant intensity at ca. 1300 nm due to hopping of electrons (or more correctly holes) between the Fe^{II} and Fe^{III} centers [102]. The valence electrons in these materials are localized on the Mössbauer timescale (ca. 10^{-7} s), and hence the Mössbauer spectra show resolved Fe^{II} and Fe^{III} sites. These results are also consistent with class II behavior [110, 111].

The nature of the interaction between the iron centers in polyferrocenylsilanes is an important question which has sparked significant attention. It does not appear to be simply an electrostatic or coulombic effect whereby a positive charge on one iron center influences the ease of electron removal from another in close proximity. Indeed, studies of linear and cyclic oligomers (and the corresponding high polymers, see Section 3.3.7) show that there is a strong dependence of $\Delta E_{1/2}$ on the nature of the bridging elements as well as the distance between the iron sites [75]. Although, in principle, d-π-σ conjugation through the Fe–Cp–Si orbitals is possible, the degree of ground-state electron delocalization of this type in polyferrocenylsilanes appears to be rather low. Thus, in contrast to π-conjugated polymers such as polyacetylenes and σ-conjugated polymers such as polysilanes and polystannanes, which show a decrease in band gap with increased chain length as the HOMO-LUMO transition moves to lower energy, an analogous effect for polyferrocenylsilanes has not been detected by UV/vis spectroscopy [65]. Thus, the λ_{max} and extinction coefficient for the linear dimer $FcSiMe_2Fc$, the cyclic dimer $[fcSiMe_2]_2$, and the high polymer **3.22** (R = R′ = Me) are very similar. As an explanation, it has been advocated that the variation of the metal-metal interactions depends on the nature of the bridging group, which influences the "molecular-scale dielectric constant" of the medium between the iron centers [112]. As the dielectric constant of the medium determines the interactions detected, more polarizable atoms would be expected to lead to increased redox coupling, which has in fact been observed in practice.

When polyferrocenylsilanes are oxidized, they undergo a color change from amber to blue. This interesting, reversible, electrochromic behavior has been studied in some detail for several polymers [110, 113]. Pristine high molecular weight polyferrocenylsilanes are insulating ($\sigma = 10^{-14}$ S cm^{-1}); when partially oxidized or "p-doped" by I_2, the amorphous samples exhibit conductivities in the weak semiconductor range ($\sigma = 10^{-8}$–10^{-7} S cm^{-1}), whereas for the oriented crystalline samples (**3.22**, R = R′ = *n*-Bu) the conductivities are in the semiconductor range (up to ca. 2×10^{-4} S cm^{-1}) [79]. Detailed studies have indicated that iodine-doping is partially reversible and, at high I_2 concentration, an $[I_5]^-$ species forms, which may play a role in mediating metal-metal interactions and charge transport [111, 114].

The semiconductive nature of polyferrocenylsilanes makes them excellent candidates for applications where some conductivity is needed but high values are not

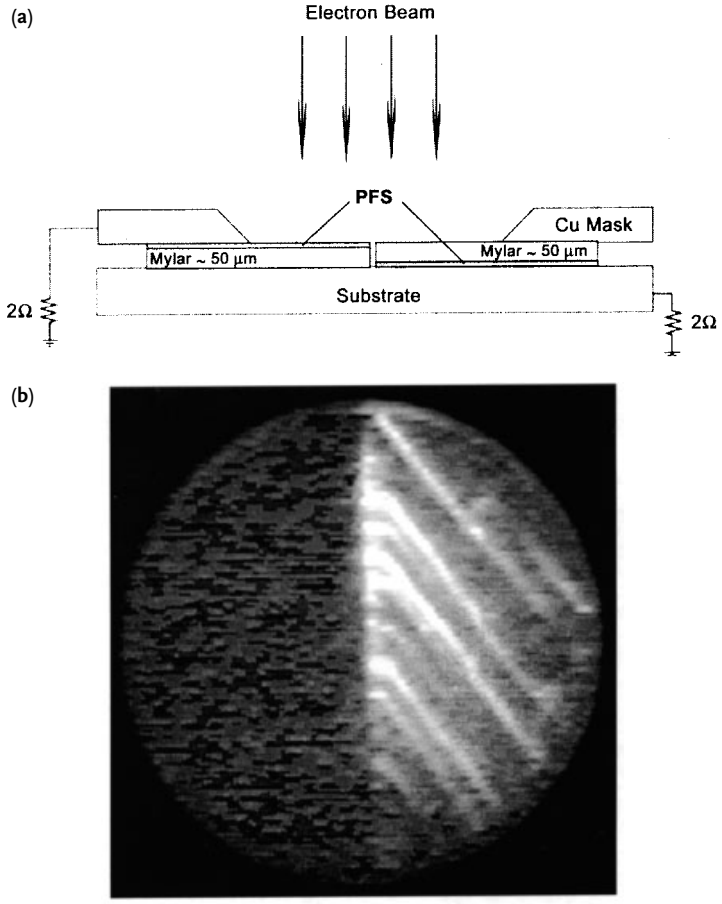

Fig. 3.10 (**a**) Schematic representation of a split specimen device used in charging experiments with PFS films. The Mylar surface coated with the polymer film was cut in half and, with one half inverted, was placed in the device. (**b**) Arc discharge tracks for the 50 μm thick Mylar sample, half of which (left) has been coated with a 15 μm thick layer of **3.22** (R = Me, R′ = Ph). The circular aperture is 4.5 cm in diameter. (Reproduced from [115])

desirable due to the associated effects of magnetic fields. For example, amorphous PFSs, such as **3.22** (R = Me, R′ = Ph), possess appreciable hole mobilities (ca. 10^{-5} cm^2 V^{-1} s^{-1}) [79] and appear promising as charge dissipation materials with potential applications as protective coatings for dielectrics [115]. Thus, on exposure to low-energy electrons (20 keV), an apparent combination of electron scattering by the iron atoms and some degree of electron conductivity in the polymer film prevents appreciable charge build-up. In contrast, for insulating organic polymers such as Mylar, poly(ethylene terephthalate), an accumulation of the negative charge in the material leads to arcing, which will inevitably result in material breakdown. Fig. 3.10 illustrates the effect of coating a 50 μm thick Mylar layer

with a 15 μm thick film of amorphous poly(ferrocenylmethylphenylsilane) in charging experiments; here, arc-discharging was clearly evident on the exposed Mylar surface, but not on the polyferrocene-coated surface.

The magnetic properties of TCNE-oxidized, low molecular weight polyferrocenylsilanes ($M_w \approx 1500$) have been investigated. These studies indicated the presence of electron delocalization and, in some cases, the presence of ferromagnetic ordering at low temperature [116]. Attempts to reproduce this behavior with a variety of high molecular weight samples were reported to be unsuccessful [117]. Photooxidation of PFS in the presence of chloroform has also been demonstrated, and the resultant oxidized materials were found to be photoconducting [118].

3.3.6.4 Redox-Active Polyferrocenylsilane Gels

The incorporation of transition metals into crosslinked polymer networks leads to gels with interesting properties. Ultimately, such materials represent possibilities for the formation of electrochemical actuators or switches. Controlled crosslinking of polyferrocenylsilanes has been achieved to yield redox-active gels that swell in solvents [119]. A crosslinked network **3.48** [$(x+y):z = 1:0.02–0.15$] can be obtained, and the degree of crosslinking can be controlled by using appropriate amounts of the spirocyclic [1]ferrocenophane **3.47** in the thermal polymerization mixtures (Eq. 3.20). From the measurement of the swelling response in various solvents, the solubility parameter (δ) for the linear poly(ferrocenyldimethylsilane) **3.22** (R = R′ = Me) was estimated to be 18.7(7) $MPa^{1/2}$ [119].

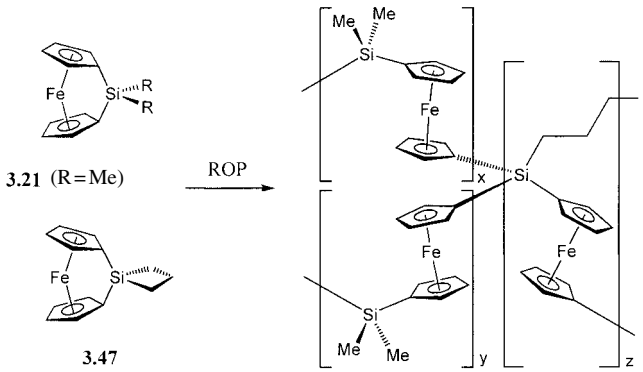

(3.20)

3.48

The metal-metal interactions in the polymer network were investigated by controlled potential electrolysis with the aid of an optically transparent thin-layer electrochemistry (OTTLE) cell. In the visible/near-IR spectrum of the fully reduced deep-red/orange gel the lowest-energy visible band is assigned to a d–d transition. Upon oxidation, two new absorption peaks emerge: one at 640 nm is due to a ligand-to-metal charge-transfer (LMCT) of the ferrocenium moiety, whereas the

other peak, a broad absorption band centered at 1300 nm, is assigned to an intervalence electron-transfer (IVCT). The color of the gel was observed to darken to a deep-blue with increasing oxidation. The reversibility of the process was demonstrated by reversing the potential and allowing the gel to return to the fully reduced state, as indicated by its original deep-red/orange color and the disappearance of the LMCT and IVCT bands of the oxidized polymer [119].

The swelling of the polyferrocenylsilane gel in an organic solvent depends on the degree of oxidation of the iron sites. This has allowed the development of planar colloidal photonic crystal devices, in which silica microspheres are periodically arrayed in a matrix of a cross-linked polyferrocenylsilane [120]. The optical Bragg diffraction peak (stop-band) position, width, and intensity could then be tuned over a broad wavelength range through reversible redox processes or by changing the solvent as a result of an anisotropic expansion of the photonic lattice. The optical response of the material was exceptionally fast, and it attained its fully swollen state from the dry shrunken state on a sub-second time scale.

By means of an alternative sol-gel hydrolytic approach, poly(ferrocenylalkoxysilane)s have also been incorporated into gels and oxide matrices. For example, poly(ferrocenylalkoxysilane)s **3.25** (OR = OMe, O^{i}Pr, or OCH_2Ph) (see Eq. 3.11, p. 84) were hydrolyzed in water using fluoride catalysts to afford orange, insoluble solids, which retained the electrochemical properties of the ferrocene units [121].

3.3.6.5 Thermal Stability and Conversion to Nanostructured Magnetic Ceramics

The use of processable polymeric ceramic precursors is an attractive way of circumventing the difficulty inherent in the processing of ceramic materials into desired shapes (see Chapter 1, Section 1.3.2). Ceramics obtained as films, coatings, fibers, or bulk shapes are especially appealing for practical applications. Polymers are of interest as precursors to ceramic monoliths, films, and fibers, provided that the yield on pyrolysis is high. Polyferrocenylsilanes such as **3.22** (R = R′ = Me) are thermally stable up to 350–400 °C. Above 500 °C, magnetic ceramic composites are formed, which consist of iron particles in an essentially amorphous SiC/C matrix [122]. However, the ceramic yields are low (only 35–40% at 1000 °C). The insoluble, semicrystalline poly(ferrocenyldihydrosilane) **3.22** (R = R′ = H) and materials with acetylenic side groups, e.g. **3.22** (R = Me, R′ = C≡CPh), give the highest ceramic yields, with weight retentions of 63% and 81% at 1000 °C and 900 °C, respectively [80, 123].

The use of highly crosslinked polyferrocenylsilane networks **3.48** ($x = y = 0$) leads to much improved ceramic yields (ca. 90%) and the pyrolytic formation of shaped, magnetic ceramics is efficient. The crosslinked network can be formed by heating the [1]silaferrocenophane, **3.47**, in a mold (for 7 h at 150 °C and then for 16 h at 180 °C). The shape of the resulting crosslinked network **3.48** ($x = y = 0$) resembles the mold used, such as a pentagon (Fig. 3.11).

Pyrolysis of molded samples of **3.48** ($x = y = 0$) above 500 °C leads to ceramics with a very small associated weight loss and contraction (< 10%), which allows retention of the overall shape (Fig. 3.11 a) [124, 125]. Furthermore, at 600 °C, the for-

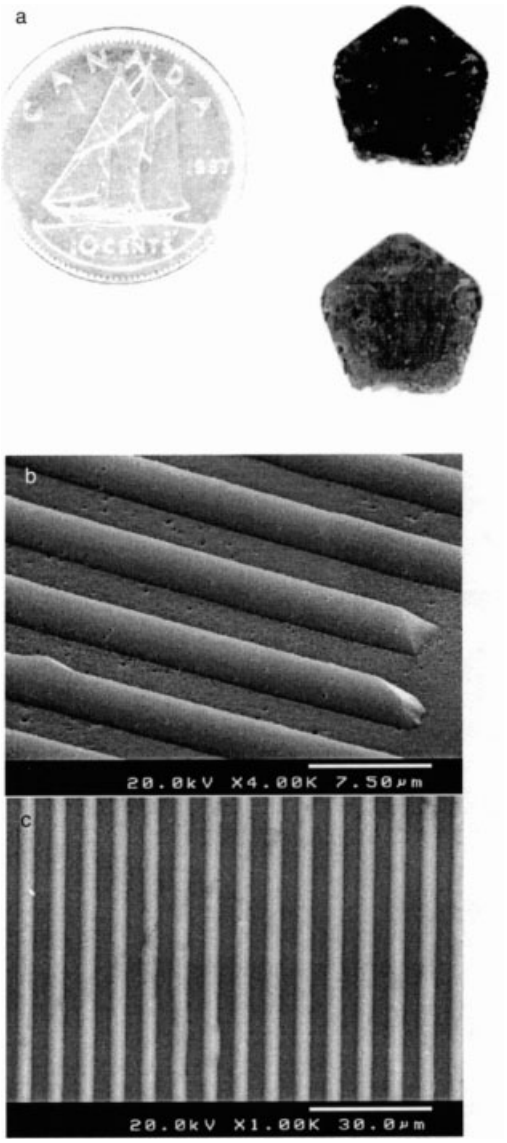

Fig. 3.11 (**a**) Photograph of a bulk organometallic polymer cast in a pentagonal Teflon mold before (bottom) and after (top) pyrolysis at 600 °C. The ceramic retains the shape of the precursor polymer and shows only a small contraction after pyrolysis (pyrolysis was not performed in a mold). (**b**) SEM micrograph of a micron-scale patterned polymer film made by soft lithographic techniques. Micromolding of **3.47** within soft-lithographically patterned and anisotropically etched channels housed inside silicon wafers enables the formation of pre-determined designs of the cross-linked polyferrocenylsilane network **3.48** ($x=y=0$) following thermal ROP. (**c**) SEM micrograph of the resulting patterned ceramic film following pyrolysis at 600 °C under nitrogen. (Reproduced from [125])

mation of small iron clusters dispersed within an amorphous "carbosilane" matrix is apparent. As the pyrolysis temperature is further raised to 1000 °C, an increase in iron particle size is detected by PXRD and TEM. Magnetization measurements on ceramics formed at 650 °C and 850 °C show evidence for smaller, superparamagnetic Fe_n clusters, while for those formed at higher temperatures (1000 °C) the size of the Fe_n clusters is large enough for ferromagnetic behavior to be displayed. Flexible films could also be formed from **3.48** ($x=y=0$), and subsequent pyrolysis at 600 °C provides a route to rigid, superparamagnetic ceramic films.

The polymer precursor approach can also be used in conjunction with soft-lithography techniques to permit the formation of micron-scale magnetic patterns [125]. For example, micromolding of monomer **3.47** within anisotropically etched channels in a silicon wafer followed by thermal ROP yielded patterned polyferrocenylsilane films, and subsequent pyrolysis yielded a patterned magnetic ceramic film with 10% feature size contraction (see Fig. 3.11 b and c). Honeycomb-like cross-linked polyferrocenylsilane inverse opal structures have been prepared by the thermal ROP of spirocyclic [1]silaferrocenophanes such as **3.47** confined within the interstitial void spaces of sacrificial colloidal crystal silica templates. These organometallic polymer inverse opals were converted in high yield to honeycomb-like magnetic ceramic replicas through pyrolysis at 900 °C [126]. Such approaches may allow the formation of shaped ceramic structures of interest for photonics applications, catalysis, nanofiltration, or as magnetically actuated components of microelectromechanical systems (MEMS).

The pyrolysis of polyferrocenylsilanes within the channels of the mesoporous silica MCM-41 and the creation of nanostructured magnetic ceramic nanocomposite materials has also been achieved [127]. In addition, the use of sacrificial porous alumina templates yields organometallic and magnetic ceramic nanofibers [128]. Hyperbranched polyferrocenylsilanes have also been synthesized, and pyrolysis of these interesting materials has been found to lead to superparamagnetic ceramics [129]. Furthermore, pyrolysis of polyferrocenylsilanes with pendant Co clusters yields ceramics containing hybrid Fe/Co alloy nanoparticles [130].

3.3.6.6 **Charge-Tunable and Preceramic Microspheres**

Microspheres based on metal-containing polymers should exhibit interesting redox, semiconductive, and photonic properties intrinsic to the polymeric materials, and may prove useful for a variety of applications. The most common methods for microsphere preparation involve the use of steric stabilizers, which may adversely affect the properties of the resultant materials. This problem can be avoided by the use of a precipitation polymerization methodology, which allows the autostabilization of the polymer microspheres without addition of stabilizers. This approach, which has been used for the formation of crosslinked polystyrene microspheres, has been adapted to allow the preparation of microspheres comprised of polyferrocenylsilane [131].

PFS microspheres comprising **3.48** ($x+y=1$, $z=1$) can be formed by the reaction of monomers **3.21** (R = R′ = Me) and **3.47** in a 1 : 1 ratio in a mixture of xylenes and decane containing a Pt(0) catalyst at 60 °C. Under gentle agitation, over a period of 18 h polymer microspheres with diameters of ca. 2 μm are formed with a reasonably narrow size dispersity (Fig. 3.12 a). Chemical oxidation of the resulting microspheres with iodine leads to positively charged particles, which electrostatically self-assemble with negatively charged silica nanospheres (diameter ca. 0.4 μm). SEM revealed the formation of composite superstructures in which the larger polyferrocenylsilane core was surrounded by the smaller, negatively charged silica particles (Fig. 3.12 b).

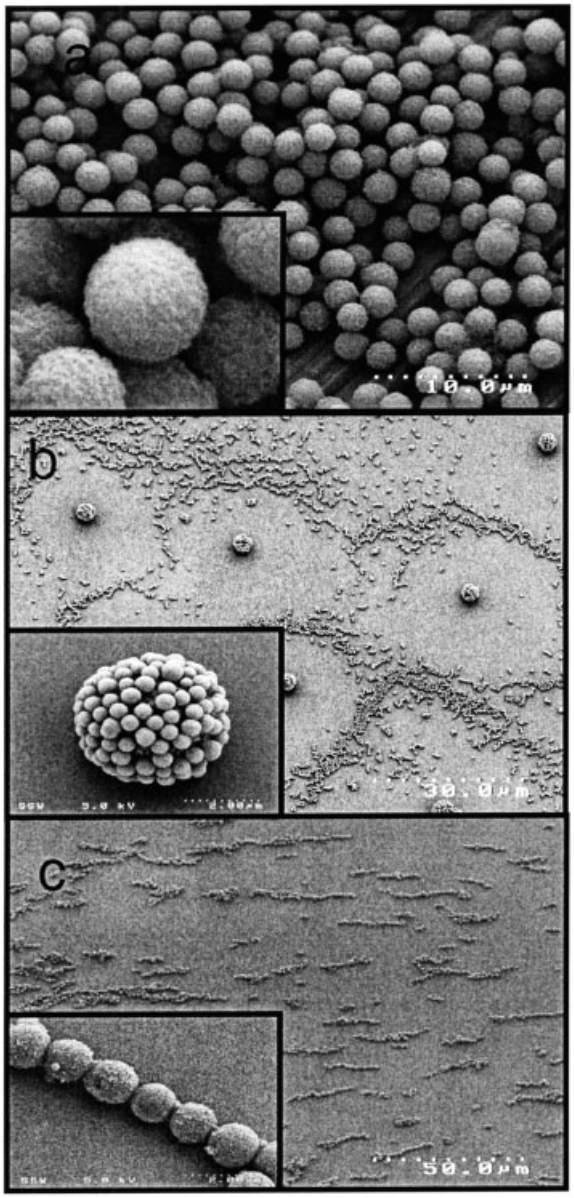

Fig. 3.12 SEM micrographs of: (**a**) Polyferrocenylsilane microspheres formed by precipitation polymerization methods with average particle diameters of 2.1 µm; (**b**) oxidized polyferrocenylsilane microspheres self-assembled with negatively charged silica particles. The silica particles become electrostatically bound to the surface of the oxidized, organometallic microspheres, which are circumscribed by regions of silica particles when deposited on the surface of a silicon wafer; (**c**) ceramic particles obtained by pyrolysis of the polyferrocenylsilane microspheres at 900 °C that display ordering in an external magnetic field. Long strands of magnetic ceramic microspheres are formed, which align parallel to the applied magnetic field lines. (Reproduced from [131])

The development of magnetic particles is of intense interest for theoretical studies, as well as for potential applications in recording media and imaging. The crosslinked PFS microspheres can be used as precursors to spherical magnetic ceramic particles. Upon pyrolysis at either 600 °C or 900 °C, there is a contraction of the microspheres from 2 μm to 1.7 μm in diameter (Fig. 3.12c). Furthermore, the magnetic properties of the microspheres were found to be dependent on the pyrolysis conditions. As with the bulk crosslinked material **3.48** ($x=y=0$), at lower temperatures (600 °C) smaller, superparamagnetic Fe clusters are formed, while at higher temperatures (900 °C) the resulting clusters are larger and display room temperature ferromagnetic behavior. As a result of the magnetic properties associated with the particles, their assembly into well-ordered arrays by interaction with an applied magnetic field becomes feasible [131].

3.3.6.7 Water-Soluble Polyferrocenylsilanes: Layer-by-Layer Assembly Applications

Water-soluble organic polymers are of considerable commercial importance, whereas few examples of water-soluble metal-containing polymers have been reported. Both cationic and anionic water-soluble polyferrocenylsilanes have been prepared by a variety of different synthetic methodologies [132–138]. These materials are of potential interest as electrode materials and as redox-active polymeric electrolytes, the ionic conductivity of which might be tuned by oxidation of the iron centers. Based on the potential formation of micellar aggregates, these materials may also prove useful as redox-active encapsulation agents [139]. Furthermore, various water-soluble ferrocenium salts have been shown to display anti-cancer activity [140].

A typical water-soluble PFS polyelectrolyte, the cationic polyferrocenylsilane **3.50**, can be prepared by thermal ROP of monomer **3.49** followed by quaternization of the resulting polymer with Me_2SO_4 (Eq. 3.21) [133].

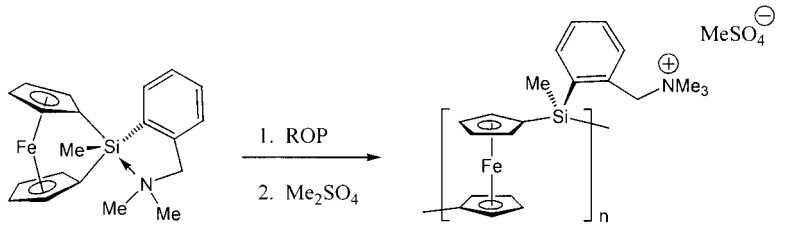

(3.21)

3.49 **3.50**

A key application for these materials involves the creation of electrostatic superlattices by layer-by-layer assembly [135–138]. The technique involves the sequential adsorption of polycationic and polyanionic monolayers from aqueous solutions to form nanoscale multilayer polymer films of controlled thickness. Such film architectures can be manipulated to achieve unique physical properties, and orchestrated for the construction of a range of devices. For example, well-characterized organic/organometallic polymer electrostatic superlattices have been prepared by alternate adsorp-

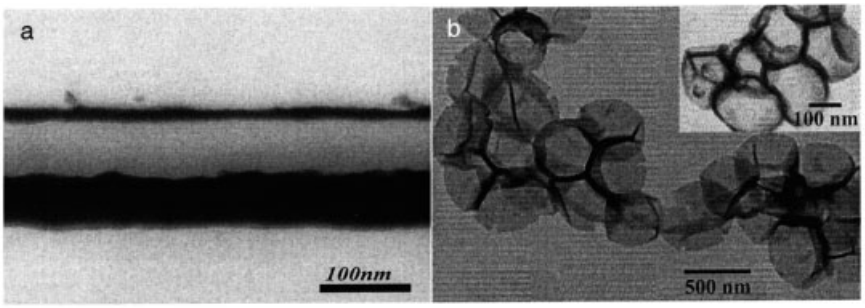

Fig. 3.13 (**a**) 30 Bilayer film of an all-organometallic superlattice imaged by TEM; (**b**) SEM image of hollow PFS microspheres. (Reproduced from [137])

tion of anionic poly(styrenesulfonate) (PSS) and cationic PFS **3.50** on Si and Au substrates [135]. The wettability of the film surface is dependent on the outermost layer of the multilayer assembly, as shown by the advancing contact angle measurements. All-organometallic superlattices constructed from cationic and anionic polyferrocenylsilane polyelectrolytes have also been prepared [137, 138], and a cross-section of such a film on Au can be visualized by TEM after the film surface is sputtered with a layer of Au (Fig. 3.13 a) [137]. In addition, superlattices can be prepared on negatively charged silica microspheres. Subsequent selective etching of the silica with HF yields hollow organometallic microspheres (Fig. 3.13 b) [137].

3.3.6.8 Applications as Variable Refractive Index Sensors and as Nonlinear Optical Materials

Polyferrocenylsilanes are promising materials as coatings for optical-fiber gas sensors [141]. These devices function on the principle that environmentally induced changes in the refractive index of a thin (ca. 0.4 μm) PFS coating lead to changes in the power transmitted through the optical fiber. An example of NH_3-sensing by a device that uses a polyferrocenylsilane coating (**3.22**, R = Me, R′ = Ph, see Eq. 3.10) is shown in Fig. 3.14. The sensor also works well for CO_2, but not for N_2O. In addition, Langmuir-Blodgett films of polyferrocenylsilanes have been studied and are of potential interest as chemomechanical sensors, where changes in mechanical properties are induced by analytes [142]. Potential applications as second-order NLO materials have also been investigated [143].

3.3.7 Properties of Other Ring-Opened Polymetallocenes and Related Materials

Similar ROP methods to those described for silicon-bridged [1]ferrocenophanes have been successfully used for germanium-bridged [1]ferrocenophanes [89, 144]. The resulting high molecular weight polyferrocenylgermanes **3.27** (see Eq. 3.12) are amber materials that exhibit similar electrochemical and thermal transition behavior to polyferrocenylsilanes but with slightly lower T_g values [89, 144]. Polyferrocenylger-

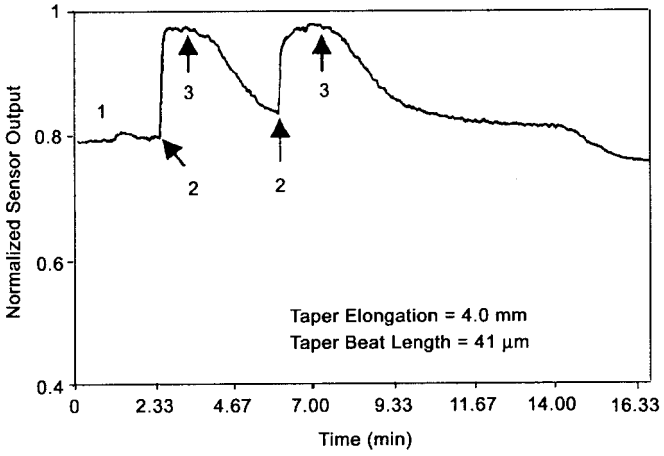

Fig. 3.14 Response of a PFS sensor to NH_3. Point 1 is the response under vacuum, points 2 mark the introduction of NH_3, and at points 3 reevacuation was initiated. (Reproduced from [141])

manes that are symmetrically substituted on germanium also tend to crystallize, as in the case of polyferrocenylsilane analogues. Random copolymers of polyferrocenylgermanes and polyferrocenylsilanes have been prepared from mixtures of [1]germa- and [1]silaferrocenophanes using either thermal or transition metal-catalyzed ROP [88, 89].

Tin-bridged [1]ferrocenophanes have also been successfully prepared by the use of sterically bulky substituents at the bridging element, and undergo ROP to yield polyferrocenylstannanes **3.35** [75, 145]. Polyferrocenylphosphines **3.29** (see Eq. 3.13), polyferrocenylphosphinesulfides **3.30**, and polyelectrolytes derived from the ROP of phosphonium-bridged [1]ferrocenophanes have also been studied [45, 72, 146, 147]. The polyferrocenes with organophosphorus spacers appear to be amorphous, presumably due to their atactic nature. The redox properties of the polyferrocenylphosphines seem, in some cases, to be more complex than those of the corresponding polymers with Group 14 element spacers. This appears to be a consequence of possible electron removal from the lone pair at phosphorus in addition to that from the ferrocene moieties [148]. Polyferrocenylphosphines with narrow polydispersities have been prepared by living anionic ROP of [1]phosphaferrocenophanes and have also been studied [146].

Polyferrocenylsulfides **3.32** have been prepared by the ROP of highly strained sulfur-bridged [1]ferrocenophanes and, based on electrochemical measurements, appear to possess more substantial metal-metal interactions (redox coupling $\Delta E_{1/2} > 0.30$ V) than the analogous polyferrocenylsilanes [73]. Polyferrocenylboranes **3.34** are sensitive to moisture, which has hindered detailed studies of their properties [74].

Disilane-bridged [2]ferrocenophanes are insufficiently strained to undergo ROP [64]. However, random polymers **3.38** with ferrocenylsilane and oligosilane units in the main chain have been prepared by the thermal copolymerization of silicon-

bridged [1]ferrocenophanes and cyclic tetrasilanes (see Eq. 3.15). The resulting copolymers show interesting properties. For example, the Si–Si bonds in these materials can be photochemically cleaved by UV light, and the conjugation in the backbone only appears to involve the σ-delocalized oligosilane segments. The random copolymers also possess appreciable hole mobilities [79].

ROP of hydrocarbon-bridged [2]ferrocenophanes yields polyferrocenylethylenes **3.37** (M = Fe, $E_1 = E_2 = CH_2$, R = H or Me) (see Eq. 3.14). Due to the more insulating hydrocarbon bridge in these materials, only slight communication between the iron centers is observed by cyclic voltammetry (redox coupling of $\Delta E_{1/2}$ = 0.09 V). Nevertheless, cooperative magnetic behavior has been reported in TCNE-oxidized materials at low temperature [149].

3.3.8
Polyferrocenylsilane Block Copolymers

3.3.8.1 Synthetic Scope

Living anionic ROP of strained silicon-bridged [1]ferrocenophanes (Section 3.3.3) provides an excellent route to PFS block copolymers with controlled block lengths and narrow polydispersities (PDI < 1.1) [82–84]. Diblock, triblock, and more complex architectures are now known for a wide variety of organic, inorganic, or even other polyferrocene coblocks. The prototypical materials prepared in the mid-1990s were the diblock copolymers polyferrocenylsilane-*b*-polydimethylsiloxane (PFS-*b*-PDMS) **3.52** and polystyrene-*b*-polyferrocenylsilane (PS-*b*-PFS) **3.54** [83]. As shown in Scheme 3.4, initial anionic polymerization of monomer **3.21**

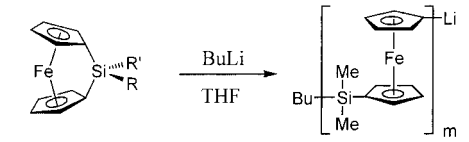

3.21 R = R' = Me

3.51

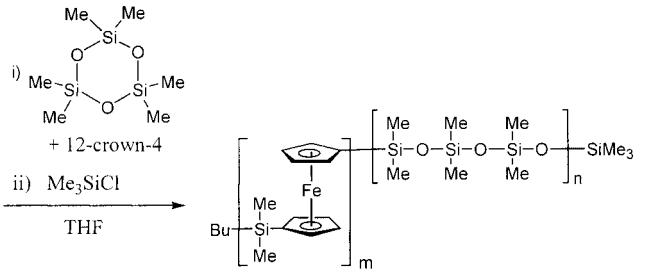

PFS-*b*-PDMS

3.52

Scheme 3.4

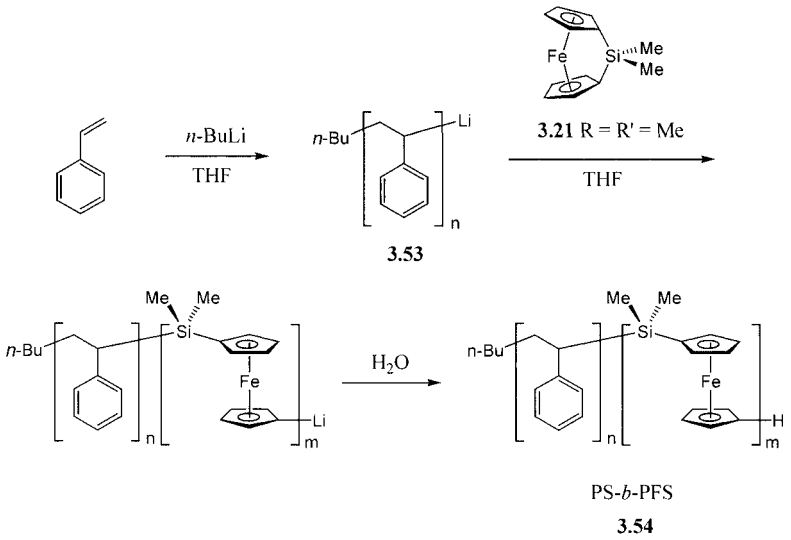

Scheme 3.5

(R = R′ = Me) gives a living polyferrocenyllithium species **3.51**, which can be subsequently used to initiate the ROP of a comonomer such as a cyclic siloxane to prepare **3.52**. The ROP of ferrocenophane **3.21** can also occur in the presence of the living anions of a preformed block. For example, copolymer PS-*b*-PFS **3.54** can be prepared by anionic polymerization of styrene followed by ROP of **3.21**, initiated by the lithiated polystyrene species **3.53** (Scheme 3.5).

PFS block copolymers can also be accessed by transition metal-catalyzed ROP of silicon-bridged [1]ferrocenophanes (Section 3.3.4) in the presence of a polymer terminated with a reactive Si–H bond [90]. This technique has been successfully used for the synthesis of both diblock and triblock copolymers. For example, water-soluble PFS-*b*-PEO **3.55** (PEO = poly(ethylene oxide)) has been prepared from monomer **3.21** (R = R′ = Me) and commercially available poly(ethylene glycol) modified at the end group (Scheme 3.6) [92]. In such cases, the polydispersity of the PFS blocks is higher than that obtained from anionic ROP (typically PDI = 1.4), and the polydispersity of the coblock is determined by that of the original Si–H functionalized material. Nevertheless, block copolymer syntheses that use the transition metal-catalyzed approach are very convenient, as the stringent purification and experimental requirements for living anionic polymerizations are unnecessary.

3.3.8.2 Self-Assembly in Block-selective Solvents

Based on the studies of organic block copolymers (see Chapter 1, Section 1.2.5), polyferrocenylsilane block copolymers can be expected to self-assemble in solvents which are selective for one of the blocks. In the case of organic block copolymers, most studies have led to the identification of spherical structures, where the less

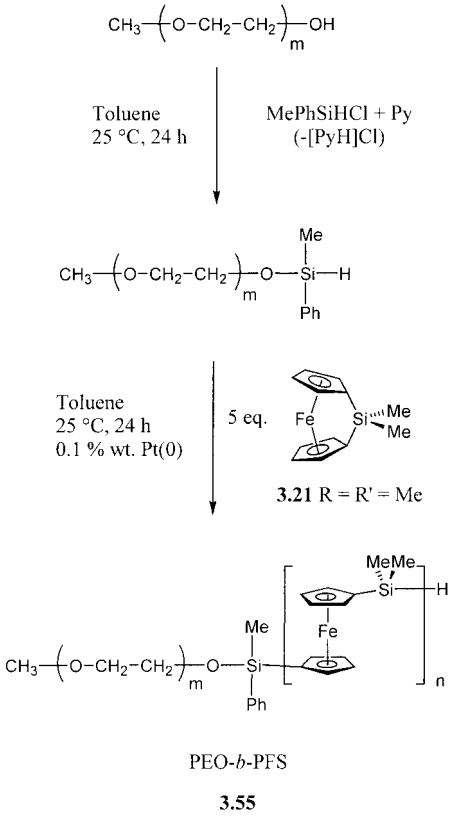

Scheme 3.6

soluble block constitutes the core within a corona formed by the more soluble block. Only since the mid-1990s have non-spherical structures become more commonly reported [150].

Initial studies on the solution micellization of PFS block copolymers involved investigations of the aggregation of PFS-*b*-PDMS block copolymers **3.52** in a selective solvent for the PDMS block [151]. Interesting cylindrical micellar architectures can be generated by simply dissolving the amber, tacky block copolymer in *n*-hexane at room temperature (Fig. 3.15). Worm-like micelles were obtained in the case of a material with a PFS : PDMS block ratio of 1 : 6. These structures maintain their integrity after solvent evaporation, and the iron-rich cores can be readily visualized by transmission electron microscopy (TEM) (Fig. 3.16 a). When the micelles are prepared above the T_m of the poly(ferrocenyldimethylsilane) block (ca. 120–145 °C), spherical aggregates are formed. Spherical structures are also generated when an amorphous poly(ferrocenylmethylphenylsilane) or poly(ferrocenylmethylethylsilane) block is used in the copolymer. These results suggest that the crystallization of the core polymer is the driving force for the unexpected formation of worm-like micelles below T_m [152]. In the case of even longer corona-forming PDMS blocks, cylindrical struc-

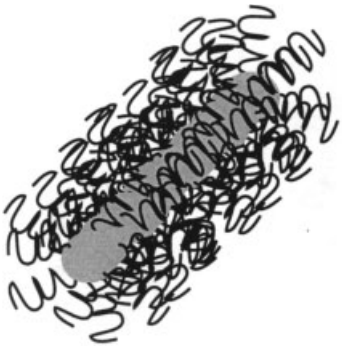

Fig. 3.15 Schematic cross-sectional diagram of PFS-*b*-PDMS (**3.52**) cylindrical micelles showing the polyferrocenylsilane core and a poly(dimethylsiloxane) corona.

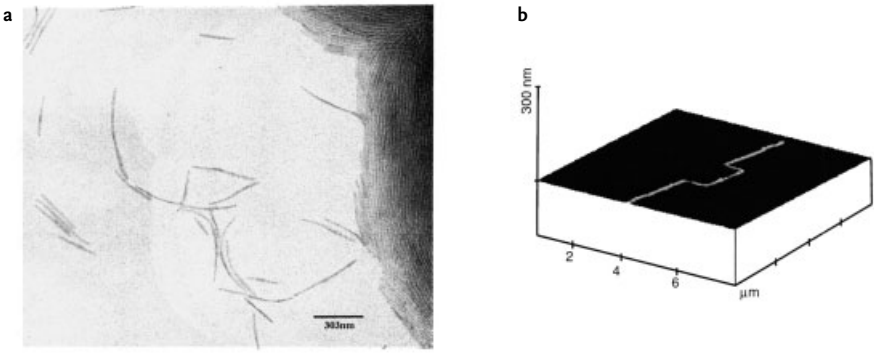

Fig. 3.16 (**a**) Transmission electron micrograph of cylindrical micelles of PFS-*b*-PDMS **3.52** (M_n = 35,100, PDI = 1.1) aerosol-sprayed from *n*-hexane solution onto mica. The cylinders have an average contour length of 440 nm and an average diameter of 20 nm. The micrograph shows a region where the cylinders are starting to pack and form a two-dimensional film and regions where there are isolated cylinders. No staining of the sample is necessary as the PFS cores are readily observable due to high electron density contrast. (**b**) Scanning force micrograph after the oriented deposition of PFS-*b*-PDMS diblock copolymer cylinders along pre-patterned grooves on a resist film, lift-off with acetone, followed by hydrogen plasma treatment. This process leads to aligned nanoscopic lines with a height of approximately 4 nm, composed of cylindrical clusters of Fe, Si, O and C. (Reproduced from [151] and [157])

tures that possess an appreciably hollow cavity are formed (e.g. for a PFS : PDMS ratio of 1 : 12) [153].

The lengths of the cylindrical structures can be increased to over 10 µm by controlling the preparation technique. The cylinders show considerable stability in solution and are unchanged in size after heating to 80 °C. However, ultrasonication of samples of the cylindrical micelles leads to a shortening of their length, as indicated by light-scattering and TEM studies.

Cylindrical and tape-like morphologies have been identified in the case of PI-*b*-PFS (PI = polyisoprene) where the PFS block crystallizes [154]. Water-soluble polyferrocenyldimethylsilane-*b*-poly(aminoalkylmethacrylate) copolymers of narrow

polydispersity have also been prepared, and cylindrical micelles have been identified [155]. Block copolymers generated by transition metal-catalyzed ROP, such as PFS-*b*-PDMS-*b*-PFS triblock materials, have been shown to self-assemble in hexanes to yield a variety of remarkable architectures that include flower-like assemblies in which the PFS block is semicrystalline [156]. In several systems, morphologies such as vesicles and compound micelles in addition to spheres and cylinders have been identified.

The cylindrical micelles formed by PFS-*b*-PDMS consist of a wire-like core of PFS surrounded by a sheath or corona of insulating poly(dimethylsiloxane) and are of interest as semiconducting nanowires and as precursors to magnetic wire-like ceramic structures. These structures are sufficiently stable to permit fabrication by spin- or dip-coating onto substrates. The cylindrical micelles have been positioned on the surface of a GaAs wafer by capillary forces along grooves that had previously been formed by electron-beam etching of the surface [157]. After reactive ion etching of the micelles with hydrogen plasma, connected ceramic lines of reduced size, with potentially interesting conductive and magnetic properties, were generated (Fig. 3.16 b). In some cases, such a technique allows the formation of lines that have widths of less than 10 nm and lengths greater than 500 nm through this combined "top-down/bottom-up" approach [158]. It should be noted that structures of such small dimensions are difficult to fabricate using other techniques. Furthermore, these well-defined aggregates may be of use as etching resists for semiconducting substrates such as GaAs or Si, and offer potential access to magnetic or semiconducting nanoscopic patterns on various substrates. As the accessibility of smaller and smaller width scales by conventional lithographic techniques becomes limited, the use of such methods becomes attractive. For example, the formation of micellar etching resists for use in the production of quantum wires with large aspect ratios in semiconducting substrates may be possible.

3.3.8.3 **Self-Assembly in the Solid State**

Polyferrocenylsilane block copolymers in which the blocks are immiscible (which is generally the case) would be expected to self-assemble to form phase-separated organometallic domains in the solid state. Based on the classical behavior of organic block copolymers, thin films of polyferrocene diblock copolymers would be expected to form domains such as spheres, cylinders, double diamonds (or gyroids) (or their antistructures), or lamellae (Chapter 1, Section 1.2.5). The preferred domain structure would be expected to be controlled by the ratio of the blocks, their degree of immiscibility (as defined by the Flory-Huggins interaction parameter χ), and the overall molecular weight of the block copolymer [159].

The first studies of polyferrocenylsilane block copolymer films were reported in 1996 and utilized DSC and TEM to analyze the phase separation in the materials [83]. In the case of PS-*b*-PFS (**3.54**) and PFS-*b*-PDMS (**3.52**), it was demonstrated that the electron-rich Fe atoms of the polyferrocenylsilane block cause sufficient electron scattering to provide contrast with the organic or inorganic coblocks, so that selective staining of one of the blocks, which is generally required for all-or-

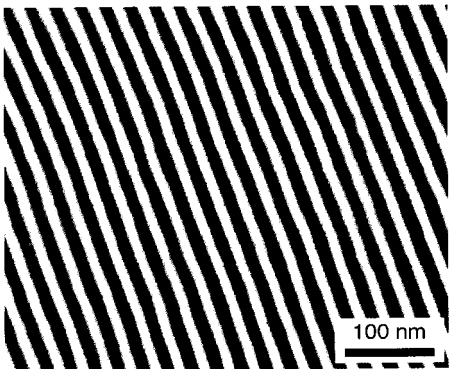

Fig. 3.17 TEM image of films of PS-*b*-PFS (block ratio = ca. 1:1) after annealing at 180 °C showing lamellar ordering (domain spacing of 31 nm). The white regions are PS domains while the darker regions are PFS domains. (Reproduced from [160])

ganic materials, is unnecessary [83, 151]. Detailed systematic studies confirmed that spherical, cylindrical, and lamellar domains are formed by using the expected block ratio variations [160–163]. An example of the formation of a lamellar structure by a PS-*b*-PFS block copolymer is shown in Fig. 3.17. A detailed analysis of the thermodynamic interactions in PS-*b*-PFS (**3.54**) using birefringence, SAXS, and neutron-scattering techniques has also been performed [164]. The phase-separation can be influenced by the crystallization of the polyferrocenyldimethylsilane block, and analogous materials with amorphous PFS blocks that order more readily without the need to anneal above the T_m, have therefore also been studied [84].

The difference in etch-resistance between the blocks in a copolymer can be used to pattern surfaces on the nanometer scale through exposure of phase-separated thin films to etching plasmas [165]. Such processes are particularly efficient if one of the blocks contains inorganic elements [166]. Block-selective ablation of thin films of phase-separated PFS block copolymers would therefore be expected to be useful for the nanopatterning of surfaces [161]. An example that elegantly illustrates this approach utilizes PS-*b*-PFS materials (**3.54**), which provide a spherical PFS morphology within a matrix of PS [167]. The high relative etching resistance of the PFS block compared to the PS block has allowed the production of lithographic templates from such films upon plasma treatment. Subsequent use of the template in patterning substrates such as cobalt metal has generated arrays of magnetic cobalt nanodots with potential applications in data storage (Fig. 3.18) upon plasma treatment.

Pyrolysis of phase-separated PFS block copolymer films also allows the formation of metal-rich nanostructures. For example, pyrolysis of a thin film of PS-*b*-PFS, with cylinders of the amorphous PFS block oriented perpendicular to the substrate within a crosslinked PS matrix, at 600 °C yields iron-containing dots of size ca. 20 nm on a substrate (Fig. 3.19) [168].

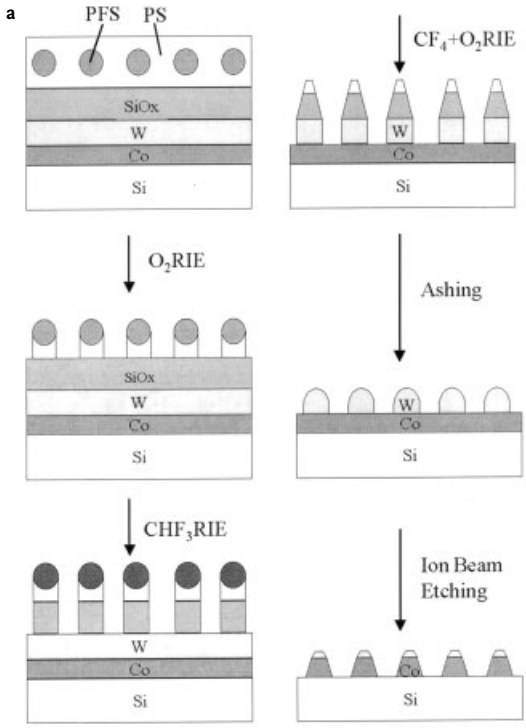

Fig. 3.18 (**a**) Single-domain cobalt dot arrays with high magnetic particle density, patterned over large areas (e.g., 10 cm diameter wafers) using self-assembled block copolymer lithography with PS-*b*-PFS **3.54** as a template. A thin film consisting of spheres of PFS in a matrix of PS is cast on a multilayer of silica, tungsten, and cobalt. The exposed PS is removed by O_2 reactive ion etching (RIE), and then the silica is patterned using a CHF_3-RIE. The tungsten is patterned using a CF_4+O_2 RIE, and the silica and residual polymer are removed by high-pressure CHF_3-RIE in an ashing step. The cobalt dots are formed by ion-beam etching. (**b**) A tilted SEM image of a typical array of Co dots with tungsten caps obtained by this procedure. (Reproduced from [167] with permission. We thank Prof. C.A. Ross and J.Y. Cheng (Dept. of Materials Science and Engineering, Massachusetts Institute of Technology) for the figures.)

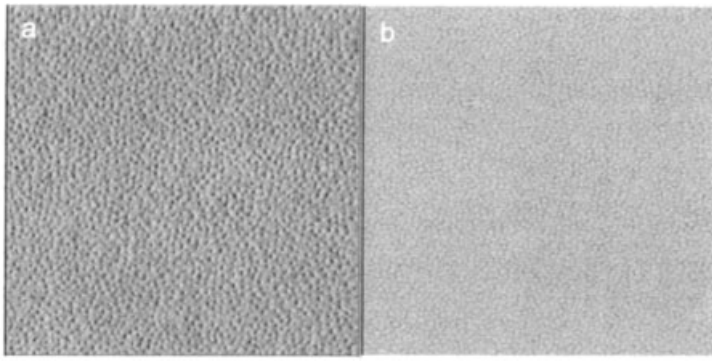

Fig. 3.19 AFM images (2 μm×2 μm) of (**a**) a thin film (200 nm) and (**b**) a pyrolyzed (600 °C, 2 h, N_2) sample of a thin film (25 nm) of PS-*b*-PFS in which the PS matrix had been crosslinked by UV radiation.
PFS = poly(ferrocenylmethylethylsilane). (Reproduced from [168])

3.3.9
Polyferrocenylphosphine Block Copolymers

It is also possible to form block copolymers by living anionic ROP of phosphorus-bridged ferrocenophanes (Section 3.3.3) [45, 146]. Diblock copolymers such as PI-*b*-PFP (**3.57**) (PFP = polyferrocenylphosphine) can be prepared by the sequential anionic polymerization of isoprene and the ferrocenophane **3.56** (Scheme 3.7). These materials yield spherical micelles in *n*-hexane with an amorphous PFP core and a PI corona. The PI corona can be cross-linked by radical reactions to yield a permanently crosslinked shell, which retains its integrity even in good solvents

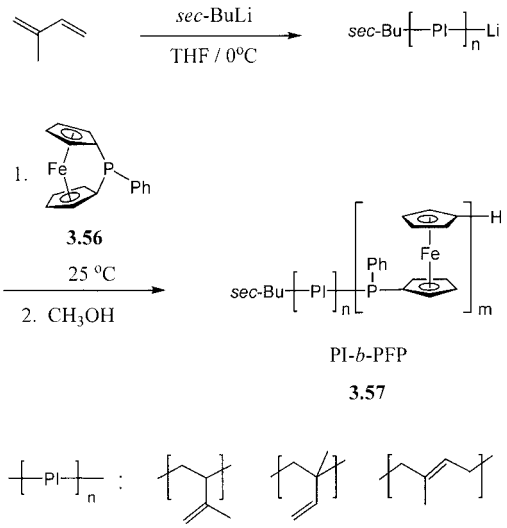

Scheme 3.7

for both blocks [169]. With PFP block copolymers, the possibility of the coordination of various transition metal moieties to the phosphorus centers may prove useful for catalysis and for materials science applications.

3.4
Transition Metal-Catalyzed Ring-Opening Metathesis Polymerization (ROMP) of Metallocenophanes

The synthesis of poly(ferrocenylenevinylene) by ring-opening metathesis polymerization (ROMP) of the vinylene-bridged [2]ferrocenophane (**3.58**) was reported in 1997 [170]. The monomer was obtained from the McMurry coupling of 1,1′-ferrocenedicarbaldehyde. In the presence of a molybdenum ROMP catalyst, **3.58** was found to undergo polymerization (Scheme 3.8) to give an insoluble orange powder **3.59**, which exhibited a conductivity of 10^{-3} Scm^{-1} after iodine-doping. Partially soluble block copolymers **3.60** were also obtained from ferrocenophane **3.58** and norbornene via the ROMP route (Scheme 3.8). When a ratio of [Mo]-catalyst : norbornene : **3.58** = 1 : 10 : 10 was used, the reaction gave a red gel and a soluble fraction with an M_w value of 1710, as determined by GPC analysis (*vs.* polystyrene standards) and a slightly higher M_n of 3000 by end-group analysis. Similar material generated from a reaction mixture with a catalyst : norbornene : **3.58** ratio of 1 : 50 : 10 showed a considerably higher M_w of 21,000 by GPC. The cyclic voltammograms of **3.60** showed two reversible redox waves with a separation of 0.25 mV, which is similar to that of polyferrocenylsilanes **3.22** ($\Delta E_{1/2}$ = 0.20–0.25 V), thus indicating a significant degree of interaction between the Fe centers [170].

Also of relevance at this juncture due to the analogous synthetic approach, ROMP of [4]ferrocenophane **3.61** (R = H) with unsaturated –C=C–C=C– bridges (Eq. 3.22) has been used to obtain related polyferrocenylenedivinylenes **3.62**

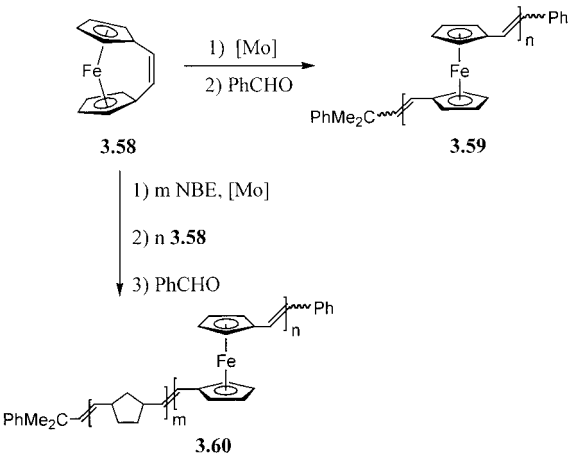

Scheme 3.8

(R = H) with a π-conjugated structure [171]. These materials are rather insoluble, but copolymerization with *sec*-butylcyclooctatetraene yields more soluble materials with molecular weights up to M_w = 24,400 (PDI = 2.1). ROMP has also been used to prepare soluble, high molecular weight materials **3.62** (R = *t*-Bu) (M_w > 300,000) from substituted [4]ferrocenophane **3.61** bearing a solubilizing *t*-butyl group [172].

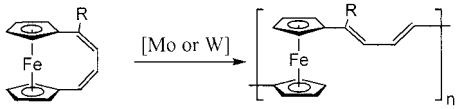

(3.22)

3.61 **3.62**

R = H or *t*-Bu

3.5 Atom Abstraction-Induced Ring-Opening Polymerization of Chalcogenido-Bridged Metallocenophanes

In early 1992, a novel atom-abstraction-induced ROP process was described [60]. Using this method, the synthesis of well-defined poly(ferrocenylene persulfide)s (**3.64**) was achieved by desulfurization of [3]trithiaferrocenophane (**3.63**) with PBu_3 (Eq. 3.23). The resultant yellow materials proved to be soluble only when the ferrocene unit was substituted with alkyl groups. The rate of the desulfurization reaction and the nature of the resultant polymers have been reported to be solvent-dependent [173–175]. The molecular weights have been determined to be in the range M_w = 12,000–359,000 for **3.64** (R = *n*-Bu, R′ = H) and 25,000 in the case of a less soluble copolymer formed from monomers **3.63** with (R = R′ = H) : (R = ^{n}Bu, R′ = H) in a ratio of 53 : 47 [173, 175]. Polymerization of mono- and disubstituted *t*-Bu derivatives yielded highly soluble polymers **3.64** with M_w values of up to 26,000 (R = *t*-Bu, R′ = H) and high polydispersities (PDI = 1.9–7.9) [174]. These polymers have been fully characterized and exhibit very interesting properties. The materials are air-stable in the solid state but are photosensitive in solution. The persulfide bond can be reductively cleaved with $Li[BEt_3H]$ and subsequently regenerated upon oxidation with I_2 [174]. Electrochemical studies of **3.64** (R = R′ = *t*-Bu) showed two reversible oxidation waves, as observed for polyferrocenylsilanes, that can be attributed to initial oxidation of alternating iron sites along the polymer chain [174, 175]. A wave separation of $\Delta E_{1/2}$ = ca. 0.29 V (Fig. 3.20) suggests that the interaction between iron sites is slightly greater than that observed in polyferrocenylsilanes (Fig. 3.9) [108].

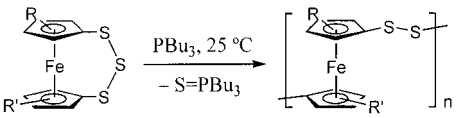

(3.23)

3.63 **3.64**

R = R′ = H, *t*–Bu
R = *n*–Bu, *t*–Bu R′ = H

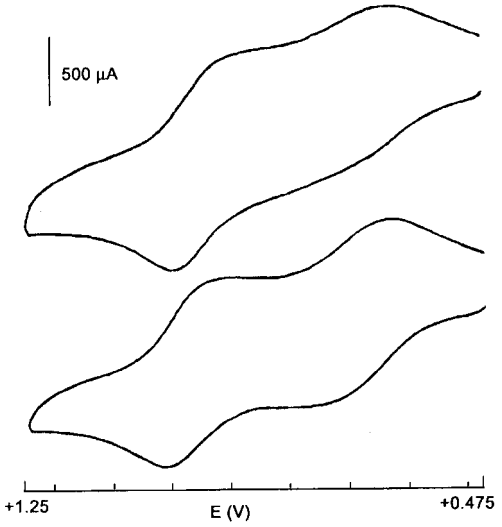

Fig. 3.20 Cyclic voltammograms of poly(ferrocenylene persulfide)s **3.64** (top: R=R′=*t*-Bu; bottom: R=*t*-Bu, R′=H) showing two reversible oxidation waves separated by a redox coupling $\Delta E_{1/2}$ of ca. 0.29 V for both polymers (in 0.1 M $[Bu_4N][PF_6]$ in CH_2Cl_2). (Reproduced from [174])

This atom-abstraction route has also been used for the preparation of polymeric networks from alkylated [3,3′]bis(trithia)ferrocenophanes [173]. A bimodal molecular weight distribution, with maxima at $M_n \approx 5000$ and 5×10^5, was obtained by GPC for the material, from which a polymer fraction was isolated ($M_n=8.5\times10^5$). Low molecular weight poly(ferrocenylene perselenide)s have also been prepared from the selenium analogue of **3.63**. These materials also undergo photodegradation upon exposure to UV light in air [175].

3.6
Face-to-Face and Multidecker Polymetallocenes Obtained by Condensation Routes

Multidecker sandwich structures can be classified in the forms shown in Fig. 3.21 (a) and (b) and contrast with the linear polymer structures discussed so far (Fig. 3.21 c).

Several attempts have been made to synthesize these types of polymeric structures, but in most cases dimeric complexes, or double- or triple-decker structures, were produced. A synthesis of novel polymeric metallocenes (Fig. 3.21, type b) held face-to-face by naphthalene or binaphthyl spacer groups has been developed. The condensation route involved palladium-catalyzed cross-coupling of chlorozincferrocenes or ruthenocenes with 1,8-diiodonaphthalene [176, 177]. Since the ferrocene reagent is very reactive and cannot be prepared in pure form, it is difficult to achieve the exact stoichiometry of reactants required for a high degree of polymerization. Also, the rigidity of the polymer framework makes these materials relatively insoluble and, consequently, only materials with M_n up to 4000 have been prepared. Crystallographic studies on a trimetal oligomer, as a model for a segment of the polymer, showed a cisoid arrangement of the naphthalene rings. Ex-

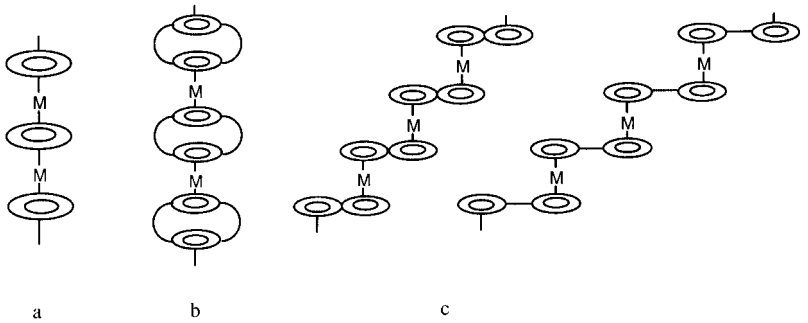

Fig. 3.21 Polymeric Multidecker Sandwich Complexes (**a**) and (**b**) and the Structure of Linear Polymetallocenes (**c**) for comparison

trapolation would suggest a helical structure for the polymer [178]. An alternative, more successful route, in which a ferrocene monomer (**3.65**) is polymerized by treatment with sodium bis(trimethylsilyl)amide and $FeCl_2$ at room temperature (Eq. 3.24), has been reported by the same group [179]. The introduction of long hydrocarbon chains as substituents in the monomer unit clearly improves the solubility; thus, polymers **3.66** (M = Fe) with values of M_n up to 18,000 can be easily prepared and, in some cases, components of higher molecular weight were also detected.

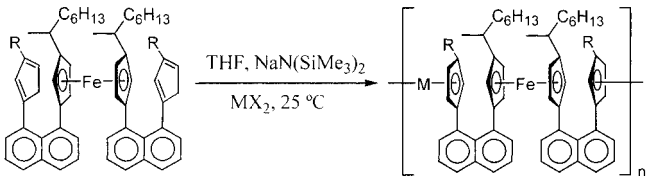

3.65 **3.66**

M = Fe, Co X = Cl
M = Ni, X = CH_3COO
R = H, 2-octyl

(3.24)

This is a more general route to these materials and allows access to polynickelocenes by the reaction of alkylated bis(cyclopentadienyl)naphthalene with a nickel (II) reagent. Mixed nickel-iron or cobalt-iron structures can also be prepared in a similar fashion from **3.65** and the corresponding metal salts. However, to date, only low molecular weight products ($M_n < 4000$ for nickelocene polymers and < 2000 for the heterometallic materials) have been described [180]. The electrical and magnetic properties of these polymers have been investigated. When the iron-based polymers were partially oxidized with I_2, an increase in the electrical conductivity from less than 10^{-12} Scm^{-1} to 6.7×10^{-3} Scm^{-1} was detected, reflecting semiconductor behavior. This value is almost two orders of magnitude lower than that for the analogous crystalline poly(1,1′-ferrocenylene) (Section 3.2.1). The electrochemistry of oligomers reflects some degree of electronic interaction and

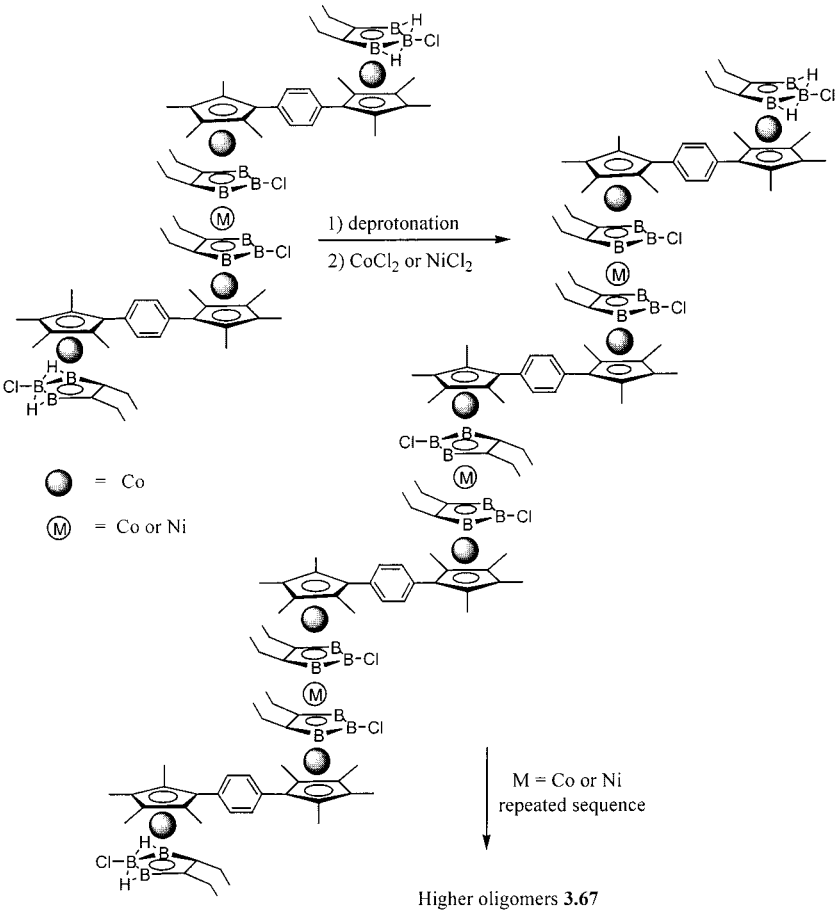

Scheme 3.9

charge delocalization between the metal centers of the partially oxidized species ($\Delta E_{1/2}$ = 0.10–0.20 V at 50 V s^{-1}). The corresponding I_2-doped polymers appear to be weakly interacting mixed-valent systems by Mössbauer spectroscopy. The bulk magnetic susceptibility was determined for the paramagnetic nickelocene polymer and heterometallic copolymers. For all of the polymers, the values were found to be greater than those for the corresponding nickelocene or cobaltocene, which was interpreted in terms of cooperative magnetic behavior [180].

The synthesis of multidecker structures (Fig. 3.21 (a)) with stacked architectures has also been explored. Tetra-decker sandwich oligomeric materials **3.67** containing carborane C_2B_3 rings have been synthesized by successive deprotonation of the reactive C_2B_3 end groups followed by metathesis reactions with the appropriate metal salts (Scheme 3.9) [181]. Oligomers having 5–17 metal atoms have been synthesized via this route. Cyclic voltammetry studies of these compounds sug-

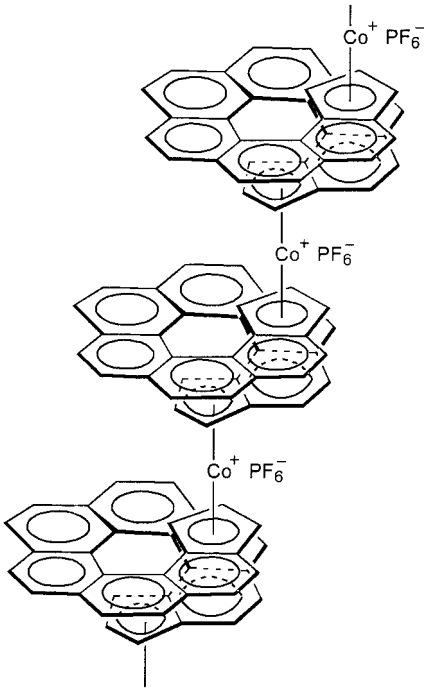

3.68

gested little inter-sandwich electronic communication, but gave good evidence for electronic delocalization within the individual tetra-decker stacks [182].

Among recent attempts to obtain polymers of combined type a and c (Fig. 3.21), in which the successive metal-ring bonding is laterally displaced, is the interesting synthesis of materials of structure **3.68** [183]. The preparation of soluble helical cobaltocenium oligomers (**3.68**, up to six units) was achieved in high yield, following the elaborate synthesis of [9]helicene hydrocarbon dianions, by treatment with $CoBr_2 \cdot DME$ and anion metathesis. These are the first examples in which metallocenes are joined by fused conjugated aromatic systems. Electrochemical studies on their properties showed a weak interaction between the metals ($\Delta E_{1/2} = 0.13$ V), similar to that in the face-to-face polymers described above.

3.7 References

1 G. J. Wilkinson, *J. Organomet. Chem.* **1975**, *100*, 273.

2 (a) N. J. Long, *Metallocenes, An Introduction to Sandwich Complexes*, Blackwell Science, Oxford, **1998**. (b) *Ferrocenes* (Eds.: A. Togni, T. Hayashi), VCH Publishers, New York, **1995**.

3 A. Togni, in *Ferrocenes* (Eds.: A. Togni, T. Hayashi), VCH Publishers, New York, **1995**, pp. 433–469.

4 S. Barlow, D. O'Hare, *Chem. Rev.* **1997**, *97*, 637.

5 J. A. Kramer, D. N. Hendrickson, *Inorg. Chem.* **1980**, *19*, 3330.

6 R. Deschenaux, J. W. Goodby, in *Ferrocenes* (Eds.: A. Togni, T. Hayashi), VCH Publishers, New York, **1995**, pp. 471–495.

7 *Inorganic Materials, 2nd ed.* (Eds.: D. W. Bruce, D. O'Hare), John Wiley & Sons, Toronto, **1996**.

8 For an overview, see: I. Manners, *Chem. Br.* **1996**, *32*, 46.

9 For interesting work on metallocene oligomers based on V, Cr, Co, and Ni, see: H. Atzkern, P. Bergerat, H. Beruda, M. Fritz, J. Hiermeier, P. Hudeczek, O. Kahn, F. H. Köhler, M. Paul, B. Weber, *J. Am. Chem. Soc.* **1995**, *117*, 997.

10 E. W. Neuse, H. Rosenberg, *J. Macromol. Sci., Rev. Macromol. Chem.* **1970**, *C4*, 1.

11 See ref. [10], pp. 130.

12 V. V. Korshak, S. L. Sosin, V. P. Alekseeva, *Doklady Akad. Nauk SSSR* **1960**, *132*, 360.

13 V. V. Korshak, S. L. Sosin, V. P. Alekseeva, *Vysokomol. Soedin.* **1961**, *3*, 1332.

14 A. N. Nesmeyanov, V. V. Korshak, V. V. Voevodski, N. S. Kochetkova, S. L. Sosin, R. B. Materikova, T. N. Bolotnikova, V. M. Chibrikin, N. M. Bazhin, *Doklady Akad. Nauk S.S.S.R.* **1961**, *137*, 1370.

15 H. Rosenberg, E. W. Neuse, *J. Organomet. Chem.* **1966**, *6*, 76.

16 For a detailed overview, see ref. [10], pp. 30–33.

17 A. N. Nesmeyanov, V. N. Drozd, V. A. Sazonova, V. I. Romanenko, A. K. Prokofev, L. A. Nikonova, *Izv. Akad. Nauk SSSR, Otd. Khim. Nauk* **1963**, 667.

18 P. V. Roling, M. D. Rausch, *J. Org. Chem.* **1972**, *37*, 729.

19 H. Watanabe, I. Motoyama, K. Hata, *Bull. Chem. Soc. Jpn.* **1966**, *39*, 790.

20 I. J. Spilners, J. P. Pellegrini, *J. Org. Chem.* **1965**, *30*, 3800.

21 F. L. Hedberg, H. Rosenberg, *Tetrahedron Lett.* **1969**, *10*, 4011.

22 M. D. Rausch, *J. Org. Chem.* **1963**, *28*, 3337.

23 E. W. Neuse, R. K. Crossland, *J. Organomet. Chem.* **1967**, *7*, 344.

24 A. Bradley, J. P. Hammes, *J. Electrochem. Soc.* **1963**, *110*, 15.

25 T. Izumi, A. Kasahara, *Bull. Chem. Soc. Jpn.* **1975**, *48*, 1955.

26 L. Bednarik, R. C. Gohdes, E. W. Neuse, *Transition Met. Chem.* **1977**, *2*, 212.

27 C. U. Pittman, Jr., B. Surynarayanan, Y. Sasaki in *Inorganic Compounds with Unusual Properties* (Ed.: R. B. King) *Adv. Chem. Ser. 150*, Chapter 4, p 46–55 (1976).

28 C. U. Pittman, Jr., Y. Sasaki, *Chem. Lett.* **1975**, 383.

29 D. O. Cowan, J. Park, C. U. Pittman, Jr., Y. Sasaki, T. K. Mukherjee, N. A. Diamond, *J. Am. Chem. Soc.* **1972**, *94*, 5110.

30 D. O. Cowan, C. LeVanda, *J. Am. Chem. Soc.* **1972**, *94*, 9271.

31 U. T. Mueller-Westerhoff, P. Eilbracht, *J. Am. Chem. Soc.* **1972**, *94*, 9272.

32 D. O. Cowan, F. Kaufman, *J. Am. Chem. Soc.* **1970**, *92*, 219.

33 E. W. Neuse, L. Bednarik, *Macromolecules* **1979**, *12*, 187.

34 K. Sanechika, T. Yamamoto, A. Yamamoto, *Polymer J.* **1981**, *13*, 255.

35 T. Yamamoto, K. Sanechika, A. Yamamoto, M. Katada, I. Motoyama, H. Sano, *Inorg. Chim. Acta* **1983**, *73*, 75.

36 H. Meier, *Organic Semiconductors*, Verlag Chemie, Weinheim, FRG, **1974**.

37 N. Oyama, Y. Takizawa, H. Matsuda, T. Yamamoto, K. Sanechika, *Denki Kagaku oyobi Kogyo Butsuri Kagaku* **1988**, *56*, 781.

38 (a) K. Seki, H. Tanaka, T. Ohta, K. Sanechika, T. Yamamoto, *Chem. Phys. Lett.* **1991**, *178*, 311; (b) for theoretical calcula-

tions see M.C. Böhm, *J. Chem. Phys.* **1984**, *80*, 2704.
39 (a) T. Hirao, M. Kurashina, K. Aramaki, H. Nishihara, *Dalton Trans.* **1996**, 2929. (b) H. Nishihara, T. Hirao, K. Aramaki, K. Aoki, *Synth. Met.* **1997**, *84*, 935.
40 P. Park, A.J. Lough, D.A. Foucher, *Macromolecules* **2002**, *35*, 3810.
41 E.W. Neuse, *J. Macromol. Sci., Chem.* **1981**, *A16*, 3.
42 E.W. Neuse, G.J. Chris, *J. Macromol. Sci., Chem.* **1967**, *A1*, 371.
43 C.U. Pittman, Jr., *J. Polym. Sci., Polym. Chem. Ed.* **1967**, *5*, 2927.
44 H.P. Withers, Jr., D. Seyferth, J.D. Fellmann, P.E. Garrou, S. Martin, *Organometallics* **1982**, *1*, 1283.
45 C.H. Honeyman, T.J. Peckham, J.A. Massey, I. Manners, *J. Chem. Soc., Chem. Commun.* **1996**, 2589.
46 J.D. Fellmann, P.E. Garrou, H.P. Withers, D. Seyferth, D.D. Traficante, *Organometallics* **1983**, *2*, 818.
47 H. Rosenberg, M.D. Rausch, US Patent 3060215, **1962**.
48 H. Rosenberg, US Patent 3426053, **1969**.
49 J. Park, Y. Seo, S. Cho, D. Whang, K. Kim, T. Chang, *J. Organomet. Chem.* **1995**, *489*, 23.
50 A.G. Osborne, R.H. Whiteley, R.E. Meads, *J. Organomet. Chem.* **1980**, *193*, 345.
51 D. Seyferth, H.P. Withers, *Organometallics* **1982**, *1*, 1275.
52 T. Itoh, H. Saitoh, S. Iwatsuki, J. *Polym. Sci., Polym. Chem.* **1995**, *33*, 1589.
53 H. Plenio, J. Hermann, J. Leukel, *Eur. J. Inorg. Chem.* **1998**, 2063.
54 H. Plenio, J. Hermann, A. Sehring, *Chem. Eur. J.* **2000**, *6*, 1820.
55 O. Nuyken, V. Burkhardt, T. Pöhlmann, M. Herberhold, *Makromol. Chem., Macromol. Symp.* **1991**, *44*, 195.
56 M. Herberhold, H.D. Brendel, O. Nuyken, T. Pöhlmann, *J. Organomet. Chem.* **1991**, *413*, 65.
57 O. Nuyken, T. Pöhlmann, M. Herberhold, *Macromolecular Rep.* **1992**, *A29*, 211.
58 S.A. Giddings, *Inorg. Chem.* **1964**, *3*, 684.
59 J.J. Salzmann, *Helv. Chim. Acta* **1968**, *51*, 903.
60 P.F. Brandt, T.B. Rauchfuss, *J. Am. Chem. Soc.* **1992**, *114*, 1926.
61 D.A. Foucher, B.Z. Tang, I. Manners, *J. Am. Chem. Soc.* **1992**, *114*, 6246.
62 (a) A.G. Osborne, R.H. Whiteley, *J. Organomet. Chem.* **1975**, *101*, C27. (b) M. Herberhold, *Angew. Chem. Int. Ed. Engl.* **1995**, *34*, 1837.
63 A.B. Fischer, J.B. Kinney, R.H. Staley, M.S. Wrighton, *J. Am. Chem. Soc.* **1979**, *101*, 6501.
64 W. Finckh, B.Z. Tang, D.A. Foucher, D.B. Zamble, R. Ziembinski, A. Lough, I. Manners, *Organometallics* **1993**, *12*, 823.
65 Review: I. Manners, *Adv. Organomet. Chem.* **1995**, *37*, 131.
66 Review: K. Kulbaba, I. Manners, *Macromol. Rapid Commun.* **2001**, *22*, 711.
67 M.J. MacLachlan, A.J. Lough, I. Manners, *Macromolecules* **1996**, *29*, 8562.
68 P. Nguyen, G. Stojcevic, K. Kulbaba, M.J. MacLachlan, X.-H. Liu, A.J. Lough, I. Manners, *Macromolecules* **1998**, *31*, 5977.
69 J.K. Pudelski, I. Manners, *J. Am. Chem. Soc.* **1995**, *117*, 7265.
70 F. Jäkle, R. Rulkens, G. Zech, J.A. Massey, I. Manners, *J. Am. Chem. Soc.* **2000**, *122*, 4231.
71 D.A. Foucher, M. Edwards, R.A. Burrow, A.J. Lough, I. Manners, *Organometallics* **1994**, *13*, 4959.
72 C.H. Honeyman, D.A. Foucher, F.Y. Dahmen, R. Rulkens, A.J. Lough, I. Manners, *Organometallics* **1995**, *14*, 5503.
73 R. Rulkens, D.P. Gates, D. Balaishis, J.K. Pudelski, D.F. McIntosh, A.J. Lough, I. Manners, *J. Am. Chem. Soc.* **1997**, *119*, 10976.
74 A. Berenbaum, H. Braunschweig, R. Dirk, U. Englert, J.C. Green, F. Jäkle, A.J. Lough, I. Manners, *J. Am. Chem. Soc.* **2000**, *122*, 5765.
75 F. Jäkle, R. Rulkens, G. Zech, D.A. Foucher, A.J. Lough, I. Manners, *Chem. Eur. J.* **1998**, *4*, 2117.
76 J.M. Nelson, H. Rengel, I. Manners, *J. Am. Chem. Soc.* **1993**, *115*, 7035.
77 J.M. Nelson, A.J. Lough, I. Manners, *Angew. Chem. Int. Ed. Engl.* **1994**, *33*, 989.

78 R. Resendes, J.M. Nelson, A. Fischer, F. Jäkle, A. Bartole, A.J. Lough, I. Manners, *J. Am. Chem. Soc.* **2001**, *123*, 2116.

79 R. Rulkens, R. Resendes, A. Verma, I. Manners, K. Murti, E. Fossum, P. Miller, K. Matyjaszewski, *Macromolecules* **1997**, *30*, 8165.

80 J.K. Pudelski, R. Rulkens, D.A. Foucher, A.J. Lough, P.M. Macdonald, I. Manners, *Macromolecules* **1995**, *28*, 7301.

81 K.C. Hultzsch, J.M. Nelson, A.J. Lough, I. Manners, *Organometallics* **1995**, *14*, 5496.

82 (a) R. Rulkens, A.J. Lough, I. Manners *J. Am. Chem. Soc.* **1994**, *116*, 797. (b) R. Rulkens, Y.Z. Ni, I. Manners, *J. Am. Chem. Soc.* **1994**, *116*, 12121.

83 Y.Z. Ni, R. Rulkens, I. Manners, *J. Am. Chem. Soc.* **1996**, *118*, 4102.

84 K. Temple, J.A. Massey, Z. Chen, N. Vaidya, A. Berenbaum, M.D. Foster, I. Manners, *J. Inorg. Organomet. Polym.* **1999**, *9*, 189.

85 I. Manners, *Polyhedron* **1996**, *15*, 4311.

86 K. H. Pannell, H. K. Sharma, *Organometallics* **1997**, *16*, 3077.

87 Y.Z. Ni, R. Rulkens, J.K. Pudelski, I. Manners, *Macromol. Rapid Commun.* **1995**, *16*, 637.

88 N.P. Reddy, H. Yamashita, M. Tanaka, *J. Chem. Soc., Chem. Commun.* **1995**, 2263.

89 T.J. Peckham, J.A. Massey, M. Edwards, I. Manners, D.A. Foucher, *Macromolecules* **1996**, *29*, 2396.

90 P. Gómez-Elipe, R. Resendes, P.M. Macdonald, I. Manners, *J. Am. Chem. Soc.* **1998**, *120*, 8348.

91 D.L. Zechel, K.C. Hultzsch, R. Rulkens, D. Balaishis, Y.Z. Ni, J.K. Pudelski, A.J. Lough, I. Manners, D.A. Foucher, *Organometallics* **1996**, *15*, 1972.

92 R. Resendes, J. Massey, H. Dorn, M.A. Winnik, I. Manners, *Macromolecules* **2000**, *33*, 8.

93 K.N. Power-Billard, I. Manners, *Macromol. Rapid Commun.* **2002**, *23*, 607.

94 K. Temple, F. Jäkle, J.B. Sheridan, I. Manners, *J. Am. Chem. Soc.* **2001**, *123*, 1355.

95 K. Mochida, N. Shibayama, M. Goto, *Chem. Lett.* **1998**, 339.

96 T. Baumgartner, F. Jäkle, R. Rulkens, G. Zech, A.J. Lough, I. Manners, J. *Am. Chem. Soc.* **2002**, *124*, 10062.

97 T. Mizuta, M. Onishi, K. Miyoshi, *Organometallics* **2000**, *19*, 5005.

98 J. Rasburn, D.A. Foucher, W.F. Reynolds, I. Manners, G.J. Vancso, *Chem. Commun.* **1998**, 843.

99 J.A. Massey, K. Kulbaba, M.A. Winnik, I. Manners, *J. Polym. Sci., Polym. Phys.* **2000**, *28*, 3032.

100 R.G.H. Lammertink, M.A. Hempenius, I. Manners, G.J. Vancso, *Macromolecules* **1998**, *31*, 795.

101 Z. Chen, M.D. Foster, W. Zhou, H. Fong, D.H. Reneker, R. Resendes, I. Manners, *Macromolecules* **2001**, *34*, 6156.

102 (a) R. Rulkens, A.J. Lough, I. Manners, S.R. Lovelace, C. Grant, W.E. Geiger, *J. Am. Chem. Soc.* **1996**, *118*, 12683. (b) H. Nishihara, *Adv. Inorg. Chem.* **2002**, *53*, 41.

103 S. Barlow, A.L. Rohl, S. Shi, C.M. Freeman, D. O'Hare, *J. Am. Chem. Soc.* **1996**, *118*, 7578.

104 V.S. Papkov, M.V. Gerasimov, I.I. Dubovik, S. Sharma, V.V. Dementiev, K.H. Pannell, *Macromolecules* **2000**, *33*, 7107.

105 (a) X.-H. Liu, D.W. Bruce, I. Manners, *J. Chem. Soc., Chem. Commun.* **1997**, 289. (b) X.-H. Liu, D.W. Bruce, I. Manners, *J. Organomet. Chem.* **1997**, *548*, 49.

106 J.C. Medina, C. Li, S.G. Bott, J.L. Atwood, G.W. Gokel, *J. Am. Chem. Soc.* **1991**, *113*, 366.

107 K. Kulbaba, I. Manners, P.M. Macdonald, *Macromolecules* **2002**, *35*, 10014.

108 D.A. Foucher, C.H. Honeyman, J.M. Nelson, B.Z. Tang, I. Manners, *Angew. Chem. Int. Ed. Engl.* **1993**, *32*, 1709.

109 M.T. Nguyen, A.F. Diaz, V.V. Dement'ev, K.H. Pannell, *Chem. Mater.* **1993**, *5*, 1389.

110 D.A. Foucher, R. Ziembinski, R. Rulkens, J.M. Nelson, I. Manners, in *Inorganic and Organometallic Polymers II: Advanced Materials and Intermediates, ACS Symp. Ser. 572 (Eds.:* P. Wisian-Neilson, H.R. Allcock, K.J. Wynne), American Chemical Society, Washington, D.C., **1994**, p. 442.

111 L. Espada, K.H. Pannell, V. Papkov, L. Leites, S. Bukalov, I. Suzdalev, M. Ta-

naka, T. Hayashi, *Organometallics* **2002**, *21*, 3758.
112 G.E. Southard, M.D. Curtis, *Organometallics* **2001**, *20*, 508.
113 M.T. Nguyen, A.F. Diaz, V.V. Dement'ev, K.H. Pannell, *Chem. Mater.* **1994**, *6*, 952.
114 L. Bakueva, E.H. Sargent, R. Resendes, A. Bartole, I. Manners, *J. Mater. Sci., Mater. Electr.* **2001**, *12*, 21.
115 R. Resendes, A. Berenbaum, G. Stojevic, F. Jäkle, A. Bartole, F. Zamanian, G. Dubois, C. Hersom, K. Balmain, I. Manners, *Adv. Mater.* **2000**, *12*, 327.
116 M. Hmyene, A. Yassar, M. Escorne, A. Percheron-Guegan, F. Garnier, *Adv. Mater.* **1994**, *6*, 564.
117 J.K. Pudelski, D.A. Foucher, C.H. Honeyman, P.M. Macdonald, I. Manners, S. Barlow, D. O'Hare, *Macromolecules* **1996**, *29*, 1894.
118 P. Cyr, M. Tzolov, I. Manners, E.H. Sargent, *Macromol. Chem. Phys.* **2003**, *204*, 915.
119 K. Kulbaba, M.J. MacLachlan, C.E.B. Evans, I. Manners, *Macromol. Chem. Phys.* **2001**, *202*, 1768.
120 A.C. Arsenault, H. Miguez, V. Kitaev, G.A. Ozin, I. Manners, *Adv. Mater.* **2003**, *15*, 503.
121 G. Calléja, G. Cerveau, R.J.P. Corriu, *J. Organomet. Chem.* **2001**, *621*, 46.
122 R. Petersen, D.A. Foucher, B.-Z. Tang, A. Lough, N.P. Raju, J.E. Greedan, I. Manners, *Chem. Mater.* **1995**, *7*, 2045.
123 A. Berenbaum, A.J. Lough, I. Manners, *Organometallics* **2002**, *21*, 4415.
124 M.J. MacLachlan, M. Ginzburg, N. Coombs, T.W. Coyle, N.P. Raju, J.E. Greedan, G.A. Ozin, I. Manners, *Science* **2000**, *287*, 1460.
125 M. Ginzburg, M.J. MacLachlan, S.M. Yang, N. Coombs, T.W. Coyle, N.P. Raju, J.E. Greedan, R.H. Herber, G.A. Ozin, I. Manners, *J. Am. Chem. Soc.* **2002**, *124*, 2625.
126 J. Galloro, M. Ginzburg, H. Míguez, S.M. Yang, N. Coombs, A. Safa-Sefat, J.E. Greedan, I. Manners, G.A. Ozin, *Adv. Func. Mater.* **2002**, *12*, 382.
127 M.J. MacLachlan, M. Ginzburg, N. Coombs, N.P. Raju, J.E. Greedan, G.A. Ozin, I. Manners, *J. Am. Chem. Soc.* **2000**, *122*, 3878.
128 M. Ginzburg-Margau, S. Fournier-Bidoz, N. Coombs, G.A. Ozin, I. Manners, *Chem. Commun.* **2002**, 3022.
129 Q. Sun, J.W.Y. Lam, K. Xu, H. Xu, J.A.K. Cha, P.C.L. Wong, G. Wen, X. Zhang, X. Jing, F. Wang, B.Z. Tang, *Chem. Mater.* **2000**, *12*, 2617.
130 A. Berenbaum, M. Ginzburg, N. Coombs, A.J. Lough, A. Safa-Sefat, J.E. Greedan, G.A. Ozin, I. Manners, *Adv. Mater.* **2003**, *15*, 51.
131 K. Kulbaba, A. Cheng, A. Bartole, S. Greenberg, R. Resendes, N. Coombs, A. Safa-Sefat, J.E. Greedan, H.D.H. Stöver, G.A. Ozin, I. Manners, *J. Am. Chem. Soc.* **2002**, *124*, 12522.
132 K.N. Power-Billard, I. Manners, *Macromolecules* **2000**, *33*, 26.
133 F. Jäkle, Z. Wang, I. Manners, *Macromol. Rapid Commun.* **2001**, *21*, 1291.
134 Z. Wang, A.J. Lough, I. Manners, *Macromolecules* **2002**, *35*, 7669.
135 M. Ginzburg, J. Galloro, F. Jäkle, K.N. Power-Billard, S. Yang, I. Sokolov, C.N.C. Lam, A.W. Neumann, I. Manners, G.A. Ozin, *Langmuir* **2000**, *16*, 9609.
136 M.A. Hempenius, N.S. Robins, R.G.H. Lammertink, G.J. Vancso, *Macromol. Rapid Commun.* **2001**, *22*, 30.
137 (a) J. Halfyard, J. Galloro, M. Ginzburg, Z. Wang, N. Coombs, I. Manners, G.A. Ozin, *Chem. Commun.* **2002**, 1746. (b) J. Halfyard, M. Ginzburg, J. Galloro, I. Manners, G.A. Ozin, unpublished results.
138 M.A. Hempenius, M. Péter, N.S. Robins, E.S. Kooij, G.J. Vancso, *Langmuir* **2002**, *18*, 7629.
139 (a) J.C. Medina, I. Gay, Z. Chen, L. Echegoyen, G.W. Gokel, *J. Am. Chem. Soc.* **1991**, *113*, 365. (b) T. Saji, K. Hoshino, Y. Ishii, M. Goto, *J. Am. Chem. Soc.* **1991**, *113*, 450. (c) Y. Kakizawa, H. Sakai, A. Yamaguchi, Y. Kondo, N. Yoshino, M. Abe, *Langmuir* **2001**, *17*, 8044.
140 P. Koepf-Maier, H. Koepf, E.W. Neuse, *Angew. Chem. Int. Ed. Engl.* **1984**, *96*, 456.

141 L. I. Espada, M. Shadaram, J. Robillard, K. H. Pannell, *J. Inorg. Organomet. Polym.* **2000**, *10*, 169.

142 H. Yim, M. D. Foster, D. Balaishis, I. Manners, *Langmuir* **1998**, *14*, 3921.

143 Y. Y. Liu, X. Zhang, H. D. Tang, T. J. Wang, J. G. Qin, D. Y. Liu, S. J. Li, C. Ye, *Chinese J. Chem.* **2002**, *20*, 1199.

144 M. Castruita, F. Cervantes-Lee, J. S. Mahmoud, Y. Zhang, K. H. Pannell, *J. Organomet. Chem.* **2001**, *637*, 664.

145 H. K. Sharma, F. Cervantes-Lee, J. S. Mahmoud, K. H. Pannell, *Organometallics* **1999**, *18*, 399.

146 T. J. Peckham, J. A. Massey, C. H. Honeyman, I. Manners, *Macromolecules* **1999**, *32*, 2830.

147 T. J. Peckham, A. J. Lough, I. Manners, *Organometallics* **1999**, *18*, 1030.

148 D. A. Durfey, R. U. Kirss, C. Frommen, W. Feighery, *Inorg. Chem.* **2000**, *39*, 3506.

149 J. M. Nelson, P. Nguyen, R. Petersen, H. Rengel, P. M. Macdonald, A. J. Lough, I. Manners, N. P. Raju, J. E. Greedan, S. Barlow, D. O'Hare, *Chem. Eur. J.* **1997**, *3*, 573.

150 L. Zhang, A. Eisenberg, *J. Am. Chem. Soc.* **1996**, *118*, 3168.

151 J. A. Massey, K. N. Power, I. Manners, M. A. Winnik, *J. Am. Chem. Soc.* **1998**, *120*, 9533.

152 J. A. Massey, K. Temple, L. Cao, Y. Rharbi, J. Raez, M. A. Winnik, I. Manners, *J. Am. Chem. Soc.* **2000**, *122*, 11577.

153 J. Raez, I. Manners, M. A. Winnik, *J. Am. Chem. Soc.* **2002**, *124*, 10381.

154 L. Cao, I. Manners, M. A. Winnik, *Macromolecules* **2002**, *35*, 8258.

155 X.-S. Wang, M. A. Winnik, I. Manners, *Macromol. Rapid Commun.* **2002**, *23*, 210.

156 R. Resendes, J. A. Massey, K. Temple, L. Cao, K. N. Power-Billard, M. A. Winnik, I. Manners, *Chem. Eur. J.* **2001**, *7*, 2414.

157 J. A. Massey, M. A. Winnik, I. Manners, V. Z.-H. Chan, J. M. Ostermann, R. Enchelmaier, J. P. Spatz, M. Möller, *J. Am. Chem. Soc.* **2001**, *123*, 3147.

158 L. Cao, J. A. Massey, M. A. Winnik, I. Manners, V. Z.-H. Chan, J. P. Spatz, J. M. Ostermann, R. Enchelmaier, M. Möller, *Adv. Func. Mater.* **2003**, *13*, 271.

159 F. S. Bates, *Science* **1991**, *251*, 898.

160 J. A. Massey, K. N. Power, M. A. Winnik, I. Manners, *Adv. Mater.* **1998**, *10*, 1559.

161 I. Manners, *Chem. Commun.* **1999**, 857.

162 R. G. H. Lammertink, M. A. Hempenius, E. L. Thomas, G. J. Vancso, *J. Polym. Sci., Polym. Phys.* **1999**, *37*, 1009.

163 W. Li, N. Sheller, M. D. Foster, D. Balaishis, I. Manners, B. Annis, J.-S. Lin, *Polymer* **2000**, *41*, 719.

164 H. B. Eitouni, N. P. Balsara, H. Hahn, J. A. Pople, M. A. Hempenius, *Macromolecules* **2002**, *35*, 7765.

165 M. Park, C. Harrison, P. M. Chaikin, R. A. Register, D. H. Adamson, *Science* **1997**, *276*, 1401.

166 V. Z.-H. Chan, J. Hoffman, V. Y. Lee, H. Latrou, A. Avgeropoulos, N. Hadjichristidis, R. D. Miller, E. L. Thomas, *Science* **1999**, *286*, 1716.

167 J. Y. Cheng, C. A. Ross, V. Z.-H. Chan, E. L. Thomas, R. G. H. Lammertink, G. J. Vancso, *Adv. Mater.* **2001**, *13*, 1174.

168 K. Temple, K. Kulbaba, K. N. Power-Billard, I. Manners, A. Leach, T. Xu, T. P. Russell, C. J. Hawker, *Adv. Mater.* **2003**, *15*, 297.

169 L. Cao, I. Manners, M. A. Winnik, *Macromolecules* **2001**, *34*, 3353.

170 M. A. Buretea, T. D. Tilley, *Organometallics* **1997**, *16*, 1507.

171 C. E. Stanton, T. R. Lee, R. H. Grubbs, N. S. Lewis, J. K. Pudelski, M. R. Callstrom, M. S. Erickson, M. L. McLaughlin, *Macromolecules* **1995**, *28*, 8713.

172 R. W. Heo, F. B. Somoza, T. R. Lee, *J. Am. Chem. Soc.* **1998**, *120*, 1621.

173 C. P. Galloway, T. B. Rauchfuss, *Angew. Chem. Int. Ed. Engl.* **1993**, *32*, 1319.

174 D. L. Compton, T. B. Rauchfuss, *Organometallics* **1994**, *13*, 4367.

175 D. L. Compton, P. F. Brandt, T. B. Rauchfuss, D. F. Rosenbaum, C. F. Zukoski, *Chem. Mater.* **1995**, *7*, 2342.

176 R. Arnold, S. A. Matchett, M. Rosenblum, *Organometallics* **1988**, *7*, 2261.

177 B. M. Foxman, M. Rosenblum, *Organometallics* **1993**, *12*, 4805.

178 B. M. Foxman, D. A. Gronbeck, M. Rosenblum, *J. Organomet. Chem.* **1991**, *413*, 287.

179 H. M. Nugent, M. Rosenblum, *J. Am. Chem. Soc.* **1993**, *115*, 3848.

180 M. Rosenblum, H.M. Nugent, K.-S. Jang, M.M. Labes, W. Cahalane, P. Klemarczyk, W.M. Reiff, *Macromolecules* **1995**, *28*, 6330.

181 X. Meng, M. Sabat, R.N. Grimes, *J. Am. Chem. Soc.* **1993**, *115*, 6143.

182 J.R. Pipal, R.N. Grimes, *Organometallics* **1993**, *12*, 4459.

183 T.J. Katz, A. Sudhakar, M.F. Teasley, A.M. Gilbert, W.E. Geiger, M.P. Robben, M. Wuensch, M.D. Ward, *J. Am. Chem. Soc.* **1993**, *115*, 3182.

4
Main-Chain Metallopolymers Containing π-Coordinated Metals and Long Spacer Groups

4.1
Introduction

Polymers with main-chain metal-containing units in close spatial proximity (i.e., when the spacer groups comprise three atoms or fewer), in which the metal atoms can interact, are dominated by metallocene-based materials, and this area was the focus of the previous chapter. Macromolecules in which longer spacer groups are present between the metal centers have also been explored. The chemistry that has been successfully used to prepare metal-containing polymers with long spacers is much more diverse, and a variety of π-hydrocarbon ligands other than cyclopentadienyl groups have been productively utilized. Nevertheless, apart from several impressive exceptions, the studies reported to date have been, in general, less in-depth and relatively few properties and applications have been investigated in detail. This chapter surveys work in this general area.

4.2
Polymetallocenes with Long Insulating Spacer Groups

4.2.1
Organic Spacers

The thermal stability and interesting physical properties of ferrocene provided the initial motivation for the inclusion of ferrocene moieties into polymer chains [1–3]. In the 1960s, numerous attempts to produce ferrocene-containing organic polymers, which included polyketones, polyesters, polyamines, polyamides, polyurethanes, polyureas, and materials with heterocyclic groups, were reported [4]. The synthetic methodologies that were used involved polycondensation methods at high temperatures, and frequently involved side reactions that led to impure materials or cross-linking. In general, the resulting polymers were very poorly characterized and were of low molecular weight ($M_n < 6000$). Often, no analytical data or structural characterization was provided. Room temperature interfacial polycondensation methods were also investigated as a convenient alternative to

Synthetic Metal-Containing Polymers. Ian Manners

ISBN: 3-527-29463-5

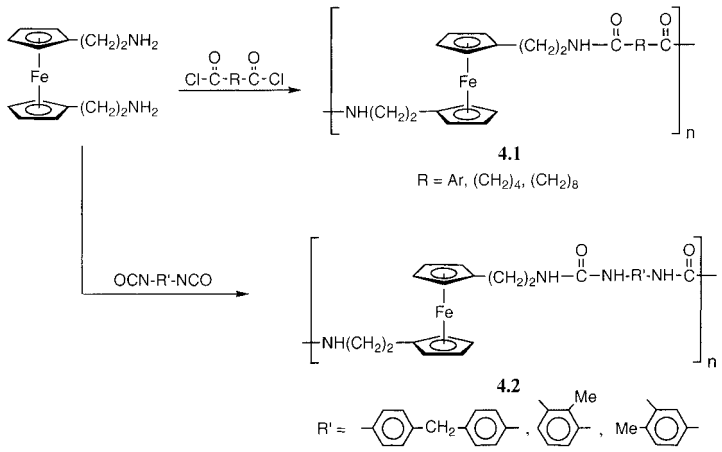

Scheme 4.1

classical polycondensations. Such methods were first reported for the preparation of polyamides and polyesters by the reaction of 1,1′-ferrocenyldicarbonyl chloride with several diamines and diols [5]. The synthesis of polyurethanes using this technique was also reported and involved the condensation of 1,1′-ferrocenedimethanol and 1,1′-bis(dihydroxyethyl)ferrocene with diisocyanates. Once again, however, these polymers possessed low molecular weights [6]. The early research in these areas has been summarized and critically reviewed [4] and will not be discussed further here.

In the 1980s, the successful synthesis of elastomeric polyamides (**4.1**) of high molecular weight (M_n = 10,000–18,000) was reported by the polycondensation of 1,1′-bis(β-aminoethyl)ferrocene with diacid chlorides (Scheme 4.1) [7]. Also, polyureas (**4.2**) were prepared from the same ferrocene monomer and diisocyanates, and polyesters and polyurethanes were prepared from 1,1′-bis(β-hydroxyethyl)ferrocene. However, the latter materials had much lower molecular weights and were characterized only by scanning electron microscopy, X-ray elemental analysis, and IR spectroscopy. The introduction of ferrocenes in which the functional groups are separated from the cyclopentadienyl ring by at least two methylene units was crucial in order to reduce steric effects and to avoid the instability found previously in polymers of α-functionalized ferrocene due to the α-ferrocenyl carbonium ion stability [8].

The same type of methodology was also used to prepare ferrocene-containing arylidene polyesters (**4.3**) in good yields from dicarboxyl ferrocenes and organic diols. These materials were characterized by elemental analysis, IR spectroscopy, viscometry, and WAXS [9]. The polymers were found to be semicrystalline, but were soluble in polar organic solvents. Conductivity studies showed an n-type semiconductor behavior ($\sigma = 3 \times 10^{-10}$ Scm^{-1} at room temperature) that followed a one-term Arrhenius-type equation with increasing conductivity over the range 25–220 °C.

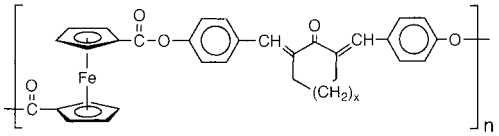

4.3
x = 0, 1, 2

Ferrocene-containing polymers with long spacers have been prepared as new nonlinear optical (NLO) materials for second harmonic generation (SHG) applications (e.g. frequency doubling) [10]. The use of ferrocene derivatives in this area is attractive as a result of their demonstrated large hyperpolarizability values combined with their thermal and photochemical stabilities [11]. These factors make polyferrocenes desirable candidates for use as processable NLO materials. The polyurethane copolymer **4.4** was synthesized using a functional ferrocene monomer (Eq. 4.1) and has been well-characterized; the molecular weight was estimated by GPC to be $M_n = 7600$. The two possible orientations of the ferrocene NLO chromophore monomer unit, which correspond to opposite dipole orientations, were both present in the main chain.

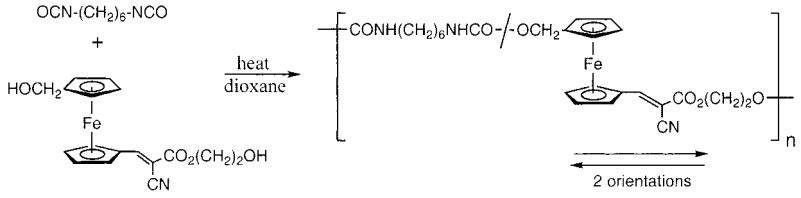

4.4

(4.1)

Contrary to previous results concerning related materials with a single orientation of the ferrocene-based NLO chromophores in the main chain, copolymer **4.4** displays SHG activity after corona poling at 150 °C with reasonable stability of the SHG signal [12]. This suggests that the chain packing in the solid state, that cancels dipole additive effects in the former materials, does not operate for the latter polymers, which leads to a positive response to poling.

A range of well-characterized ferrocene-containing copolyesters, such as **4.5**, have been prepared by $Ti(O^iPr)_4$-catalyzed melt polycondensations at 140–170 °C [13]. The polymers had molecular weights in the range 9000–30,300 (by capillary viscometry) and were analyzed by NMR, IR, and DSC. When ferrocene groups were incorporated into the main chain of the polyesters, an increase in the oxidation potential by ≈ 40 mV was detected, presumably due to a charge-transfer through-space interaction between the electron-poor ester group and the ferrocene unit as the separation was four to six σ-bonds. The first study of the rheological consequences of the incorporation of ferrocene groups into the main chain of a

polymer was performed using dynamical mechanical analysis (DMA). Comparison with analogous iron-free polyesters demonstrated the strong influence of the ferrocene unit on the rheological properties, with unusual, rubber-like behavior being observed. A tentative explanation was proposed in terms of the metallocene functioning as a large but highly flexible unit that lowers the critical entanglement molecular weight.

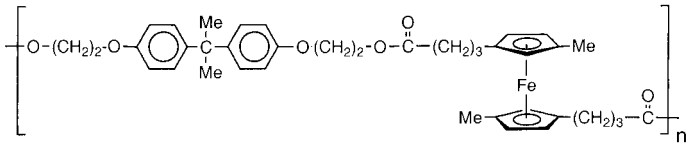

4.5

A wide variety of group 4 (Ti, Zr, Hf) metallocene-containing polyethers, polythioethers, polyesters, polyamines, polyoximes, and polyamidoximes have also been reported [14, 15]. Their synthesis, which is based on the polycondensation (with HCl elimination) of Cp_2MCl_2 with difunctional organic species such as diols, dithiols, etc. (Scheme 4.2), was carried out either in aqueous solution or by using interfacial condensation techniques, depending on the solubility of the difunctional base [16–19]. The materials varied in color from yellow to orange for titanium and from white to light-grey for zirconium and hafnium. Molecular weights ranged from values characteristic of oligomers up to ca. 10^6, although the solubility of the polymers was generally low. Characterization was often limited to IR, which showed characteristic bands for both the metallocene and organic fragments. This allowed an estimation of metal content since, in most cases, elemental analyses for carbon were inconsistent with expected values, possibly due to the high stability of thermal degradation products.

An interesting variant of the polycondensation approach involved the use of fluorescent dyes as the difunctional organic monomers [20, 21]. Thus, soluble, high molecular weight titanium polydyes (e.g. $M_w = 5.3 \times 10^5$ by light-scattering measurements for the titanium polymer derived from the diphenol monomer bromophenol blue) were synthesized in yields that depended on the reaction conditions and the dye used. Structural characterization was achieved by IR and, in some cases, by elemental analysis. Their claimed advantage over monomeric dyes and dye/polymer dispersions was their potentially permanent, non-leaching nature. These metallopolymeric dyes are fluorescent and, when used as coloring or doping agents in paper, cloth, paint, and plastic, they provided access to materials in which this property was retained [20, 21].

The synthesis of polymers containing main-chain cobaltocenium units has also been studied as this 18-electron organometallic moiety is isoelectronic with ferrocene. The synthesis of partially soluble polyesters (**4.6**, E = O, R = $(CH_2)_4$, $CH_2C_6H_4CH_2$) was reported using solution condensation polymerization techniques, and the soluble fractions were of low molecular weight ($M_n \approx$ 2500–4000,

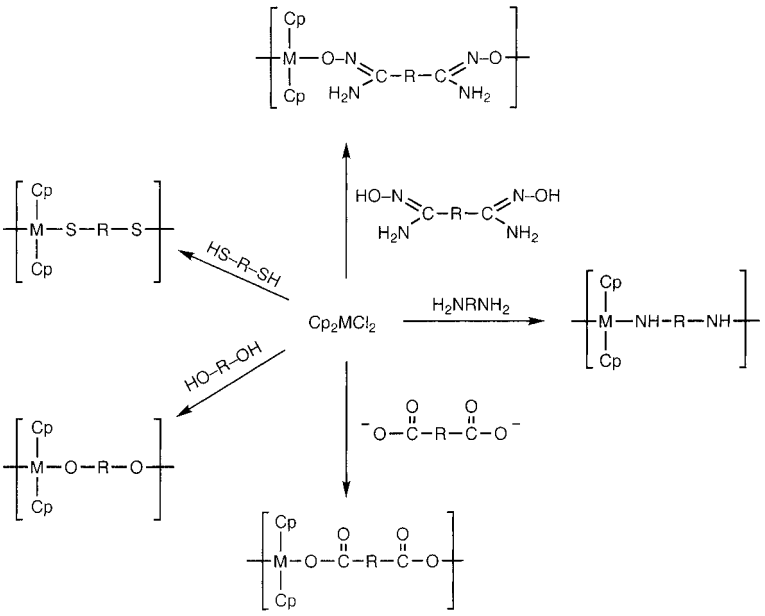

Scheme 4.2

with some material up to $M_n = 8000$) (Eq. 4.2) [22–24]. The products contained mixtures of $[PF_6]^-$ and Cl^- ions and were characterized by IR spectroscopy. Thermally-induced polycondensations at 175–200 °C were also performed, but failed to lead to the formation of soluble materials with substantially higher molecular weights (extensive decomposition was noted). Similar results were obtained when attempts were made to extend the synthetic routes to the formation of the analogous polyamides **4.6** (E = NH) [24].

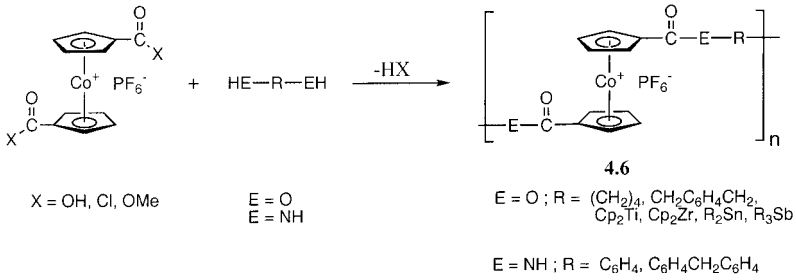

4.6

X = OH, Cl, OMe

E = O
E = NH

E = O ; R = $(CH_2)_4$, $CH_2C_6H_4CH_2$, Cp_2Ti, Cp_2Zr, R_2Sn, R_3Sb

E = NH ; R = C_6H_4, $C_6H_4CH_2C_6H_4$

(4.2)

Attempts to produce soluble high molecular weight polyesters by the polycondensation copolymerization of cobaltocenium 1,1′-dicarboxylic acid with titanocene, zirconocene, tin, and antimony dihalides (**4.6**; E = O, R = Cp_2Ti, Cp_2Zr, R_2Sn,

R_3Sb) were reported in the 1970s [24]. These materials were isolated in 30–80% yields and were characterized by IR, TGA, and DSC, but showed limited solubility in organic solvents or water. Nevertheless, molecular weights (by intrinsic viscosity measurements in 2-chloroethanol) of approximately 80,000 (for R = Cp_2Ti or Cp_2Zr) and 5000 (for R = R_2Sn and R_3Sb) were determined [24–28]. TGA indicated a temperature for 10% weight loss (T_{10}) of around 350 °C for the Co/Ti and Co/Zr polymers and of around 250 °C for the lower molecular weight Co/Sn and Co/Sb materials. Hydrolytic instability of all of the polymers was noted on stirring with aqueous salt solutions [24].

Well-characterized cobaltocenium polyamides **4.6** (E = NH), on the other hand, have been successfully prepared by the reaction of aromatic diamines with 1,1′-dicarboxylcobaltocenium chloride in molten antimony trichloride at 150–175 °C [29]. The products were isolated as $[PF_6]^-$ salts upon treatment with $[NH_4][PF_6]$, and were characterized by IR, ^1H NMR, and elemental analysis, all of which supported the assigned linear polyamide structure. Unfortunately, although the materials were soluble in DMSO and acids, and were slightly soluble in water and ethanol, viscosity and VPO measurements proved inconclusive due to polydissociation in solution. The authors based the assignment of their polymeric nature on their film-forming properties, and the low concentration of carboxyl end groups with respect to that of the NH groups as detected by IR [29].

Well-characterized polymers with ferrocene units connected by sulfur-containing moieties containing an alkyl spacer between the ferrocene and the thiol groups, have also been reported [30]. Thus, polyaddition of 1,1′-bis(2-mercaptopropylthio)ferrocene to divinylsulfone afforded a soluble, orange, low molecular weight ($M_n \approx 3000$) material in 90% yield that was characterized by NMR and elemental analysis. A series of sulfur-containing ferrocene polymers has also been prepared from 1,1′-dimercaptoferrocene by base-catalyzed polyaddition to activated diolefins containing electron-withdrawing substituents (e.g. **4.7**) or by interfacial condensation with acid dichlorides for the synthesis of poly(thioesters) (e.g. **4.8**). This afforded yellow, soluble polymers with low molecular weights ($M_n < 5000$ by GPC; PDI ≈ 1.6–5.0) that were characterized by several analytical and spectroscopic methods.

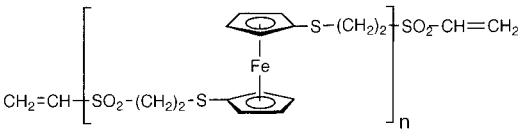

4.7

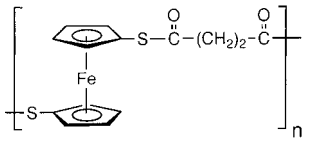

4.8

4.2.2
Organosilicon Spacers

Structural modification of polysiloxanes (silicones) has also been an important area of interest and ferrocene has been introduced into organosilicon polymers, including siloxanes and carbosilanes. The first approaches to such siloxanes were made in the 1960s by means of the controlled hydrolysis of diethoxysilyl- or chlorosiloxanylsilyl-ferrocene derivatives [31, 32]. Unfortunately, the products were oils with very low molecular weights, due in part (in the former case) to intramolecular condensation side reactions [4]. The first examples of well-characterized, high molecular weight polyferrocenylsiloxanes (**4.9**) were reported in 1974, prepared by the condensation reaction in melt or solution, at 100–110 °C of 1,1′-bis(dimethylaminodimethylsilyl) ferrocene with three different disilanols [33]. Molecular weights (M_n) were in the range 9000–20,000 (by GPC), with melt polymerization giving the highest values and narrowest distributions. Intramolecular cyclization is favored over intermolecular condensation when using diphenylsilanediol. DSC studies revealed sharp melt transitions between 40 and 80 °C for these soluble, fibrous polymers. The polymer **4.9b** was found to be as thermally stable (up to 400 °C) and as stable to hydrolysis (in THF/H_2O) as the corresponding arylene polysiloxane without ferrocene moieties in the backbone.

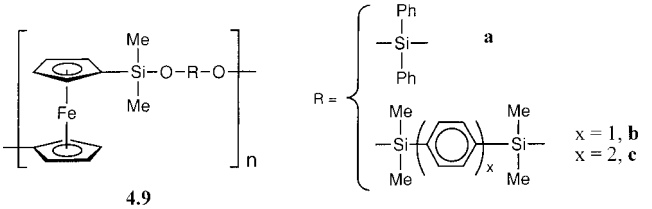

4.9

The use of Diels-Alder and platinum-catalyzed polyaddition reactions of divinyl ferrocene derivatives to prepare ferrocene-containing polycarbosilanes has also been described [32, 34, 35]. These reactions were also used to prepare materials with additional functional groups that led to ferrocene- and silicon-containing polyesters, polyamides, and polyurethanes. Molecular weights varied in the range 3800–6000 and products were liquids or elastomers. The authors only carried out comparative studies of the thermal stabilities of these polymers.

Novel organometallic accordion-type copolymers [36] were prepared in 1992 through the Knoevenagel polycondensation of a bis(ferrocene aldehyde)silane with several bis(cyanoacetate)s [37]. The reaction produced soluble copolymers (**4.10**) that consisted of biferrocenylsilane units with long organic spacers in isomeric (*E*/*Z*) mixtures. They were fully characterized by spectroscopic and analytical methods and possessed reasonably high molecular weights (M_n= 9100–26,600).

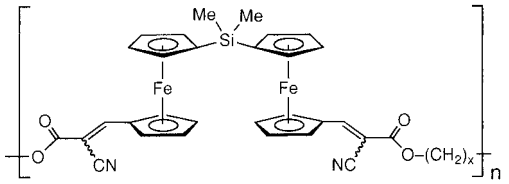

4.10
x = 4, 6, 8

An efficient and versatile approach to yellow-orange, film-forming ferrocene- and silicon-containing polyamides such as **4.11** and **4.12** has been developed [38]. Solution or interfacial polycondensation reactions at room or low temperature, between difunctional ferrocene acid chlorides and diaminosiloxanes or between ferrocene diamines and difunctional arenesiloxane acid chlorides, yielded materials for which molecular weights (M_n) of 10,600–12,500 were determined by VPO. These polymers were very well-characterized structurally by a range of techniques including NMR and IR. The iron centers are non-interacting, as shown by the presence of a single reversible oxidation wave in a cyclic voltammogram (Fig. 4.1). The polymers are of interest for the chemical modification of electrodes; evaporatively-deposited films on different electrodes (Pt, glassy carbon) exhibited the characteristic behavior of surface-confined redox couples.

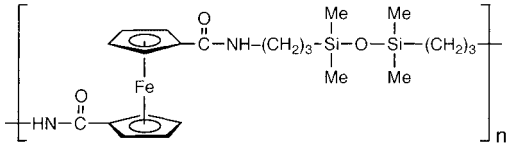

4.11

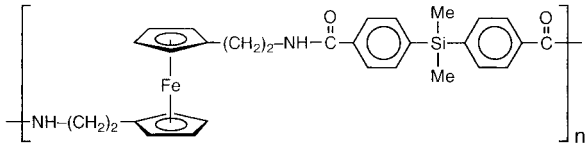

4.12

An interesting Rh- and Ru-catalyzed dehydrocoupling approach to polyferrocenes has also been reported [39]. The reaction involved treatment of ferrocenedithiol with diarylsilanes (Eq. 4.3), and the resultant polymers **4.13** possessed M_n values of 2700–4600 and PDI values of 1.4–1.6.

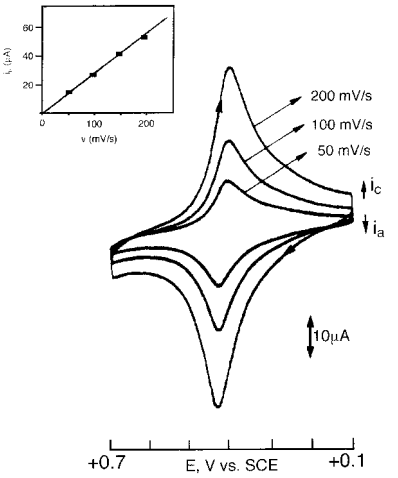

Fig. 4.1 Cyclic voltammogram of a film of ferrocene-containing polyamide (**4.11**) evaporatively deposited on a Pt-disc electrode measured in CH_3CN/0.1 M $[Bu_4N][PF_6]$. Inset shows a plot of current versus scan rate. (Adapted from [38])

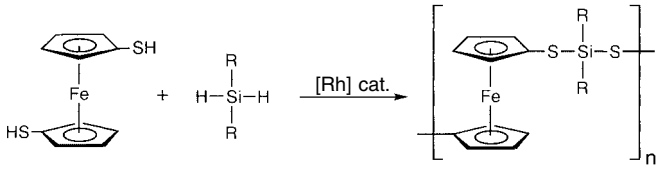

(4.3)

4.13

R = C_6H_4R'-p
R' = M, OMe, F

4.2.3 Siloxane Spacers

The synthesis of polymetallosiloxanes by controlled hydrolytic condensation of Cp_2MX_2 (M = Ti, Zr, Hf; X = Cl or OR) with dichloro- or dialkoxysiloxanes has been investigated based on the possible improvements in heat resistance that might be realized through the introduction of the metal moiety into the polysiloxane backbone. The results obtained in the area were critically reviewed, since partial cleavage of the metal-ring bond occurred in all the cases and viscous, putty-like products were produced; these were poorly characterized, with virtually no data being provided [40]. Only when $Cp_2Ti(SH)_2$ and dichlorosiloxanes were used as reagents in the presence of triethylamine were linear oligomers (**4.14**, $n = 6$) formed with minimal M–Cp bond cleavage. Even in this case, the materials were hydrolytically sensitive [41].

An interesting new approach in this area has been reported with the synthesis of novel polymeric zirconocene-silsesquioxanes (**4.15**) with R = cyclohexyl [42, 43]. The condensation of zirconocene derivatives with polyhedral silsesquioxanes led to amorphous polymers in high yields ($\approx$ 90%) that were characterized by NMR spectroscopy and elemental analysis. These high molecular weight ($M_n = 14{,}000$) materials exhibited high thermal stability (to ca. 475–515 °C) and, surprisingly, **4.15 a** was found to be stable to both air and hydrolysis.

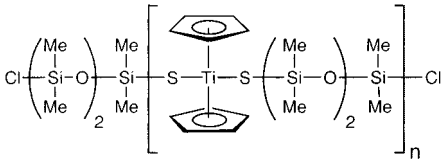

4.14

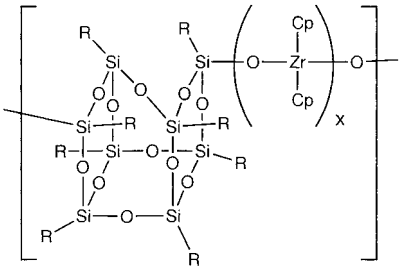

4.15a x = 1
b x = 2

4.3
Polymetallocenes with Long Conjugated Spacer Groups

Polyferrocenylene exhibits significant electrical conductivity when doped (see Chapter 3, Section 3.2.1) and, thus, the introduction of ferrocene units into the main chain of polymers with σ-, σ-π- or π-conjugation in the backbone is a potentially appealing research objective. Studies of materials with short spacers were reviewed in Chapter 3; here, we focus on polymers with spacers longer than three atoms.

Conjugated organic polymers such as polyacetylene, poly(*p*-phenylene) or poly(*p*-phenylene vinylene) are typically insoluble, rigid materials that are difficult to process. Several attempts have been made to introduce skeletal ferrocene units into the main chain of these materials, where they might be expected to increase both the flexibility and solubility [44–50]. Unfortunately, most of the materials reported still had low molecular weights ($M_w < 5000$) and poor solubility. An important development has been the effective use of metal-catalyzed polycondensations to make such materials. For example, the successful use of a Pd-catalyzed coupling procedure has been reported for the preparation of high molecular weight, soluble polyferrocenes with *p*-oligophenylene spacers such as **4.16** (Eq. 4.4), with molecular weights (M_w) up to 35,500 as determined by light-scattering [50]. Such studies revealed that the presence of the ferrocene unit adds significant chain flexibility relative to the rigid-rod organic polymer analogue poly(*p*-phenylene). It was suggested that the presence of the ferrocene units introduces kink angles of at least 60° into the polymer backbone. DSC and polarizing microscopy studies of **4.16** showed the materials to be semicrystalline, and TGA curves showed that they

possess improved thermal stability with regard to weight loss when compared to their poly(*p*-phenylene) analogues.

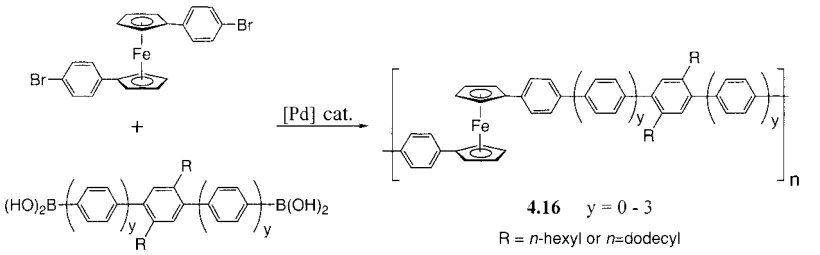

4.16 y = 0 - 3
R = *n*-hexyl or *n*-dodecyl

(4.4)

A wide range of analogous polymers (e.g. **4.17**) with acetylenic spacers have been prepared by Pd-catalyzed polycondensation reactions between diiodoferrocenes and diethynyl arenes, and these have been very well characterized [51]. While polymer **4.17** (R = H) was found to be only partly soluble in organic solvents, the alkyl-substituted analogue **4.17** ($R = C_{12}H_{25}$) and related species with diethynylthiophene spacers were reported to be completely soluble. An analogous material with a diethynylpyridine spacer was found to be partly soluble in organic solvents, but dissolved completely in formic acid. Structural characterization was achieved by NMR and IR spectroscopy. Light-scattering analysis of the soluble fraction of **4.17** (R = H) in $CHCl_3$ gave an M_w value of 1.5×10^3, and for **4.17** ($R = C_{12}H_{25}$) GPC gave an M_w value of 6.9×10^3 with a PDI = 1.47 relative to polystyrene standards. The highest molecular weight values were found for the materials with diethynylthiophene and diethynylpyridine spacers (M_w up to 3.4×10^4 by light-scattering). TGA showed that polymers **4.17** (R = H or $C_{12}H_{25}$) are stable to weight loss up to ca. 400 °C under nitrogen. Cyclic voltammetry showed single, broad oxidation waves at 0.23–0.25 V *vs.* ferrocene/ferrocenium. The authors attributed the broadening of the CV peak to an exchange of electrons (ca. 1 s on the CV time scale) between metal centers through the π-conjugated chain. However, Mössbauer spectra of an I_2-oxidized sample of polymer **4.17** (R = H) showed no coalescence of the Fe^{II} and Fe^{III} quadrupolar doublets at ca. 0 °C, and indicated only slow exchange of electrons between the Fe^{II} and Fe^{III} sites on the time-scale of this experiment (10^{-7} s). The unoxidized samples of polymers **4.17** (R = H) were found to be insulating ($\sigma = 1.0\times10^{-12}$ S cm^{-1}); however, upon oxidation with I_2, the electrical (presumably p-type) conductivity increased to 1.3×10^{-4} Scm^{-1}. Interestingly, an Na-doped sample of the analogous polymer with a diethynylpyridine spacer exhibited an electrical conductivity of 1.2×10^{-5} Scm^{-1}, which suggested n-type behavior.

The red-orange polymer **4.18** and analogous materials were also prepared by Pd-catalyzed polycondensation reactions, and analysis by cyclic voltammetry showed the presence of weak metal-metal coupling ($\Delta E_{1/2} = 0.07$–0.12 V) between the widely spaced iron centers [49]. Low molecular weight ferrocene polymers **4.19** with fluorinated arene ligand spacers have also been prepared and, intriguingly, show no detectable metal-metal communication [52, 53]. Low molecular

weight metal-containing polycarbosilanes **4.20** ($M_w < 4000$) with ferrocene moieties in the main chain have been prepared in high yield by polycondensation routes that involve the use of the di-Grignard reagent of diacetylene and 1,1′-bis(chlorodiorganosilyl)ferrocenes as difunctional monomers [54]. These materials were characterized by NMR and IR spectroscopies, and elemental analysis. Pyrolysis of the ferrocene-containing polycarbosilanes **4.20** at 1350 °C under argon afforded complex multiphase $Fe_xSi_yC_z$ ceramics in high yield (75–85%). Such high yields suggest that excellent shape retention would occur if shaped polymer samples, such as fibers or films, were used. The high ceramic yields were attributed to a facile thermally-induced crosslinking via the acetylenic groups [54].

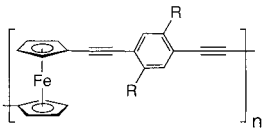

4.17

R = H or $C_{12}H_{25}$

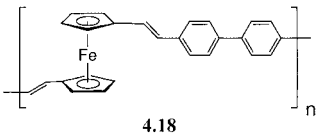

4.18

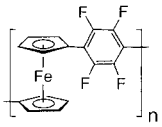

4.19

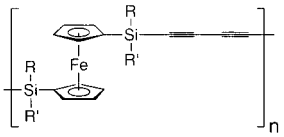

4.20

Polyferrocenes with hexasilane spacers (**4.21**) have also been synthesized in an attempt to obtain polymers in which ferrocenes are joined to σ-delocalized polysilane segments in a regular alternating structure [55]. The condensation of dilithioferrocene and 1,6-dichlorododecamethylhexasilane gave a soluble, well-characterized polymer that showed a monomodal molecular weight distribution by GPC with a maximum at $M_w \approx 3500$. After doping with I_2, conductivity values ($\sigma = 3 \times 10^{-5}$ Scm^{-1}) were three orders of magnitude higher than that of octadecasilane. This suggested that conjugation between ferrocene and the hexasilanediyl linker contributes to the conductivity, although the values observed were lower than those for the corresponding polyferrocenylenes [56].

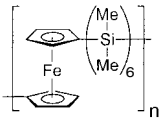

4.21

Thiophene units have also been employed in order to bridge ferrocenes so as to obtain conjugated polymers [57]. The reaction of a di-zinc ferrocene derivative with dibromothiophene afforded a polyferrocenylenethienylene (**4.22**) with moder-

ate molecular weight ($M_n \approx 4500$) that was characterized by NMR spectrometry and elemental analysis. Studies on doped materials with $[SbCl_6]^-$, $[BF_4]^-$, and $[TCNQ]^-$ counteranions showed the presence of weak antiferromagnetic interactions.

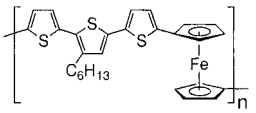

4.22

Condensation routes to well-characterized polyferrocenes with arene (**4.23**) and thiophene (**4.24**) spacers have been developed (Eqs. 4.5 and 4.6) [58, 59]. These materials are soluble, with molecular weights (M_w) of 42,000–52,000 and broad polydispersities (PDI = 10–15). (Analogous materials formed by ROMP were described in Chapter 3, Section 3.4.)

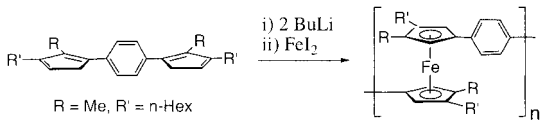

4.23 (4.5)

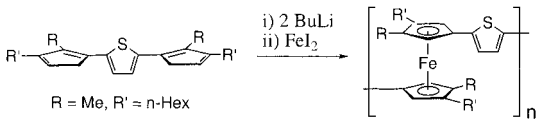

4.24 (4.6)

The magnetic properties of the oxidized materials have been studied, and were interpreted in terms of the temperature dependence of the magnetic moment of the ferrocene units. Cyclic voltammetry studies on **4.23** (Fig. 4.2) and **4.24** showed the presence of two reversible oxidation waves with redox couplings ΔE of 0.17 V and 0.19 V, respectively. This is consistent with the presence of moderate Fe · · · Fe interactions.

The nature of the metal-metal interactions in **4.23** and **4.24**, and in related polymeric materials, has been analyzed in terms of a published theoretical analysis [58]. The conclusion reached was that the bridging groups affect the molecular scale dielectric constant between the metal sites, which, in turn, mediates the essentially through-space interaction. Based on this concept, more polarizable atoms would be expected to lead to stronger metal-metal coupling, and this has indeed been observed. For example, the less polarizable fluorinated arene groups in **4.19** lead to no detectable Fe · · · Fe interaction by cyclic voltammetry, whereas polarizable atoms such as sulfur (see Chapter 3, Section 3.3.7) lead to large $\Delta E_{1/2}$ values.

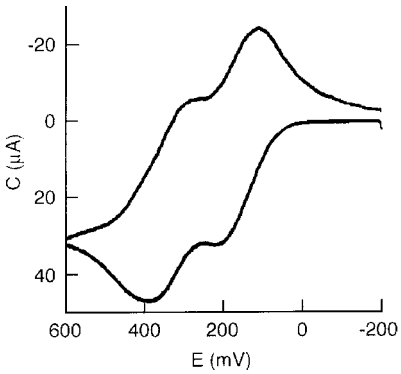

Fig. 4.2 Cyclic voltammogram of a solution of polyferrocene **4.23** in CH_2Cl_2 containing 0.1 M $[Bu_4N][PF_6]$, obtained at a scan rate of 100 mV s^{-1} with ferrocene (E = 0) as a reference. (Adapted from [58])

4.4 Other Metal-Containing Polymers with π-Coordinated Metals and Long Spacer Groups

4.4.1 π-Cyclobutadiene Ligands

Cyclobutadiene moieties in the main chain provide a useful site for the attachment of metals to polymeric structures. For example, a variety of well-characterized rigid-rod organocobalt polymers **4.25 a** with complexed cyclobutadiene units in the main chain have been prepared by Pd-catalyzed Heck coupling (Eq. 4.7), whereby M_w values of 7400–65,000 and PDIs of ca. 1.7–5.0 (by GPC) were achieved [60]. These materials were isolated as yellow solids and were found to exhibit interesting thermotropic liquid-crystal behavior (Fig. 4.3) [60].

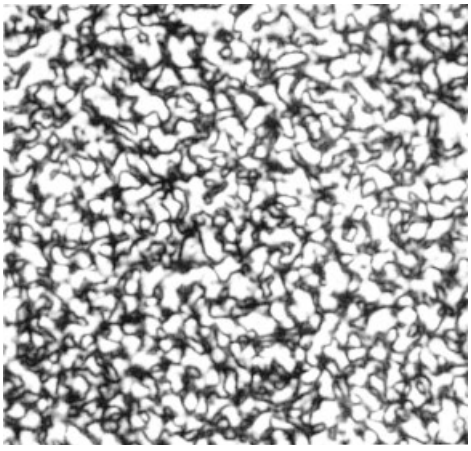

Fig. 4.3 Schlieren texture of a film of polymer **4.25 a** (R^2 = hexyl, $R^1 = SiMe_3$) at 165 °C under a polarizing microscope. (Adapted from [60 a])

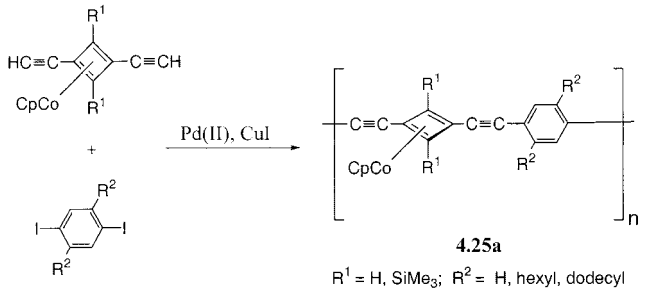

(4.7)

4.25a

R^1 = H, $SiMe_3$; R^2 = H, hexyl, dodecyl

The use of acyclic diyne metathesis (ADIMET) provides an alternative synthetic approach to analogous Co polymers of type **4.25b** with M_w values of 1.3×10^5 to 3.1×10^5 (PDI = 2.9–3.7) (Eq. 4.8). These materials showed lyotropic liquid-crystalline phases and chiroptical properties as a result of aggregation in poor solvents; TEM and polarizing microscopy studies indicated the formation of lamellar or irregular honeycomb-shaped morphologies (Fig. 4.4). The results indicate that the presence of the organocobalt substituents leads to fundamentally different behavior from that of the parent poly(*p*-phenylene)s [60].

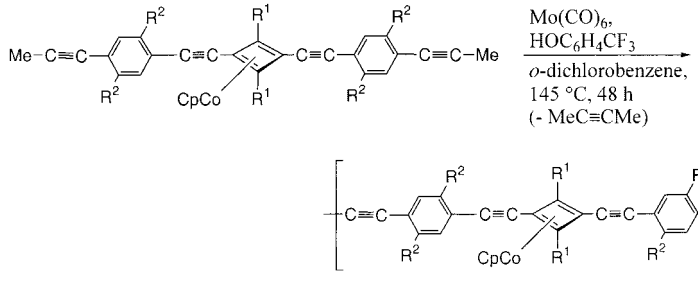

(4.8)

4.25b

R^1 = $SiMe_3$; R^2 = hexyl, 2-ethylhexyl, (*S*)-3,7-dimethyloctyl, dodecyl

Analogous ochre-yellow polymers **4.26** that contain thiophene in the main chain (M_w = 11,300–35,300; PDI = 1.5–2.7) have also been prepared [61]. Upon slow concentration of their solutions in chlorinated solvents, such as chloroform, lyotropic nematic liquid-crystalline phases form. In one case, a lyotropic smectic state was identified.

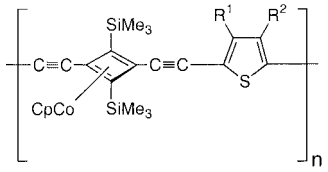

4.26

R^1, R^2 = H, hexyl, dodecyl

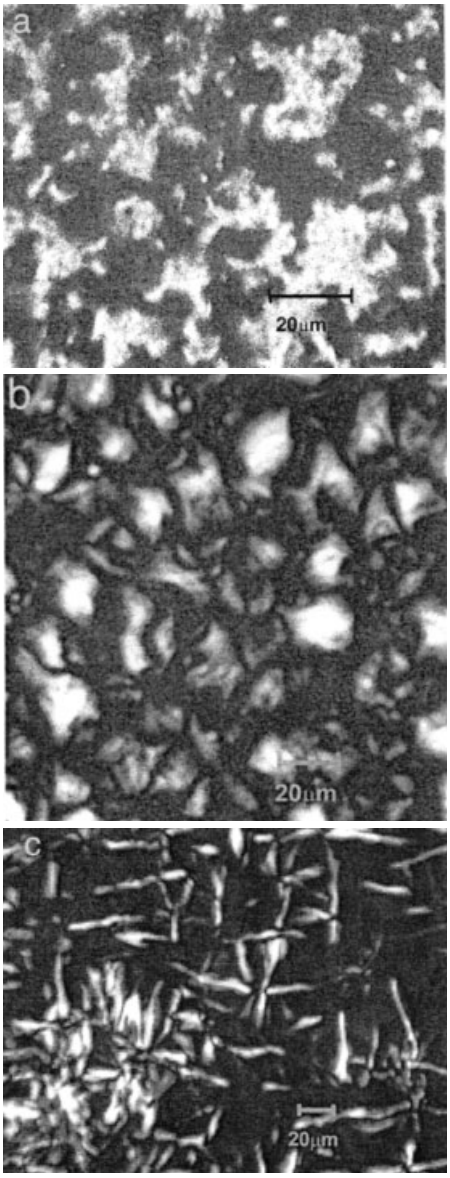

Fig. 4.4 Schlieren textures of the frozen lyotropic phase of (a) polymer **4.25 b** (R^2 = 2-ethylhexyl, $R^1 = SiMe_3$), (b) polymer **4.25 b** (R^2 = (*S*)-3,7-dimethyloctyl, $R^1 = SiMe_3$) under cross-polarizers. The baton texture of polymer **4.25 b** (R^2 = (*S*)-3,7-dimethyloctyl, $R^1 = SiMe_3$) shown in (c) is indicative of a higher, lamellar ordered structure. (Adapted from [60 b])

Materials with butadiene bridging units in the main chain (**4.27**) and with $DP_n > 17$ have been prepared by Hay's oxidative coupling of diterminal alkyne monomers [62–64]. Organocobalt polymers **4.27** possess a conjugated backbone, as shown by the decrease in wavelength of one of the lowest-energy visible absorption peaks relative to small molecule analogues. Thus, studies of the optical properties of linear model oligomers **4.27** ($n = 2$ to 7) showed a bathochromic shift in the UV/vis absorption with a concomitant increase in peak intensity as the chain

length increased [64]. The effective conjugation length appeared to be achieved at $n=7$ (heptamer), since the UV/vis spectrum of this species is almost superimposable with that of **4.27** ($n=8$ or 9) and polymeric **4.27**. The optical properties of the polymers **4.27** have been studied in detail and the involvement of the metal in the electronic transitions has been elucidated [65, 66].

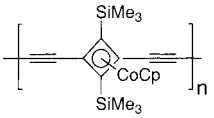

4.27

Polymers **4.29** containing cyclobutadiene units in the main chain have also been obtained by the rearrangement of main-chain metallocyclopentadiene units of polymers **4.28** (see Chapter 5, Section 5.3) (Eq. 4.9) [67–72]. The similarity of molecular weights found for **4.28** and **4.29** indicated that no significant chain cleavage or side reactions occurred during this process [68]. Moreover, UV/vis data indicated that the presence of conjugated spacers R leads to a shift to longer wavelength in the polymers relative to model compounds. This is indicative of electron delocalization in the main chain [69].

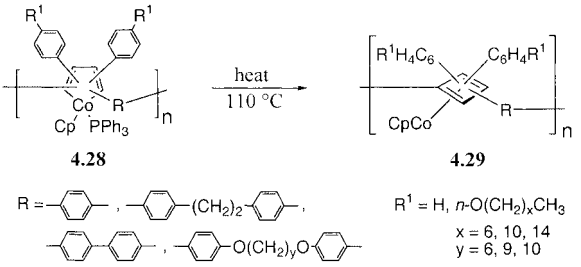

(4.9)

The thermal reaction of cobalt polymers **4.28** with isocyanates at 120 °C leads to 2-pyridone-containing polymers such as **4.30** [70]. Well-characterized, yellow polyesters **4.31** containing skeletal (cyclobutadiene)cobalt moieties in the main chain have been prepared by interfacial polycondensation approaches [73]. The use of solubilizing alkoxy substituents R afforded materials with $M_n=5{,}400$–$16{,}300$ (PDI = 1.3–1.8). Analogous materials to **4.31** with a 1,3-disposition of the main-chain substituents on the cyclobutadiene ligands have also been studied [73, 74]. Thermotropic liquid crystallinity was detected by polarizing microscopy, with, in some cases, mesophases stable over the temperature range from about 110 to > 250 °C.

An analogous synthetic approach based on Ni(0)-catalyzed dehalogenative polycondensation [75, 76] yielded, for example, yellow polymers **4.32** with $M_n=8000$–$13{,}600$ and PDI = 1.3–2.1 by GPC (Eq. 4.10) [76]. Comparison of the UV/vis spectrum of the polymer with that of the model dimer was consistent with the presence of a π-conjugated structure. Polarizing microscopy and powder X-ray diffraction studies suggested that a nematic mesophase was formed. For example, polymer **4.32** (R = *n*-dodecyl) formed a mesophase in the temperature range 146–184 °C [76].

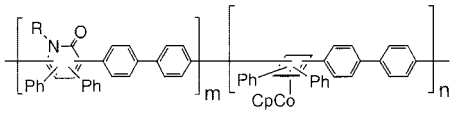

4.30

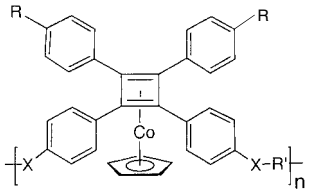

4.31

X = O, CO_2
R' = $(CH_2)_x$ (x = 5, 10, etc.), C_6H_4, C_6H_4-C_6H_4, etc.

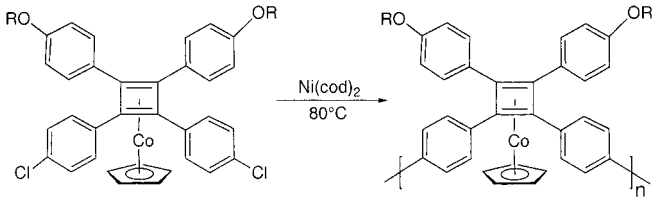

4.32

R = C_6, $C_{12\text{-}16}$ *n*-alkyl chains

(4.10)

4.4.2
π-Cyclopentadienyl Ligands

Cymantrene-containing organometallic polymers (**4.33**) have been prepared by Suzuki coupling reactions (Eq. 4.11). These materials were unstable in air and had molecular weights (M_n) of ca. 1.1×10^4 and broad polydispersities of ca. 6 [77]. Analogous 1,2-substituted oligomeric (**4.34**) and polymeric (**4.35**) materials with butadiyne bridging units in the main chain have been prepared by Hay's oxidative coupling of diterminal alkyne monomers [78]. The brown, film-forming polymers **4.35** were also unstable in air and were found to have an M_w value of 15,200 and a PDI of 1.58 by GPC (relative to polystyrene standards).

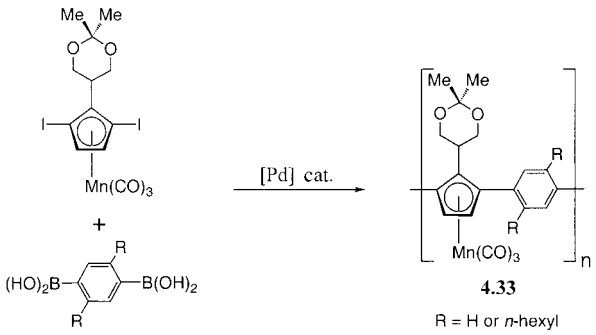

4.33

R = H or *n*-hexyl

(4.11)

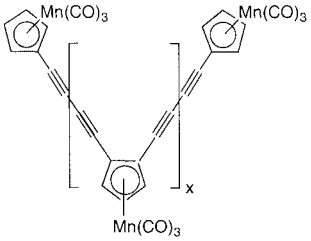

4.34

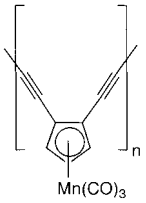

4.35

Analogous materials with cyclopentadienyliron units coordinated to cyclopentadienyl ligands in the main chain, but with shorter C_2 spacers, were described in Chapter 3, Section 3.2.2. Polymers with cyclopentadienyl cobalt groups in the main chain have been produced by the treatment of precursor materials containing cobaltacyclopentadiene groups (e.g. **4.28**) first with *t*-butyl isocyanide and then with MeI [79].

4.4.3
π-Arene Ligands

Soluble π-complexed aromatic polyamides (**4.36**) have been prepared by polycondensation of (*p*-phenylenediamine)$Cr(CO)_3$ with terephthaloyl chloride in *N,N*-dimethylacetamide (Eq. 4.12) [80]. The highly viscous solution of **4.36** exhibited lyotropic liquid-crystalline behavior with a nematic texture that was visible by polarizing optical microscopy. The intrinsic viscosity for **4.36** in *N,N*-dimethylacetamide was determined to be 4.52 dL g^{-1}, and gel-permeation chromatography analysis using a viscosity detector gave an absolute molecular weight (M_w) of 78,000 (polydispersity = 1.7). The analogous polymer in which only half of the diamines are complexed to $Cr(CO)_3$ has also been reported. The trimethylphosphine derivative **4.37** was prepared similarly by polycondensation of (*p*-phenylenediamine)$Cr(CO)_2PMe_3$ with terephthaloyl chloride. These materials are of importance, as the coordination solubilizes poly(*p*-phenyleneterephthalamide) (used for making Kevlar fibers for bullet-proof vests, etc.) in common organic solvents, but still allows for the formation of ordered, liquid-crystalline solutions.

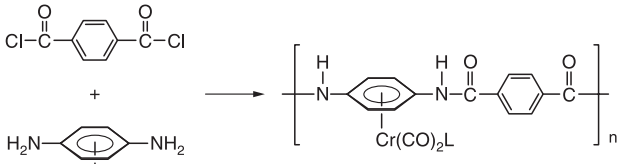

(4.12)

4.36 L = CO
4.37 L = PMe_3

Soluble π-complexed aromatic polysulfides **4.38** have also been prepared with (η^5-C_5Me_5)Ru moieties (Eq. 4.13) [81]. A variety of polymers with Fe(η^5-C_5H_5) groups attached to arene groups in the polymer main chain have been reported.

These include polyethers, polythioethers, and polyamines [82–85]. In addition to linear materials, star-shaped polymers such as **4.39** have been reported [86]. These materials are redox-active as a result of the presence of the cationic ArFe(η^5-C_5H_5) moieties, which undergo reversible reduction at –40 °C. The materials are photochemically labile and exposure to UV light of $\lambda = 200$ nm results in decomplexation to afford the corresponding organic polymers.

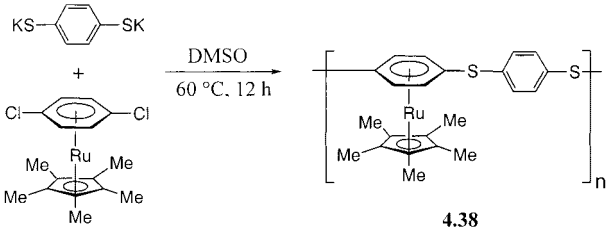

(4.13)

4.38

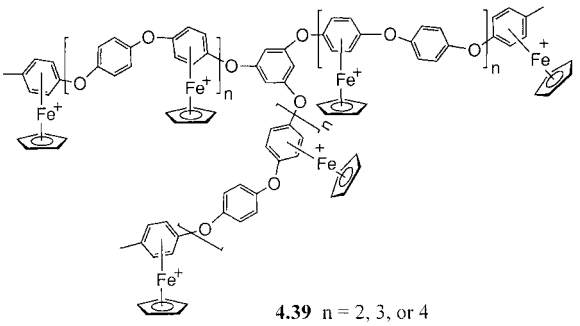

4.39 n = 2, 3, or 4

Polymers **4.40** containing cationic (arene)Fe(η^5-C_5H_5) units in the main chain together with azo dyes in the side-group structure have also be developed (Scheme 4.3) [87]. Photolysis in the presence of H_2O_2 led to photobleaching.

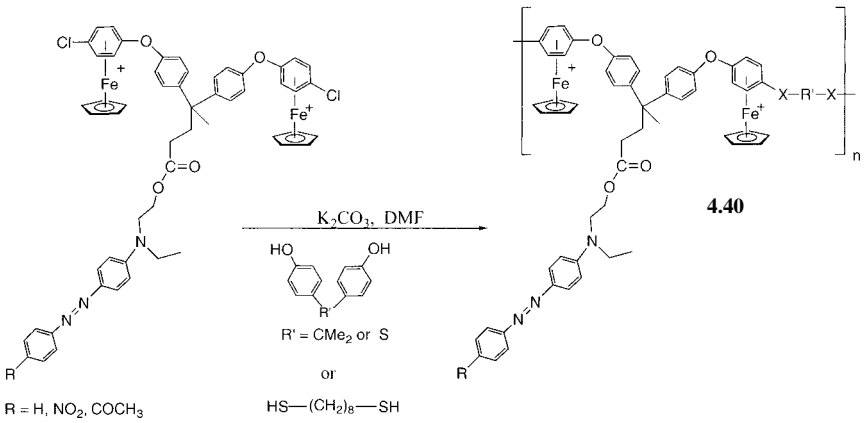

R = H, NO_2, $COCH_3$

4.40

Scheme 4.3

The complexation of Fe(η^5-C_5H_5) groups to ca. 60% of the main-chain arene moieties in low molecular weight samples (M_n = 1700) of poly(*n*-hexylphenylene) to yield **4.41** has also been reported [88]. Interchain cross-linking appears to be induced by electrochemical reduction, resulting in the formation of an insoluble polymer film on the electrode. Attachment of the FeCp group also leads to a modification of the photoluminescence intensity and emission wavelength.

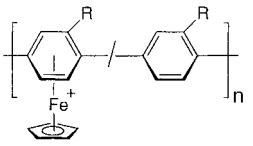

4.41

R = *n*-hexyl

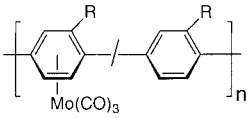

4.42

R = *n*-hexyl

Similar polymers with around 20% of the main-chain arene groups complexed by $Mo(CO)_3$ (**4.42**) have also been reported [89]. The quenching of photoluminescence detected for **4.41** and **4.42** results from the presence of the metal-based LUMO between the valence and conduction bands of the conjugated polymer chain. This leads to a pathway for non-radiative decay after photoexcitation that involves electron transfer to the 3d LUMO on the metal, which occurs prior to recombination with holes [88, 90].

An analogous polymer with diethynyldiphenylene spacers, **4.43**, which possesses complexation of arene groups to $Cr(CO)_3$ moieties, has been prepared [91]. Its solubility was low, even though molecular weights (M_n) of ca. 7800 were estimated. In this case, the synthesis involved a cross-coupling reaction of the *p*-dichloroarene complex with the bis(trimethylstannyl)dialkyne [91]. Similar materials with diethynylthiophene spacers have also been described [92].

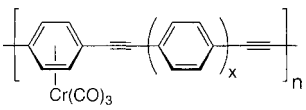

4.43 x = 1 or 2

4.4.4
π-Alkyne Ligands

Soluble π-complexed polymers have also been prepared by means of coordination to alkyne groups in a polymer main chain. Both non-conjugated (e.g. alkynylsiloxanes [93]) and conjugated materials have been studied.

Treatment of π-conjugated poly(phenylenediacetylene) with controlled amounts of $Pt(C_2H_4)(PPh_3)_2$ led to the formation of polymers **4.44** with 20–50% complexa-

tion of the main chain alkyne groups [94]. Subsequent pyrolysis at 600 °C led to the formation of conducting glassy carbon matrixes containing coalescence-stable Pt nanoclusters which function as catalysts for H^+ and O_2 reduction [94–97]. Complexation of alkyne units of conjugated polymers to platinum can also lead to crosslinked materials **4.45** [98–100]. These networks can possess substantially increased charge carrier mobilities in comparison to the all-organic conjugated polymer precursor and may lead to improved semiconductor devices [100].

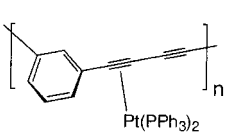

4.44

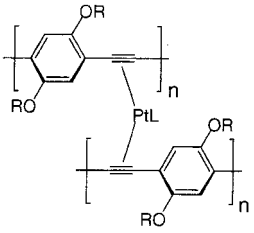

4.45

4.5 References

1 *Ferrocenes* (Eds.: A. Togni, T. Hayashi), VCH Publishers, New York, **1995**.

2 N. J. Long, *Metallocenes*, Blackwell Science, Oxford, **1998**.

3 *Inorganic Materials* (Eds.: D. W. Bruce, D. O'Hare), John Wiley & Sons, Toronto, **1992**.

4 E. W. Neuse, H. Rosenberg, *J. Macromol. Sci. – Revs. Macromol. Chem.* **1970**, *C4*, 1.

5 F. W. Knobloch, W. H. Rauscher, *J. Polym. Sci., Part A1* **1961**, *54*, 651.

6 M. Okawara, Y. Takemoto, H. Kitaoka, E. Haruki, E. Imoto, *Kogyo Kagaku Zasshi* **1962**, *65*, 685.

7 K. Gonsalves, L. Zhan-ru, M. D. Rausch, *J. Am. Chem. Soc.* **1984**, *106*, 3862.

8 C. U. Pittman, M. D. Rausch, *Pure Appl. Chem.* **1986**, *58*, 617.

9 M. M. Abd-Alla, M. F. El-Zohry, K. I. Aly, M. M. Abd-El-Wahab, *J. Appl. Polym. Sci.* **1993**, *47*, 323.

10 M. E. Wright, E. G. Toplikar, H. S. Lackritz, J. T. Kerney, *Macromolecules* **1994**, *27*, 3016.

11 S. R. Marder, J. W. Perry, B. G. Tiemann, W. P. Schaefer, *Organometallics* **1991**, *10*, 1896.

12 M. E. Wright, E. G. Toplikar, *Macromolecules* **1992**, *25*, 6050.

13 G. Wilbert, A. Wiesemann, R. Zentel, *Macromol. Chem. Phys.* **1995**, *196*, 3771.

14 *Organometallic Polymers* (Eds.: C. E. Carraher, Jr., J. E. Sheats, C. U. Pittman, Jr.), Academic Press, New York, **1978**, p. 79.

15 *Metal-Containing Polymeric Systems* (Eds.: E. Sheats, C. E. Carraher, Jr., C. U. Pittman, Jr.), Plenum Press, New York, **1985**, p. 1.

16 *Interfacial Synthesis, Vol. II* (Eds.: F. Millich, C. E. Carraher, Jr.), Marcel Dekker Inc., New York, **1977**, p. 367.

17 C. E. Carraher, Jr., S. T. Bajah, *Polym. J.* **1973**, *14*, 42.

18 C. E. Carraher, Jr., S. T. Bajah, *Polymer* **1974**, *15*, 9.

19 a) *Interfacial Synthesis, Vol. III* (Eds.: C. E. Carraher, Jr., J. Preston), Marcel Dekker Inc., New York, **1982**, p. 77; b) C. E. Carraher, Jr., M. J. Christensen, *Angew. Makromol. Chem.* **1978**, *69*, 61; c) C. E. Carraher, Jr., J. Lee, *J. Macromol. Sci.* **1975**, *A-9*, 19.

20 *Interfacial Synthesis, Vol. III* (Eds.: C. E. Carraher, Jr., J. Preston), Marcel Dekker Inc., New York, **1982**, p. 93.

21 C. E. Carraher, Jr., R. A. Schwarz, J. A. Schroeder, M. Schwarz, H. M. Molloy, *Am. Chem. Soc. Div. Org. Coat. Plast. Chem.* **1980**, *43*, 798.

22 C. U. Pittman, Jr., O. E. Ayers, S. P. McManus, J. E. Sheats, C. E. Whitten, *Macromolecules* **1971**, *4*, 360.

23 C. U. Pittman, Jr., O. E. Ayers, B. Suryanarayanan, S. P. McManus, J. E. Sheats, *Makromol. Chem.* **1974**, *175*, 1427.

24 *Organometallic Polymers* (Eds.: C. E. Carraher, Jr., J. E. Sheats, C. U. Pittman, Jr.), Academic Press, New York, **1978**, p. 87.

25 C. E. Carraher, Jr., J. E. Sheats, *Makromol. Chem.* **1973**, *166*, 23.

26 C. E. Carraher, Jr., *Macromolecules* **1971**, *4*, 263.

27 C. E. Carraher, Jr., G. F. Peterson, J. E. Sheats, T. Kirsch, *Makromol. Chem.* **1974**, *175*, 3089.

28 J. E. Sheats, C. E. Carraher, Jr., D. Bruyer, M. Cole, *Am. Chem. Soc. Div. Org. Coat. Plast. Chem.* **1974**, *34*, 474.

29 *Organometallic Polymers* (Eds.: C. E. Carraher, Jr., J. E. Sheats, C. U. Pittman, Jr.), Academic Press, New York, **1978**, p. 95.

30 O. Nuyken, T. Pöhlmann, M. Herberhold, *Macromol. Chem. Phys.* **1996**, *197*, 3343.

31 R. L. Schaaf, P. T. Kan, C. T. Lenk, *J. Org. Chem.* **1961**, *26*, 1790.

32 G. Greber, M. L. Hallensleben, *Makromol. Chem.* **1966**, *92*, 137.

33 W. J. Patterson, S. P. McManus, C. U. Pittman, Jr., *J. Polym. Sci. Polym. Chem.* **1974**, *12*, 837.

34 G. Greber, M. L. Hallensleben, *Makromol. Chem.* **1967**, *104*, 90.

35 G. Greber, M. L. Hallensleben, *Makromol. Chem.* **1965**, *83*, 148.

36 J. S. Moore, S. I. Stupp, *Macromolecules* **1990**, *23*, 65.

37 M. E. Wright, M. S. Sigman, *Macromolecules* **1992**, *25*, 6055.

38 C. M. Casado, M. Morán, J. Losada, I. Cuadrado, *Inorg. Chem.* **1995**, *34*, 1668.

39 I. Yamaguchi, H. Ishii, T. Sakano, K. Osakada, T. Yamamoto, *Appl. Organomet. Chem.* **2001**, *15*, 197.

40 E. W. Neuse, H. J. Rosenberg, *J. Macromol. Sci. – Revs. Macromol. Chem.* **1970**, *C4*, 119.

41 E. W. Neuse, H. Rosenberg, *J. Macromol. Sci. – Revs. Macromol. Chem.* **1970**, *C4*, 121.

42 J. D. Lichtenhan, *Comments Inorg. Chem.* **1995**, *17*, 115.

43 T. S. Haddad, J. D. Lichtenhan, *J. Inorg. Organomet. Polym.* **1995**, *5*, 237.

44 (a) A. Kasahara, T. Izumi, *Chem. Lett.* **1978**, 21; (b) R. Gooding, C. P. Lillya, C. W. Chien, *J. Chem. Soc., Chem. Commun.* **1983**, 151.

45 A. S. Gamble, J. T. Patton, J. M. Boncella, *Makromol. Chem. Rapid Commun.* **1992**, *13*, 109.

46 R. Bayer, T. Pöhlmann, O. Nuyken, *Makromol. Chem. Rapid Commun.* **1993**, *14*, 359.

47 R. Knapp, M. Rehahn, *Makromol. Chem. Rapid Commun.* **1993**, *14*, 451.

48 S. L. Ingham, M. S. Khan, J. Lewis, N. J. Long, P. R. Raithby, *J. Organomet. Chem.* **1994**, *470*, 153.

49 M. Bochmann, J. Lu, R. D. Cannon, *J. Organomet. Chem.* **1996**, *518*, 97.

50 R. Knapp, U. Velten, M. Rehahn, *Polymer* **1998**, *39*, 5827.

51 (a) T. Yamamoto, T. Morikita, T. Maruyama, K. Kubota, M. Katada, *Macromolecules* **1997**, *30*, 5390; (b) T. Morikita, T. Maruyama, T. Yamamoto, K. Kubota, M. Katada, *Inorg. Chim. Acta* **1998**, *269*, 310; (c) T. Morikita, T. Yamamoto, *J. Organomet. Chem.* **2001**, *637–639*, 809.

52 C. B. Hollandsworth, W. G. Hollis, Jr., C. Slebodnick, P. A. Deck, *Organometallics* **1999**, *18*, 3610.

53 P. A. Deck, M. J. Lane, J. L. Montgomery, C. Slebodnick, *Organometallics* **2000**, *19*, 1013.

54 (a) R. J. P. Corriu, N. Devylder, C. Guerin, B. Henner, A. Jean, *Organometallics* **1994**, *13*, 3194; (b) R. J. P. Corriu, N. Devylder, C. Guerin, B. Henner, A. Jean, *J. Organomet. Chem.* **1996**, *509*, 249.

55 M. Tanaka, T. Hayashi, *Bull. Chem. Soc. Jpn.* **1993**, *66*, 334.

56 T. Yakamoto, K. Sanechika, A. Yakamoto, M. Katado, I. Motoyama, H. Sano, *Inorg. Chim. Acta* **1983**, *73*, 75.

57 M. Hmyene, A. Yassar, M. Escorne, A. Percheron-Guegan, F. Garnier, *Adv. Mater.* **1994**, *6*, 564.

58 G. E. Southard, M. D. Curtis, *Organometallics* **2001**, *20*, 508.

59 G. E. Southard, M. D. Curtis, *Organometallics* **1997**, *16*, 5618.

60 (a) M. Altmann, U. H. F. Bunz, *Angew. Chem. Int. Ed. Engl.* **1995**, *34*, 569; (b) W. Steffen, B. Köhler, M. Altmann, U. Sherf, K. Stitzer, H.-C. zur Loye, U. H. F. Bunz, *Chem. Eur. J.* **2001**, *7*, 117.

61 M. Altmann, V. Enkelmann, G. Lieser, U. H. F. Bunz, *Adv. Mater.* **1995**, *7*, 726.

62 U. H. F. Bunz, *Pure & Appl. Chem.* **1996**, *68*, 309.

63 M. Altmann, U. H. F. Bunz, *Makromol. Chem. Rapid Commun.* **1994**, *15*, 785.

64 M. Altmann, V. Enkelmann, F. Beer, U. H. F. Bunz, *Organometallics* **1996**, *15*, 394.

65 B. C. Harrison, J. M. Seminario, U. H. F. Bunz, M. L. Myrick, *J. Phys. Chem. A* **2000**, *104*, 5937.

66 H. Rengel, M. Altmann, D. Neher, B. C. Harrison, M. L. Myrick, U. H. F. Bunz, *J. Phys. Chem. B* **1999**, *103*, 10335.

67 A. Ohkubo, K. Aramaki, H. Nishihara, *Chem. Lett.* **1993**, 271.

68 I. Tomita, A. Nishio, T. Endo, *Macromolecules* **1994**, *27*, 7009.

69 J. C. Lee, A. Nishio, I. Tomita, T. Endo, *Macromolecules* **1997**, *30*, 5205.

70 I. Tomita, A. Nishio, T. Endo, *Macromolecules* **1995**, *28*, 3042.

71 I. Tomita, A. Nishio, T. Endo, *Appl. Organomet. Chem.* **1998**, *12*, 735.

72 I. L. Rozhanskii, I. Tomita, T. Endo, *Macromolecules* **1996**, *29*, 1934.

73 I. L. Rozhanskii, I. Tomita, T. Endo, *Polymer* **1999**, *40*, 1581.

74 I. L. Rozhanskii, I. Tomita, T. Endo, *Macromolecules* **1997**, *30*, 1222.

75 I. L. Rozhanskii, I. Tomita, T. Endo, *Chem. Lett.* **1997**, 477.

76 Y. Sawada, I. Tomita, T. Endo, *Macromol. Chem. Phys.* **2000**, *201*, 510.

77 S. Setayesh, U. H. F. Bunz, *Organometallics* **1996**, *15*, 5470.

78 U. H. F. Bunz, V. Enkelmann, F. Beer, *Organometallics* **1995**, *14*, 2490.

79 I. Tomita, J. C. Lee, T. Endo, *J. Organomet. Chem.* **2000**, *611*, 570.

80 A. A. Dembek, R. R. Burch, A. E. Feiring, *J. Am. Chem. Soc.* **1993**, *115*, 2087.

81 A. A. Dembek, P. J. Fagan, M. Marsi, *Macromolecules* **1993**, *26*, 2992.

82 A. S. Abd-El-Aziz, K. M. Epp, C. R. de Denus, G. Fisher-Smith, *Organometallics* **1994**, *13*, 2299.

83 A. S. Abd-El-Aziz, C. R. de Denus, M. J. Zaworotko, L. R. MacGillivray, *J. Chem. Soc., Dalton Trans.* **1995**, 3375.

84 A. S. Abd-El-Aziz, C. R. de Denus, E. K. Todd, S. A. Bernardin, *Macromolecules* **2000**, *33*, 5000.

85 A. S. Abd-El-Aziz, E. K. Todd, G. Z. Ma, *J. Polym. Sci. Polym. Chem.* **2001**, *39*, 1216.

86 A. S. Abd-El-Aziz, E. K. Todd, T. H. Afifi, *Macromol. Rapid Commun.* **2002**, *23*, 113.

87 A. S. Abd-El-Aziz, T. H. Afifi, W. R. Budakowski, K. J. Friesen, E. K. Todd, *Macromolecules* **2002**, *35*, 8929.

88 H. Funaki, K. Aramaki, H. Nishihara, *Synth. Met.* **1995**, *74*, 59.

89 H. Funaki, K. Aramaki, H. Nishihara, *Chem. Lett.* **1992**, 2065.

90 J. Matsuda, K. Aramaki, H. Nishihara, *J. Chem. Soc., Faraday Trans.* **1995**, *91*, 1477.

91 M. E. Wright, *Macromolecules* **1989**, *22*, 3256.

92 Y. Morisaki, H. Chen, Y. Chujo, *Polym. Bull.* **2002**, *48*, 243.

93 T. Kuhnen, M. Stradiotto, R. Ruffolo, D. Ulbrich, M. J. McGlinchey, M. A. Brook, *Organometallics* **1997**, *16*, 5048.

94 N. L. Pocard, D. C. Alsmeyer, R. L. McCreery, T. X. Neenan, M. R. Callstrom, *J. Am. Chem. Soc.* **1992**, *114*, 769.

95 O. J. A. Schueller, N. L. Pocard, M. E. Huston, R. J. Spontak, T. X. Neenan, M. R. Callstrom, *Chem. Mater.* **1993**, *5*, 11.

96 H. D. Hutton, N. L. Pocard, D. C. Alsmeyer, O. J. A. Schueller, R. J. Spontak, M. E. Huston, W. H. Huang, R. L. McCreery, T. X. Neenan, M. R. Callstrom, *Chem. Mater.* **1993**, *5*, 1727.

97 T. X. Neenan, M. R. Callstrom, O. J. A. Schueller, *Macromol. Symp.* **1994**, *80*, 315.

98 C. Huber, F. Bangerter, W. R. Caseri, C. Weder, *Am. Chem. Soc.* **2001**, *123*, 3857.

99 A. Kokil, C. Huber, W. R. Caseri, C. Weder, *Macromol. Chem. Phys.* **2003**, *204*, 40.

100 A. Kokil, I. Shiyanovskaya, K. D. Singer, C. Weder, *Am. Chem. Soc.* **2002**, *124*, 9978.

5
Metallopolymers with Metal-Carbon σ-Bonds in the Main Chain

5.1
Introduction

Polymers with metal-carbon bonds in the main chain represent one of the most extensive, interesting, and broad classes of metal-containing polymers. Rigid-rod transition metal acetylide polymers or polymetallaynes are the most extensively studied subgroup of these metallopolymers. Although initial developments were reported in this area in the 1960s, it was not until the late 1970s that a series of well-characterized, soluble, high molecular weight materials that contained Pd and Pt was described. The key to this success was the discovery of efficient catalytic, step-growth polycondensation processes that involved difunctional monomers which were available in high purity and that proceeded to high conversion. This enabled the strict stoichiometry and conversion requirements necessary for the formation of high molecular weight materials by step-growth polycondensations to be successfully satisfied (see Chapter 1, Section 1.5.2.2.2). In the 1980s and early 1990s, the diversity of polymetallaynes was extended to include other metals, and a series of materials with metallocyclopentadiene units containing Co and Zr in the main chain was also described. Various other polymers with metal-carbon single and multiple bonds in the main chain that involve sp^3- and sp^2-hybridized carbon centers, respectively, were also reported during the same period. A feature of the work on virtually all of these materials is the excellent structural characterization of the polymers by means of a wide variety of spectroscopic and analytical techniques. However, although absolute methods have been used in a number of cases, molecular weight characterization has often relied on the convenient but relative method of gel-permeation chromatography (GPC) with polystyrene standards for column calibration (see Section 1.2.1). For the rigid structures common to many of the polymers discussed in this chapter, appreciable differences in hydrodynamic behavior from that of polystyrene would be anticipated. It is important, therefore, to bear in mind that the molecular weight data reported for many of the polymers is likely to be inaccurate (see Section 5.2.3.2).

Synthetic Metal-Containing Polymers. Ian Manners

ISBN: 3-527-29463-5

5.2
Rigid-Rod Transition Metal Acetylide Polymers

5.2.1
Polymer Synthesis

An array of versatile and efficient step-growth polycondensation methodologies has been developed for the synthesis of transition metal acetylide polymers. In this section, a representative review of the types of routes available and materials accessible is given.

Polymeric Cu- and Hg-acetylides **5.1** (M = Cu or Hg, L = no substituent), produced by oxidative coupling of diyne precursors (Scheme 5.1, Eq. 5.1) were briefly reported in the 1960s. These materials were proposed to have a linear geometry; however, they were generally found to be intractable, which precluded their purification and definitive characterization [1, 2]. In the mid- to late 1970s, the first soluble polymetallaynes **5.1** (M = Pt) and **5.2** (M = Pd) that contained metal atoms in the main chain were reported, and these were prepared by a similar route. Subsequent work resulted in the general development of this and other routes to Group 10 metal-containing polyynes. Since 1990, a variety of new routes that allow the incorporation of metals from Groups 8, 9, and 10 into the polymer backbone have been described.

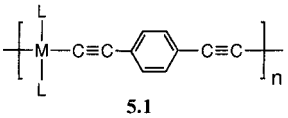

5.1

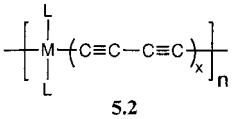

5.2

The first soluble transition metal polyyne oligomers **5.1** and **5.2** ($x = 2$) were reported in 1975 and consisted of $Pt(P^nBu_3)_2$ and $Pd(P^nBu_3)_2$ moieties in the main chain connected by butadiyne and diethynylbenzene bridging units. These were isolated as air-stable, orange-yellow solids with average molecular weights (M_n) of 7300 and 5700, respectively, as determined by vapor-pressure osmometry [3]. These materials were prepared by the oxidative coupling method shown in Scheme 5.1 (a). Subsequent work, reported in 1977, showed that Group 10 metal-acetylide polymers with improved molecular weights ($M_w > 10^5$) could be prepared through the use of three main approaches: oxidative coupling, dehydrohalogenation, and alkynyl ligand exchange (see Scheme 5.1 (a–c)) [4–12].

The first method involves oxidative homo-coupling of bis(terminal alkynyl) complexes in the presence of a catalytic amount of a copper(I) halide and O_2 as the oxidizing agent (Scheme 5.1, Eq. 5.1) [10]. The use of this catalyst system in organic synthesis is extensive and is better known as Hay's coupling reaction [11]. Extension of this methodology to organometallic synthesis was demonstrated by the conversion of *trans*-bis(acetylide) monomers into polymeric complexes. It is

(a) Oxidative Coupling

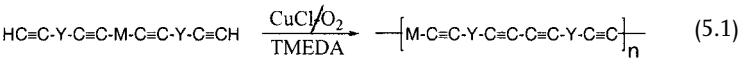

(5.1)

(b) Dehydrohalogenation

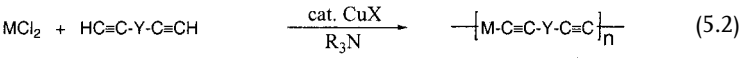

(5.2)

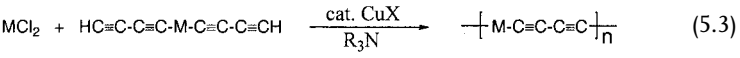

(5.3)

(c) Alkynyl Ligand Exchange

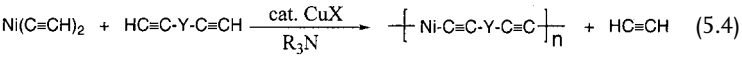

(5.4)

M = *trans*-$Pt(PR_3)_2$, *trans*-$Pd(PR_3)_2$
Ni = *trans*-$Ni(PR_3)_2$

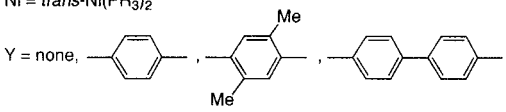

Scheme 5.1

worth noting that this method is dependent only on one monomer type; stoichiometric balance is therefore already present, and so high degrees of polymerization are usually obtained (see Chapter 1, Section 1.5.2.2.2).

The second method involves a polycondensation reaction between metal halides and di-terminal alkynes by a copper(I) halide-catalyzed dehydrohalogenation process (Scheme 5.1, Eqs. 5.2 and 5.3) [3, 4–9]. The reactions are typically performed in amine solvents, such as diethylamine or piperidine under reflux conditions, and afford high molecular weight polymers. In the case of gaseous alkynes such as acetylene or butadiyne, the polymers are most conveniently obtained by polycondensation of the corresponding mononuclear metal bis(alkynyl) complexes and metal halides. The degree of polymerization achieved through use of the dehydrohalogenation approach is dependent upon the exact ratio of the difunctional monomer pairs involved.

The aforementioned two methods work well for a majority of cases, particularly for platinum, and afford high molecular weight macromolecules, as estimated by gel-permeation chromatography, with $M_w = 60{,}000–160{,}000$ depending on the nature of the bridging alkynes. In the case of palladium, significantly lower molecular weights (M_w values up to 26,000) were obtained [10]. However, neither of these two methods is applicable to nickel due to the inherent instability of dihalonickel complexes in amine solvents and of dialkynylnickel complexes in oxidizing media. Thus, the analogous Ni-containing acetylide polymers (with $M_w = 10{,}000–13{,}000$ by GPC) were prepared by means of an alkynyl ligand exchange process, which is catalyzed by CuI in amine solvents (Scheme 5.1, Eq. 5.4) [12].

Similar synthetic routes to those described in Scheme 5.1 have also been used to prepare the analogous polymeric species **5.3** and **5.4**, which contain mixed alkynyl ligands and/or mixed metals in the main chain [6, 8].

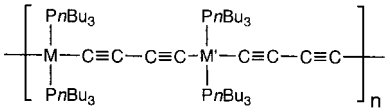

5.3

M = Pd Ni Pd M' = Pt Pt Ni

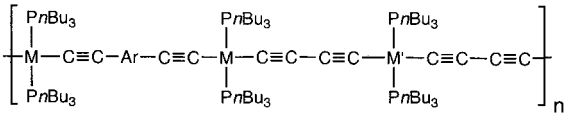

5.4

M = Pd Pt Pd M' = Pt Pd Ni Ar = 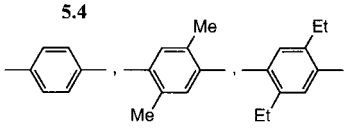

Although the aforementioned methods are generally applicable for the incorporation of Group 10 metals into metal-acetylide polymers, these approaches could not be extended to metals from Groups 8 and 9 due to the instability of the prospective monomer complexes in amine solvents. Research efforts building on the molecular chemistry of hydrido-acetylide complexes of rhodium have resulted in a facile route to Group 9 polymers **5.5** and **5.6** [13–16]. This method involves the direct oxidative addition of terminal diynes to $RhMeL_4$ or $[RhL_4]^+$ ($L = PR_3$) (Eqs. 5.5 and 5.6). The reaction, which resembles that described in an earlier report on the synthesis of $Co(PMe_3)_4(C{\equiv}CPh)$ using a terminal alkyne [17], proceeds rapidly at ambient temperature to produce soluble polymers **5.6** when $L = P^nBu_3$ or an insoluble white solid **5.5** when $L = PMe_3$. The authors did not report the molecular weight for the soluble polymer. However, the formation of free-standing films of the material upon evaporation of the THF solvent suggested that the product was macromolecular in nature.

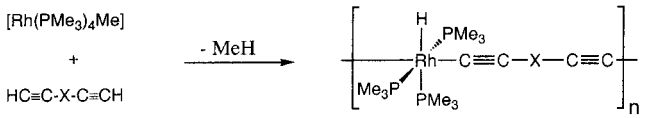

(5.5)

5.5

X = -*p*-C_6H_4-, -*p*-C_6H_4-C_6H_4-*p*-

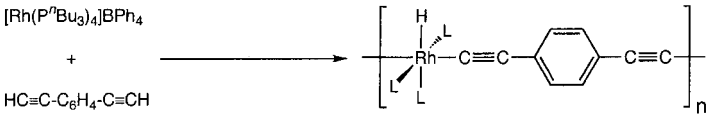

(5.6)

5.6

L= P^{n}Bu$_3$

A convenient metathesis reaction that involves trimethyltin reagents [18] has been used to prepare polyynes that contain Group 8 (Fe, Ru, Os) [19–22], Group 9 (Co, Rh) [23, 24], and Group 10 (Ni, Pd, Pt) [23–26] metals. The polymers were prepared through reaction of equimolar amounts of bis(trimethylstannyl acetylide)s and the appropriate metal halide complexes in the presence of CuI as a catalyst (Scheme 5.2, Eqs. 5.7–5.9). This method is quite general and is reported to produce platinum polymers **5.7** (M = Pt, E = P or As) with slightly higher average molecular weights compared to previously used routes as determined by GPC relative to polystyrene (M_w = 82,000–210,000). The analogous Ni and Pd polymeric complexes were obtained with much lower molecular weights (M_w = 20,000–30,000). In the case of rhodium, the polymer (**5.9**) was found to be a white, insoluble solid, similar to the polymer (**5.5**) produced by the aforementioned method [14]. Insoluble polymeric materials **5.8** were also reported for Ru coordinated with trimethylphosphine (PMe_3) and for Os with diphenylphosphinomethane (dppm) and bis(ethynyl)biphenyl ligands [22].

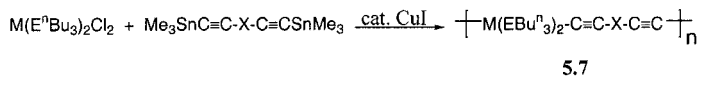

(5.7)

5.7

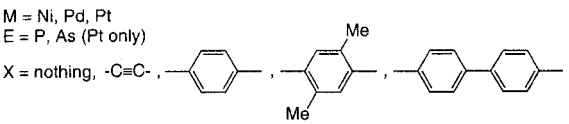

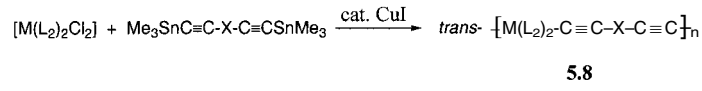

(5.8)

5.8

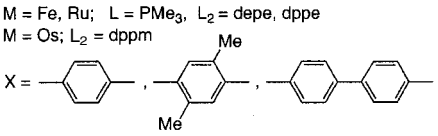

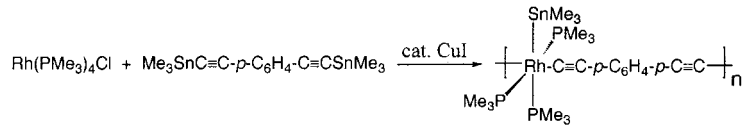

(5.9)

5.9

Scheme 5.2

A Co-acetylide polymer without phosphine ligation at the metal center has also been prepared through the use of this methodology. Thus, air-stable, yellow *trans*-$[CoN_4C{\equiv}C\text{–}p\text{-}C_6H_4\text{–}C{\equiv}C]_n$ (N_4= 3,9-dimethyl-4,8-diazaundecane-2,10-dione dioxime) (**5.10**) with M_w = 15,800 (by GPC) was obtained through reaction of *trans*-N_4CoCl_2 with an equimolar amount of $Me_3Sn\text{–}C{\equiv}C\text{–}p\text{-}C_6H_4\text{–}C{\equiv}C\text{–}SnMe_3$ in the presence of a catalytic amount of CuI in refluxing CH_2Cl_2 [27].

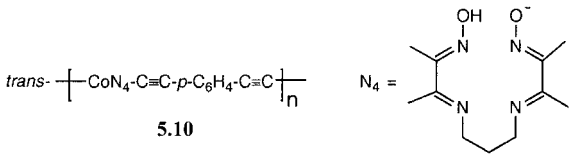

5.10

Recently, an extension of the dehydrohalogenation process to the synthesis of a new class of heterobimetallic polyyne materials (**5.11**) that contain mixed metals with alternating $Ru(dppe)_2$ and $Pd(P^nBu_3)_2$ moieties in the polymer backbone has been reported (Eq. 5.10); these were found to have M_w = 14,000 (by GPC measurements) [28]. The incorporation of ferrocene units into the polymer main chain with alternation between either $Ni(PBu_3)_2$ (**5.12**) or $Pd(PBu_3)_2$ (**5.13**) moieties has also been achieved (Eq. 5.11); the molecular weights of the resulting polymers were M_w = 26,100 and 21,400, respectively [28, 29].

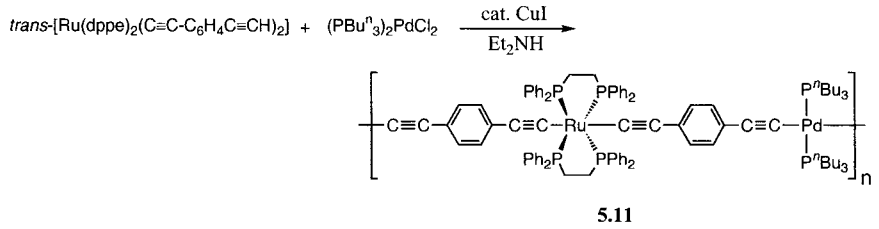

5.11

(5.10)

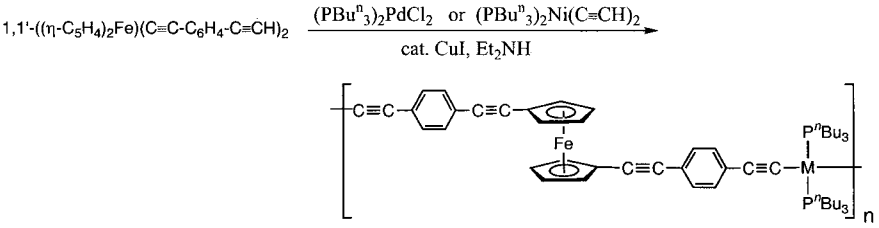

5.12 M = Ni
5.13 M = Pd

(5.11)

Gold(I)-containing polyynes **5.14–5.16**, with diphosphine and diacetylide spacers, have been prepared either by the reaction of gold acetylide precursors with the corresponding diphosphines or from the reactions of [AuCl(SMe_2)] with the appropriate diethynylarene in the presence of a base [30]. The resultant materials were found to be insoluble in most organic solvents, but were partially soluble in THF, dichloromethane, and chloroform; they had average molecular weights of 15,000–18,000, as estimated by GPC (relative to polystyrene standards).

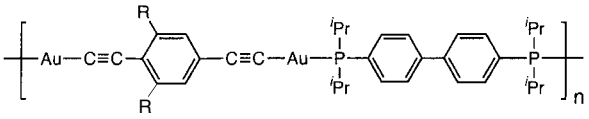

5.14 R = H
5.15 R = Me

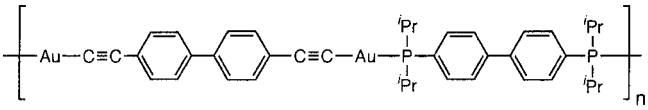

5.16

The synthesis of rigid-rod oligomeric Au^I complexes (**5.17** and **5.18**), with (isocyanoaryl)acetylide bridging ligands, has been achieved by elimination of ^{t}BuC≡CH from the precursor ^{t}BuC≡C–Au–C≡N–Ar–C≡CH [31, 32]. However, direct molecular weight determinations of the resultant materials were not possible due to insolubility. Similarly, the synthesis of the insoluble polymeric materials (**5.19**) with Au^I centers bridged by diisocyanides and diacetylides has also been described [33, 34].

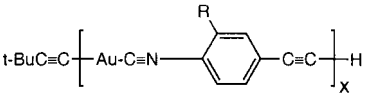

5.17 R = H
5.18 R = Me

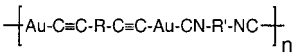

5.19

R = C_6H_4, C_6H_4-C_6H_4, $C_6H_2Me_2$, CH_2O-C_6H_4-CMe_2-C_6H_4-OCH_2,
R' = C_6H_4, C_6H_3Me, $C_6H_2Me_2$, C_6Me_4, $C_6H_2{}^tBu_2$, $C_6H_2Me_2$-$C_6H_2Me_2$

A novel route to polymer chains **5.20** that contain metal moieties as terminal groups has been reported, which involved multiple (up to 100) insertions of aryl isocyanides into the Pd–C bond of the heterodinuclear μ-acetylide complex [$Cl(PR_3)_2Pd$–C≡C–$Pt(PR_3)_2Cl$] (Eq. 5.12) [35]. Crosslinked Pt-containing polymers have been obtained by reacting 1,3,5-triethynylbenzene with the *trans*-dihalo com-

plexes by the dehydrohalogenation route. The 2-D hexagonal graphite-like polymers (**5.21** and **5.22**) were found to have very low solubility [36].

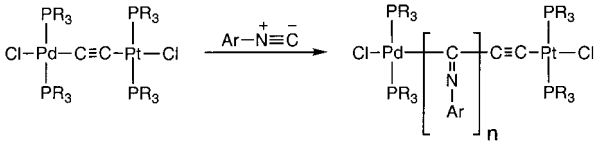

(5.12)

5.20

R = Et, ^{n}Bu
Ar = C_6H_5, C_6H_4-C_4H_9-*p*, C_6H_4-C_8H_{17}-*p*, C_6H_4-NO_2-*p*, C_6H_4-CH_3-*p*

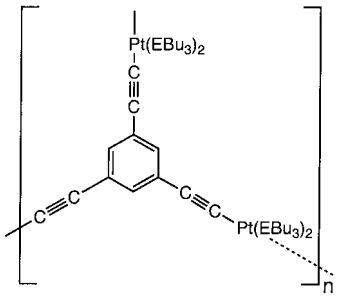

5.21 E = P
5.22 E = As

Improved solubility was achieved by preparing polymer **5.23** through the use of co-monomer mixtures of 1,3,5-triethynylbenzene and 2,5-diethynyl-*p*-xylene in various molar ratios (1:10, 1:50, 1:100) with *trans*-dichlorobis(tri-*n*-butylphosphine) platinum. The high degree of cross-linking for the 1:10 mixture resulted in an insoluble material, whereas soluble copolymers were obtained with M_w = 58,000 and 27,000 (by GPC relative to polystyrene) for the 1:50 and 1:100 molar ratios, respectively [36].

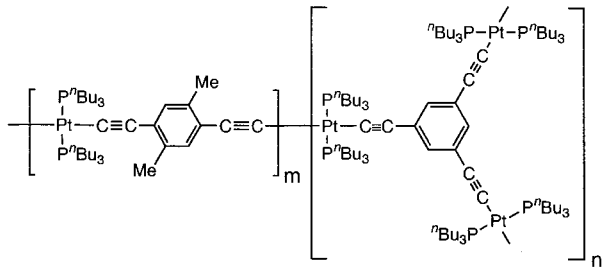

5.23

An interesting class of cationic polyyne polymers (**5.24**) was prepared by reaction of the bimetallic complex μ-butadiynyl-bis[*trans*-chlorobis(tri-*n*-butylphosphine)palladium] with an equimolar amount of 4,4′-bipyridyl in the presence of excess $K[PF_6]$. The resultant polyelectrolyte **5.24** possessed alternating butadiyne and pyridyl spacer units in the main chain (Eq. 5.13). Other analogous polyelectrolytes have been obtained similarly by the use of the appropriate dihalide complex and bipyridyl derivatives [37].

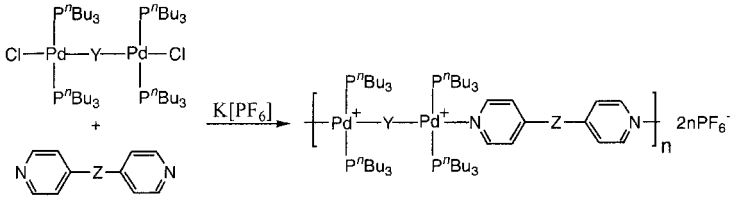

5.24

(5.13)

Y = -C≡C-C≡C-, Z = no substituent
Y = -C≡C-C≡C-, Z = CH_2CH_2
Y = -C≡C-C≡C-, Z = CH=CH

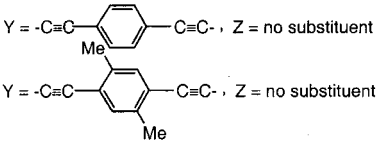

The synthesis of platinum polyynes with heteroaromatic organic spacer groups has also been readily accomplished; for example, species (**5.25**) with skeletal pyridyl units have been prepared either by the dehydrohalogenation method (Scheme 5.1(b)) or by an Me_3SnCl elimination procedure analogous to that in Eq. 5.7 (Scheme 5.2) [38]. The resultant polymers could be quaternized at nitrogen with methyl iodide and triflate. Materials such as **5.26** with a bithiazole spacer have also been prepared by the dehydrohalogenation method [39].

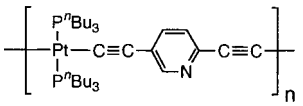

5.25

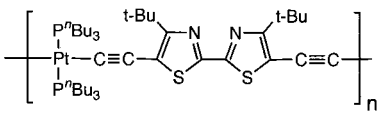

5.26

Electropolymerization has also been used to generate polymetallayne films on an electrode surface. For example, the transition metal-polythiophene hybrid material **5.27** (Eq. 5.14) has been prepared using this approach, which appears to be highly promising for the creation of a broad range of intriguing polymers [40, 41].

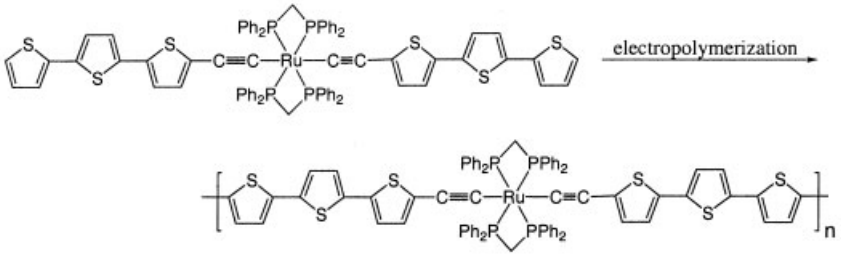

5.27

(5.14)

5.2.2

Structural and Theoretical Studies of Polymers and Model Oligomers

Retention of the *trans* configuration around the metal centers in the aforementioned Pt-polymers such as **5.1** and **5.2** (M = Pt) is evident from spectroscopic analysis of model compounds that contain one to six Pt centers, as well as from single-crystal X-ray diffraction studies of representative species [5, 42, 43]. For example, a detailed study of the molecular structures and crystal-packing arrangements for a series of symmetric and unsymmetric bis(acetylide) complexes, $[Pt(PMe_2Ph)_2(C{\equiv}CC_6H_4{-}p\text{-}R)(C{\equiv}CC_6H_4{-}p\text{-}R')]$ (R, R′ = OMe, SMe, NH_2, NMe_2, CN, NO_2), and the analogous bis(butadiyne) complex has been described [16]. X-ray diffraction provided conclusive proof of the *trans* configuration at the Pt center. The *trans* disposition of the acetylide units has also been established for the Ni and Pd analogues, as well as for Group 8 and 9 complexes such as octahedral *trans*-$[Ru(dppe)_2(C{\equiv}CC_6H_5)_2]$ and *mer, trans*-$[Rh(PMe_3)_3(H)(C{\equiv}CC_6H_5)_2]$, respectively [43–45]. The binuclear Rh^I complex $[Rh(PMe_3)_4(C{\equiv}C{-}C_6H_4{-}C{\equiv}C)Rh(PMe_3)_4]$ has also been characterized crystallographically [14]. Model compounds with organic heteroatomic spacers have also been studied [39, 46–48]. An illustrative example of work in this general area is provided by an X-ray structural study of a Pt-oligothiophene ferrocenylacetylene oligomer (**5.28**), the structure of which is illustrated in Fig. 5.1 [46].

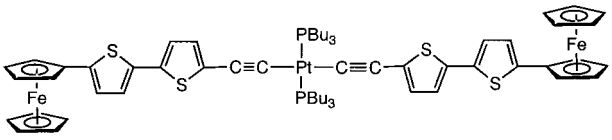

5.28

^{31}P NMR spectroscopy has also provided an exceptional tool for the determination of the configuration at the metal centers in polymers as well as oligomers [3–7, 10]. For example, the *trans* configuration of phosphine ligands in Pt-bis(acetylide) com-

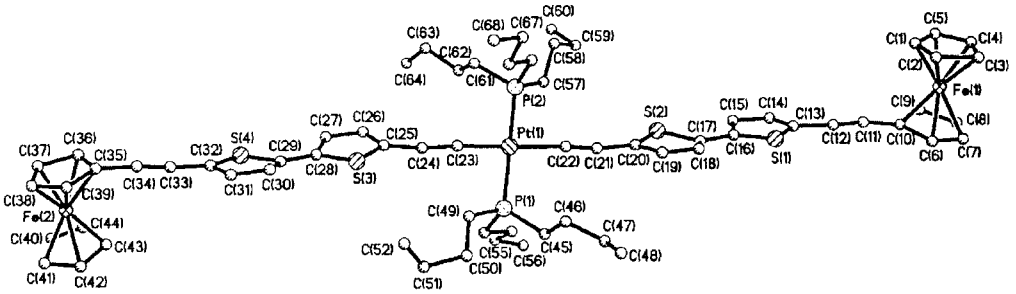

Fig. 5.1 Molecular structure of oligomer **5.28** showing the *trans* disposition of the ligation at the Pt center. (Adapted from [46])

plexes gives rise to a ^{31}P signal at $\delta = 3.0$ to 5.0 ppm, whereas the *cis* configuration gives rise to a signal at $\delta = -2.0$ to -4.0 ppm (referenced to 85% phosphoric acid). In the Pt-containing polymers **5.1** and **5.2** and similar materials, as well as the Pd and Ni analogues, no resonances are detected in the region assigned to the *cis* configuration. Thus, these polymers are believed to possess a rod-like structure with an all-*trans* configuration at the square-planar metal centers. Additional IR spectral analysis was also consistent with the above assignment [5].

In a multinuclear solid-state NMR study carried out on the platinum complex *trans*-[ClPt(P^nBu_3)$_2$–C≡C–*p*-C_6H_4–C≡C–Pt(P^nBu_3)$_2$Cl] and the corresponding polymers **5.1** (M = Pt, L = E^nBu_3, E = P or As), strong evidence for a *trans* geometry at the Pt centers was provided by a ^{31}P NMR study, which gave a chemical shift of $\delta = 4.5$ and ^{31}P-^{195}Pt coupling constants of 2440 Hz (dimer) and 2450 Hz (polymer) in the case of L = P^nBu_3 [49].

Selected area electron diffraction and low-dose, high-resolution TEM imaging techniques have also been employed to obtain structural information on the Pt polyyne [Pt($AsBu_3$)$_2$–C≡C–*p*-C_6H_4–C≡C]$_n$ of structural type **5.1** [50, 51]. The results show a well-defined arrangement of the molecular chains into crystallites (ca. 50 nm in diameter) with grain and dislocation defects. The proposed monoclinic unit cell has measured parameters of $a = 2.08$ nm, $c = 1.20$ nm, $90^\circ \leq \beta \leq 93^\circ$ and a calculated value of $b = 1.9$ nm [50, 51]. The authors attributed the variation in β to the openness of the packing and the tendency of the polymer chains to align upon extension.

Many studies have been directed at gaining insight into the degree of conjugation and electron delocalization in the main chain of polymetallaynes with the aim of controlling the band gap (E_g) and band width, and the hence electronic properties and potential applications of these interesting materials. Studies of the bonding in metal alkynyl, butadiynyl, and bis(alkynyl) complexes by means of photoelectron spectroscopy and/or molecular orbital calculations [52–54] have provided much useful information, and support previous calculational findings [55] that indicate that there is considerable mixing of the filled metal d orbitals with the filled π-system of the alkynyl moiety [43]. The energy mismatch between the metal d-levels and alkynyl π^*-levels, at least in cases in which there are no strong π-acceptor substituents

in conjugation with the alkynyl moiety, apparently leads to a lack of significant π-backbonding. However, the perturbation of the filled metal d-levels by the π-donor character of the alkynyl groups leads to low-lying metal-ligand charge-transfer (MLCT) absorptions. An in-depth compilation and analysis of data obtained primarily from X-ray diffraction, electronic, and vibrational studies that aims at probing the nature of bonding in metal-alkynyl complexes has been reported [43].

Extended Hückel band calculations [56] on metal polyynes have indicated that in $[L_nM–C\equiv C–Ar–C\equiv C\text{-}]_x$ systems the highest occupied crystal orbital (HOCO, which is roughly analogous to the HOMO in a molecular system) is predominantly metal-d in character and is delocalized along the chain through the ML_n groups for $n=2$ (square planar) and $n=4$ (octahedral) geometries. The calculations indicated that the lowest unoccupied crystal orbital (LUCO) is predominantly alkynyl-π* in character. It was suggested, based on these studies, that the electrical conductivity of polymetallaynes can be improved through alteration of the character of the HOCO and the LUCO. The nature of the metal is expected to play a significant role in affecting the HOCO energy level in such a way that the higher the energy and the more diffuse the d orbitals, the higher the HOCO level will be. On the other hand, extending the π-conjugation length in the alkynyl spacer groups would be expected to lower the optical (HOCO-LUCO) band gap in metal polyyne systems, predominantly by lowering the energy of the LUCO. These calculations indicated that electrical conductivity is favored for polymetallaynes containing four-coordinate d^8 square-planar metal centers over those with six-coordinate d^6 octahedral metal centers, due mainly to the greater conduction bandwidth in the former case (by ca. 0.4 eV). Other authors have reported similar extended Hückel calculations on Pt-containing polymers and also concluded that the Pt centers do contribute to some electronic delocalization along the polymer chain [57]. In addition, a vibrational spectroscopic study of these Pt polyynes, of types **5.1** and **5.2**, in the solid state has suggested that the alkyne spacer units still possess their essentially acetylenic character and that π-conjugation is reduced in the presence of phenylene rings in the polymer main chain [58].

Overall, although many details are still open to question, both theory and experiment (see Sections 5.2.3.3–5.2.3.5) support the assertion that a significant degree of electron delocalization is present in the polymetallayne main chain. Furthermore, as shown below, the structure can be successfully tuned to influence the electronic properties. However, a key challenge for the future is the development of materials in which electron delocalization is even further enhanced.

5.2.3
Polymer Properties

A wide variety of high molecular weight polymetallaynes have been reported that possess mainly d^8 square-planar metals (Ni, Pd, Pt) or six-coordinate d^6 octahedral metals such as Ru. Many of these materials have been very well-characterized and, as a group, they provide fascinating insight into the role that main-chain metal atoms can play in influencing polymer properties.

5.2.3.1 Thermal and Environmental Stability

Group 10 metal polyynes of types **5.1** and **5.2** are yellow solids which generally show good stability in air in the solid state [5]. The thermal stability of samples of these and related materials with M_w in the range $1.0\times10^4-1.2\times10^5$ has been investigated by means of TGA, and the results indicated that the platinum-containing polymers are considerably more stable than their palladium and nickel analogues (Table 5.1). In air, the polymers decompose explosively with a weight loss of ca. 35–60% [5]. The Pt materials are also significantly more stable than the Pd and Ni analogues in solution. Even the Pt materials tend to lose small amounts of the ligands (e.g. phosphine) at the metal center, and association in solution through complexation of alkyne functionalities on neighboring chains has been proposed on the basis of viscosity measurements [5]. Little has been reported on polymers containing metals of Groups 8 and 9 with regard to thermal and environmental stability.

Table 5.1 Thermal stability of Group 10 metal polyyne polymers (measured by TGA at a heating rate of 5 °C/min) [5]

Polymer	$M_w\times10^3$	*Decomposition temp. (°C)*	
		in air	*in N_2*
$[Pt(P^nBu_3)_2\text{-}C\equiv C\text{-}C\equiv C]_n$	120	270	350
$[Pd(P^nBu_3)_2\text{-}C\equiv C\text{-}C\equiv C]_n$	24	150	200
$[Ni(P^nBu_3)_2\text{-}C\equiv C\text{-}C\equiv C]_n$	10	150	165
$[Pt(P^nBu_3)_2\text{-}C\equiv C\text{-}C_6H_4\text{-}C\equiv C]_n$	72	230	300
$[Pd(P^nBu_3)_2\text{-}C\equiv C\text{-}C_6H_4\text{-}C\equiv C]_n$	25	145	170
$[Ni(P^nBu_3)_2\text{-}C\equiv C\text{-}C_6H_4\text{-}C\equiv C]_n$	13	135	140
$[Pt(P^nBu_3)_2(\text{-}C\equiv C\text{-}C\equiv C\text{-})_2]_n$	30	210	210
$[Pt(P^nBu_3)_2(\text{-}C\equiv C\text{-}C_6H_4\text{-}C\equiv C\text{-})_2]_n$	120	250	250
$[Pt(P^nBu_3)_2(\text{-}C\equiv C\text{-}C\equiv C\text{-})\text{-}Pt(P^nBu_3)_2(\text{-}C\equiv C\text{-}C_6H_4\text{-}C\equiv C\text{-})]_n$	34	–	330

5.2.3.2 Solution Properties

The high solubility of many metal polyynes in common organic solvents, such as benzene, toluene, tetrahydrofuran, and dichloromethane, is attributed to the presence of organic substituents on the ancillary ligands attached to the metal or organic spacer unit, which promotes good solvent-polymer chain segment interactions. As noted earlier, molecular weight measurements have generally involved the use of GPC with polystyrene standards for column calibration. This relative technique generally provides only approximate estimates of the molecular weight as it is assumed that the hydrodynamic size of the polymers under study is similar to that of the calibration standard (generally polystyrene) of the same molecular weight. This is clearly unrealistic for polymers with rigid backbones. However, the sedimentation equilibrium method has been used to provide absolute mea-

surements of the molecular weight of several platinum polyynes, and these clearly established the macromolecular nature of these materials. For example, samples of the representative polymer **5.2** ($ML_2 = Pt(P^nBu_3)_2$, $x = 2$) were found to possess a molecular weight $M_w > 10^5$ by the sedimentation method [4, 7]. The intrinsic viscosities of this and related polymers, $[\eta] = 1.19–1.25$ dL g^{-1}, were found to be independent of the nature of the solvent in the solubility parameter (δ) range of 6.6–9.7 (cal/mL)$^{1/2}$ [5, 7]. In addition, the α-value in the Mark-Houwink equation (ca. 1.7) was also determined, and this indicated that this type of polymer has a stiff rod-like structure in solution [5, 7]. It is noteworthy, however, that subsequent studies on the same polymer have led to the suggestion that the polymer chain is more flexible and can be represented by a worm-like model [59, 60].

The generally rigid, extended nature of metal polyynes is also evident from their tendency to form lyotropic liquid-crystalline phases [5, 61, 62]. Homometallic polymers, as well as mixed-metal systems, that contain Pt, Ni, and Pd have all been shown to exhibit liquid-crystalline phases in trichloroethene (Fig. 5.2) [61, 62]. The formation of a nematic phase, as observed between crossed polarizers, was reported for the platinum polyyne **5.2** ($ML_2 = Pt(P^nBu_3)_2$, $x = 2$) (Fig. 5.3) [61]. The lyotropic liquid-crystalline phases formed by these polymers have also been detected by high-resolution ^{31}P NMR spectroscopy [63, 64]. The orientation of the polymer chain exhibits a strong response to magnetic and electric perturbations, and this leads to either parallel or perpendicular alignment with respect to the applied magnetic field. It was established that the preferred direction of the mesogenic macromolecules with respect to the magnetic field is determined by the magnetic anisotropy of the polymer and its structure [63, 64].

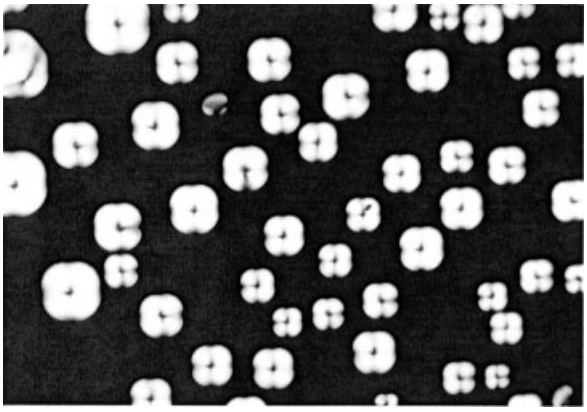

Fig. 5.2 Liquid crystals of polymetallayne **5.3** (M = Pd, M′ = Pt) observed between cross-polarizers in trichloroethene (200× magnification). (Reproduced from [5])

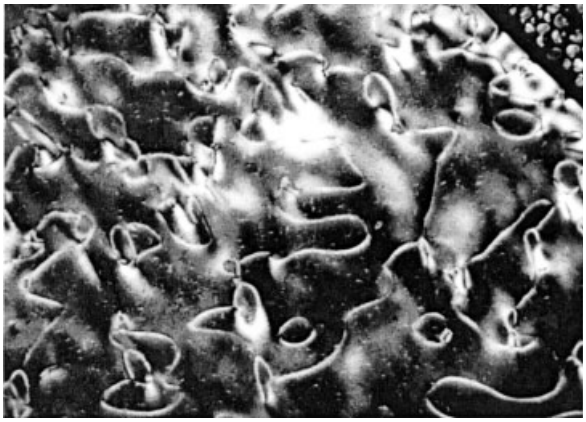

Fig. 5.3 Nematic liquid crystals of polymetallayne **5.2** (M = Pt, L = P^nBu_3, $x = 2$, $n \approx 100$) observed between cross-polarizers in trichloroethene at 25 °C. (We thank Prof. S. Takahashi, Osaka University, for the figure)

5.2.3.3 **Optical Properties**

Metal-to-alkyne ligand charge-transfer (MLCT) transitions are a common spectral feature in all of the linear rigid-rod metal polyynes. Their optical absorption and emission properties have been examined in some detail [26, 50, 65–67]. The optical band gap that corresponds to the lowest-energy transition between the valence band and conduction band varies depending upon the metal centers and their coordination geometry, the ancillary ligands, and the nature of the alkyne bridging units [65–67]. This transition was investigated as a function of chain length for a series of materials of the type [R–(Pt(P^nBu_3)$_2$–C≡C–*p*-C_6H_4–C≡C)$_{n-1}$–Pt(P^nBu_3)$_2$–R] ($n = 2$–5, R = C≡CC_6H_5) [42]. It was found that the low-energy band undergoes a red shift as n increases, but the magnitude of the shift rapidly decreases with increasing n value (Table 5.2). However, no further significant bathochromic shift was observed on moving from the pentaplatinum species ($\lambda_{max} = 378$ nm) to the high polymer ($\lambda_{max} = 380$ nm) [7, 42]. It was also found that the optical transitions for the polymers occur at lower energies than those for the free alkyne ligands. These observations both suggest that appreciable π-conjugation occurs through the metal centers [67]. Further extension of the π-conjugation within the alkyne spacer has a significant effect on the lowest-energy optical transitions, as illustrated in Table 5.3. It is apparent that the triacetylenic bridge ($m = 1$) exhibits a lower optical gap than the diacetylenic analogue ($m = 0$) ($E_g = 3.12$ eV *vs.* 3.23 eV) [26], and likewise the band-gap excitation for the more extended bis(aryleneethynyl)benzene [67] is red-shifted in comparison with that of the comparable diethynylbenzene material [26, 66] ($E_g = 3.13$ eV *vs.* 3.26 eV). The more extended anthracene spacer, which contains three fused benzene rings, is most effective in promoting the delocalization of π-electrons along the polymer backbone [67]. Thiophene and oligothiophene spacer units were also found to be

Table 5.2 λ_{max} (nm) for the lowest optical absorption band for a series of oligo- and polyplatinaynes [7, 42]

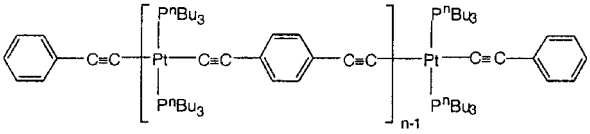

n	λ_{max} *(nm)*
2	363
3	371
4	376
5	378
ca. 80	380

Table 5.3 Lowest optical transition measurements as a function of the alkynyl ligand spacer [26, 67]

Compound	E_g *(eV)*
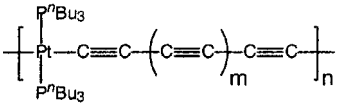	3.23 (m = 0) 3.12 (m = 1)
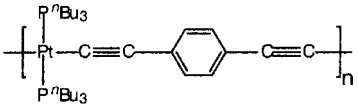	3.26
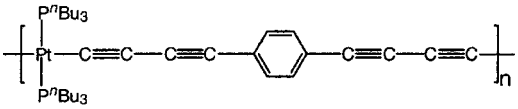	3.13
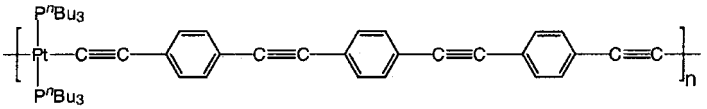	3.11
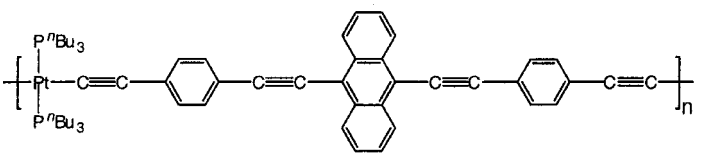	2.48
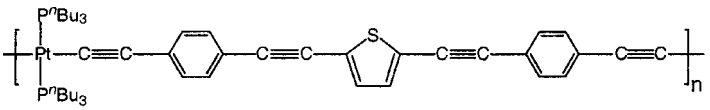	2.70

more effective than arene spacers, whereas, in comparison, silyl spacers (SiR_2) have been found to reduce delocalization [67–69].

Most polymetallaynes have band gaps of ca. 2.4–3.2 eV, but the value can be reduced substantially to ca. 1.7 eV by the use of alternating donor (bis(phosphine)platinum acetylide) and acceptor (electron-deficient thienopyrazine) units in the backbone, as in polymer **5.29** [70]. Similarly, donor–acceptor interactions appear to be important in polymer **5.30**, which possesses a ferrocenylfluorenyl spacer and has a band gap of 2.1 eV. In the absence of the metallocene group, the analogous polymer has a substantially wider gap (E_g=2.9 eV) [71].

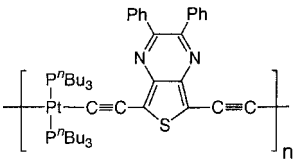

5.29

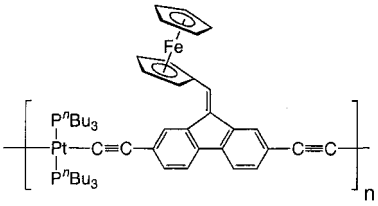

5.30

π-Conjugated organic polymers are of widespread interest with respect to their light-emissive properties, which permit applications in, for example, lasers, photocells, and light-emitting diodes [72–74]. Light emission is possible from excited singlet states, but is spin-forbidden from excited triplet states. The presence of transition metals in the π-conjugated framework of polymetallaynes introduces sufficient spin-orbit coupling for emission from excited triplet states to also become significant [47]. For example, the polymers shown in Table 5.3 exhibit photoluminescence at room temperature and, for the lower three polymers in the table, the emission quantum yields (4–8%) were found to be about one-tenth of those for the free ligands (30–60%) [67]. The lower quantum yields detected for the Pt polymers were attributed to the population of long-lived triplet states that were easily quenched under the conditions of the experiment. Photoluminescence experiments performed at liquid-helium temperature allow the observation of the emission from the triplet states. For example, the photoluminescence spectra of thin films of the polymetallayne **5.31** at 10 K and 300 K are shown in Fig. 5.4 [47]. The high-energy emission at 450–600 nm is assigned to fluorescence from the excited S_1 state and the low-energy band at 670–850 nm, which is only detected at 10 K, was assigned to phosphorescence from the excited triplet state T_1.

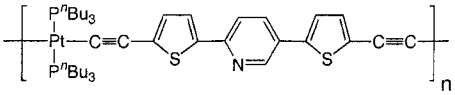

5.31

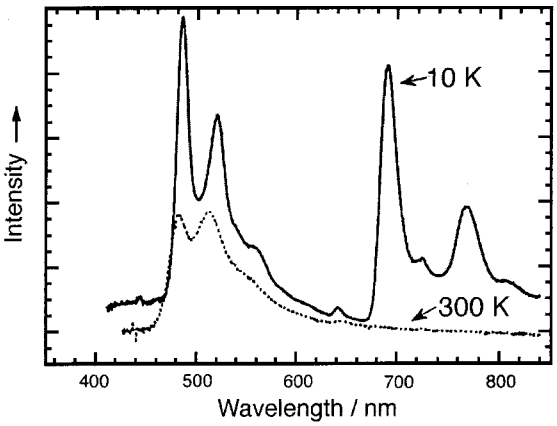

Fig. 5.4 Photoluminescence spectra of a thin film of polyplatinayne **5.31** at 10 K and 300 K. The excitation wavelength was 334–364 nm. (Adapted from [47])

Detailed studies have been performed on the photophysics of a range of Pt polyynes [68, 75–77], and the energy-gap law for triplet states in a series of platinum polyynes has been established [78]. Convincing evidence for π-conjugation between metal sites in the main chain has been provided by some of the experiments [75]. The photophysics of polymers with fluorene and carbazole spacers has also been investigated in depth, and the studies indicate that the singlet state extends over more than one repeat unit whereas the triplet state is strongly localized [79].

Studies of polymetallaynes that contain metals other than Pt are much more rare. However, the photophysical properties of rigid-rod, conjugated gold(I) polymers **5.17–5.19** have been investigated, and these materials were found to exhibit weak luminescence in the solid state at ca. 585 and 600 nm at room temperature when excited with UV light [34].

5.2.3.4 **Nonlinear Optical Properties**

The ability to manipulate light in new ways is critical to the creation of new photonic devices. Materials that exhibit nonlinear optical (NLO) effects offer potential applications in many areas such as switching and frequency doubling or tripling [80]. It is well known that extended π-electron-delocalized systems such as conjugated organic polymers exhibit appreciable third-order nonlinear optical susceptibilities. Significantly, the absence of a center of symmetry is not a structural requirement for third-order NLO materials, which provides a significant potential advantage over second-order NLO materials [80]. Thus, metal polyyne polymers, which possess low oxidation state transition metals with highly polarizable d electrons in the conjugated backbone, should show enhanced hyperpolarizability. Indeed, studies of the third-order nonlinear optical properties [81–87] of a series of platinum polyynes have shown that these polymers exhibit large hyperpolarizabilities, comparable with those of inorganic semiconductors such as InSb (1700×10^{-36} esu) and elemental Ge (2300×10^{-36} esu) [84]. Table 5.4 lists the third-

Table 5.4 Third-order nonlinear optical coefficients for some Pt-polyynes [84]

Polymer	*n*	γ' *(10^{-36} esu)*	γ'' *(10^{-36} esu)*
$[Pt(P^nBu_3)_2\text{-}C\equiv C\text{-}C_6H_4\text{-}C\equiv C]_n$	112	102	3401
$[Pt(P^nBu_3)_2\text{-}C\equiv C\text{-}C_6H_4\text{-}C\equiv C\text{-}C\equiv C\text{-}C_6H_4\text{-}C\equiv C]_n$	>144	856	3570
$[Pt(P^nBu_3)_2\text{-}C\equiv C\text{-}C_6H_2(Me_2)\text{-}C\equiv C]_n$	26	56	1199
$[Pt(P^nBu_3)_2\text{-}C\equiv C\text{-}C_6H_2(Me_2)\text{-}C\equiv C\text{-}C\equiv C\text{-}C_6H_2(Me_2)C\equiv C]_n$	52	181	4366

order hyperpolarizabilities for some platinum polyynes, measured by the optical Kerr gate technique, along with the corresponding chain lengths. The large values of γ' (real component) and γ'' (imaginary component), where the former refers to nonlinear refraction and the latter to nonlinear absorption, suggest that these materials are potentially of interest for the construction of NLO devices [84].

5.2.3.5 **Electrical and Photoconductive Properties**

The electrical conductivity and photoconductivity of metal polyynes have been studied in some detail [88]. For instance, it has been demonstrated that in the unoxidized state **5.2** (M = Cu, L = no substituent, $x = 1$) is an insulator ($\sigma = 10^{-9}$ Scm^{-1}), but upon doping with I_2 the conductivity is increased to ca. 10 Scm^{-1} [89]. Polyynes such as **5.1** (M = Ni, Pd, Pt; L = E^{n}Bu$_3$; E = P or As) can either be oxidized with nitric acid or doped with I_2 [50]. Measurements on undoped films showed low conductivity values of ca. 10^{-7} Scm^{-1}, which improved to ca. 10^{-6} Scm^{-1} in the I_2-doped samples [50]. The Pt-acetylide polymers **5.25** with pyridyl groups in the spacer unit showed conductivities of 2.5×10^{-3} Scm^{-1} upon doping with iodine. Quaternization followed by iodine doping gave a similar value (3.4×10^{-3} Scm^{-1}). These values appear to be the highest reported for soluble polymetallaynes [38].

Electrochemical studies of several polymetallaynes have also been reported [70, 71, 79]. Reduction of organic spacer groups can be achieved, and the oxidation of substituents (e.g. ferrocene) can be reversible. However, electrochemical oxidation of the platinum centers in at least some polymetallaynes appears to occur in two irreversible redox steps (presumably involving Pt^{II}/Pt^{III} and Pt^{III}/Pt^{IV} couples). This observation suggests that the chemical doping experiments that were used to increase the electrical conductivities of the polymers described above may not involve simple processes.

The photoconductivity of platinum polyynes has been examined, and photocells (Fig. 5.5) have been fabricated using the materials **5.32** ($M_w = 2.9\times10^4$, PDI = 1.71) and **5.33** ($M_w = 1.9\times10^4$, PDI = 2.14). The quantum efficiencies detected were ca. 0.01%, a common value for single-layer devices. The photocurrent was found to increase with an increase in bias voltage [79]. Similar studies of Pt polyynes **5.34** and **5.35** ($M_w = 8.3\times10^4$–1.8×10^5, PDI = 1.2–3.2), with thiophene and oligothiophene spacers, respectively, have also been reported and quantum efficiencies

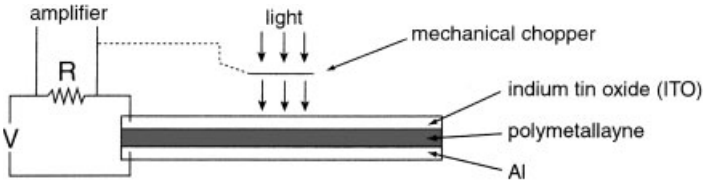

Fig. 5.5 Photocells constructed from single layers of platinum polyynes **5.32** and **5.33**.

were found to be around 0.04% [68]. In analogous work, the most promising photocurrent quantum yield of ca. 1% has been reported for the donor-acceptor polymer **5.29**. This value is unusually high for a single-layer device [70].

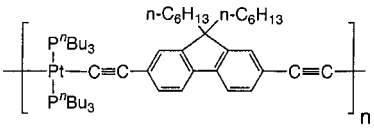

5.32

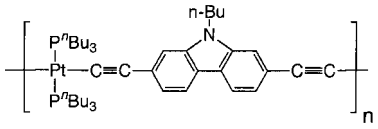

5.33

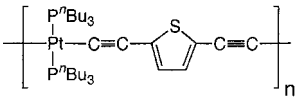

5.34

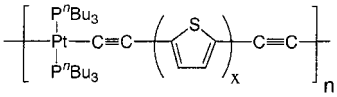

5.35
x = 2 or 3

5.3
Polymers with Skeletal Metallocyclopentadiene Units

The first members of an interesting new class of organometallic π-conjugated polymers that contain metallocyclopentadiene units in the main chain were reported in 1993 [90, 91]. The addition of acetylenes to $CpCo(PPh_3)_2$ allowed the preparation of polymers **5.36** (Eq. 5.15). These materials were found to be intractable in common organic solvents; their degree of polymerization was estimated to be ca. 20 by IR spectroscopy [90].

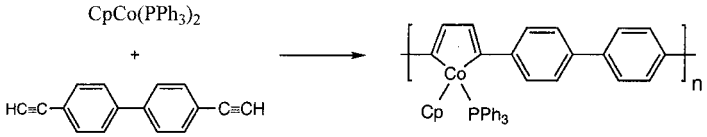

(5.15)

5.36

A similar synthetic approach was used to prepare Co polymers **5.37** (Eq. 5.16), which possessed improved solubility as a result of the presence of flexible aliphatic spacers in the main chain [91].

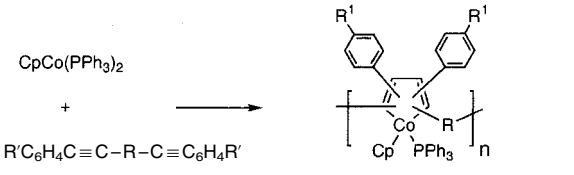

(5.16)

5.37

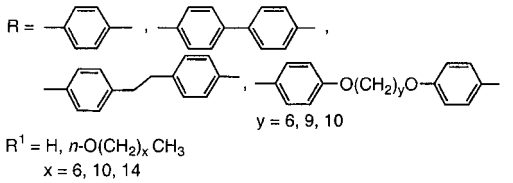

Molecular weights for the soluble, orange-brown polymers **5.37** were determined by GPC (versus polystyrene standards) to be ca. $M_w = 9000–16{,}000$, with PDI values in the range 1.3–1.5 [92]. Solubility can also be enhanced through the attachment of *n*-hexyl groups to the Cp ligands [93]. Regioregular polycobaltacyclopentadienes **5.38** have been prepared by a nickel-catalyzed route (Eq. 5.17), and these materials possess molecular weights up to $M_w = 5.6 \times 10^5$, with PDI = 2.8 [94].

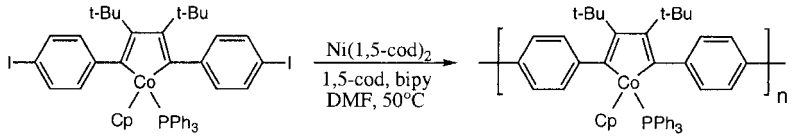

5.38

(5.17)

The polycobaltacyclopentadienes of types **5.36–5.38** are of interest as metal-containing analogues of π-conjugated organic polymers such as polythiophene and polypyrrole. This has led to substantial interest in their physical properties [92–97]. UV/vis studies show that there is a shift in the lowest-energy absorption band with an increased degree of polymerization, which is indicative of a significant degree of π-conjugation in the polymer main chain [92, 93]. Band gaps of ca. 2.1–2.3 eV have been determined by measurement of the absorption edge of UV/vis spectra, and these values are comparable with the value of 2.0 eV for polythiophene [93]. In the dark, polycobaltacyclopentadienes show low conductivity ($\sigma \approx 10^{-12}$ Scm^{-1}). However, upon irradiation with white light a very substantial photoconductivity effect has been demonstrated [93]. Cyclic voltammograms of the polymers show quasi-reversible oxidations and irreversible reductions. Electro-

chemical studies of **5.38** revealed weak metal-metal interactions with $\Delta E_{1/2}$ values around 20% of those in poly(1,1′-di(*n*-hexyl)ferrocenylene). The relatively weak interactions were attributed to an energy mismatch between the Co d-orbitals and the phenylene π-orbitals or to the lack of coplanarity for the cobaltacyclopentadiene and arene units [94].

Cobaltacyclopentadiene polymers undergo thermal rearrangement to the more stable (η^4-cyclobutadiene)cobalt derivatives, and reaction with isocyanates affords new polymers containing 2-pyridone moieties in the polymer backbone (for details, see Chapter 4, Section 4.4.1) [98–100].

A novel extension of the metal-induced coupling of diynes involves the preparation of the red, moisture-sensitive zirconocene-containing polymer **5.39** (Eq. 5.18) with $M_w = 37{,}000$ (PDI = 2.1) by GPC (relative to polystyrene) [101]. Related organosilicon polymers and macrocycles derived from the zirconocene coupling of $MeC{\equiv}CSiMe_2C_6H_4SiMe_2C{\equiv}CMe$ have also been reported [102, 103].

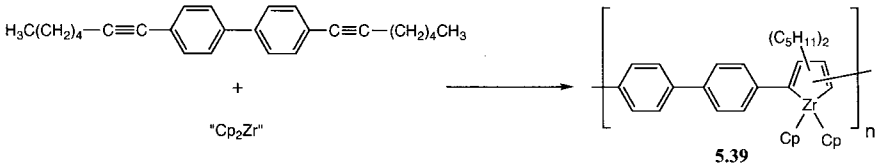

5.39

(5.18)

The Zr polymers **5.39** are not just of intrinsic interest, but they also permit chemical modification reactions in which the Zr atom is replaced [101, 103, 104]. This allows the introduction of diene, thiophene, phosphole, and aromatic functionalities to yield novel π-conjugated organic polymers (**5.40–5.43**) with controlled structures and electronic properties (Scheme 5.3).

5.4 Other Polymers with M–C σ-Bonds in the Main Chain

A step-growth polycondensation route has been successfully devised to prepare well-characterized nickel polymers **5.45** with arene spacer groups. The procedure involves the polycondensation of the fluorinated dilithiated species **5.44** and a Ni^{II} complex (Eq. 5.19) [105]. The rod-like structure of these polymers was established by dilute-solution viscosity measurements, and the results were similar to those reported for the related platinum polyyne polymers **5.2** (M = Pt, L = P^nBu_3, $x = 2$) (Section 5.2.3.2).

The absolute molecular weights of these materials were established by GPC by means of the universal calibration technique that involved the acquisition of intrinsic viscosity data. As with the aforementioned platinum polyyne polymers **5.2** ($ML_2 = Pt(P^nBu_3)_2$, $x = 2$), the intrinsic viscosities were found to be independent of the nature of the solvent, and a Mark-Houwink α-value of 1.5 was determined, which is indicative of a rod-like structure. Interestingly, it was found that in this

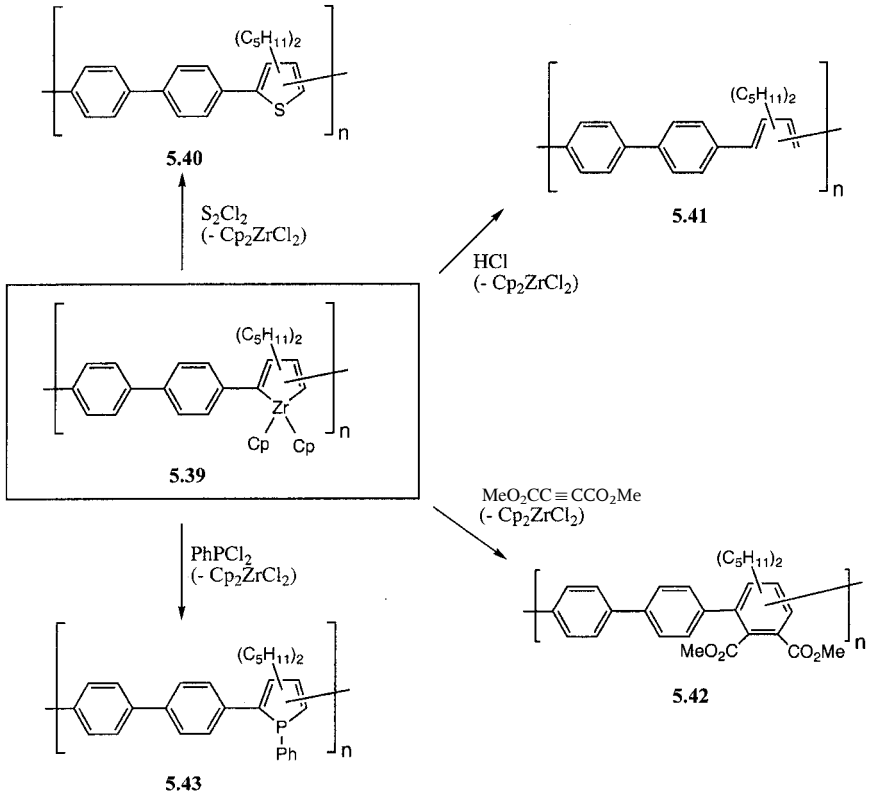

Scheme 5.3

case GPC using polystyrene standards *underestimates* the true molecular weight of the polymers. This was attributed to the high molar mass of a repeat unit in the Ni polymer **5.45** compared to polystyrene, which overcompensates for the effect of the rigid-rod structure that would be expected to lead to the opposite situation. Absolute values of M_w of up to ca. 1×10^5 were determined for the polymer samples studied [106].

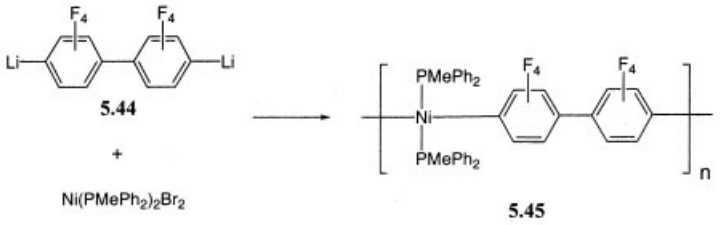

(5.19)

Polymers with M–C bonds in the main chain where the carbon atom is sp^3 hybridized are rare. Such materials have been successfully prepared by acyclic diene

metathesis (ADMET) polymerization, which has been used to prepare polycarbostannanes **5.47** with molecular weights (M_w) up to 36,000 (PDI = 2.1), with ethene as the by-product (Eq. 5.20). The reaction is unusual in that the divinyl stannane **5.46** can function as both the monomer and the co-catalyst in the case of the W-catalyzed reaction [107].

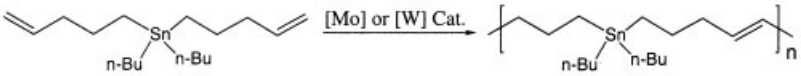

5.46 **5.47** (5.20)

As another interesting variant on materials with M–C linkages, formally conjugated polymers **5.48** and **5.49** have been prepared by polycondensation routes, and have been characterized in the solid state [108–110]. In the case of the intriguing metal-carbyne polymers **5.49**, the materials are fluorescent at room temperature [109], unlike monomeric species such as $(RO)_3W{\equiv}CR$ (R = alkyl or aryl). Polymers such as **5.48** and **5.49** and analogues thereof [110] represent very exciting targets for future study.

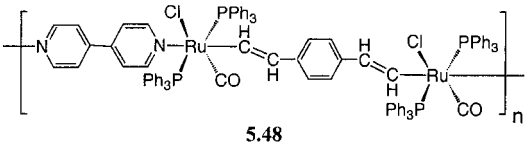

5.48

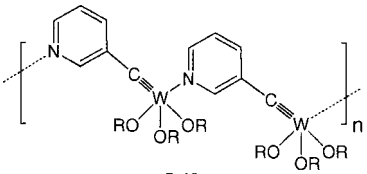

5.49

5.5 References

1 V.V. Korshak, A.M. Sladkov, Y.P. Kudryavtsev, *Vysokomol. Soedin.* **1960**, *2*, 1824.

2 A.S. Hay, *J. Polym. Sci. A-1* **1969**, *7*, 1625.

3 Y. Fujikura, K. Sonogashira, N. Hagihara, *Chem. Lett.* **1975**, 1067.

4 K. Sonogashira, S. Takahashi, N. Hagihara, *Macromolecules* **1977**, *10*, 879.

5 N. Hagihara, K. Sonogashira, S. Takahashi, *Adv. Polym. Sci.* **1981**, *41*, 149.

6 K. Sonogashira, S. Kataoka, S. Takahashi, N. Hagihara, *J. Organomet. Chem.* **1978**, *160*, 319.

7 S. Takahashi, M. Kariya, T. Yatake, K. Sonogashira, N. Hagihara, *Macromolecules* **1978**, *11*, 1063.

8 S. Takahashi, Y. Ohyama, E. Murata, K. Sonogashira, N. Hagihara, *J. Polym. Sci., Polym. Chem. Ed.* **1980**, *18*, 349.

9 S. Takahashi, H. Morimoto, E. Murata, S. Kataoka, K. Sonogashira, N. Hagihara, *J. Polym. Sci., Polym. Chem. Ed.* **1982**, *20*, 565.

10 S. Takahashi, E. Murata, K. Sonogashira, N. Hagihara, *J. Polym. Sci., Polym. Chem. Ed.* **1980**, *18*, 661.

11 A. S. Hay, *J. Org. Chem.* **1962**, *27*, 3320 and references therein.

12 K. Sonogashira, K. Ohga, S. Takahashi, N. Hagihara, *J. Organomet. Chem.* **1980**, *188*, 237.

13 H. B. Fyfe, M. Mlekuz, D. Zargarian, T. B. Marder, in *Organic Materials for Non-linear Optics II* (Eds.: R. A. Hahn, D. Bloor), The Royal Society of Chemistry, Cambridge, **1991**, p 204.

14 H. B. Fyfe, M. Mlekuz, D. Zargarian, N. J. Taylor, T. B. Marder, *Chem. Commun.* **1991**, 188.

15 H. B. Fyfe, M. Mlekuz, G. Stringer, N. J. Taylor, T. B. Marder, *Inorganic and Organometallic Polymers with Special Properties* (Ed.: R. M. Laine), NATO ASI Series, Series E, **1992**, *206*, p. 331.

16 T. B. Marder, G. Lesley, Z. Yuan, H. B. Fyfe, P. Chow, G. Stringer, I. R. Jobe, N. J. Taylor, I. D. Williams, S. K. Kurtz, *Materials for Nonlinear Optics: Chemical Perspectives* (Eds.: G. D. Stucky, S. R. Marder, J. Sohn), American Chemical Society Symp. Ser. 455, Washington D.C., **1991**, p. 605.

17 H.-F. Klein, H. H. Karsch, *Chem. Ber.* **1975**, *108*, 944.

18 C. J. Cardin, D. J. Cardin, M. F. Lappert, *J. Chem. Soc., Dalton Trans.* **1977**, 767.

19 S. J. Davies, B. F. G. Johnson, J. Lewis, P. R. Raithby, *J. Organomet. Chem.* **1991**, *414*, C51.

20 B. F. G. Johnson, A. K. Kakkar, M. S. Khan, J. Lewis, *J. Organomet. Chem.* **1991**, *409*, C12.

21 M. S. Khan, A. K. Kakkar, S. L. Ingham, P. R. Raithby, J. Lewis, B. Spencer, F. Wittman, R. H. Friend, *J. Organomet. Chem.* **1994**, *472*, 247.

22 (a) C. W. Faulkner, S. L. Ingham, M. S. Khan, J. Lewis, N. J. Long, P. R. Raithby, *J. Organomet. Chem.* **1994**, *482*, 139; (b) Z. Atherton, C. W. Faulkner, S. L. Ingham, A. K. Kakkar, M. S. Khan, J. Lewis, N. J. Long, P. R. Raithby, *J. Organomet. Chem.* **1993**, *462*, 265.

23 S. J. Davies, B. F. G. Johnson, M. S. Khan, J. Lewis, *Chem. Commun.* **1991**, 187.

24 M. S. Khan, S. J. Davies, A. K. Kakkar, D. Schwartz, B. Lin, B. F. G. Johnson, J. Lewis, *J. Organomet. Chem.* **1992**, *424*, 87.

25 B. F. G. Johnson, A. K. Kakkar, M. S. Khan, J. Lewis, A. E. Dray, R. H. Friend, F. Wittman, *J. Mater. Chem.* **1991**, *1*, 485.

26 J. Lewis, M. S. Khan, A. K. Kakkar, B. F. G. Johnson, T. B. Marder, H. B. Fyfe, F. Wittman, R. H. Friend, A. E. Dray, *J. Organomet. Chem.* **1992**, *425*, 165.

27 M. S. Khan, N. A. Pasha, A. K. Kakkar, P. R. Raithby, J. Lewis, K. Fuhrmann, R. H. Friend, *J. Mater. Chem.* **1992**, *2*, 759.

28 O. Lavastre, M. Even, P. H. Dixneuf, A. Pacreau, J.-P. Vairon, *Organometallics* **1996**, *15*, 1530.

29 O. Lavastre, J. Plass, P. Bachmann, S. Guesmi, C. Moinet, P. H. Dixneuf, *Organometallics* **1997**, *16*, 184.

30 G. Jia, R. J. Puddephatt, J. D. Scott, J. J. Vittal, *Organometallics* **1993**, *12*, 3565.

31 G. Jia, R. J. Puddephatt, J. J. Vittal, N. C. Payne, *Organometallics* **1993**, *12*, 263.

32 G. Jia, N. C. Payne, J. J. Vittal, R. J. Puddephatt, *Organometallics* **1993**, *12*, 4771.

33 M. J. Irwin, G. Jia, N. C. Payne, R. J. Puddephatt, *Organometallics* **1996**, *15*, 51.

34 M. J. Irwin, J. J. Vittal, R. J. Puddephatt, *Organometallics* **1997**, *16*, 3541.

35 K. Onitsuka, T. Joh, S. Takahashi, *Angew. Chem. Int. Ed. Engl.* **1992**, *31*, 851.

36 M. S. Khan, D. J. Schwartz, N. A. Pasha, A. K. Kakkar, B. Lin, P. R. Raithby, J. Lewis, *Z. Anorg. Allg. Chem.* **1992**, *616*, 121.

37 K. Onitsuka, H. Ogawa, T. Joh, S. Takahashi, *Chem. Lett.* **1988**, 1855.

38 K. A. Bunten, A. K. Kakkar, *Macromolecules* **1996**, *29*, 2885.

39 W. Y. Wong, S. M. Chan, K. H. Choi, K. W. Cheah, W. K. Chan, *Macromol. Rapid Commun.* **2000**, *21*, 453.

40 M. O. Wolf, *Adv. Mater.* **2001**, *13*, 545.

41 Y. Zhu, D. B. Millet, M. O. Wolf, S. J. Rettig, *Organometallics* **1999**, *18*, 1930.

42 Y. Fujikura, K. Sonogashira, N. Hagihara, *Chem. Lett.* **1975**, 1067.

43 J. Manna, K. D. John, M. D. Hopkins, *Adv. Organomet. Chem.* **1995**, *38*, 79.

44 Z. Atherton, C. W. Faulkner, S. L. Ingham, A. K. Kakkar, M. S. Khan, J. Lewis, N. J. Long, P. R. Raithby, *J. Organomet. Chem.* **1993**, *462*, 265.

45 P. Chow, D. Zargarian, N. J. Taylor, T. B. Marder, *Chem. Commun.* **1989**, 1545.

46 W. Y. Wong, G. L. Lu, K. F. Ng, K. H. Choi, Z. Lin, *J. Chem. Soc., Dalton Trans.* **2001**, 3250.

47 M. S. Khan, M. R. A. Al-Mandhary, M. K. Al-Suti, N. Feeder, S. Nahar, A. Köhler, R. H. Friend, P. J. Wilson, P. R. Raithby, *J. Chem. Soc., Dalton Trans.* **2002**, 2441.

48 M. S. Khan, M. R. A. Al-Mandhary, M. K. Al-Suti, A. K. Hisahm, P. R. Raithby, B. Ahrens, M. F. Mahon, L. Male, E. A. Marseglia, E. Tedesco, R. H. Friend, A. Köhler, N. Feeder, S. J. Teat, *J. Chem. Soc., Dalton Trans.* **2002**, 1358.

49 M. J. Duer, M. S. Khan, A. K. Kakkar, *Solid State Nucl. Magn. Reson.* **1992**, *1*, 13.

50 A. E. Dray, F. Wittmann, R. H. Friend, A. M. Donald, M. S. Khan, J. Lewis, B. F. G. Johnson, *Synth. Met.* **1991**, *41-43*, 871.

51 A. E. Dray, R. Rachel, W. O. Saxton, J. Lewis, M. S. Khan, A. M. Donald, R. H. Friend, *Macromolecules* **1992**, *25*, 3473.

52 D. L. Lichtenberger, S. K. Renshaw, A. Wong, C. D. Tagge, *Organometallics* **1993**, *12*, 3522.

53 D. L. Lichtenberger, S. K. Renshaw, R. M. Bullock, *J. Am. Chem. Soc.* **1993**, *115*, 3276.

54 J. N. Louwen, R. Hengelmolen, D. M. Grove, A. Oskam, R. L. DeKock, *Organometallics* **1984**, *3*, 908.

55 N. M. Kostic, R. F. Fenske, *Organometallics* **1982**, *1*, 974.

56 G. Frapper, M. Kertesz, *Inorg. Chem.* **1993**, *32*, 732.

57 O. Lhost, J. M. Toussaint, J. L. Bredas, H. F. Wittmann, K. Fuhrmann, R. H. Friend, M. S. Khan, J. Lewis, *Synth. Met.* **1993**, *55–57*, 4525.

58 R. D. Markwell, I. S. Butler, A. K. Kakkar, M. S. Khan, Z. H. Al-Zakwani, J. Lewis, *Organometallics* **1996**, *15*, 2331.

59 M. Motowoka, T. Norisuye, A. Teramoto, H. Fujita, *Polym. J.* **1979**, *11*, 665.

60 A. Abe, N. Kimura, S. Tabata, *Macromolecules* **1991**, *24*, 6238.

61 S. Takahashi, E. Murata, M. Kariya, K. Sonogashira, N. Hagihara, *Macromolecules* **1979**, *12*, 1016.

62 S. Takahashi, H. Morimoto, Y. Takai, K. Sonogashira, N. Hagihara, *Mol. Cryst. Liq. Cryst.* **1981**, *72*, 101.

63 S. Takahashi, Y. Takai, H. Morimoto, K. Sonogashira, N. Hagihara, *Mol. Cryst. Liq. Cryst.* **1982**, *82*, 139.

64 S. Takahashi, Y. Takai, H. Morimoto, K. Sonogashira, *Chem. Commun.* **1984**, 3.

65 B. F. G. Johnson, A. K. Kakkar, M. S. Khan, J. Lewis, A. E. Dray, R. H. Friend, F. Wittmann, *J. Mater. Chem.* **1991**, *1*, 485.

66 H. F. Wittmann, K. Fuhrmann, R. H. Friend, M. S. Khan, J. Lewis, *Synth. Met.* **1993**, *55–57*, 56.

67 M. S. Khan, A. K. Kakkar, N. J. Long, J. Lewis, P. Raithby, P. Nguyen, T. B. Marder, F. Wittmann, R. H. Friend, *J. Mater. Chem.* **1994**, *4*, 1227.

68 N. Chawdhury, A. Köhler, R. H. Friend, W. Y. Wong, J. Lewis, M. Younus, P. R. Raithby, T. C. Corcoran, M. R. A. Al-Mandhary, M. S. Khan, *J. Chem. Phys.* **1999**, *110*, 4963.

69 (a) W. Y. Wong, C. K. Wong, G. L. Lu, K. W. Cheah, J. X. Shi, Z. Lin, *J. Chem. Soc., Dalton Trans.* **2002**, *24*, 4587; (b) W. Y. Wong, C. K. Wong, G. L. Lu, A. W. M. Lee, K. W. Cheah, J. X. Shi, *Macromolecules* **2003**, *36*, 983.

70 M. Younus, A. Köhler, S. Cron, N. Chawdhury, M. R. A. Al-Mandhary, M. S. Khan, J. Lewis, N. J. Long, R. H. Friend, P. R. Raithby, *Angew. Chem. Int. Ed.* **1998**, *37*, 3036.

71 W. Y. Wong, W. K. Wong, P. R. Raithby, *J. Chem. Soc., Dalton Trans.* **1998**, 2761.

72 N. Tessler, G. J. Denton, R. H. Friend, *Nature* **1996**, *382*, 695.

73 G. Yu, J. Gao, J. C. Hummelen, F. Wudl, A. J. Heeger, *Science* **1995**, *270*, 1741.

74 A. Kraft, A. C. Grimsdale, A. B. Holmes, *Angew. Chem. Int. Ed.* **1998**, *37*, 402.

75 D. Belijonne, H. F. Wittmann, A. Köhler, S. Graham, M. Younus, J. Lewis, P. R. Raithby, M. S. Khan, R. H. Friend, J. L. Brédas, *J. Chem. Phys.* **1996**, *105*, 3868.

76 J. S. Wilson, A. Köhler, R. H. Friend, M. K. Al-Suti, M. R. A. Al-Mandhary, M. S. Khan, P. R. Raithby, *J. Chem. Phys.* **2000**, *113*, 7627.

77 N. Chawdhury, A. Köhler, R. H. Friend, M. Younus, N. J. Long, P. R. Raithby, J. Lewis, *Macromolecules* **1998**, *31*, 722.

78 (a) J. S. Wilson, N. Chawdhury, M. R. A. Al-Mandhary, M. Younus, M. S. Khan, P. R. Raithby, A. Köhler, R. H. Friend, *J. Am. Chem. Soc.* **2001**, *123*, 9412; (b) A. Köhler, J. S. Wilson, R. H. Friend, M. K. Al-Suti, M. S. Khan, A. Gerhard, H. Bässler, *J. Chem. Phys.* **2002**, *116*, 9457.

79 W. Y. Wong, G. L. Lu, K. H. Choi, J. X. Shi, *Macromolecules* **2002**, *35*, 3506.

80 N. J. Long, *Angew. Chem. Int. Ed. Engl.* **1995**, *34*, 21.

81 C. C. Frazier, S. Guha, W. P. Chen, M. P. Cockerham, P. L. Porter, E. A. Chauchard, C. H. Lee, *Polymer* **1987**, *28*, 553.

82 *Nonlinear Optical Properties of Organic Materials*, Proc. SPIE No. 971, The International Society for Optical Engineering, Washington DC, **1988**, p. 186.

83 C. C. Frazier, E. A. Chauchard, M. P. Cockerham, P. L. Porter, *Mat. Res. Soc. Symp. Proc.* **1988**, *109*, 323.

84 S. Guha, C. C. Frazier, P. L. Porter, K. Kang, S. E. Finberg, *Opt. Lett.* **1989**, *14*, 952.

85 *Organic Molecules for Nonlinear Optics and Photonics* (Eds.: J. Messier, F. Kajzar, P. Prasad), NATO ASI Series E, vol 194, Kluwer Academic, Dordrecht, **1991**, p 391.

86 W. J. Blau, H. J. Byrne, D. J. Cardin, A. P. Davey, *J. Mater. Chem.* **1991**, *1*, 245.

87 A. P. Davey, H. Page, W. Blau, H. J. Byrne, D. J. Cardin, *Synth. Met.* **1993**, *55–57*, 3980.

88 H. Nishihara, in *Handbook of Organic Conductive Molecules and Polymers, Vol. 2: Conductive Polymers: Synthesis and Electrical Properties* (Ed.: H. S. Nalwa), Wiley, New York, **1997**, p. 799.

89 H. Matsuda, H. Nakanishi, M. Kato, *J. Polym. Sci., Polym. Lett.* **1984**, *22*, 107.

90 A. Ohkubo, K. Aramaki, H. Nishihara, *Chem. Lett.* **1993**, 271.

91 I. Tomita, A. Nishio, T. Igarashi, T. Endo, *Polym. Bull.* **1993**, *30*, 179.

92 I. L. Rozhanskii, I. Tomita, T. Endo, *Macromolecules* **1996**, *29*, 1934.

93 T. Shimura, A. Ohkubo, N. Matsuda, I. Matsuoka, K. Aramaki, H. Nishihara, *Chem. Mater.* **1996**, *8*, 1307.

94 I. Matsuoka, K. Aramaki, H. Nishihara, *J. Chem. Soc., Dalton Trans.* **1998**, 147.

95 M. Murata, T. Hoshi, I. Matsuoka, T. Nankawa, M. Kurihara, H. Nishihara, *J. Inorg. Organomet. Polym.* **2000**, *10*, 209.

96 I. Matsuoka, H. Yoshikawa, M. Kurihara, H. Nishihara, *Synth. Met.* **1999**, *102*, 1519.

97 I. Matsuoka, H. K. Aramaki, H. Nishihara, *Mol. Cryst. Liq. Cryst.* **1996**, *285*, 199.

98 I. Tomita, A. Nishio, T. Endo, *Macromolecules* **1995**, *28*, 3042.

99 I. Tomita, A. Nishio, T. Endo, *Macromolecules* **1994**, *27*, 7009.

100 I. Tomita, A. Nishio, T. Endo, *Appl. Organomet. Chem.* **1998**, *12*, 735.

101 S. S. H. Mao, T. D. Tilley, *Macromolecules* **1997**, *30*, 5566.

102 S. S. H. Mao, T. D. Tilley, *J. Am. Chem. Soc.* **1995**, *117*, 5365.

103 S. S. H. Mao, T. D. Tilley, *J. Organomet. Chem.* **1996**, *521*, 425.

104 B. L. Lucht, S. S. H. Mao, T. D. Tilley, *J. Am. Chem. Soc.* **1998**, *120*, 4354.

105 K. C. Sturge, A. D. Hunter, R. McDonald, B. D. Santarsiero, *Organometallics* **1992**, *11*, 3056.

106 X. A. Guo, K. C. Sturge, A. D. Hunter, M. C. Williams, *Macromolecules* **1994**, *27*, 7825.

107 P. S. Wolfe, F. J. Gomez, K. B. Wagener, *Macromolecules* **1997**, *30*, 714.

108 G. Jia, W. F. Wu, R. C. Y. Yeung, H. P. Xia, *J. Organomet. Chem.* **1997**, *539*, 53.

109 T. P. Pollagi, S. J. Geib, M. D. Hopkins, *J. Am. Chem. Soc.* **1994**, *116*, 6051.

110 K. D. John, M. D. Hopkins, *Chem. Commun.* **1999**, 589.

6
Polymers with Metal-Metal Bonds in the Main Chain

6.1
Introduction

The remarkable properties of high molecular weight polysilanes **6.1** and polygermanes **6.2**, which were first prepared in the late 1970s and early 1980s by Wurtz coupling procedures (Eq. 6.1), have led to considerable interest in the development of polymer chains based on the heavier Group 14 element, tin, as well as other metals [1–4]. To appreciate the reasons for the interest in polymers containing metal-metal bonds in the backbone, it is very useful to first consider some of the unique features of polysilanes, which have now been thoroughly studied.

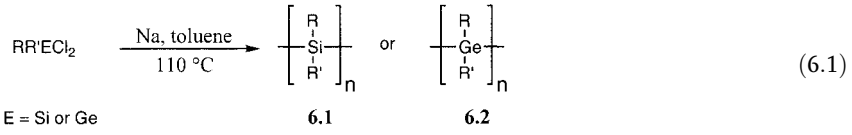

(6.1)

One of the most novel characteristics of the all-silicon backbone in polysilanes is that it possesses delocalized σ-electrons, a phenomenon that is virtually unknown in carbon chemistry [3, 5–8]. This can be understood in terms of the nature of the molecular orbitals associated with the Si–Si σ-bonds. These are more diffuse than those associated with C–C σ-bonds as they are constructed from higher energy 3s and 3p atomic orbitals and silicon is less electronegative than carbon. This leads to significant interactions between the adjacent Si–Si σ-bonds along a polysilane chain, a situation analogous to that for the π-bonds in π-delocalized polymers such as polyacetylene. Thus, a band model, rather than a localized model, is more appropriate for these catenated structures [3, 8]. As a consequence of the delocalization of σ-electrons, the σ-σ^* transition that occurs at around 220 nm in $Me_3Si–SiMe_3$ moves to lower energy as the number of silicon atoms in the chain increases. In the high polymers, the σ-σ^* band-gap transitions occur in the near-UV region, at ca. 300–400 nm [2, 3, 8, 9]. The electron delocalization also leads to appreciable electrical conductivity upon doping. For example, conductivities of up to 0.5 S cm^{-1} have been reported after doping with AsF_5 [8]. In addition, many of the polymers are thermochromic, as the conformations that they

Synthetic Metal-Containing Polymers. Ian Manners

ISBN: 3-527-29463-5

adopt change with temperature and consequently alter the degree of σ-delocalization along the main chain. Due to their low-energy σ-σ^* transitions, polysilanes are photosensitive and have attracted considerable attention as photoresist materials in microlithography [3, 8]. Polygermanes **6.2** appear to possess even more extensive σ-delocalization than polysilanes and the σ-σ^* band-gap transition for the high polymers is significantly red-shifted, by ca. 20 nm, in comparison to the silicon analogues [10–12].

6.2 Polystannanes

6.2.1 Oligostannanes

The preparation of cyclic and linear catenated structures based on tin atoms has attracted significant attention in the literature, and prior to 1990 a range of oligomers and remarkable clusters were reported [13, 14]. Because of the lower electronegativity of Sn compared to Si and Ge, polystannanes would be expected to possess even more σ-delocalized structures and have therefore been regarded as a very desirable synthetic target [13–15]. Important work that underlined the potential significance of high polymeric polystannanes was carried out in 1987 [13]. Researchers successfully prepared linear oligostannanes **6.3**, with three to six catenated tin atoms (x=1–4), by a salt-elimination procedure (Eq. 6.2).

(6.2)

6.3
x = 1–4

Each of the discrete oligomers was characterized by single-crystal X-ray diffraction, and the structures are shown in Fig. 6.1. The Sn–Sn bond lengths varied in the range 2.80–2.97 Å, and each oligomer was shown to possess a *trans*-planar conformation.

Most interestingly, studies of the discrete oligomers by UV/vis spectroscopy showed that the σ-σ^* transition moves dramatically to lower energy as the chain length is increased (Fig. 6.2). Indeed, whereas the trimer **6.3** (x=1) is colorless, the linear hexamer **6.3** (x=4) is yellow. The spectroscopic evidence for the formation of a band structure, in a manner similar to the well-known decrease in HOMO-LUMO gap with increasing chain length for π-conjugated materials, led to the proposed term "molecular metals" for these oligomers and prospective high molecular weight analogues [13].

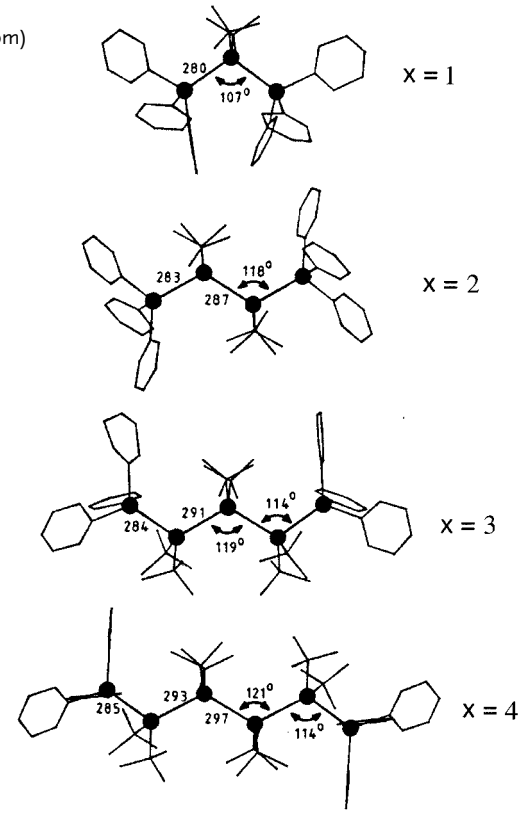

Fig. 6.1 X-ray structures of oligostannanes **6.3** with $x=1$–4. Bond lengths (pm) and angles (°) are indicated. (Adapted from [13])

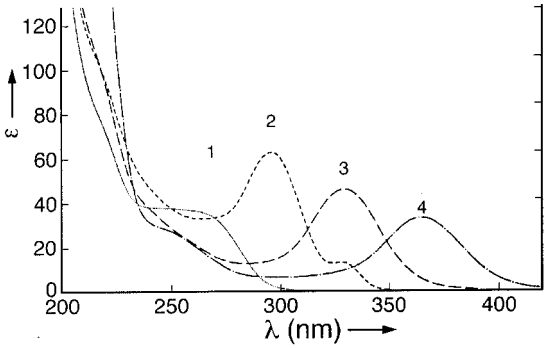

Fig. 6.2 UV/vis spectra of oligostannanes **6.3** with three to six tin atoms ($x=1$–4). (Adapted from [13])

6.2.2
Polystannane High Polymers

Prior to the early 1990s, attempts to generate high molecular weight polystannanes by Wurtz coupling were unsuccessful and yielded only low molecular weight oligomers and reduction products. The lack of success compared with the corresponding silicon and germanium polymers was attributed to the relative ease of reduction of Sn^{IV} and the weakness of the Sn–Sn bond. The key breakthrough in this area was reported in 1993, when it was shown that transition metal-catalyzed dehydrogenative coupling reactions, which had been extensively applied to the synthesis of polysilanes, could be applied to secondary stannanes R_2SnH_2 (Eq. 6.3) [16]. Yellow poly(dialkylstannane)s **6.4** (e.g. R = *n*-butyl, *n*-hexyl, or *n*-octyl) of substantial molecular weight (up to $M_n \approx 22{,}000$) were prepared with the aid of various zirconium catalysts. These materials indeed possess extensively delocalized σ-electrons, as illustrated by the band-gap σ-σ^* transition that occurs at 384–388 nm (in THF). In addition, exposure of thin films of the polymers to the oxidant AsF_5 leads to significant electronic conductivities of ca. 0.01–0.3 Scm^{-1} [17].

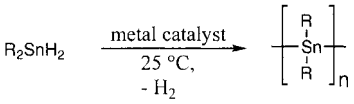

(6.3)

6.4

Even smaller band gaps are present in polystannanes with aryl substituents at tin [18, 19]. For example, dehydropolymerization of R_2SnH_2 (R = *p*-^{t}BuC$_6$H$_4$ or *p*-^{n}HexC$_6$H$_4$) afforded linear polymers (contaminated with some cyclics) with M_n values up to 20,000. The materials, which are also yellow in color, possess λ_{max} values for the Sn σ-σ^* transition of 423–436 nm; this represents a red-shift by 30–40 nm compared to the values for poly(dialkylstannane)s and is suggestive of significant σ-π conjugation involving the Sn backbone and the aryl substituents.

The proposed mechanism for the formation of the polystannanes involves σ-bond metathesis and is thought to be analogous to that for the catalytic dehydrocoupling route to polysilanes from primary silanes $RSiH_3$. The Zr precatalyst is believed to generate a metal hydride species that participates in a step-growth process that involves four-centered transition states (Scheme 6.1) [17].

Highly branched polystannane materials have been prepared by a dehydropolymerization/rearrangement process [20]. Whereas Ti and Zr metallocene precatalysts afford linear polystannanes by dehydropolymerization of ^{n}Bu$_2$SnH$_2$, the Rh^I complex RhH(CO)(PPh$_3$)$_3$ was found to react to afford either cyclic oligomers or branched polymers, depending upon the reaction conditions. The dark-yellow, gummy polymer formed, **6.4** (R = ^{n}Bu) ($M_n = 3.5 \times 10^4$, PDI = 1.4), was shown to possess a branched structure by ^{119}Sn NMR, and by analysis of the cleavage products obtained after treatment with I_2 followed by PhMgBr, which included BuSnPh$_3$ as well as Bu$_2$SnPh$_2$. As a result of the branching, the λ_{max} in the UV/vis spectrum of the material (in pentane) was 394 nm, slightly but significantly

Scheme 6.1

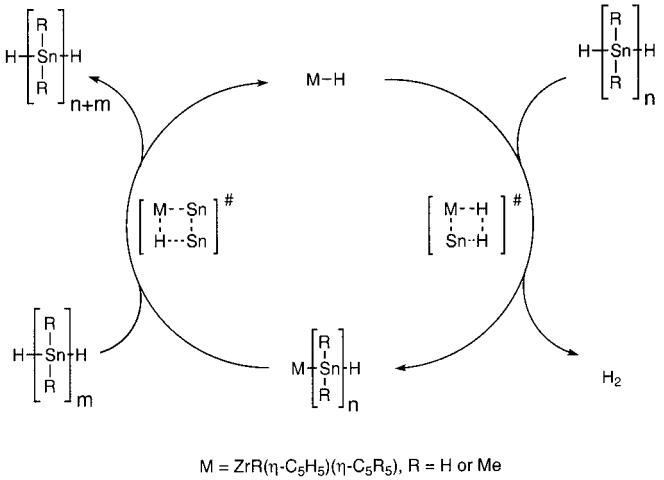

Table 6.1 UV/vis and GPC molecular weight data for selected polystannanes **6.4** (R = alkyl or aryl) formed by means of dehydrocoupling

R	*Dehydrocoupling precatalyst* [a]	λ_{max} *(nm, 25 °C)* [b]	M_n [c]	*PDI* [c]	*Ref.*
^{n}Bu	$Me_2CCp'_2ZrMe(Si(SiMe_3)_3)$	384 (THF)	2.0×10^4	3.3	17
^{n}Bu	Cp_2ZrMe_2	–	1.4×10^4	3.3	17
^{n}Bu	$CpCp^*ZrMe_2$	–	1.3×10^4	5.6	17
^{n}Bu	$CpCp^*ZrMe(Si(SiMe_3)_3)$	–	7.8×10^3	2.2	17
^{n}Bu	$RhH(CO)(PPh_3)_3$	394 (pentane) [d]	3.5×10^3	1.4	20
^{n}Hex	$CpCp^*ZrMe(Si(SiMe_3)_3)$	384 (THF)	1.5×10^4	2.4	17
^{n}Oct	$CpCp^*ZrMe(Si(SiMe_3)_3)$	–	1.4×10^4	6.7	17
^{n}Oct	Cp_2ZrMe_2	388 (THF)	2.1×10^4	4.3	17
p-^{t}BuC_6H_4	Cp_2ZrMe_2	432 (THF)	1.5×10^4	1.35	18
p-^{n}HexC_6H_4	Cp_2ZrMe_2	436 (THF)	2.0×10^4	2.4	18

a) Cp = (η-C_5H_5), Cp* = (η-C_5Me_5), Cp′ = (η-C_5H_4), reaction conditions vary; consult reference for details.
b) Limiting values for polymers with $M_n > 1\times10^4$.
c) Obtained from GPC analysis of polymer in THF relative to polystyrene standards; $PDI = M_w/M_n$.
d) Branched polymer.

red-shifted from that of linear poly(di-*n*-butylstannane) (λ_{max} = 378–380 nm in the same solvent). The branched material was reported to possess greater stability to air-oxidation and light in the solid state than the linear polymeric analog. A representative list of selected polystannanes prepared by means of dehydrocoupling procedures is compiled in Table 6.1.

Careful reinvestigations of Wurtz coupling procedures have now also successfully led to the isolation of high molecular weight polystannanes. The first detailed report of the preparation of polystannanes by Wurtz coupling in a refereed journal was

published in 1996 [21]. Poly(di-*n*-butylstannane) was prepared from the reaction of $^{n}Bu_2SnCl_2$ with a sodium dispersion in toluene, in the presence of 15-crown-5 at 60 °C in the dark (Eq. 6.4). The maximum yield of polymer was reached after 4 h and very high molecular weight material was formed ($M_n > 10^6$). Prolonged reaction times gave rise to chain scission. The spectroscopic data were consistent with the earlier reports on the same polymer formed by means of the dehydrocoupling route. Electrochemical reduction of dialkyldichlorostannanes $^{n}Bu_2SnCl_2$ and $^{n}Oct_2SnCl_2$ has also been reported, and affords moderate molecular weight polystannanes **6.4** (R = ^{n}Bu or ^{n}Oct) with $M_n = 3.5–5.6 \times 10^3$ (PDI = 1.3–2.6) [22].

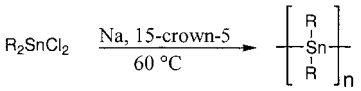

(6.4)

6.4

The σ-delocalization in polystannanes has attracted significant theoretical interest [15, 23]. Recent synthetic methods have permitted access to oligostannanes **6.5** with 3–15 catenated tin atoms [23, 24]. The Sandorfy C model, which regards the polystannane backbone as a linear chain of interacting sp^3 hybrid orbitals, allows for an excellent degree of correlation between the experimental and calculated σ-σ^* transition energies with increasing chain length [23].

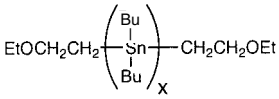

6.5
x = 3—15

In the Sandorfy C model, the degree of delocalization can be appreciated by consideration of the ratio β_{gem}/β_{vic} of the resonance integrals β for geminal (same atom) and vicinal (adjacent atom) interactions (Fig. 6.3). In the case of perfect delocalization, the ratio β_{gem}/β_{vic} would be unity, whereas perfect localization of electrons would correspond to a value of zero [3]. A resonance integral ratio $\beta_{gem}/\beta_{vic} = 0.75$ has been calculated for polystannanes from this data, which indicates that polystannanes possess substantial delocalization of σ-electrons in the tin chain [23].

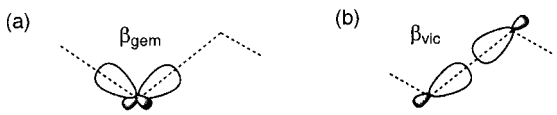

Fig. 6.3 Resonance integrals β for **(a)** geminal and **(b)** vicinal overlap of sp^3-hybridized orbitals.

Band structure calculations have also been reported for hypothetical polystannanes **6.4** (R = R′ = H), and the results have been compared with those for analogous polysilanes and polygermanes [15]. The band gap (E_g) was calculated to decrease in the

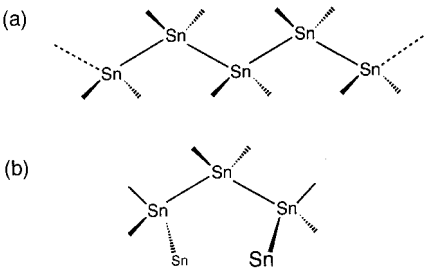

Fig. 6.4 Polystannane conformations: **(a)** *trans*-planar and **(b)** *gauche*-helical.

Table 6.2 Calculated band parameters for polystannane $[SnH_2]_n$ (**6.4** R=H) and analogous Group 14 polymers $[SiH_2]_n$ (**6.1** R=R′=H) and $[GeH_2]_n$ (**6.2**) (R=R′=H)

Polymer	*Conformation*	*Band gap E_g (eV)*	*Effective hole mass at valence band edge m_n^{*} a)*	*Effective electron mass at conduction band edge m_e^{*} a)*	*Ref.*
$[CH_2]_n$	*trans* planar	–	0.21	–	5
$[CH=CH]_n$	*trans* planar	–	0.12	–	5
$[SiH_2]_n$	*trans* planar	3.89 b)	0.14	0.10	15
	gauche helical	5.94 c)	7.84	0.88	15
$[GeH_2]_n$	*trans* planar	3.31 b)	0.13	0.10	15
	gauche helical	5.13 c)	5.39	0.57	15
$[SnH_2]_n$	*trans* planar	2.80 b)	0.12	0.09	15
	gauche helical	4.65 c)	9.66	2.32	15

a Units are in mass of a free electron m_e.
b Direct band gap.
c Indirect band gap.

order Si > Ge > Sn for the *trans*-planar and *gauche*-helical structures (Table 6.2, Fig. 6.4). The degree of delocalization was calculated to be much greater in the *trans*-planar configuration than in the *gauche*-helical conformation. This is illustrated in Fig. 6.5, which shows the calculated band structures in each case. The band dispersion (or band width) is noticeably less in the case of the *gauche*-helical structures. Direct band gaps exist in those cases where the polymers adopt a *trans*-planar conformation.

Based on further calculations, the intriguing possibility of gaining access to a metallic state for polystannanes appears to exist, in which the valence band and conduction band overlap. This might be achieved if, for example, pressure is used to widen the bond angles along the polymer main chain to greater than ca. 150°. This bond angle is significantly greater than the value found in linear hexamers such as **6.3** ($x=4$), in which the skeletal Sn–Sn–Sn angles are 114 and 121°.

A significant drawback with regard to the practical application of polystannanes is their air- and moisture sensitivity. This is not so severe in the solid state, but the materials are appreciably sensitive in solution. Nevertheless, the properties of these

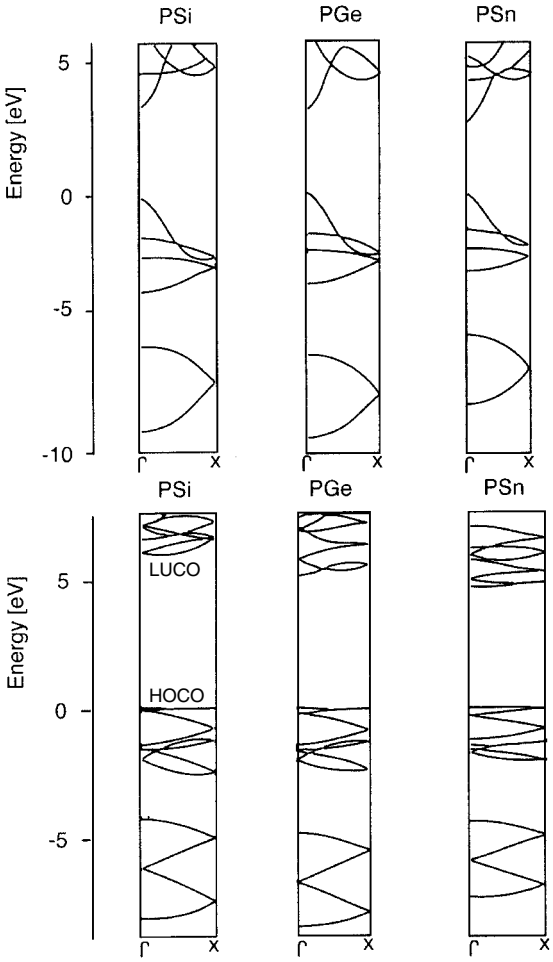

Fig. 6.5 Band structures for polysilanes (PSi), polygermanes (PGe), and polystannanes (PSn) (top, *trans*-planar conformation; below, *gauche*-helical conformation). (Adapted from [15])

fascinating materials are under detailed scrutiny [25]. The polymers are reasonably thermally stable up to ca. 270 °C; polystannane **6.4** (R = *p*-^{t}BuC$_6$H$_4$) yields tin metal when heated under nitrogen to 400 °C, and tin oxides when heated in air, with a decomposition onset of around 225 °C. Polystannanes are highly photosensitive and exhibit photobleaching behavior and, upon UV-irradiation, depolymerize to yield cyclic oligomers (Fig. 6.6). Green fluorescence has also been reported for polystannane **6.4** (R = ^{n}Bu) after UV excitation [16]. The dependence of the degree of σ-conjugation on conformation is expected to be significant based on work on polysilanes, and it is likely that the smallest band gaps for these materials have yet to be achieved.

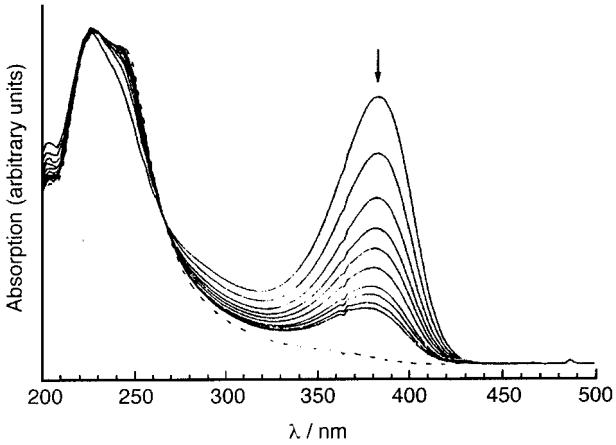

Fig. 6.6 Photobleaching of polystannane (**6.4** R=*n*-Bu) in pentane upon irradiation by room light. Measurements were taken every 30 s. The final spectrum is given by the dotted line. (Adapted from [16])

6.3 Polymers Containing Main-Chain Metal-Metal Bonds That Involve Transition Elements

Polymers that contain covalent metal-metal bonds in the polymer backbone might be expected to possess novel conductive and photochemical properties. This is an area in which considerable synthetic challenges must be overcome if progress is to be made. In general, comparatively little work has been carried out so far, but the area is so intriguing that the efforts made are of particular note.

In 1989, polycondensation routes to polyurethanes that contain Mo–Mo bonds (**6.6**, R=urethane linkage) or Fe(μ-CO)$_2$Fe units (**6.7**) in the polymer backbone were reported (Eq. 6.5) [26–29]. Polyurea and polyamide analogues and poly(ether urethane) copolymers with Mo–Mo and Fe–Fe bonds in the polymer backbone were also reported by the same group [30–32]. These materials were generally of low molecular weight, with M_n values usually less than 10,000. For example, different samples of the red, powdery material **6.6** possessed M_n=4800–6000 (by vapor-pressure osmometry), which corresponds to ca. six to eight repeat units, whereas **6.7**, a red-brown powder, possessed an M_n value of only 1500, which corresponds to two to three repeat units [28]. Despite the low molecular weights, the polymers are of interest as photoreactive materials, as the metal-metal bonds can be cleaved photochemically by visible light. In contrast, conventional polymers generally require ultraviolet light for photodegradation.

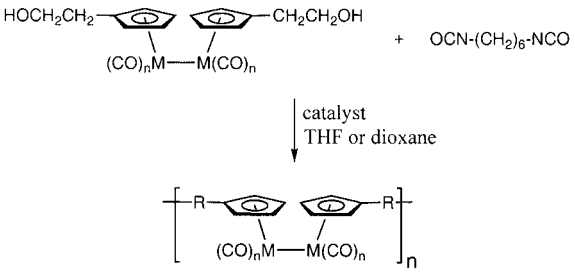

(6.5)

6.6 $(CO)_nM\text{-}M(CO)_n$ = $(CO)_3Mo—Mo(CO)_3$

6.7 $(CO)_nM\text{-}M(CO)_n$ = 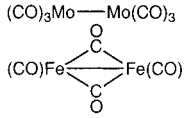

As mentioned above, the M–M-bonded polymers are of interest as photochemically labile materials (Scheme 6.2). The quantum yields for the photodegradation of these polymers, and model complexes, decrease as the chain length is increased. This effect has been observed in other polymer systems and several explanations are possible. One invokes the theory that radiationless decay is faster in molecules with more vibrational modes and that this would thus lower the quantum yield for the formation of requisite radical cage pair as the chains get longer [32, 33].

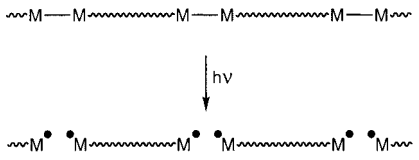

Scheme 6.2

Studies of a series of polymers containing Mo–Mo bonds showed that both light and oxygen were necessary for degradation to take place in the solid state [28–31]. Oxygen was found to react with the metal radicals produced by irradiation, otherwise the M–M bonds reformed by radical recombination. Studies of materials **6.8** with chlorine atoms that can act as "built-in" radical traps showed that photochemical degradation occurs over 5 days upon irradiation under nitrogen, and IR spectroscopy revealed the appearance of bands characteristic of $CpMo(CO)_3Cl$ units [31]. Nevertheless, the photodegradation was still found to be faster in air, presumably due to the higher concentration of oxygen radical trap present.

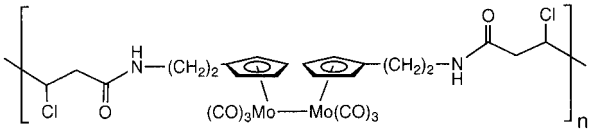

6.8

The synthesis of a further class of polymers with cyclopentadienylirondicarbonyl dimer units in the backbone has been described [34]. These materials possess organosiloxane spacers and were prepared by condensation reactions, as illustrated for the case of **6.9** (Eq. 6.6).

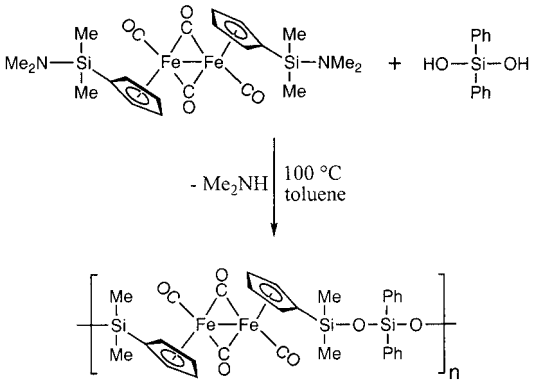

(6.6)

6.9

The materials were of low to medium molecular weight (M_n = 4000–13,500) and showed very interesting electrochemical behavior. Studies of model compounds showed that upon reduction or oxidation the Fe–Fe bond is cleaved. The polymers, on the other hand, show reversible two-electron oxidation processes in THF/[^{n}Bu$_4$N][BF$_4$] at fast scan rates, as the Fe–Fe bonds reform after cleavage due to the fact that Fe atoms are held in close proximity by the bridging organosiloxane units.

Polymers with Pt–Pt bonds as part of the polymer main chain have also been reported (Eq. 6.7) [35, 36]. These yellow materials (e.g. **6.10**) are particularly interesting as they possess conjugated rigid-rod structures, but are essentially insoluble or are only sparingly soluble in organic solvents; studies to date have been comparatively limited in scope. Analogues of **6.10** with diphosphine spacers, as well as neutral analogues with acetylide spacers, have also been prepared and were also found to be insoluble in common solvents [36].

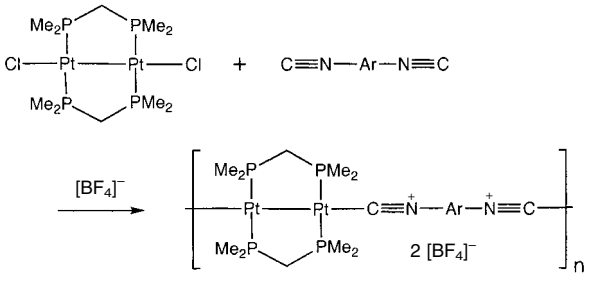

(6.7)

6.10

The successful synthesis of a series of soluble polymers with varying degrees of metal-metal interactions has been achieved by the use of chelating isocyanide ligands [37, 38]. The reaction of linear Pt_4 isocyanide-bridged complexes with difunctional diphosphines $Ph_2P–(CH_2)_x–PPh_2$ (x=4–6) yielded orange-red amorphous soluble polymers **6.11** with molecular weights (M_w) estimated to be in the range 8.4×10^4–3.1×10^5 [39]. Extended Hückel calculations suggest that the HOMO and LUMO of polymer **6.11** are both dσ* orbitals that arise from the four interacting Pt atoms, and the major low-energy UV/vis band at ca. 394 nm in EtOH, that is analogous to that for a Pt_4 monomer complex with PPh_3 end groups (λ_{max}=405 nm), was assigned to dσ*-dσ* transitions. Studies of a model complex suggest that the Pt–Pt bond order is around 0.5. Although the materials **6.11** were not luminescent at room temperature after photoexcitation, phosphorescent emission was detected at 77 K [39].

Related materials with Ag (**6.12**) or Cu (**6.13**) atoms in the main chain have been prepared by reaction of the respective metal salts with the diisocyanide. The white Ag materials were found to be rather insoluble, and soluble fractions appeared to be only oligomeric in nature. However, for the yellow-beige Cu polymers, molecular weights (M_w) of up to 1.6×10^5 were measured by static light-scattering techniques in MeCN [40–42]. These materials were also found to show no luminescence at room temperature, but intense blue emissions were detected at 77 K. Detailed analysis of the emission, and comparison with that of monomeric species, provided evidence for the existence of significant M–M interactions along the polymer main chain for both **6.12** and **6.13** [40].

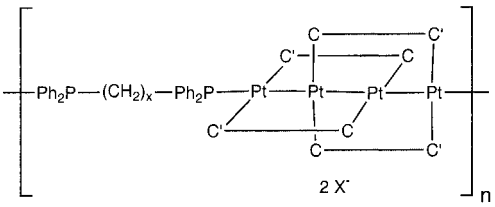

6.11

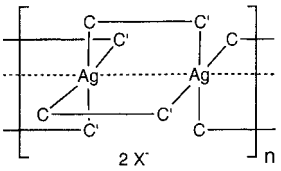

6.12

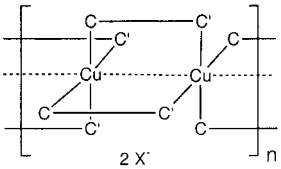

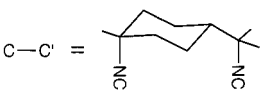

6.13

A range of very exciting "metal string" complexes has been prepared, in which a series of metal-metal bonds is present. An example is the remarkable heptanickel complex $Ni_7L_4Cl_2$ (**6.14**) where L is a heptadentate amidopyridine ligand

that binds to the metal atoms as depicted in Fig. 6.7 [43]. Compound **6.14** was prepared by the reaction of $NiCl_2$ with the diprotonated ligand, H_2L, in the presence of the base K[O^{t}Bu]. The X-ray structure of **6.14** is shown in Fig. 6.8; the penta-nickel and cobalt analogues of this species have also been prepared [44].

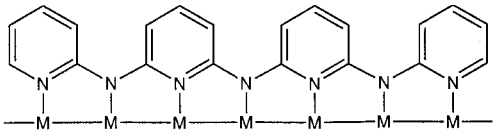

Fig. 6.7 Depiction of the heptadentate ligand L present in the structure of **6.14**.

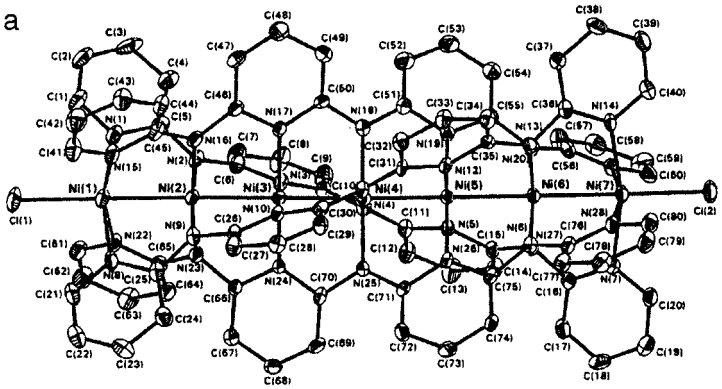

6.14

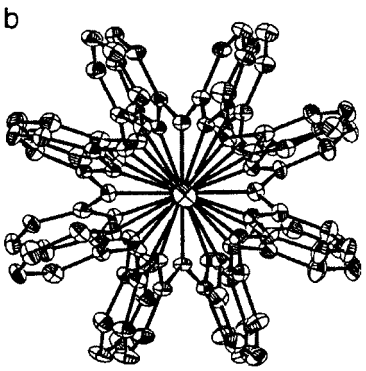

Fig. 6.8 Molecular structure of $Ni_7L_4Cl_2$ (**6.14**) determined by X-ray diffraction: **(a)** side view and **(b)** view along Ni–Ni axis. (Adapted from [43])

Polymers that contain bonds between main group metals and transition elements represent an area that is at a very early stage of development and the challenges associated with the synthesis of high polymeric materials are substantial. Nevertheless, glimpses of the possibilities can be found in some linear and cyclic oligomers that have been prepared as model systems for prospective high polymeric analogues. For example, the hexametallic dimer **6.15** has been synthesized (Eq. 6.8) as a model for analogous high polymers [45].

$$Na_2[\{Fe(CO)_2(\eta\text{-}C_5H_4)\}_2CH_2] + 2\ (\eta\text{-}C_5H_5)(CO)_2Fe\text{-}SnPh_2Cl \longrightarrow \textbf{6.15} \tag{6.8}$$

Attempts to prepare analogous polymers **6.16** have been briefly reported and have led to CH_2Cl_2-soluble materials with $M_n = 8500$ when osmometry was used for molecular weight measurements (Eq. 6.9) [46].

$$Na_2[\{Fe(CO)_2(\eta\text{-}C_5H_4)\}_2X_2] + Ph_2SnCl_2 \longrightarrow \textbf{6.16}\quad X = CH(NMe_2) \tag{6.9}$$

A remarkable 12-membered ring, $[Os(CO)_4SnPh_2]_6$ (**6.17**), has been isolated from the reaction of $Na_2[Os(CO)_4]$ with Ph_2SnCl_2, and has been characterized by X-ray crystallography (Fig. 6.9 a) [47]. Polymeric analogues with this type of catenated structure would clearly be fascinating to study and do indeed exist in the case of $[Fe(CO)_4BiR]_n$ ($R = {}^n Bu$) (**6.18**), at least in the solid state (Fig. 6.9 b) [48].

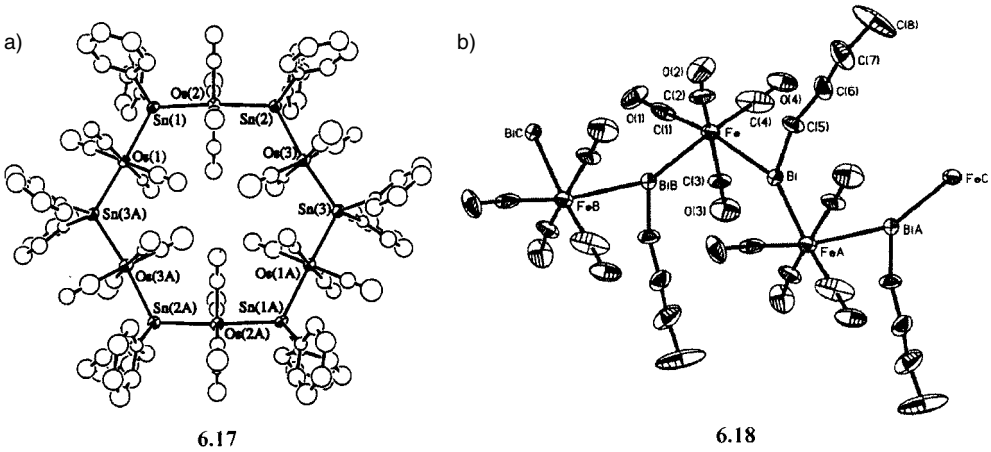

6.17 6.18

Fig. 6.9 X-ray structures of **(a) 6.17** and **(b)** a segment of polymer **6.18**. (Reproduced from [47] and [48])

We conclude this section with a mention of another area of considerable interest and future potential. It concerns the synthesis and study of soluble polymers that contain metal-metal multiple bonds in the backbone. Desirable targets include materials with perpendicular (**6.19**) and parallel (**6.20**) orientations of the multiple bonds (Fig. 6.10) [49–51].

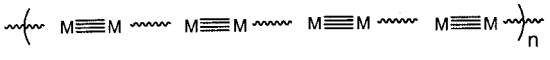

6.19

6.20

Fig. 6.10 Possible perpendicular (**6.19**) and parallel (**6.20**) arrangements of metal-metal multiple bonds in prospective polymeric structures.

An example of the model complexes that point the way to potentially fascinating polymers in the future is given by the tetranuclear species **6.21** [49]. Remarkable square arrays of molybdenum–molybdenum quadruple bonds with oxalate spacers have also been prepared by simple assembly procedures, as illustrated by the formation of the complex $Mo_8(oxalate)_4(N–N)_8$ (**6.22**) (N–N = di(*p*-methoxyphenyl)formamidinate) (Fig. 6.11) from $[Mo_2(N–N)_2(NCMe)_2]^{2+}$ and $[oxalate]^{2-}$ [52].

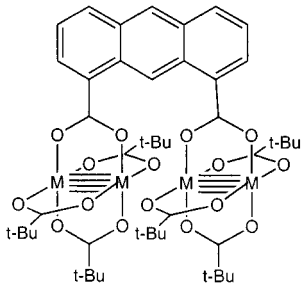

6.21

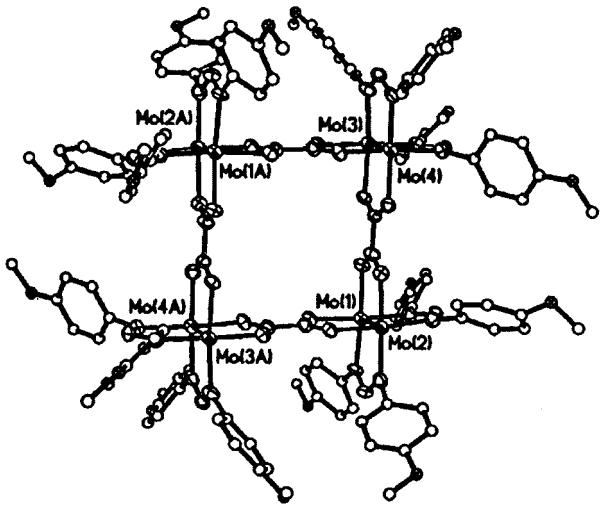

6.22

Fig. 6.11 Molecular structure of $Mo_8(oxalate)_4(N–N)_8$ (**6.22**) (N–N = di(*p*-methoxyphenyl)formamidinate). (Adapted from [52])

6.4
Polymers that Contain Metal Clusters in the Main Chain

Metal cluster complexes exhibit many interesting catalytic, optical, and other potentially useful properties for materials science applications, and many impressive advances have been made with respect to their synthesis [53–55]. The incorporation of these remarkable metal-containing units into the main chain of polymer structures clearly offers exciting possibilities [56], but this area is, in general, poorly developed. The following three examples of linear structures illustrate the growing interest and broad potential of this area. Dendritic structures that contain metal clusters are discussed in Chapter 8.

In 2000, the dark-brown cluster polymer **6.23**, obtained from the polycondensation of the hexanuclear ruthenium carbido species $Ru_6C(CO)_{15}$ with the diphosphinoalkyne $Ph_2PC{\equiv}CPPh_2$ in refluxing THF, was reported [57]. The structure was assigned on the basis of IR, NMR, and elemental analysis, and an estimated degree of polymerization of up to 1000 was reported based on electron microscopy techniques. Polymer **6.23** has been shown to be electron-beam sensitive and this allows the creation of Ru-based nanoparticle chains and, ultimately, conducting wires [57–59].

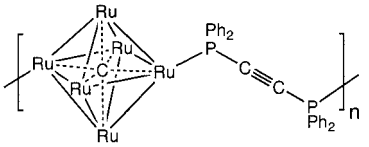

6.23

Ru = $Ru(CO)_x$

It is proposed that, on irradiation with electrons, the first step involves removal of the sheath of carbonyl ligands and that the second step involves fusion of the particles into larger clusters. Through the use of films of **6.23** and a finely focussed electron beam, wires with widths as small as 100 nm were accessible.

In 2001, an efficient step-growth polycondensation approach, reminiscent of that used to prepare metal-metal bonded polymers **6.6** and **6.7**, was successfully developed to yield polyurethanes **6.24** with Mo_2Ir_2 clusters in the backbone [60]. Well-characterized polymers with molecular weights of up to $M_w = 136{,}000$ (PDI = 3.1), which corresponds to a number average of around 30 clusters per polymer chain, were obtained. The synthetic procedure involved treatment of a diol of the Mo_2Ir_2 cluster with the diisocyanate OCN–R–NCO (R = aliphatic or aromatic spacer) in the presence of a tin catalyst. The unusual optical properties of organometallic clusters will drive applications-oriented work on these materials [60].

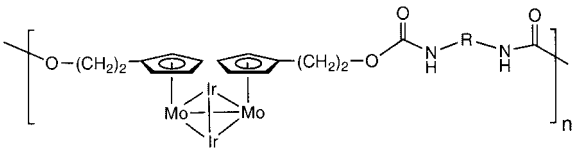

6.24

Mo_2Ir_2 = $Mo_2Ir_2(CO)_{10}$

Finally, in a position at the interface of solid-state and polymer science are the remarkable linear chain compounds $[LiMo_3Se_3]_n$, which can be dissolved in polar solvents such as propylene carbonate, DMSO, or *N*-methylformamide to form burgundy solutions. These species contain polymeric $[Mo_3Se_3^-]_n$ anions (**6.25**) that consist of polycondensed Mo_6Se_8 polyhedra (Fig. 6.12) [61, 62].

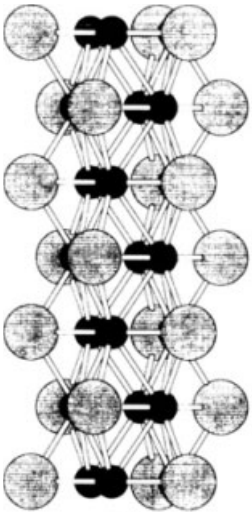

Fig. 6.12 Depiction of a segment of the structure of the polymeric anions **6.25**. The dark spheres are Mo atoms and the lighter spheres are Se atoms. (Adapted from [62])

6.25

Solutions containing **6.25** in *N*-methylformamide display nematic liquid crystallinity as a result of alignment of the polymeric rigid rods in solution [63]. Attempts to align individual rods in microchannels showed that they tend to form bundles with widths of 10–200 nm depending on solution concentration and microchannel volume (Fig. 6.13) [64]. Through the use of low concentrations and small microchannels, 1–3 nm structures, which are close to the width of individual chains, could be deposited. Placement of the structures over lithographically patterned electrodes has led to the determination of conductivities of ca. 2×10^2 S cm^{-1}. Lustrous thin films were obtained from solution by spin-coating or solvent casting, and these possess high conductivities of up to ca. 10^4 Scm^{-1}. Cation exchange in solution is possible in order to replace Li^+ ions by, for example $[NMe_4]^+$ under mild conditions in the presence of 12-crown-4. This should allow the electronic properties of the materials to be modified [65].

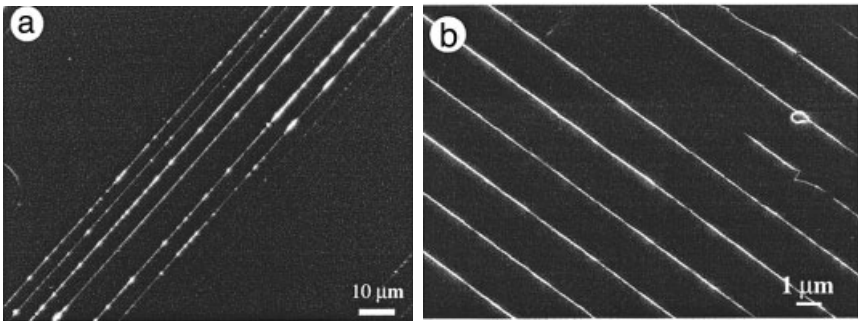

Fig. 6.13 **(a)** Cross-polarized optical image of patterns of nanowires of **6.25** generated using microchannels on a glass substrate and **(b)** FESEM image of wire arrays on a silicon substrate. (Adapted from [64])

6.5
Supramolecular Polymers That Contain Metal-Metal Interactions Involving Transition Elements

The use of self-assembly processes to generate materials with skeletal M–M interactions is a highly promising methodology. Many fascinating examples of metal-metal bonding in the solid state are known, but in most cases the interesting properties are lost in solution due to dissociation [66–69].

One of the most investigated species is Magnus's Green Salt $[Pt(NH_3)_4][PtCl_4]$ (**6.26**), which has been known since 1828 [70]. This intractable material has attracted much attention, as X-ray analysis showed that it possesses a structure (Fig. 6.14) that contains stacked square-planar $[Pt(NH_3)_4]^{2+}$ cations and $[PtCl_4]^{2-}$ anions in the solid state. This creates a linear chain of Pt atoms that have separations of 3.23–3.25 Å and leads to the generation of a band structure. The material has been shown to possess appreciable electrical conductivity (ca. 10^{-6}–10^{-2} S cm^{-1}) [71].

Recently, attempts to prepare soluble versions of **6.26** have focussed on analogues with organoamine ligation $[Pt(NH_2R)_4][PtCl_4]$ **6.27** (R = *n*-heptyl to *n*-tetradecyl). However, although these species are indeed soluble in organic solvents, the Pt–Pt distances in such materials are substantially longer (> 3.4 Å) and result in a pink color and insulating properties. This is a consequence of a tilting of the planes of the cations and anions in the stacked structure, rather than a sterically-induced elongation as was previously suggested. The use of the branched (*S*)-3,7-dimethyloctyl substituent can mitigate this effect, and materials **6.27** (R = (*S*)-3,7-dimethyloctyl) are green, possess Pt–Pt distances of 3.1 Å by powder X-ray diffraction, and are weakly semiconducting ($\sigma \approx 10^{-7}$ Scm^{-1}) [71]. Moreover, the Pt–Pt bonding is retained in solutions of the material in toluene or xylenes. Vapor-pressure osmometry indicated an M_n value of ca. 9000, which corresponds to a DP_n

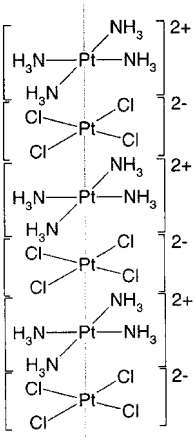

6.26

Fig. 6.14 Structure of $[Pt(NH_3)_4][PtCl_4]$ (**6.26**) in the solid state. (Reproduced from [71])

value of ca. 16. This work suggests that careful ligand choice might allow even shorter Pt–Pt distances (which might even approach the values of ca. 2.6–2.8 Å in Pt metal) and which could yield substantially higher conductivities.

Another intriguing route to supramolecular materials with Pt–Pt bonds involves the use of hydrogen bonding between O and NH groups of neighboring Pt–Pt-bonded carboxylate-bridged dimers **6.28** (Fig. 6.15). Partial oxidation yields materials with conductivities of 10^{-2}–10^{-3} S cm^{-1} [72].

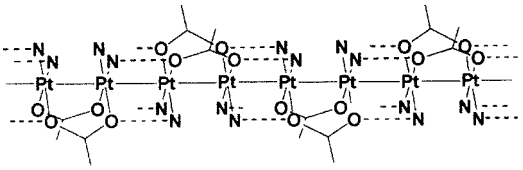

Fig. 6.15 The hydrogen-bonded structure of **6.28**. (Reproduced from [72])

In another example, weak metal-metal interactions that involve other heavy transition elements, such as Au, have recently been used to help guide the self-assembly of metallocyclic building blocks **6.29** into luminescent, superhelical fibers based on stacked structures (Fig. 6.16) [73].

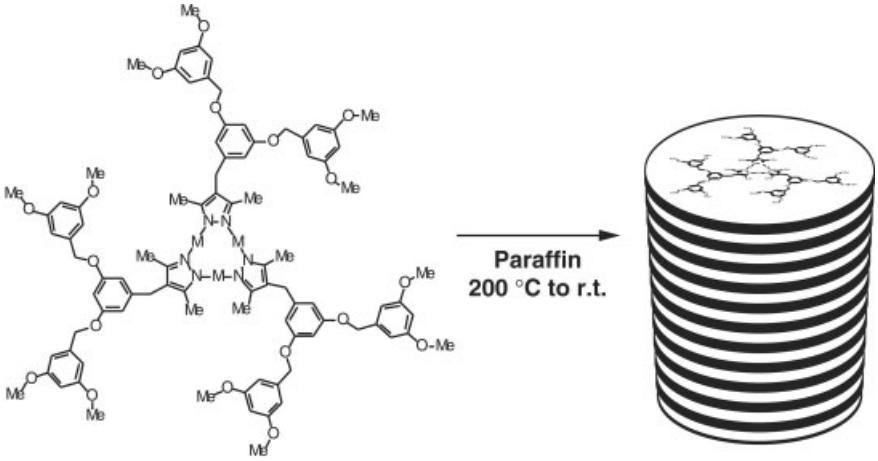

Fig. 6.16 Self-assembly of metallocycle **6.29** into stacked structures. (Adapted from [73])

6.6 References

1 K. S. Mazdiyasni, R. West, D. L. David, *J. Am. Ceram. Soc.* **1978**, *61*, 504.
2 R. West, *J. Organomet. Chem.* **1986**, *300*, 327.
3 R. D. Miller, J. Michl, *Chem. Rev.* **1989**, *89*, 1359.
4 K. Matyjaszewski, *J. Inorg. Organomet. Polym.* **1991**, *1*, 463.
5 H. Teramae, K. Takeda, *J. Am. Chem. Soc.* **1989**, *111*, 1281.
6 J. Nelson, W. J. Pietro, *J. Phys. Chem.* **1988**, *92*, 1365.
7 A. Savin, O. Jepsen, J. Flad, O. K. Andersen, H. Preuss, H. G. von Schnering, *Angew. Chem. Int. Ed. Engl.* **1992**, *31*, 187.
8 J. E. Mark, H. R. Allcock, R. West, *Inorganic Polymers*, Prentice Hall, Englewood Cliffs, New Jersey, **1992**, p 186–236.
9 The lowest absorption bands of polysilanes have also been assigned to excitonic rather than interband transitions. See H. Tachibana, M. Matsumoto, Y. Tokura, Y. Moritomo, A. Yamaguchi, S. Koshihara, R. D. Miller, S. Abe, *Phys. Rev. B* **1993**, *47*, 4363.
10 P. Trefonas III, R. West, *J. Polym. Sci. Polym. Chem. Ed.* **1985**, *23*, 2099.
11 R. D. Miller, R. Sooriyakumaran, *J. Polym. Sci. Polym. Chem. Ed.* **1987**, *25*, 111.
12 J. E. Mark, H. R. Allcock, R. West, *Inorganic Polymers*, Prentice Hall, Englewood Cliffs, New Jersey, **1992**, p. 243.
13 S. Adams, M. Dräger, *Angew. Chem. Int. Ed. Engl.* **1987**, *26*, 1255.
14 L. R. Sita, *Acc. Chem. Res.* **1994**, *27*, 191.
15 K. Takeda, K. Shiraishi, *Chem. Phys. Lett.* **1992**, *195*, 121.
16 T. Imori, T. D. Tilley, *Chem. Commun.* **1993**, 1607.
17 T. Imori, V. Lu, H. Cai, T. D. Tilley, *J. Am. Chem. Soc.* **1995**, *117*, 9931.
18 V. Lu, T. D. Tilley, *Macromolecules* **1996**, *29*, 5763.
19 V. Y. Lu, T. D. Tilley, *Macromolecules* **2000**, *33*, 2403.
20 J. R. Babcock, L. R. Sita, *J. Am. Chem. Soc.* **1996**, *118*, 12481.
21 (a) N. Devylder, M. Hill, K. C. Molloy, G. J. Price, *Chem. Commun.* **1996**, 711; (b) An earlier report of the synthesis of polystannanes by Wurtz coupling was published as a conference proceeding but the spectroscopic data reported for the claimed polymers do not match the data found subsequently. See W. Zou, N. L. Yang, *Polym. Prepr. (Am. Chem. Soc., Div. Polym. Chem.)* **1992**, *33*, 188 and refs. [16] and [17].
22 M. Okano, N. Matsumoto, M. Arakawa, T. Tsuruta, H. Hamano, *Chem. Commun.* **1998**, 1799.
23 L. R. Sita, K. W. Terry, K. Shibata, *J. Am. Chem. Soc.* **1995**, *117*, 8049 and references cited therein.
24 K. Shibata, C. S. Weinert, L. R. Sita, *Organometallics* **1998**, *17*, 2241.
25 S. S. Bukalov, L. A. Leites, V. Lu, T. D. Tilley, *Macromolecules* **2002**, *35*, 1757.
26 S. C. Tenhaeff, D. R. Tyler, *Chem. Commun.* **1989**, 1459.
27 S. C. Tenhaeff, D. R. Tyler, *Organometallics* **1991**, *10*, 473.
28 S. C. Tenhaeff, D. R. Tyler, *Organometallics* **1991**, *10*, 1116.
29 S. C. Tenhaeff, D. R. Tyler, *Organometallics* **1992**, *11*, 1466.
30 G. F. Nieckarz, D. R. Tyler, *Inorg. Chim. Acta* **1996**, *242*, 303.
31 G. F. Nieckarz, J. J. Litty, D. R. Tyler, *J. Organomet. Chem.* **1998**, *554*, 19.
32 J. L. Male, B. E. Lindfors, K. J. Covert, D. R. Tyler, *Macromolecules* **1997**, *30*, 6404.
33 J. L. Male, B. E. Lindfors, K. J. Covert, D. R. Tyler, *J. Am. Chem. Soc.* **1998**, *120*, 13176.
34 M. Morán, M. C. Pascual, I. Cuadrado, J. Losada, *Organometallics* **1993**, *12*, 811.
35 M. J. Irwin, G. Jia, J. J. Vittal, R. J. Puddephatt, *Organometallics* **1996**, *15*, 5321.
36 R. J. Puddephatt, *Chem. Commun.* **1998**, 1055.
37 P. D. Harvey, D. Fortin, *Coord. Chem. Rev.* **1998**, *171*, 351.
38 P. D. Harvey, *Coord. Chem. Rev.* **2001**, *219*, 17.

39 T. Zhang, M. Drouin, P.D. Harvey, *Inorg. Chem.* **1999**, *38*, 957.

40 D. Fortin, M. Drouin, M. Turcotte, P.D. Harvey, *J. Am. Chem. Soc.* **1997**, *119*, 531.

41 D. Fortin, M. Drouin, P.D. Harvey, *J. Am. Chem. Soc.* **1998**, *120*, 5351.

42 M. Turcotte, P.D. Harvey, *Inorg. Chem.* **2002**, *41*, 2971.

43 S.Y. Lai, T.-W. Kin, Y.-H. Chen, C.-C. Wang, G.-H. Lee, M.-H. Yang, M.-K. Leung, S.-M. Peng, *J. Am. Chem. Soc.* **1999**, *121*, 250.

44 C. Wang, W. Lo, C. Chou, G. Lee, J. Chen, S. Peng, *Inorg. Chem.* **1998**, *37*, 4059.

45 P. McArdle, L. O'Neill, D. Cunningham, *Inorg. Chim. Acta* **1999**, *291*, 252.

46 P. McArdle, L. O'Neill, D. Cunningham, A.R. Manning, *J. Organomet. Chem.* **1996**, *524*, 289.

47 W.K. Leong, R.K. Pomeroy, R.J. Batchelor, F.W.B. Einstein, C.F. Campana, *Organometallics* **1997**, *16*, 1079.

48 M. Shieh, Y. Liou, M.H. Hsu, R.T. Chen, S.J. Yeh, S.M. Peng, G.H. Lee, *Angew. Chem. Int. Ed.* **2002**, *41*, 2384.

49 R.H. Cayton, M.H. Chisholm, J.C. Huffman, E.B. Lobkovsky, *J. Am. Chem. Soc.* **1991**, *113*, 8709.

50 (a) M.H. Chisholm, *Acc. Chem. Res.* **2000**, *33*, 53; (b) M.J. Byrnes, M.H. Chisholm, *Chem. Commun.* **2002**, 2040.

51 (a) T. Ren, G.L. Xu, *Comments Inorg. Chem.* **2002**, *23*, 355; (b) W.M. Xue, F.E. Kuhn, E. Herdtweck, Q.C. Li, *Eur. J. Inorg. Chem.* **2001**, 213; (c) W.M. Xue, F.E. Kuhn, E. Herdtweck, *Polyhedron* **2001**, *20*, 791.

52 F.A. Cotton, L.M. Daniels, C. Lin, C.A. Murillo, *J. Am. Chem. Soc.* **1999**, *121*, 4538.

53 I.R. Whittall, A.M. McDonagh, M.G. Humphrey, M. Samoc, *Adv. Organomet. Chem.* **1999**, *43*, 349.

54 B.F.G. Johnson, *Coord. Chem. Rev.* **1999**, *190–192*, 1269.

55 M. Feliz, J.M. Garriga, R. Llusar, S. Uriel, M.G. Humphrey, N.T. Lucas, M. Samoc, B. Luther-Davies, *Inorg. Chem.* **2001**, *40*, 6132.

56 (a) M.R. Jordan, P.S. White, C.K. Schauer, M.A. Mosley, *J. Am. Chem. Soc.* **1995**, *117*, 5403; (b) T. Kuhnen, M. Stradiotto, R. Ruffolo, D. Ulbrich, M.J. McGlinchey, M.A. Brook, *Organometallics* **1997**, *16*, 5048.

57 B.F.G. Johnson, K.M. Sanderson, D.S. Shephard, D. Ozkaya, W. Zhou, H. Ahmed, M.D.R. Thomas, L. Gladden, M. Mantle, *Chem. Commun.* **2000**, 1317.

58 M.D.R. Thomas, H. Ahmed, K.M. Sanderson, D.S. Shephard, B.F.G. Johnson, W. Zhou, *Appl. Phys. Lett.* **2000**, *76*, 1773.

59 M.D.R. Thomas, H. Ahmed, K.M. Sanderson, D.S. Shephard, B.F.G. Johnson, D. Ozkaya, N. Sharma, C. Humphreys, *J. Appl. Phys.* **2001**, *90*, 947.

60 N.T. Lucas, M.G. Humphrey, A.D. Rae, *Macromolecules* **2001**, *34*, 6188.

61 M. Potel, R. Chevrel, M. Sergent, J.C. Armici, M. Decroux, P. Fischer, *J. Solid State Chem.* **1980**, *35*, 286.

62 J.H. Golden, F.J. DiSalvo, J.M.J. Fréchet, *Chem. Mater.* **1995**, *7*, 232.

63 P. Davidson, J.C. Gabriel, A.M. Levelut, P. Batail, *Adv. Mater.* **1993**, *5*, 665.

64 B. Messer, J.H. Song, P. Yang, *J. Am. Chem. Soc.* **2000**, *122*, 10232.

65 J.H. Song, B. Messer, Y. Wu, H. Kind, P. Yang, *J. Am. Chem. Soc.* **2001**, *123*, 9714.

66 J.K. Bera, K.R. Dunbar, *Angew. Chem. Int. Ed.* **2002**, *41*, 4453.

67 N. Masciocchi, A. Sironi, S. Chardon-Noblat, A. Deronzier, *Organometallics* **2002**, *21*, 4009.

68 T. Yamaguchi, F. Yamazaki, T. Ito, *J. Am. Chem. Soc.* **2001**, *123*, 743.

69 A.F. Heyduk, D.J. Krodel, E.E. Meyer, D.G. Nocera, *Inorg. Chem.* **2002**, *41*, 634.

70 G. Magnus, *Pogg. Ann.* **1828**, *14*, 239.

71 M. Fontana, H. Chanzy, W.R. Caseri, P. Smith, A.P.H. Schenning, E.W. Meijer, F. Gröhn, *Chem. Mater.* **2002**, *14*, 1730.

72 K. Sakai, E. Ishigami, Y. Konno, T. Kajiwara, T. Ito, *J. Am. Chem. Soc.* **2002**, *124*, 12088.

73 M. Enomoto, A. Kishimura, T. Aida, *J. Am. Chem. Soc.* **2001**, *123*, 5608.

7
Main-Chain Coordination Polymers

7.1
Introduction

Coordination polymers contain ligand-metal donor-acceptor bonds and are traditionally regarded as those materials that contain anionic or neutral N, O, S, or P donor ligands attached to the metal center. Particularly when the ligands are neutral, the metal-ligand bonds can often exhibit appreciable lability, and reversibly form and cleave under many conditions. Such bonds may therefore be considered to fall under the general category of supramolecular interactions. Indeed, polymers containing coordination bonds of this type are now increasingly referred to as "metallo-supramolecular" systems.

In the past, attempts to prepare stable main-chain coordination polymers have relied on the use of chelating ligands and have been hindered by the insolubility and consequent intractability of the products [1]. These problems arise from the inherent skeletal rigidity of these materials, and the introduction of solubilizing or flexibilizing groups, either in the polymer backbone or side-group structure, has been necessary in order to obtain useful products (see Chapter 1, Section 1.2.4). Since the mid-1990s, the area has flourished and a range of very interesting and well-characterized materials containing both d- and f-block metals have been prepared. The development of polymers in which the metal is incorporated into a π-conjugated main-chain organic framework has received particular attention. This is reflective of the dramatic growth of interest in π-conjugated organic materials such as electrically conducting polythiophene and electroluminescent poly(phenylene vinylene) (PPV) [2–6]. The incorporation of metal centers into the main chain provides an additional and potentially very versatile means of perturbing and hence tuning the very useful electronic and optical (e.g. luminescence) properties of these materials. A variety of other potential applications can be envisaged for coordination polymers; for example, as sensors, electrocatalysts, and conducting and light-emitting materials in their own right. With access to block and star coordination copolymers now achieved, a particularly exciting area for the future involves potential applications as supramolecular materials.

Most of the discussions in this chapter will focus on the work on well-characterized one-dimensional coordination polymers reported since 1990. 2-D and 3-D co-

Synthetic Metal-Containing Polymers. Ian Manners

ISBN: 3-527-29463-5

ordination polymers are best regarded as solid-state materials rather than macromolecules, and these will not therefore be discussed. It should be noted that coordination polymers that possess direct metal-metal bonds and/or metal clusters in the main chain are discussed in Chapter 6 (Section 6.3 and 6.4), side-chain coordination polymers were described in Chapter 2 (Section 2.3), and dendritic coordination polymers are discussed in Chapter 8.

7.2
Polypyridyl Coordination Polymers

7.2.1
Homopolymers with Octahedral Metals

Octahedral ruthenium(II) and osmium(II) polypyridyl complexes combine thermal and chemical stability with very interesting photophysical and electronic properties (see Chapter 2, Section 2.3.2). These considerations have prompted a range of studies that target polymers based on polypyridyl and related complexes [7]. For example, in the mid- and late 1990s, crosslinked films derived from the thermal, electro- or photopolymerization of polyfunctional monomeric complexes **7.1** and **7.2** were investigated for the fabrication of light-emitting devices based on electrochemically generated chemiluminescence (Eq. 7.1). Solvent-swollen and dry films of the polymers were studied, and were found to exhibit efficiencies similar to those constructed from organic conjugated polymers [8, 9].

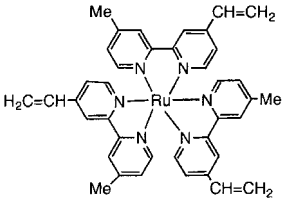

7.1

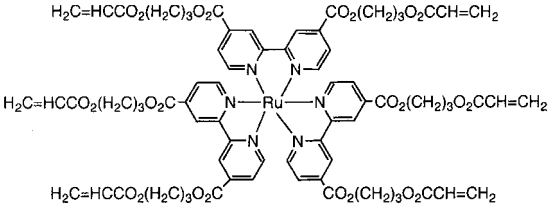

7.2

$$\begin{array}{ccccc} [Ru(bipy)_3]^{3+} & & [Ru(bipy)_3]^{2+*} & & 2\,[Ru(bipy)_3]^{2+} \\ + & \longrightarrow & + & \longrightarrow & + \\ [Ru(bipy)_3]^{+} & & [Ru(bipy)_3]^{2+} & & h\nu \end{array} \qquad (7.1)$$

Impressive results in terms of the synthesis and characterization of soluble linear Ru-polypyridyl coordination polymers were reported in 1997 [10]. Reaction of tetrapyridylphenazine (tppz) with impure ruthenium precursors $[Ru(R_2bpy)Cl_3]_x$ was found to give fairly low molecular weight polymers **7.3** with $M_n \approx 16{,}000$ ($DP_n \approx 15$) (Eq. 7.2). However, when stoichiometric balance was possible due to

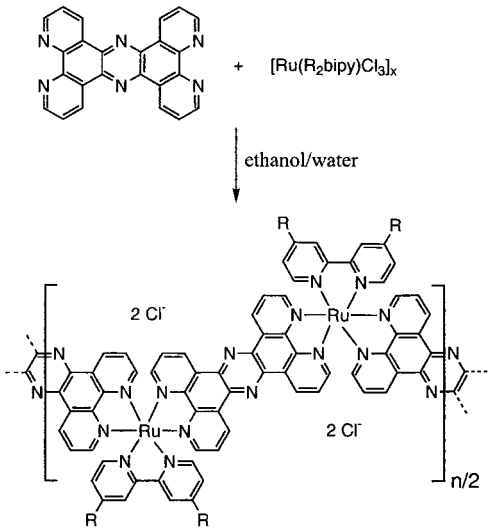

(7.2)

7.3 R = H

7.4 R = Ph

7.5 R = CH_2-adamantyl

the synthesis of pure $[Ru(R_2bpy)Cl_3]_x$ by an improved route, polycondensation afforded high molecular weight linear coordination polymers **7.3** and **7.4**. No endgroups were visible in the NMR spectra of the polymers, from which it was concluded that $DP_n > 30$. The brown-black polymers proved to be soluble in acetonitrile, dimethylacetamide, ethanol, and water.

The solubility of these interesting materials in readily available solvents provided an excellent opportunity to examine their solution properties in detail. In ethanol/water or dimethylacetamide, the polymer **7.3** displayed a pronounced polyelectrolyte effect when measurements were performed without added salt. Thus, whereas plots of η_{sp}/c (η_{sp} = specific viscosity) versus concentration (c) are usually linear, the strong intramolecular and intermolecular interactions for the high molecular weight coordination polymer **7.3** led to a dramatic increase in η_{sp}/c at fairly low concentrations (10^{-4}–10^{-5} M) in the absence of added salt. A similar, but much less dramatic, effect was observed in the case of the phenyl-substituted polymer **7.4**, for which intermolecular interactions appear to be weaker. On the other hand, in the presence of an added salt the intermolecular forces decrease due to screening effects, and intrinsic viscosities ($[\eta] \approx 12$ mL g^{-1}) were measured for **7.3** and **7.4** from the linear η_{sp}/c versus c plots. Studies of **7.3** in dilute solution by means of small-angle X-ray scattering (SAXS) suggested the formation of aggregates. However, SAXS showed the phenyl-substituted polymer **7.4** to be more soluble and studies of this material in 0.01 M $[NH_4][PF_6]$ in dimethylacetamide allowed a determination of an absolute value of M_w of ca. 47,000, which corresponded to a degree of polymerization, DP_w, of ca. 43. According to SAXS and viscosity data, polymers **7.3** and **7.4** possess a rather rigid, coiled chain conformation with densely

packed chain segments. This is consistent with the presence of random Δ and Λ configurations for the Ru centers along the main chain. Studies in solution by means of UV/vis spectroscopy showed that the spectra of the polymers **7.3** and **7.4** are similar to those of the monomeric units, which suggests that no significant π-electron delocalization occurs along the polymer main chain [10].

These studies have been extended to analogous polymers **7.5** (Eq. 7.2) with bulky adamantylmethyl groups attached to the bipyridyl substituents [11]. Viscosity measurements in the presence of added salt showed the intrinsic viscosity of **7.5** ($[\eta] \approx 23$ mL g^{-1}) to be approximately twice that of **7.3** and **7.4**, which is indicative of a much more extended chain conformation in solution.

Rod-like terpyridyl polymers **7.6** have also been accessed through step-growth polycondensation strategies (Eq. 7.3). Analogous routes those employed for the formation of **7.3–7.5** were successful in the preparation of high molecular weight materials with $DP_n > 30$ [12]. However, Pd-catalyzed polycondensation processes afforded only low molecular weight products.

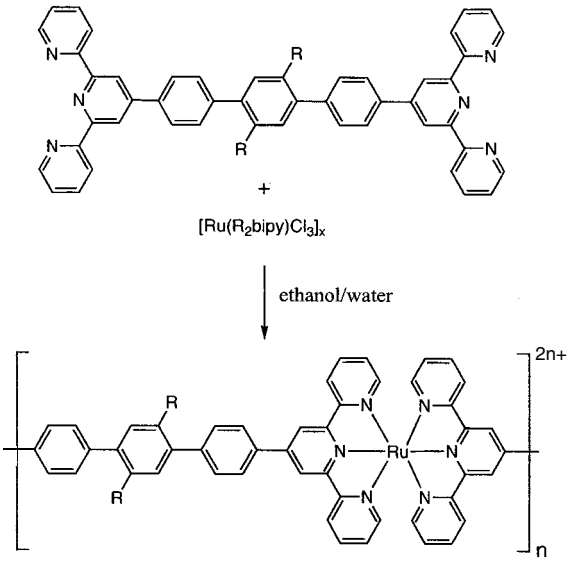

(7.3)

7.6 R = ^{n}Hex

The ruthenium terpyridyl polymers **7.6** possess rigid-rod structures with much higher intrinsic viscosities ($[\eta] \approx 300$ mL g^{-1} in 0.02 M $[NH_4][PF_6]$ in dimethylacetamide) than the coiled systems **7.3** and **7.4**. Indeed, the intrinsic viscosities are greater than for rigid-rod organic polymers such as poly(*p*-phenylene) ($[\eta] \approx 207$ mL g^{-1} when $DP_n = 37$). Again, in the absence of added salts, polyelectrolyte behavior was noted. However, as in the cases of polymers **7.3** and **7.4**, UV/vis spectroscopy indicated that little electron delocalization was present in these particular materials, despite their formally conjugated structure, and that the polymer chain appeared to behave as an array of independent ruthenium(II) complexes. Although these mate-

rials represent some of the first examples of high molecular weight coordination polymers of this type, a wide range of interesting oligomeric species have also been reported and offer promise of developments at the polymer level in the future.

Cationic Fe-terpyridyl polymers **7.7** (Fig. 7.1) have also been prepared by means of a step-growth polycondensation approach, and these materials have been used in layer-by-layer assembly applications along with oppositely charged organic polymers such as polystyrene sulfonate (PSS) [13–15]. The polymers were characterized by ^{1}H NMR and UV/vis spectroscopies, through comparison to a model complex, and by elemental analysis. Molecular weights (M_w) were estimated to be greater than ca. 14,000 by analytical ultracentrifugation methods, which corresponded to ca. 25 repeat units [13]. The formation of layer-by-layer polyelectrolyte multilayers on weakly cross-linked melamine-formaldehyde particles by sequential deposition of the cationic Fe polymer **7.7** and anionic PSS led to coated particles (see TEM image in Fig. 7.2 a). Subsequent decomposition of the core upon treatment with acid allowed for the generation of remarkable metallized hollow spheres consisting of five bilayers (Fig. 7.2 b and c) [14]. Polymers analogous to **7.7** that contain other metals such as Co are also accessible [16].

Soluble Ru-polypyridyl polyelectrolytes **7.8** have been prepared by step-growth polycondensation of the preformed Ru complex diol with $ClOC(CH_2)_{10}COCl$, and have been used to prepare similar layer-by-layer assemblies, which are of interest due to their light-emissive properties [17, 18]. For example, an Ru-containing polyester **7.8** of relatively low molecular weight ($M_n \approx 5500$) has been well characterized, and it was found that the solubility could be altered through variation of the counteranion. Solid-state light-emitting devices based on layer-by-layer assembled multilayer structures created from the water-soluble polycation **7.8** with Cl^- as the counteranion, and the sodium salt of poly(acrylic acid) as the negatively charged polyelectrolyte, were prepared on indium tin oxide, with thermally evaporated Al serving as the other electrode [18]. Light emission was noted under both positive (ITO as anode) and negative (Al as anode) bias. However, due to the multilayer structure control made possible by the use of the layer-by-layer technique, compositionally graded heterostructures that emit light only under forward or reverse bias could also be created. External quantum efficiencies for the layer-by-layer light-emitting devices were in the 1–3% range, and were found to be much high-

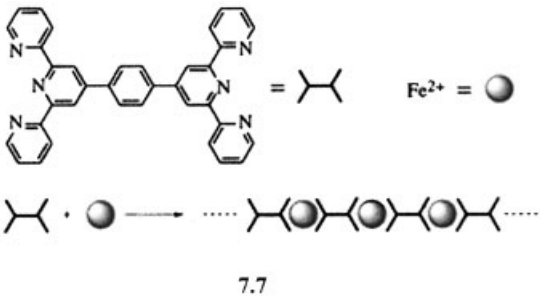

7.7

Fig. 7.1 Schematic of the structure of the iron polypyridyl coordination polymer **7.7**. (Adapted from [14])

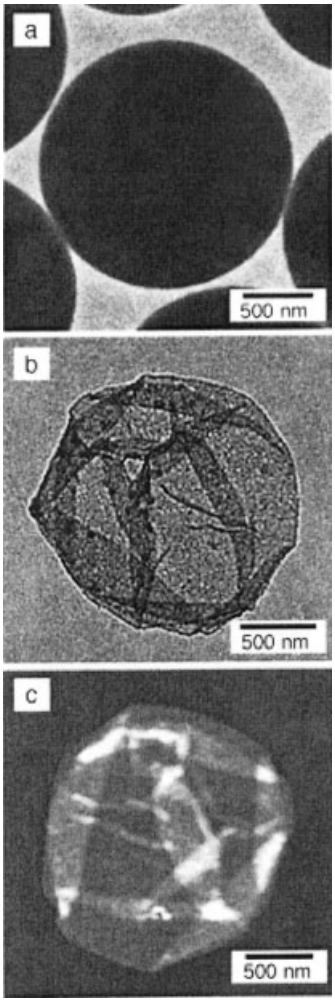

Fig. 7.2 (**a**) TEM images of multilayer-coated melamine-formaldehyde particles (diameter = 1.7 μm); (**b**) TEM and (**c**) AFM images of polyelectrolyte shells after acid-induced decomposition of the melamine-formaldehyde template. (Adapted from [14])

er than the 0.2% observed for analogous single-layer sandwich devices based on films of **7.8** formed by spin coating [18].

Main-chain polymers containing tris(bipyridyl)ruthenium units have also been used in combination with electron-conducting TiO_2 nanoparticles and hole-con-

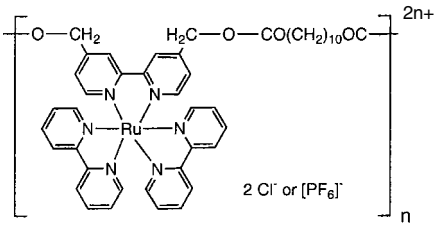

7.8

ducting graphite oxide nanoplatelets to prepare diode junctions by means of layer-by-layer self-assembly techniques [19].

A range of polyimides (e.g. **7.9**), polyesters (e.g. **7.10**), and polyamides (e.g. **7.11**) with polypyridyl Ru units in the main chain have also been prepared and have been thoroughly characterized [20, 21]. These materials were prepared by direct participation of a difunctional Ru complex in the polycondensation process (e.g. **7.9**) or by the reaction of preformed polymers with labile Ru complexes (e.g. **7.10** or **7.11**). Molecular weights (M_w) in the range 2.3×10^4 to 1.5×10^5 were determined for the polyamides. The polyimides, such as **7.9**, display appreciable hole and electron mobilities (ca. 10^{-4}–10^{-5} $cm^2\ V^{-1}\ s^{-1}$ at 25 °C). Hole transport is believed to mainly involve the Ru centers, whereas electron transport is believed to involve the diimide units. Single-layer electroluminescent devices with quantum efficiencies of ca. 0.1% have been fabricated from some of the polyimides and polyamides [20, 21]. Several of the polyamides with rigid backbones form lyotropic mesophases in sulfuric acid, and flexible chain polyesters and polyamides form thermotropic liquid-crystalline phases. A series of rhenium-containing polyimides and ruthenium-containing polybenzobis(oxazole)s and bis(thiazole)s have also been studied, and were shown to exhibit photoconductivity [22, 23].

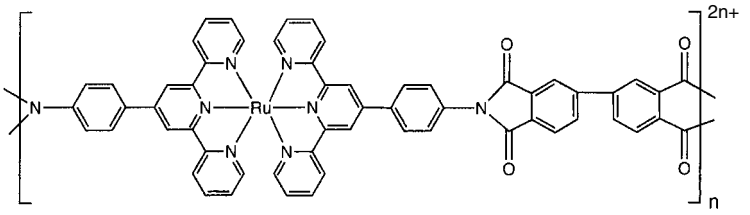

7.9

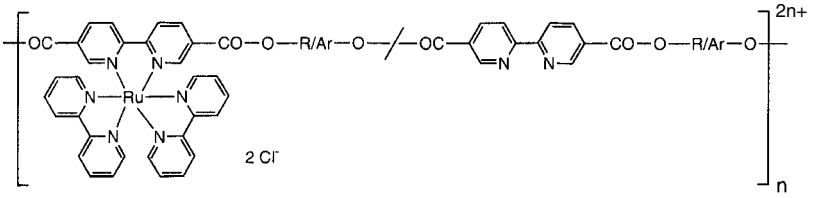

7.10

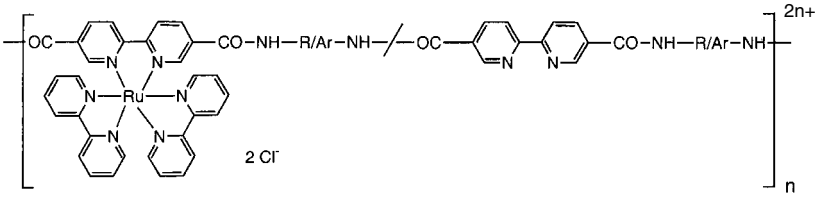

7.11

An extensive range of π-conjugated polymers with bipyridyl binding sites in the main chain have been developed. In the early 1990s, metallopolymers **7.12** containing 5 mol% Ru coordination were synthesized by the reaction of $[Ru(bpy)_2Cl_2]$ with a polybipyridyl macroligand precursor [24–27]. A significant increase in conductivity from 10^{-12} to 10^{-5} Scm^{-1} was detected on complexation with Ru. Shifts in the $Ru^{I/II}$ and $Ru^{II/III}$ potentials relative to mononuclear complexes $[Ru(bpy)_3]^{2+}$ were observed, and these were taken to be indicative of interactions between the Ru centers through the π-conjugated segments.

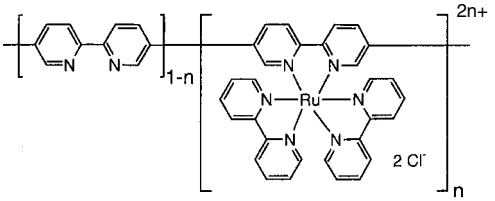

7.12

As illustrated previously, an alternative synthetic approach to complexation of a preformed polymer involves a polycondensation process that directly uses a metal complex. The Ru-containing materials **7.13** were prepared by both methods (Scheme 7.1) [28]. The shift in redox potentials for these materials provided similar evidence for significant electron delocalization.

Heck coupling procedures have been used to prepare π-conjugated metallopolymers such as **7.14** (Eq. 7.4) [29–31]. It was shown that if donor–acceptor nonlinear optical (NLO) chromophores are present as side-group substituents, these materials display photorefractivity, where the refractive index of the material can be modulated by a space charge field through the electro-optic effect. This is potentially important for optical signal processing and information storage applications. Significantly, there is appreciable overlap of the π–π^* absorption of the organic segments with that of the metal-to-ligand charge-transfer transition of the photocharge-generating Ru(bipy) moieties. The latter allow the creation of free charge carriers, and the conjugated organic segments mediate their transport and, ultimately, their trapping at defect sites. The Ru polymers were found to show much higher photorefractivity than the metal-free organic polymers.

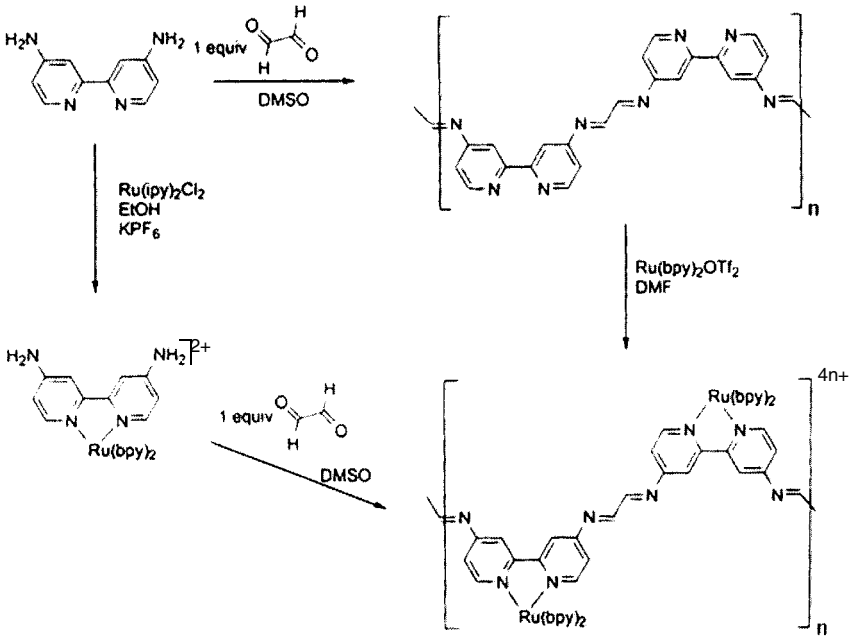

7.13

Scheme 7.1 (Adapted from [28])

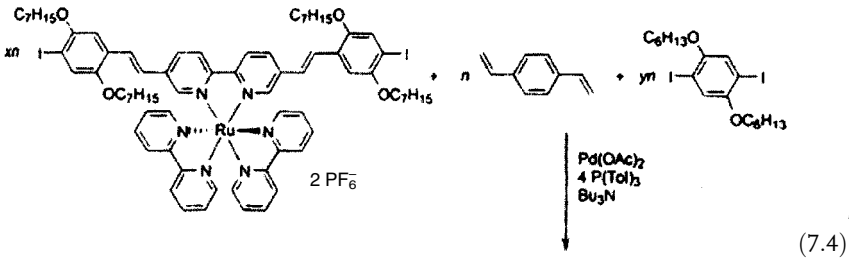

(7.4)

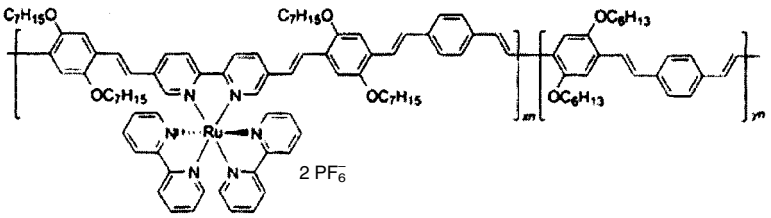

7.14

Analogous Os-containing materials have also been prepared and characterized. However, the Heck synthetic approach used to prepare the Ru and Os metallopolymers was found to introduce undesirable defects in the resultant materials, which limited their photorefractive response. Studies of the photoconductive properties of a variety of materials of type **7.14** have been reported [29, 32], and a wide range of well-characterized polymers with related structures containing octahedral Ru or Re centers have been synthesized and similarly studied [33–36]. Metal-catalyzed cross-coupling procedures have also been used to prepare polymers with alkynylarylene spacers, and the complexation of Ru or Re (e.g. to form **7.15**) leads to materials with interesting photoconducting and fluorescence properties [37, 38].

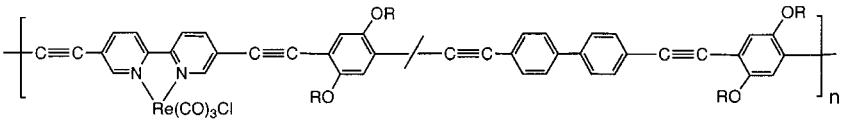

7.15
$R = C_{18}H_{37}$

Electropolymerization of Ru bipy complexes with pendant thiophene groups to form materials such as **7.16** as films on electrodes has also been explored [39]. The resultant polymers can possess appreciable redox conductivity (ca. 10^{-4} S cm^{-1}). The overlap between the metal d orbitals and the p orbitals of the ligands can be tuned by alteration of the substitution pattern, and appreciable conductivities can thereby be achieved.

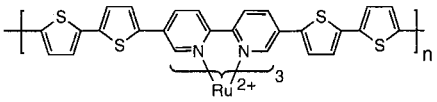

7.16

Soluble, linear polymers analogous to **7.16**, with Ru or Os coordinated to the bipyridyl center, have also been investigated in detail, and the electrochemical and photophysical studies performed support the existence of strong electronic interactions between the metal sites and the π-conjugated organic backbone [40]. Materials with terpyridyl groups bound to Ru have also been prepared by electrochemical polymerization [41].

Polymer **7.17** has been prepared by the complexation reaction of polybenzimidazole with $Ru(bpy)_2Cl_2$ [42, 43]. The dark-orange polymer was shown by GPC to possess a molecular weight of $> 5\times10^4$. Studies using techniques such as rotating disk voltammetry and impedance spectroscopy showed that charge transport is enhanced over redox conduction in this polymer as a result of the π-conjugated backbone. Analogous osmium polymers also show strong electronic communication between the metal centers through the π-conjugated polymer backbone [44].

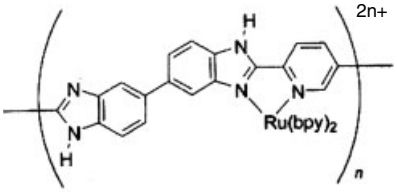

7.17

7.2.2 Homopolymers with Tetrahedral Metals

The synthesis of polypyridyl coordination polymers with tetrahedrally coordinated metals, by means of the synthetic methodology outlined in Eq. 7.5, has also been reported [45]. Red-brown copper polymers (**7.18**) and yellow silver analogues (**7.19**) were isolated as fibrous materials that were found to be stable for months in the solid state. The polymers also proved to be stable in solution in non-coordinating solvents such as chlorinated hydrocarbons, but ligand exchange occurred in solvents such as acetonitrile. Although the molecular weights of these unusual materials were not determined accurately, the lack of detectable end-group signals in their NMR spectra indicates that $DP_n > 30$. In addition, viscometry measurements indicated that the intrinsic viscosity ($[\eta] \approx 11\ \mathrm{mL\ g^{-1}}$) was similar to the value found for analogous Ru^{II} polymers with $M_w \approx 47{,}000$ (by SAXS).

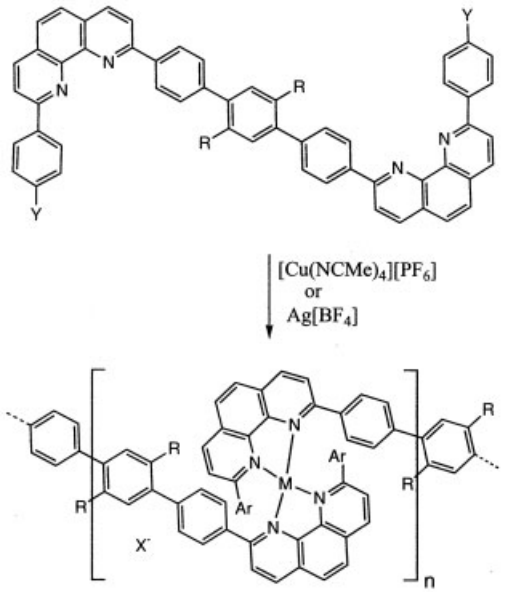

(7.5)

7.18 M = Cu, X = $[PF_6]$
7.19 M = Ag, X = $[BF_4]$

R = *n*-C_6H_{13}, Ar = C_6H_4-Y, Y = H, Cl, or OMe

The synthesis of stable coordination polymers of this type is particularly significant, as the metal complexes are kinetically labile. The presence of bulky *ortho* substituents on the phenanthroline ligands was a key to allowing stable materials to be obtained.

Another approach to Cu^{I} and Ag^{I} coordination polymers involves treatment of the preformed polymer **7.20** with metal ions (Eq. 7.6) [46]. The procedure has the advantage that the metal-free polymer precursor can be fully characterized, which is much easier to achieve than for the metal-containing polyelectrolytes that might also bear paramagnetic metal centers. Treatment of the precursor polymer in organic solvents such as chloroform and toluene with MX or $[ML_4]X$ (M = Cu or Ag) yielded gels as a result of crosslinking through $M(phen)_2$ linkages involving phenanthroline groups from different polymer chains. Performance of the reactions in the presence of excess auxiliary ligand L was found to be necessary for the formation of soluble materials **7.21** and **7.22**. Polymer **7.21**, with L = NCMe, was found to be stable in solution at room temperature, but upon heating to 80 °C insoluble gels formed, presumably as a result of thermally induced ligand exchange chemistry, whereby coordinated acetonitrile ligands are displaced by the phenanthroline ligands from adjacent polymer chains. Solution NMR studies were indicative of rapid exchange of the acetonitrile ligands, consistent with the low kinetic stability of $[M(phen)L_2]^+$ (M = Cu or Ag) complexes.

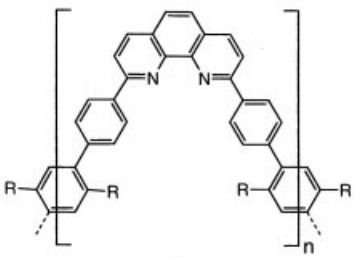

7.20

$[Cu(NCMe)_4][PF_6]$
or $Ag[BF_4]$ in MeCN
or i) $[Cu(NCMe)_4][PF_6]$
ii) 2,9-Ar_2phen (Ar = C_6H_4Br-*p*)

(7.6)

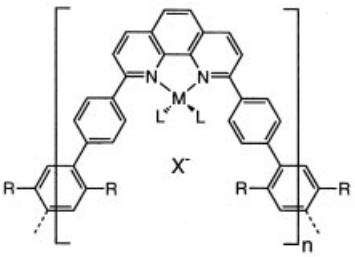

7.21 M = Cu, X = $[PF_6]$
7.22 M = Ag, X = $[BF_4]$

R = *n*-C_6H_{13}
L_2 = NCMe or 2,9-Ar_2phen (Ar = C_6H_4Br-*p*)

Addition of bidentate auxiliary ligands L_2 with bulky *ortho* substituents, such as 2,9-bis(*p*-bromophenyl)-*o*-phen, which exchange much more slowly than acetonitrile, allowed the exchange process to be slowed and well-resolved NMR spectra to be obtained. These red-brown (**7.21**) and yellow (**7.22**) brittle materials could be purified by precipitation, and were found to be stable in solution up to 80 °C without the occurrence of crosslinking and consequent gel formation [46].

Orange coordination polymers **7.23** with two phenanthroline ligands attached to the cationic Cu(I) center have also been studied. Electrochemical investigations showed that oxidation of Cu^{I} to Cu^{II} results in a coordination change that involves metal dissociation, which is fully reversible upon reduction [47]. Such materials are of interest with regard to the formation of electroresponsive membranes and controlled transport materials.

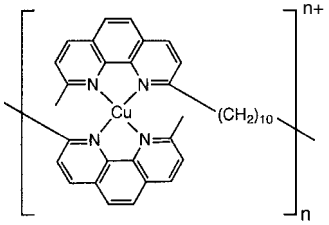

7.23

Polymetallorotaxanes **7.24** ($M = Zn^{II}$ or Cu^{I}) have been prepared by electropolymerization, which involved anodic oxidation of the pre-assembled metallorotaxane precursors (Scheme 7.2) [48]. Importantly, studies of these materials have allowed an evaluation of the individual contributions of the organic backbone and the metal-centered redox process to the overall conductivity measured on interdigitated microelectrodes. The Zn and Cu polymers behave quite differently. The Zn polymer behaves in a similar fashion to the metal-free material **7.25**, whereas the matching of the polymer and Cu-centered redox potentials in **7.24** ($M = Cu^{I}$) leads to enhancement of the communication between these two units; resistance drops by a factor of 10^6 for the Cu polymer **7.24** relative to metal-free **7.25**. In a further development in this general area, two-step electropolymerizations have been used to generate three-stranded conducting ladder polymetallorotaxanes [49].

Materials such as **7.26** and analogues thereof have been shown to exhibit metal ion responsive properties [50]. The polymers display enhanced conjugation on metal ion coordination, which can be transduced into a measurable signal in terms of the UV/vis absorption band or fluorescent emission response. The approach is remarkably versatile and is successful for a wide variety of metal ions M^{x+} from the s, p, d, and f blocks (Table 7.1).

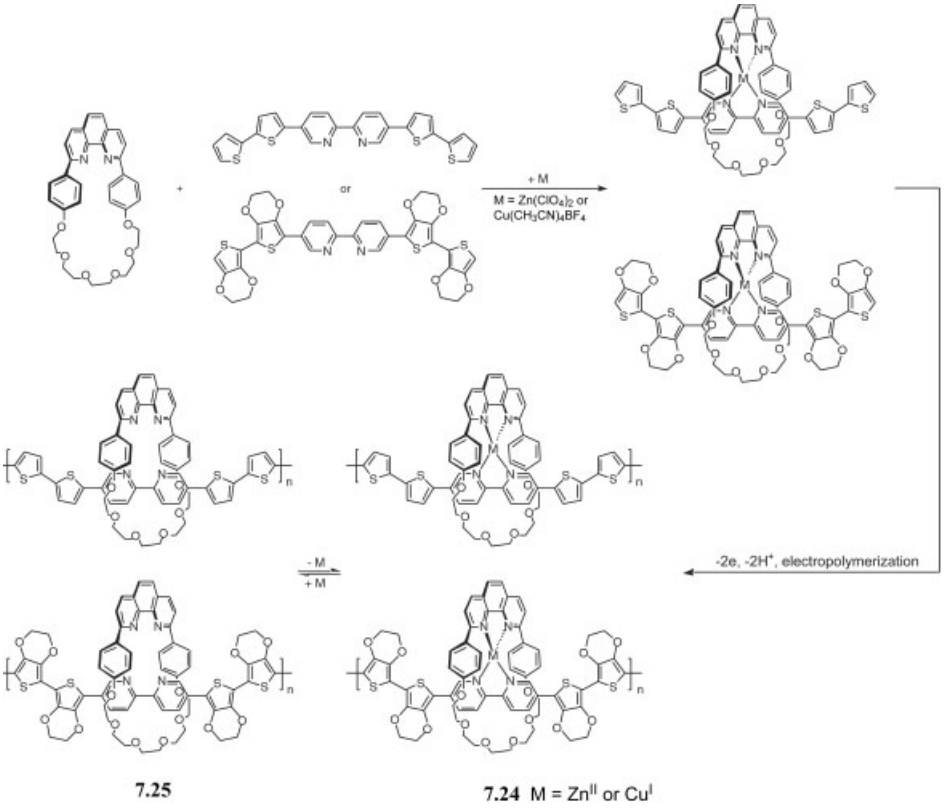

7.25 7.24 M = Zn^{II} or Cu^{I}

Scheme 7.2 (Adapted from [48])

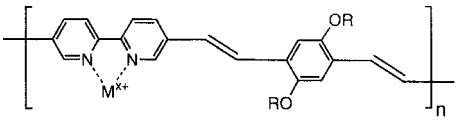

7.26
R = $C_{10}H_{21}$

7.2.3
Stars and Block Copolymers

The first developments in this area were reported in the mid-1990s. For example, Cu^{I} complexation of bipyridine units has been used to prepare the chain-extended polymer **7.27** and the crosslinked material **7.28** from polymeric precursors that contain flexible polyether segments with bipyridyl units either at the chain termini or distributed along the chain, respectively (Scheme 7.3) [51–53].

Table 7.1 Absorption and emission responses of **7.26** upon chelation of various metal ions. (Adapted from [50])

Ion	***Absorption (nm)***	***Emission***[a] (nm)	***Ion***	***Absorption (nm)***	***Emission***[a] (nm)
Ion-free	455	507	Ion-free	455	507
Zn^{2+}	513	593	Ag^{+}	503	585 (w)
Cd^{2+}	513	627	Cu^{+}	514	466 (w)
Cu^{2+}	524	q	Al^{3+}	535	590
Ni^{2+}	513	q	Fe^{3+}	527	467, 492 (m)
Co^{2+}	519	q	Sb^{3+}	556	472, 489 (w)
Hg^{2+}	512	590	La^{3+}	506	469, 499, 594
Pb^{2+}	535	468, 502 (w)	Ce^{3+}	497	469, 494, 573
Pd^{2+}	564	q	Eu^{3+}	500	466, 499, 560
Mn^{2+}	514	q	Er^{3+}	508	463, 503, 602
Sn^{2+}	558	q	Gd^{3+}	498	466, 500, 594
Fe^{2+}	529	464 (w)	Yb^{3+}	512	467, 502, 598

a q = quenched, m = medium, w = weak

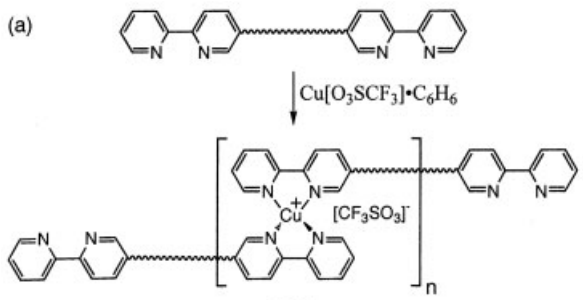

Scheme 7.3

The properties of the linear material **7.27** and the network copolymer **7.28** have been studied by dynamic mechanical analysis, DSC, and transmission electron microscopy. Evidence was obtained for the formation of highly ordered microphase-separated superstructures in the solid state from the materials **7.27**. The $Cu(bipy)_2$ moieties appear to form ordered stacks, and this leads to thermoplastic elastomer properties. In contrast, the network structure of **7.28** prevents significant microphase separation [51–53]. By means of related approaches, dinuclear Cu^I helical complexes have also been used to create block copolymers by functioning as cores [54], and polymer networks have also been formed by using diiron(II) triple helicates as cores for the formation of copolymers with methyl methacrylate [55].

Ru-terpyridyl complexes have been used as linkers between organic blocks. For example, the synthesis of the block copolymer PS_{20}-[Ru]-PEO_{70} **7.29** was accomplished by means of the procedure outlined in Scheme 7.4 [56]. These materials

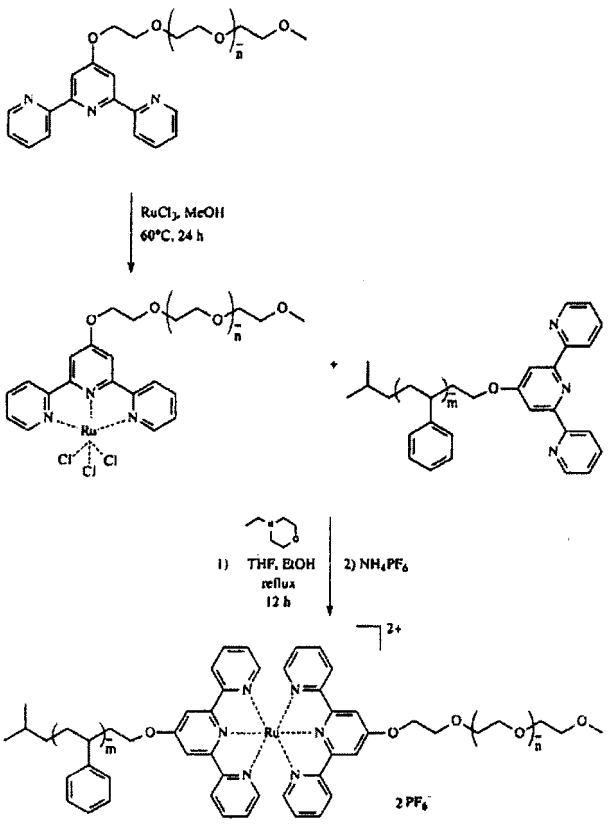

PS_{20}-[Ru]-PEO_{70}

7.29

Scheme 7.4 (Reproduced from [56])

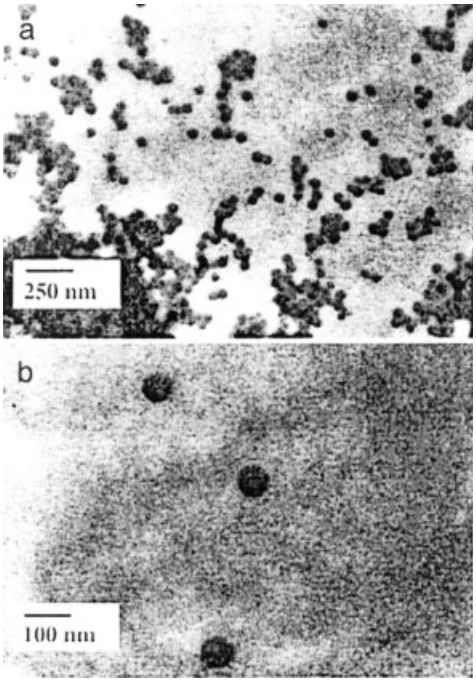

Fig. 7.3 TEM images of micelles formed from PS_{20}-[Ru]-PEO_{70} (**7.29**) in water after solvent evaporation. (Adapted from [56])

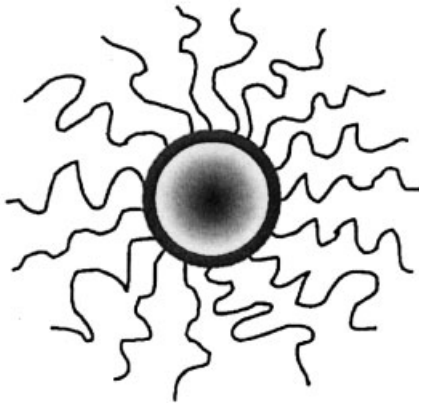

Fig. 7.4 Schematic representation of micelles of PS_{20}-[Ru]-PEO_{70} (**7.29**) showing a PS core (grey), the Ru linkers (black), and the PEO corona. (Adapted from [56])

formed micelles in water, a selective solvent for the PEO block, after initial dissolution in DMF followed by the slow addition of water and dialysis. UV/vis spectra of the bright orange-red opalescent aqueous solution of the micelles indicated that the [Ru] linker was stable in this solvent. Dynamic light-scattering studies indicated a hydrodynamic radius of 65 nm for the spherical micelles and aggregates with a radius of ca. 200 nm. Transmission electron microscopy studies, after solvent evaporation, allowed direct visualization of the spherical micelles and showed the presence of aggregates (Fig. 7.3). The micelles possessed the proposed structure shown in Fig. 7.4.

Star structures have been prepared by means of an elegant approach that uses metal-polypyridine complexes as metalloinitiators. The first results in this area were reported in 1997 when Fe and Ru tribipyridyl complexes with electrophilic halogenomethyl functionalities (X=Cl, Br or I) were used as multifunctional initiators for the ring-opening polymerization of oxazolines to afford stars **7.30** and **7.31** (Eq. 7.7) [57].

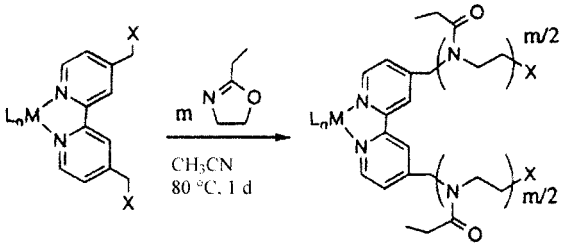

(7.7)

7.30 M=Fe
7.31 M=Ru

The violet Fe-based star polymers **7.30** were found to fragment readily and release the macroligands (Fig. 7.5), whereas the Ru-containing materials **7.31** were stable.

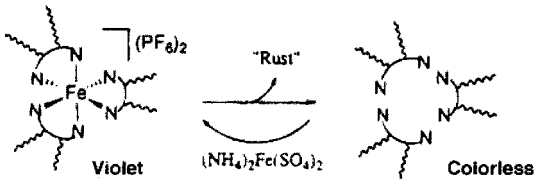

7.30

Fig. 7.5 Dissociation of star polymer **7.30** with iron as the core. (Adapted from [57])

An analogous approach to polyoxazoline polymerization was reported which uses tetrahedral Cu^{I} metalloinitiators **7.32** to create block structures **7.33** (Eq. 7.8) [58].

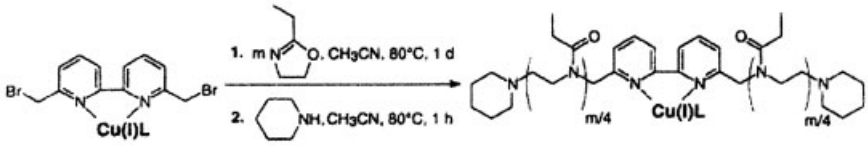

7.32 **7.33** (7.8)

The "divergent" metalloinitiator approach has been developed into a highly productive tool for the construction of a range of remarkable macromolecular structures [59–62]. Significantly, the metalloinitiators can be compatible with the highly

versatile atom-transfer radical polymerization technique, and this allows a variety of star structures to be prepared. In addition, a "convergent" approach to analogous materials involving the interaction of metal ions with macroligands has been developed. For example, reactions of bipyridyl macroligands with Ru, Fe, and Pt precursors yield the metal-centered heteroarm star polymers **7.34–7.36** with different transition metal centers as the core (Scheme 7.5) [61]. Materials with luminescent Eu complexes at block junctions and polyester arms have been similarly synthesized, and are of interest as their self-assembly should lead to materials with metals localized at microdomain boundaries [63].

Iron-centered six-arm star block copolymers **7.37** (Fig. 7.6) have been investigated in detail by small-angle X-ray scattering, TEM, and AFM [64]. When heated for ca. 2 days at 160 °C, thin films of the polymers form iron nanoclusters with diameters of ca. 20–40 nm (see TEM image, Fig. 7.7). This type of approach offers considerable potential for the single-step fabrication of nanoscale-patterned inorganic particles in polymer films.

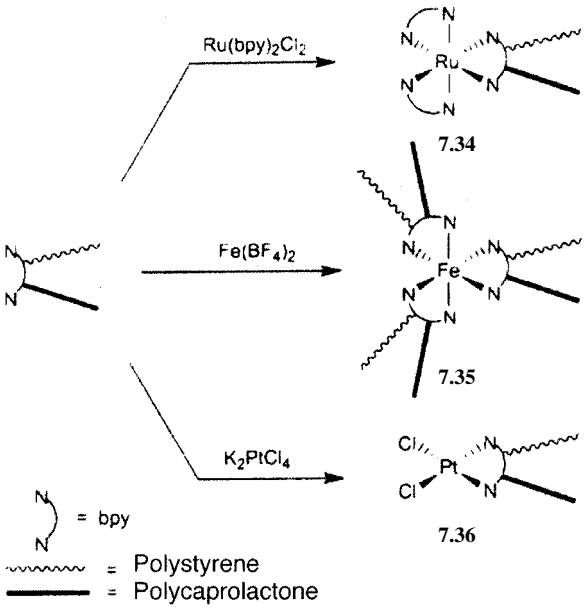

Scheme 7.5 (Adapted from [61])

7.3
Coordination Polymers Based on Schiff-Base Ligands

Schiff-base ligation has attracted significant attention as a method for creating coordination polymers with interesting morphological, catalytic, or conductive properties. For example, a series of well-characterized, thermotropic, liquid-crystalline

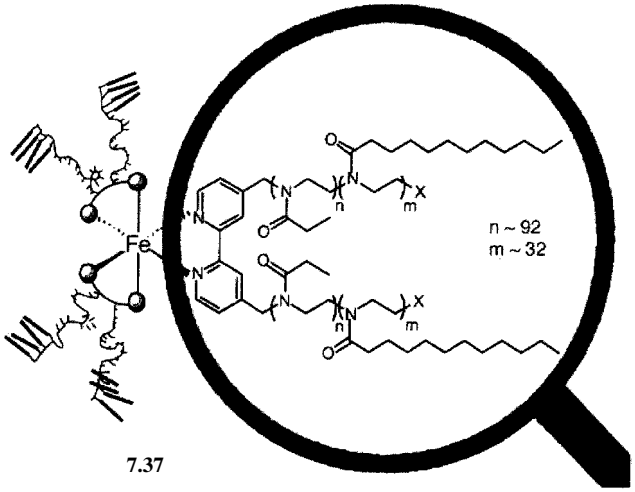

Fig. 7.6 Structure of six-arm star polymer **7.37** with an iron core. (Adapted from [64])

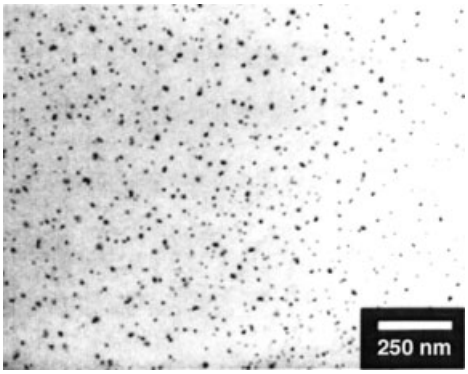

Fig. 7.7 TEM image of an annealed (160 °C) polymer film of **7.37** that shows the formation of small Fe clusters. (Adapted from [64])

coordination polymers **7.38–7.41** was described in the early 1990s [65–70]. Polymers **7.38**, which contain paramagnetic Cu^{II} centers, were prepared by interfacial polymerization between dihydroxy-functionalized Cu^{II} complexes and difunctional carboxylic acid chlorides. The liquid-crystalline properties were found to depend strongly on structural modifications involving the flexible spacer R and the substituents attached to nitrogen [65–67]. Analogous liquid-crystalline materials **7.39–7.41**, containing Ni^{II}, Pd^{II}, and V^{IV}, have been prepared by means of analogous approaches [68]. All of the polymers showed nematic phases and, in the case of oxovanadium materials **7.41**, smectic phases were also detected. The possibility of aligning paramagnetic polymers such as **7.38** and analogues thereof has received significant attention [69, 70].

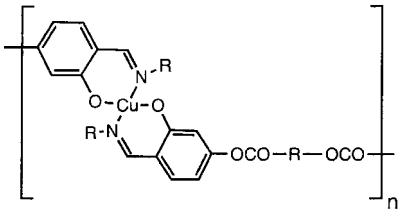

7.38

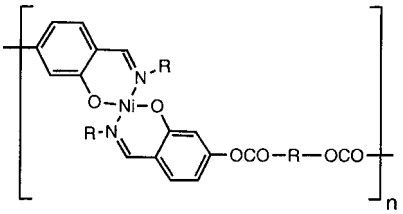

7.39

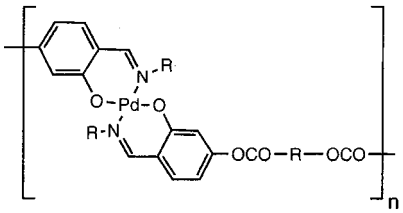

7.40

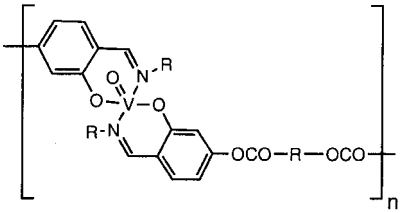

7.41

A wide range of well-characterized coordination polymers involving eight-coordinate d- and f-block metals based on Schiff-base ligation have also been described. Building on initial results in 1985, a series of high molecular weight, soluble Zr-polymers that utilize a bis(quadridentate) ligation to ensure kinetic stability was prepared and studied [71]. These materials are exemplified by the Zr-polymers **7.42**, which were prepared by the condensation procedure shown in Eq. 7.9 [72]. The materials proved to be soluble in solvents such as DMSO and NMP. After fractionation to remove oligomers, absolute molecular weights in the range M_n=6800–15,000 were determined by NMR end-group analysis. The molecular weights were also estimated by GPC with reference to polystyrene standards, which gave slightly higher values.

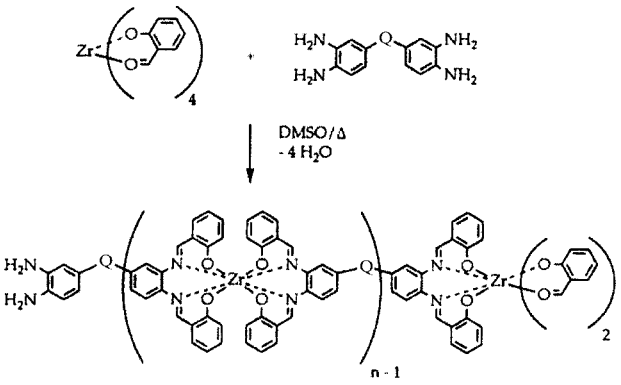

(7.9)

Q = —, CH_2, SO_2 **7.42**

Analogous procedures have been used to prepare materials containing metals such as Y^{III} (e.g. **7.43**, Scheme 7.6), La^{III}, Ce^{IV}, Eu^{III}, Yb^{III}, and Gd^{III} [72–78]. In particular, the yellow Y and Eu polymers have been examined in detail [77, 78]. Absolute molecular weights (M_n) of up to 21,600 have been determined by means of end-group analysis. The luminescence properties of the materials have been examined, and intrinsic viscosity measurements provided Mark-Houwink constants of $a = 0.52$ and $k = 0.066\ cm^3\ g^{-1}$. Mixed-metal copolymers were also prepared by means of the versatile polycondensation procedures. Conductivities of films of the Zr- and Ce-polymers were found to be ca. $10^{-7}\ Scm^{-1}$. Following doping with iodine, conductivities of up to $10^{-3}\ Scm^{-1}$ were obtained. Mixed-metal Eu/Y polyelectrolytes show enhanced luminescence relative to monomeric complexes due to a light-harvesting antenna effect [77]. Intramolecular energy transfer occurs from the Schiff-base ligand, which absorbs strongly in the near-UV/vis region, to the emitting Eu centers. The presence of Y apparently enhances luminescence, possibly by reducing Eu-Eu self-quenching.

Electropolymerization techniques have also been popular for the preparation of electrodes modified by thin films of Schiff-base metallopolymers for prospective electrocatalytic, chemical sensing, and electrochromic applications [79–85]. In

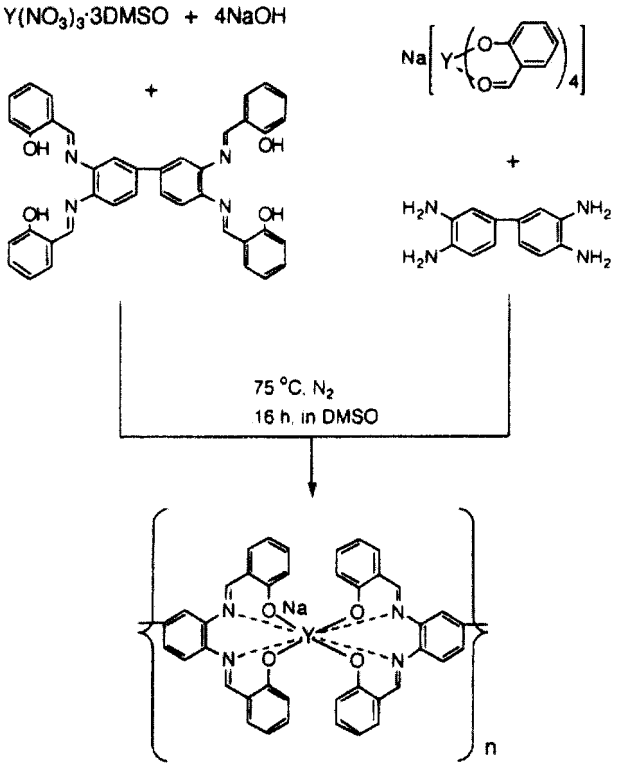

7.43

Scheme 7.6 (Adapted from [75])

many studies, the characterization has been limited to cyclic voltammetry and thin-film techniques; definitive structural analysis is generally difficult, as the resultant films are usually insoluble. Issues such as polymer chain length and the existence of structural defects, which may significantly influence electronic and optical properties, are therefore challenging to probe. Nevertheless, many very insightful studies have been performed, and the technique offers rich promise. A representative example is provided by the synthesis of the copper- or nickel-containing conjugated materials **7.44**, which were prepared by oxidative electropolymerization involving the coupling of phenyl ligands (Eq. 7.10) [82]. Evidence for the formation of the conductive polymer was provided by the increased electroactivity with each scan (Fig. 7.8).

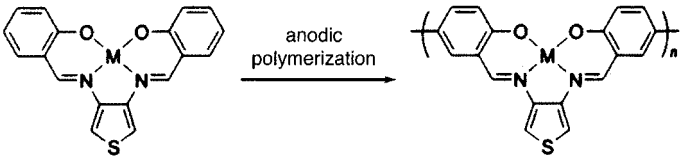

(7.10)

7.44

M = Cu^{+} or Ni^{2+}

In order to prepare highly conducting materials, redox-matching of the oxidation potentials of the organic polymer and the metal center has been productively utilized [83, 84]. For example, the thiophene-substituted Schiff-base cobalt com-

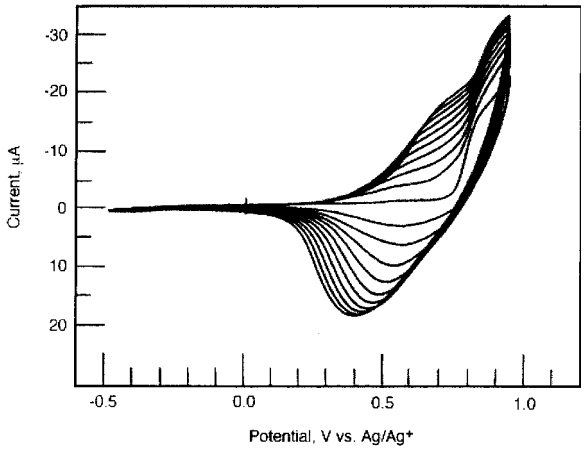

Fig. 7.8 The first ten repeated scans for the formation of polymer **7.44** (M = Cu) by oxidative electropolymerization on the working electrode. Electroactivity increases at ca. 0.6–0.7 V with each additional scan, indicating the progressive formation of a film of the metallopolymer on the electrode. Solution in CH_2Cl_2 (5×10^{-3} M in monomer) with $[Bu_4N][PF_6]$ as supporting electrolyte. Scan rate 100 mV s^{-1}. (Adapted from [82])

plex **7.45** can be prepared by treatment of a bis(salicylidene) ligand with Co^{II} salts (Eq. 7.11). Subsequent electropolymerization yields yellow films of polymer **7.46** on the Pt electrode surface (Eq. 7.12), which have been characterized by electrochemical, spectroelectrochemical, and in situ ESR measurements. In situ conductivity experiments utilizing 5 μm interdigitated microelectrodes have also been performed. Cyclic voltammetry showed overlapping broad waves for the redox processes associated with the Co^{II}/Co^{III} couple and the conjugated organic polymer backbone. The maximum conductivity detected was 44 Scm^{-1}. Decreased conductivity was detected in the presence of Lewis bases such as 2,6-lutidene due to coordination to the cobalt center and consequent lowering of the Co^{II}/Co^{III} redox potential [83, 84]. In addition to applications as sensors, cobalt polymers such as **7.46** are of interest as electrocatalysts for the reduction of oxygen. To this end, the facile electron transfer between the electrode surface and the catalytically active metal centers is believed to be highly advantageous [85].

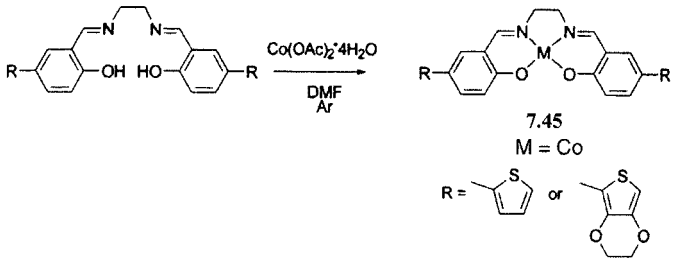

(7.11)

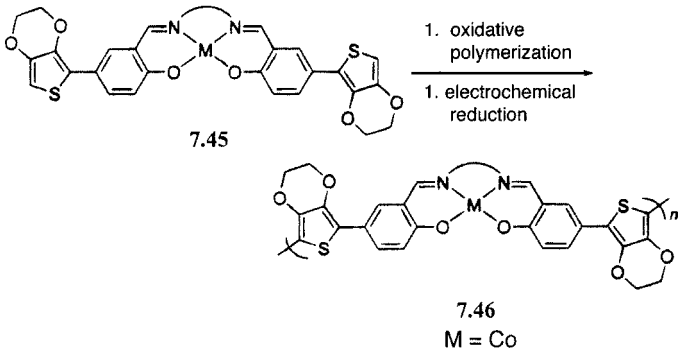

(7.12)

7.4
Coordination Polymers Based on Phthalocyanine Ligands and Related Macrocycles

Phthalocyanine-based polymers with "shish-kebab" type π-stacked structures, **7.47**, are generally prepared by two different routes. These are illustrated in Scheme 7.7, where L is typically a pyrazole, diisocyanide, or *p*-bipyridine, and a wide variety of metals (e.g. Fe, Ru, Os) and non-metals (e.g. Si, Ge) have been used. The

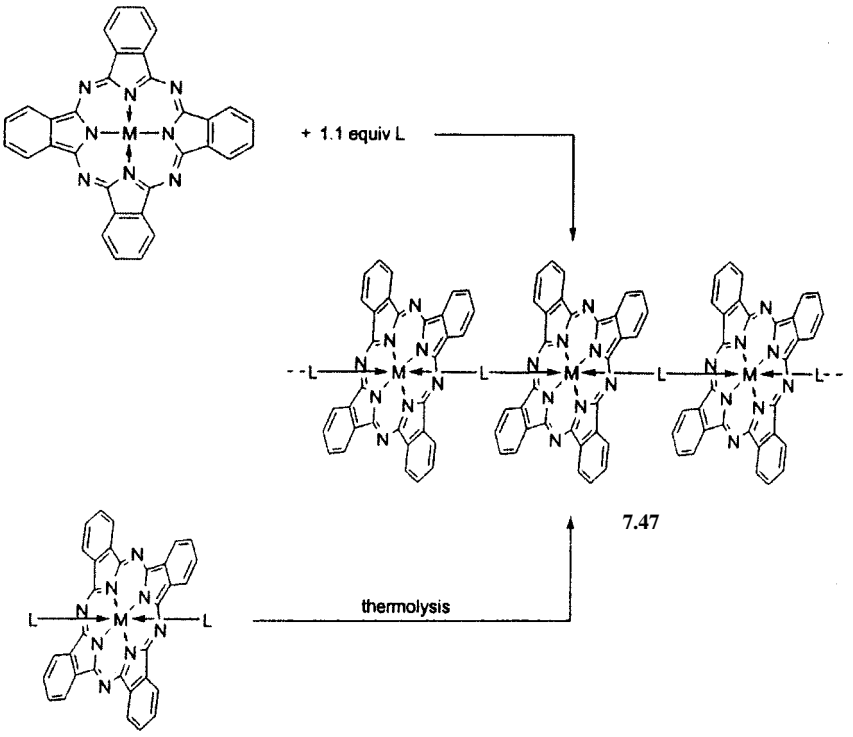

Scheme 7.7 (Adapted from [88])

materials have attracted considerable interest and significant electrical conductivities of up to ca. 0.1 S cm^{-1} have been detected for electrochemically or chemically doped materials [86, 87].

In general, due to the high skeletal rigidity of their structures, these materials are usually insoluble in solvents. Moreover, the coordination bonds that link the linear structures together are labile and dissociation can be facile; often monomeric metallophthalocyanines are reformed in the presence of strongly coordinating solvents. These materials, and related structures with similar characteristics derived from porphyrins, etc., are thus best regarded as having properties which place them at the periphery of the discussions of macromolecules covered in this book. For detailed information on these materials and the fascinating tunability of their electronic properties, the reader is therefore referred to a series of excellent reviews [86–88]. Similar arguments hold for some of the supramolecular materials possessing weak M–M interactions, which have stacked structures in the solid state but usually retain little structural integrity in solution, when dissolution is possible (Chapter 6, Section 6.5). Finally, however, it should be noted that in some rare cases, for example if flexible organic substituents are present on the periphery of the phthalocyanine ring, materials **7.47** can also be soluble (at least the low molecular weight fractions) [89].

7.5
Miscellaneous Coordination Polymers Based on Electropolymerized Thiophene Ligands

Electropolymerization techniques, which have been successfully used to prepare electrode films of metallopolymers, based on polypyridyl and Schiff-base ligation (see Sections 7.2 and 7.3), have also been shown to provide a versatile route to a variety of other interesting materials. An early example reported in 1994 is provided by Re polymers **7.48**, formed by anodic oxidation of a bis(thiazole) bearing thiophene substituents followed by complexation through treatment with $Re(CO)_5Cl$ and then $Ag[PF_6]$ (Scheme 7.8). The observed conductivities of **7.48** were, however, substantially lower than those of the uncomplexed material [90].

In 2001, Pd^{II} complexes of phosphinoterthiophene ligands were electropolymerized to afford insoluble polymers **7.49** (Scheme 7.9). These materials showed conductivities of up to 10^{-4} Scm^{-1}, and were characterized by techniques such as energy-dispersive X-ray microanalysis. Polymer **7.49** can be treated with donor ligands, such as isocyanides or phosphines, to cleave the chloride bridges that form crosslinks in order to yield soluble materials such as **7.50** [91].

Another example involves the preparation of novel polymers containing W calixarenes. Such materials, formed by the electropolymerization of species **7.51** (Scheme 7.10), show high conductivity values of up to 15.5 Scm^{-1}. It was possible to use the resultant polymers to specifically recognize *p*-xylene. For example, formation of the polymers with R=adamantyl in the presence of *p*-xylene led to films with a 10-fold increase in conductivity over those formed in the absence of xylene or in the presence of toluene [92].

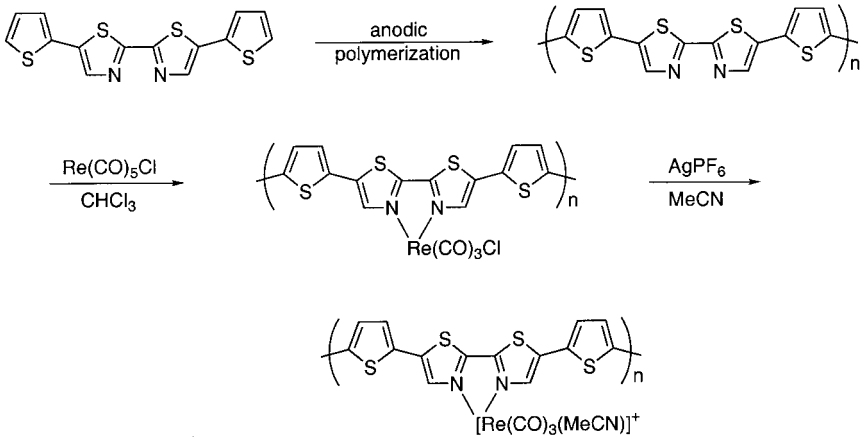

7.48

Scheme 7.8 (Adapted from [90])

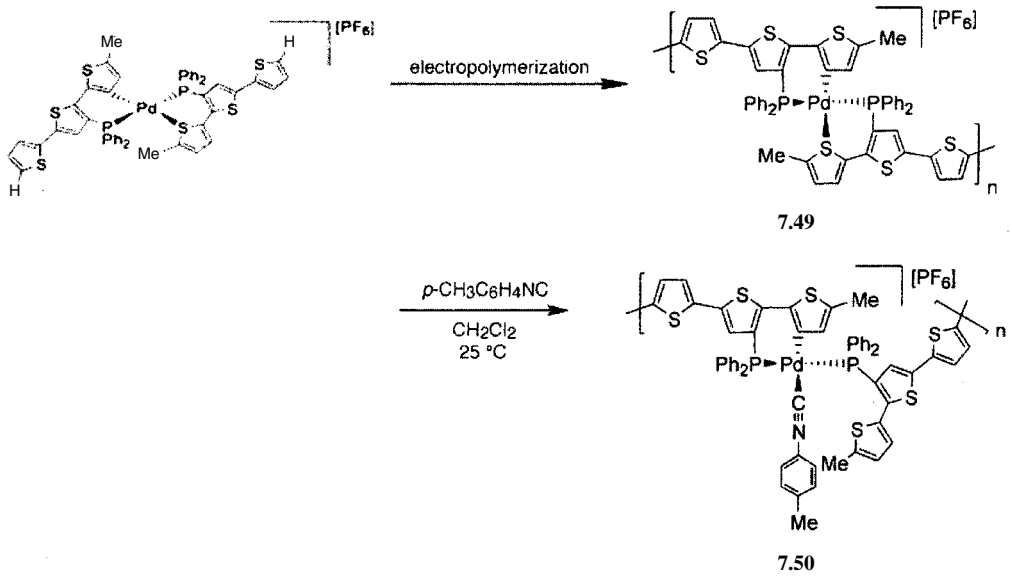

7.49

7.50

Scheme 7.9 (Adapted from [91])

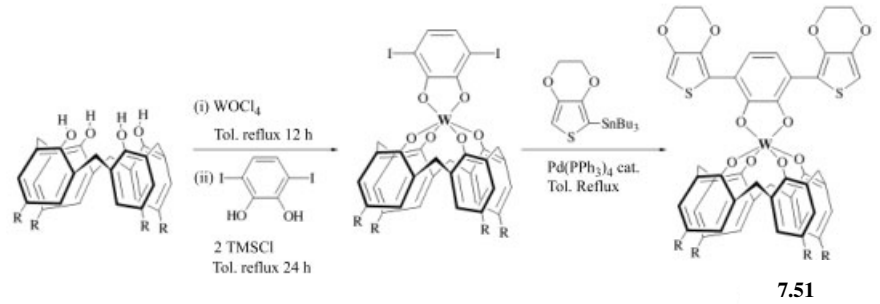

7.51

Scheme 7.10 (Adapted from [92])

Electrochemical methods have also been used to polymerize nickel dithiolene complexes with thiophene substituents in order to form conductive materials [93].

7.6 Coordination Polymers Based on DNA

DNA molecules are of great interest for use in nanoelectronic circuits, as their self-assembly and molecular recognition attributes may help to resolve the problem of wiring and positioning on the nanometer scale. The stacked aromatic bases of DNA have been proposed to function as a "π-way" for the transfer of elec-

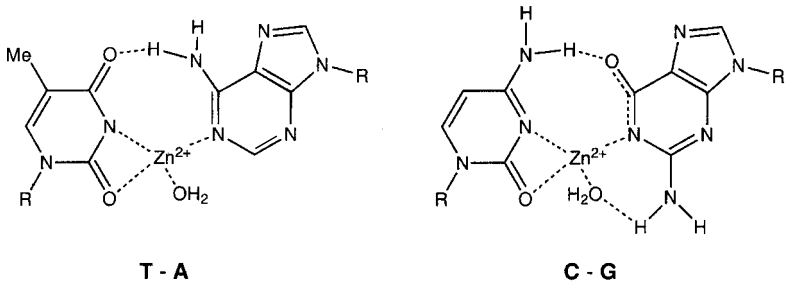

Fig. 7.9 Base pairing scheme for metallated DNA (T = tyrosine, A = adenine, C = cytosine, G = guanine)

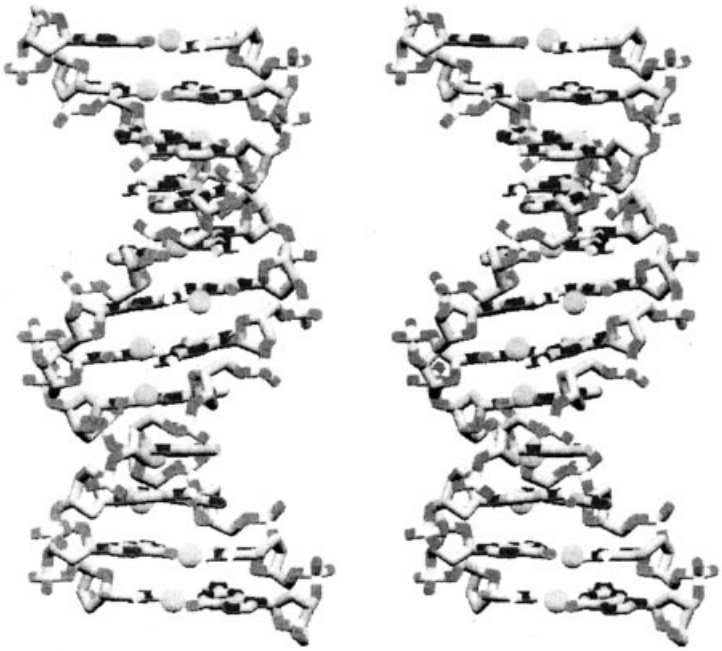

Fig. 7.10 Modelled structure of metallated (Zn) DNA. The Zn ions are shown as spheres that are buried in the center of the helix. (Adapted from [95])

trons but, although the issue is subject to intense debate, the overall behavior appears to be characteristic of a wide band-gap semiconductor. The coordination of metal ions to DNA has been seen as a possible methodology for altering the electronic properties in a controlled manner.

Metallation of DNA has been achieved by the addition of 0.1 mM Zn^{2+} at pH 9.0, whereby the imino protons of thymine and guanine are replaced (Fig. 7.9), as indicated by NMR data, and the estimated spacing of the Zn ions is ca. 4 Å (Fig. 7.10). Similar replacement is observed with Co^{2+} and Ni^{2+} [94]. Fluorescence decay mea-

surements of donor- and acceptor-labelled DNA provided evidence of more rapid electron transfer in the case of metallated (Zn) material [95]. In addition, electrical measurements on 15 μm strands of metallized and non-metallized DNA, positioned between lithographically patterned gold electrodes, have revealed a dramatic increase in conduction on metallization [96]. These exciting preliminary results suggest that metallated DNA has a potentially bright future in nanoelectronics.

7.7
Coordination Polymers Based on Other Lewis Acid/Lewis Base Interactions

The potential synthetic possibilities for the creation of coordination polymers are enormous. A variety of other types of coordination bonds have been used to create polymeric materials. In most cases, the bonds formed are sufficiently labile for depolymerization to occur in solution. For example, by layering a solution of one equivalent of bipyridine with a diborylferrocene, the coordination polymer **7.52** is formed as an insoluble black crystalline solid. Addition of picoline leads to chain cleavage and the formation of the monomeric adduct **7.53** (Eq. 7.13) [97]. Materials analogous to **7.52** have been prepared with pyrazine as the linker, and these dark-green materials show charge-transfer transitions from the iron to the electron-poor heteroaromatic ligand [98, 99].

Insoluble polymers based on bidentate M–S dithiolene and M–O dioxalato ligation have been the subject of numerous studies. Although these materials are, in general, poorly characterized they have, in some cases, been shown to exhibit promising conductive properties [100, 101]. Polymers with M–S and M–N/O ligation have also been prepared on surfaces [102, 103]. Monodentate M–N ligation has been used to prepare remarkable nanoscopic 3-D assemblies **7.54** by means of rigid, multifunctional precursors (Eq. 7.14) [104].

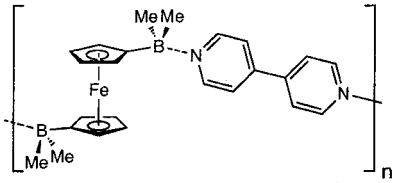

7.52

bipy ⇌ picoline (7.13)

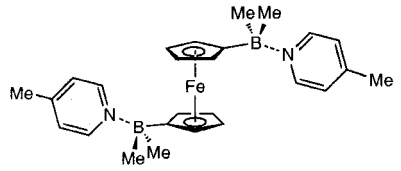

7.53

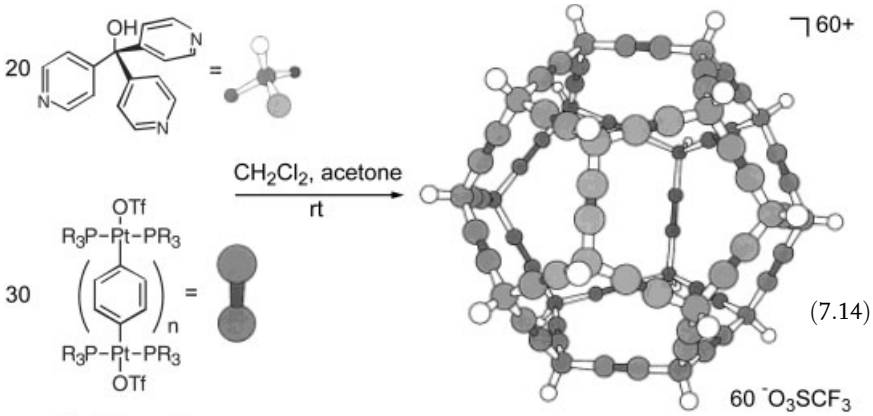

(7.14)

7.54

R = Et, n = 1, 99 %, D = ~5.5 nm
R = Ph, n = 2, 99 %, D = ~7.5 nm

Ring-opening polymerization (ROP) approaches have also been reported for the formation of coordination polymers. An early report in 1960 described the formation of beryllium polymers with β-diketonate ligation, such as **7.55**, by thermal ROP (Eq. 7.15) [105]. Structural characterization of the polymers was based on IR and elemental analysis data. Based on their intrinsic viscosities in benzene and mechanical properties, it was inferred that the polymers were of high molecular weight. More recently, coordination polymers based on metal-phosphine ligation have been prepared. For example, ROP of **7.56** in the solid state occurs to form the silver polymer **7.57** (Eq. 7.16) [106].

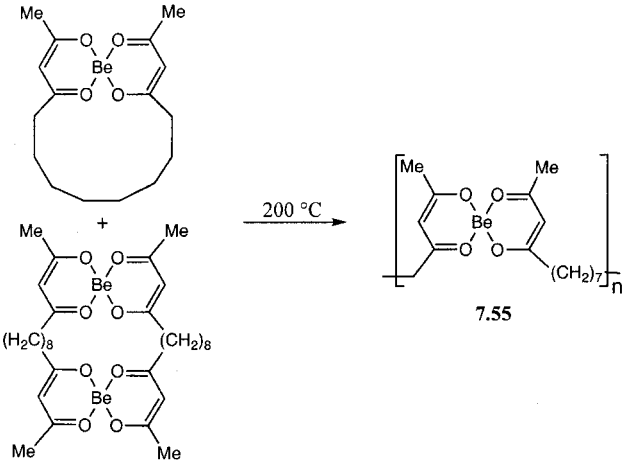

(7.15)

7.55

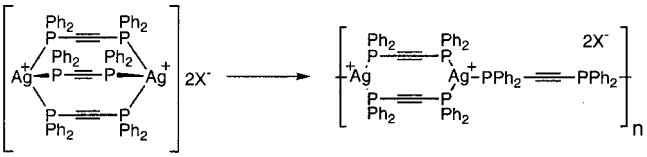

(7.16)

7.56 **7.57**

X = OTf, NO_3, BF_4

Analogous processes have been identified in the formation of gold polymers **7.58** [107]. Gold polymers with two-coordinate metal centers and mixed P/S ligation, which exist as macrocycles in solution, have also been prepared, and the insolubility of many of these materials has been traced to the presence of crystallographically characterized intermolecular Au · · · S and S · · · S interactions [108].

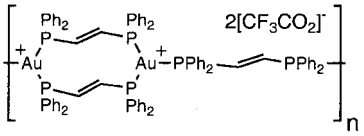

7.58

7.8 References

1 (a) R. D. Archer, *Coord. Chem. Rev.* **1993**, *128*, 49; (b) B. M. Foxman, S. W. Gersten, *Coordination Polymers*, in *Encycl. Polym. Sci. Eng.* **1987**, *4*, 175; (c) F. Ciardelli, E. Tsuchida, D. Wöhle (Eds.) *Macromolecule-Metal-Complexes*, Springer-Verlag, New York, 1996; (d) R. D. Archer, *Inorganic and Organometallic Polymers*, Wiley-VCH, New York, 2001.

2 H. Shirakawa, *Angew. Chem. Int. Ed.* **2001**, *40*, 2574.

3 G. MacDiarmid, *Angew. Chem. Int. Ed.* **2001**, *40*, 2581.

4 A. J. Heeger, *Angew. Chem. Int. Ed.* **2001**, *40*, 2591.

5 J. H. Burroughes, D. D. C. Bradley, A. R. Brown, R. N. Marks, K. Mackay, R. H. Friend, P. L. Burns, A. B. Holmes, *Nature* **1990**, *347*, 539.

6 A. Kraft, A. C. Grimsdale, A. B. Holmes, *Angew. Chem. Int. Ed.* **1998**, *37*, 402.

7 U. S. Schubert, C. Eschbaumer, *Angew. Chem. Int. Ed.* **2002**, *41*, 2892.

8 K. M. Maness, R. H. Terrill, T. J. Meyer, R. W. Murray, R. M. Wightman, *J. Am. Chem. Soc.* **1996**, *118*, 10609.

9 C. M. Elliott, F. Pichot, C. J. Bloom, L. S. Rider, *J. Am. Chem. Soc.* **1998**, *120*, 6781.

10 S. Kelch, M. Rehahn, *Macromolecules* **1997**, *30*, 6185.

11 S. Kelch, M. Rehahn, *Macromolecules* **1998**, *31*, 4102.

12 S. Kelch, M. Rehahn, *Macromolecules* **1999**, *32*, 5818.

13 M. Schütte, D. G. Kurth, M. R. Linford, H. Cölfen, H. Möhwald, *Angew. Chem. Int. Ed.* **1998**, *37*, 2891.

14 F. Caruso, C. Schüler, D. G. Kurth, *Chem. Mater.* **1999**, *11*, 3394.

15 D. G. Kurth, R. Osterhout, *Langmuir* **1999**, *15*, 4842.

16 D. G. Kurth, M. Schütte, J. Wen, *Coll. Surf. A* **2002**, *198*, 633.
17 J.-K. Lee, D. Yoo, M. F. Rubner, *Chem. Mater.* **1997**, *9*, 1710.
18 A. Wu, D. Yoo, J.-K. Lee, M. F. Rubner, *J. Am. Chem. Soc.* **1999**, *121*, 4883.
19 T. Cassagneau, J. H. Fendler, S. A. Johnson, T. E. Mallouk, *Adv. Mater.* **2000**, *12*, 1363.
20 W. Y. Ng, X. Gong, W. K. Chan, *Chem. Mater.* **1999**, *11*, 1165.
21 S. C. Yu, S. Hou, W. K. Chan, *Macromolecules* **2000**, *33*, 3259.
22 L. S. M. Lam, S. H. Chan, W. K. Chan, *Macromol. Rapid Commun.* **2000**, *21*, 1081.
23 S. C. Yu, X. Gong, W. K. Chan, *Macromolecules* **1998**, *31*, 5639.
24 T. Yamamoto, Y. Yoneda, T. Maruyama, *J. Chem. Soc., Chem. Commun.* **1992**, 1652.
25 T. Yamamoto, T. Maruyama, Z. Zhou, T. Ito, T. Fukuda, Y. Yoneda, F. Begum, T. Ikeda, S. Sasaki, H. Takezoe, A. Fukuda, K. Kubota, *J. Am. Chem. Soc.* **1994**, *116*, 4832.
26 T. Yamamoto, Z. Zhou, T. Kanbara, T. Maruyama, *Chem. Lett.* **1990**, 223.
27 T. Yamamoto, T. Maruyama, T. Ikeda, M. Sisido, *J. Chem. Soc., Chem. Commun.* **1990**, 1306.
28 S. C. Rasmussen, D. W. Thompson, V. Singh, J. D. Petersen, *Inorg. Chem.* **1996**, *35*, 3449.
29 Z. Peng, L. Yu, *J. Am. Chem. Soc.* **1996**, *118*, 3777.
30 Z. Peng, A. R. Gharavi, L. Yu, *J. Am. Chem. Soc.* **1997**, *119*, 4622.
31 Q. Wang, L. M. Wang, L. Yu, *J. Am. Chem. Soc.* **1998**, *120*, 12860.
32 Q. Wang, L. Yu, *J. Am. Chem. Soc.* **2000**, *122*, 11806.
33 W. Y. Ng, W. K. Chan, *Adv. Mater.* **1997**, *9*, 716.
34 W. K. Chan, P. K. Ng, X. Gong, S. Hou, *J. Mater. Chem.* **1999**, *9*, 2103.
35 S. C. Yu, S. Hou, W. K. Chan, *Macromolecules* **1999**, *32*, 5251.
36 P. K. Ng, X. Gong, S. H. Chan, L. S. M. Lam, W. K. Chan, *Chem. Eur. J.* **2001**, *7*, 4358.
37 (a) K. D. Ley, C. E. Whittle, M. D. Bartberger, K. S. Schanze, *J. Am. Chem. Soc.* **1997**, *119*, 3423; (b) K. D. Ley, K. S. Schanze, *Coord. Chem. Rev.* **1998**, *171*, 287; (c) K. A. Walters, D. M. Dattelbaum, K. D. Ley, J. R. Schoonover, T. J. Meyer, K. S. Schanze, *Chem. Commun.* **2001**, 1834.
38 T. Pautzsch, E. Klemm, *Macromolecules* **2001**, *35*, 1569.
39 S. S. Zhu, T. M. Swager, *Adv. Mater.* **1996**, *8*, 497.
40 K. A. Walters, L. Trouillet, S. Guillerez, K. S. Schanze, *Inorg. Chem.* **2000**, *39*, 5496.
41 J. Hjelm, E. C. Constable, E. Figgemeier, A. Hagfeldt, R. Handel, C. E. Housecroft, E. Mukhtar, E. Schofield, *Chem. Commun.* **2002**, 284.
42 C. G. Cameron, P. G. Pickup, *Chem. Commun.* **1997**, 303.
43 C. G. Cameron, P. G. Pickup, *J. Am. Chem. Soc.* **1999**, *121*, 11773.
44 C. G. Cameron, P. G. Pickup, *J. Am. Chem. Soc.* **1999**, *121*, 7710.
45 U. Velten, M. Rehahn, *Chem. Commun.* **1996**, 2639.
46 U. Velten, M. Rehahn, *Macromol. Chem. Phys.* **1998**, *199*, 127.
47 S. Bernhard, K. Takada, D. Jenkins, H. D. Abruña, *Inorg. Chem.* **2002**, *41*, 765.
48 S. S. Zhu, T. M. Swager, *J. Am. Chem. Soc.* **1997**, *119*, 12568.
49 J. Buey, T. M. Swager, *Angew. Chem. Int. Ed.* **2000**, *39*, 608.
50 B. Wang, M. R. Wasielewski, *J. Am. Chem. Soc.* **1997**, *119*, 12.
51 C. D. Eisenbach, A. Göldel, M. Terskan-Reinold, U. S. Schubert, *Macromol. Chem. Phys.* **1995**, *196*, 1077.
52 C. D. Eisenbach, A. Göldel, M. Terskan-Reinold, U. S. Schubert, *Colloid Polym. Sci.* **1998**, *276*, 780.
53 C. D. Eisenbach, A. Göldel, M. Terskan-Reinold, U. S. Schubert, *Elastomere und Kunststoffe* **1998**, *51*, 422.
54 C. D. Eisenbach, U. S. Schubert, G. R. Baker, G. R. Newkome, *J. Chem. Soc., Chem. Commun.* **1995**, 69.
55 A. Lavalette, J. Hamblin, A. Marsh, D. M. Haddleton, M. J. Hannon, *Chem. Commun.* **2002**, 3040.

56 J. F. Gohy, B. G. G. Lohmeijer, U. S. Schubert, *Macromolecules* **2002**, *35*, 4560.

57 J. J. S. Lamba, C. L. Fraser, *J. Am. Chem. Soc.* **1997**, *119*, 1801.

58 G. Hochwimmer, O. Nuyken, U. S. Schubert, *Macromol. Rapid Commun.* **1998**, *19*, 309.

59 J. E. McAlvin, C. L. Fraser, *Macromolecules* **1999**, *32*, 1341.

60 C. L. Fraser, A. P. Smith, *J. Polym. Sci. Polym. Chem.* **2000**, *38*, 4704.

61 A. P. Smith, C. L. Fraser, *Macromolecules* **2002**, *35*, 594.

62 U. S. Schubert, M. Heller, *Chem. Eur. J.* **2001**, *7*, 5253.

63 J. L. Bender, P. S. Corbin, C. L. Fraser, D. H. Metcalf, F. S. Richardson, E. L. Thomas, A. M. Urbas, *J. Am. Chem. Soc.* **2002**, *124*, 8526.

64 C. Park, J. E. McAlvin, C. L. Fraser, E. L. Thomas, *Chem. Mater.* **2002**, *14*, 1225.

65 M. Marcos, L. Oriol, J. L. Serrano, P. J. Alonso, J. A. Puértolas, *Macromolecules* **1990**, *23*, 5187.

66 U. Caruso, A. Roviello, A. Sirigu, *Macromolecules* **1991**, *24*, 2606.

67 M. Marcos, L. Oriol, J. L. Serrano, *Macromolecules* **1992**, *25*, 5362.

68 U. Caruso, A. Roviello, A. Sirigu, C. Troise, *Macromolecules* **1998**, *31*, 1439.

69 J. S. Moore, S. I. Stupp, *Polym. Bull.* **1988**, *19*, 251.

70 L. Oriol, J. L. Serrano, *Adv. Mater.* **1995**, *7*, 348.

71 (a) R. D. Archer, M. L. Illingsworth, D. N. Rau, C. J. Hardiman, *Macromolecules* **1985**, *18*, 1371; (b) R. D. Archer, B. Wang, *Inorg. Chem.* **1990**, *29*, 39; (c) R. D. Archer, *Coord. Chem. Rev.* **1993**, *128*, 49.

72 J. A. Cronin, S. M. Palmer, R. D. Archer, *Inorg. Chim. Acta* **1996**, *251*, 81.

73 H. Chen, J. A. Cronin, R. D. Archer, *Macromolecules* **1994**, *27*, 2174.

74 R. D. Archer, A. Lauterbach, V. O. Ochaya, *Polyhedron* **1994**, *13*, 2043.

75 H. Chen, R. D. Archer, *Macromolecules* **1995**, *28*, 1609.

76 H. Chen, J. A. Cronin, R. D. Archer, *Inorg. Chem.* **1995**, *34*, 2306.

77 H. Chen, R. D. Archer, *Macromolecules* **1996**, *29*, 1957.

78 R. D. Archer, H. Chen, L. C. Thompson, *Inorg. Chem.* **1998**, *37*, 2089.

79 C. P. Horwitz, R. W. Murray, *Mol. Cryst. Liq. Cryst. Sci. Tech. Sect. A* **1988**, *160*, 389.

80 P. Audebert, P. Capdevielle, M. Maumy, *New J. Chem.* **1992**, *16*, 697.

81 P. Capdevielle, M. Maumy, P. Audebert, B. Plaza, *New J. Chem.* **1994**, *18*, 519.

82 J. L. Reddinger, J. R. Reynolds, *Macromolecules* **1997**, *30*, 673.

83 R. P. Kingsborough, T. M. Swager, *Adv. Mater.* **1998**, *10*, 1100.

84 R. P. Kingsborough, T. M. Swager, *J. Am. Chem. Soc.* **1999**, *121*, 8825.

85 R. P. Kingsborough, T. M. Swager, *Chem. Mater.* **2000**, *12*, 872.

86 T. J. Marks, *Angew. Chem. Int. Ed. Engl.* **1990**, *29*, 857.

87 M. Hanack, M. Lang, *Adv. Mater.* **1994**, *6*, 819.

88 R. P. Kingsborough, T. M. Swager, *Prog. Inorg. Chem.* **1999**, *48*, 171.

89 M. Hanack, A. Hirsch, H. Lehmann, *Angew. Chem. Int. Ed. Engl.* **1990**, *29*, 1467.

90 M. O. Wolf, M. S. Wrighton, *Chem. Mater.* **1994**, *6*, 1526.

91 O. Clot, M. O. Wolf, B. O. Patrick, *J. Am. Chem. Soc.* **2001**, *123*, 9963.

92 A. Vigalok, Z. Zhu, T. M. Swager, *J. Am. Chem. Soc.* **2001**, *123*, 7917.

93 C. L. Kean, P. G. Pickup, *Chem. Commun.* **2001**, 815.

94 J. S. Lee, L. J. P. Latimer, R. S. Reid, *Biochem. Cell Biol.* **1993**, *71*, 162.

95 P. Aich, S. L. Labiuk, L. W. Tari, L. J. T. Delbaere, W. J. Roesler, K. J. Falk, R. P. Steer, J. S. Lee, *J. Mol. Biol.* **1999**, *294*, 477.

96 A. Rakitin, P. Aich, C. Papadopoulos, Y. Kobzar, A. S. Vedeneev, J. S. Lee, J. M. Xu, *Phys. Rev. Lett.* **2001**, *86*, 3670.

97 M. Fontani, F. Peters, W. Scherer, W. Wachter, M. Wagner, P. Zanello, *Eur. J. Inorg. Chem.* **1998**, 1453.

98 M. Grosche, E. Herdtweck, F. Peters, M. Wagner, *Organometallics* **1999**, *18*, 4669.

99 S. Gou, F. Peters, F. F. de Biani, J. W. Bats, E. Herdtweck, P. Zanello, M. Wagner, *Inorg. Chem.* **2001**, *40*, 4928.

100 C.W. Dirk, M. Bousseau, P.H. Barrett, F. Moreas, F. Wudl, A.J. Heeger, *Macromolecules* **1986**, *19*, 266.
101 For an excellent overview of this area, see: R.P. Kingsborough, T.M. Swager, *Prog. Inorg. Chem.* **1999**, *48*, 123–130.
102 M. Pyrasch, D. Amirbeyki, B. Tieke, *Adv. Mater.* **2001**, *13*, 1188.
103 D.L. Thomsen III, T. Phely-Bobin, F. Papadimitrakopoulos, *J. Am. Chem. Soc.* **1998**, *120*, 6177.
104 B. Olenyuk, M.D. Levin, J.A. Whiteford, J.E. Shield, P.J. Stang, *J. Am. Chem. Soc.* **1999**, *121*, 10434.
105 R.W. Kluiber, J.W. Lewis, *J. Am. Chem. Soc.* **1960**, *82*, 5777.
106 E. Lozano, M. Nieuwenhuyzen, S.L. James, *Chem. Eur. J.* **2001**, *7*, 2644.
107 M.C. Brandys, R.J. Puddephatt, *J. Am. Chem. Soc.* **2001**, *123*, 4839.
108 W.J. Hunks, M.C. Jennings, R.J. Puddephatt, *Chem. Commun.* **2002**, 1834.

8
Metallodendrimers

8.1
Introduction

Since their discovery in the late 1970s to early 1980s [1–3], scientific interest in dendrimers – well-defined, highly branched and regularly repeating 3-D macromolecular architectures – has blossomed [4–8]. Different synthetic approaches that involve either "divergent" [1–4] or "convergent" [9–12] strategies are possible, and structures that involve a core and various numbers of layers or "generations" can thereby be constructed (see earlier discussion in Chapter 1, Section 1.2.6) [4–8]. The introduction of metals into such structures to create "metallodendrimers" offers many additional possibilities for applications as functional materials. For example, structures with metal-containing cores are of interest as models of biological systems such as metalloenzymes, surface-metallized architectures have potential for sensing and catalytic applications, and materials with metals distributed throughout the structure can exhibit antenna effects and have possible uses in light-harvesting. Metallodendrimers can be subdivided on the basis of the location of the metallic moiety, which can be present in the core, on the surface, or throughout the structure.

Since the first examples were described in the early 1990s, a vast range of metallodendritic materials have been reported [13–17]. In keeping with the philosophy of other chapters, the survey here is not intended to be rigorously exhaustive in terms of listing every metallodendrimer reported in the literature, but instead aims to illustrate the most important structural classes of these materials. Moreover, where possible, attention is focussed on examples where studies of properties and potential functions have been performed.

As a result of their ready solubility, dendritic materials can be analyzed by means of standard polymer characterization techniques, such as NMR and GPC. However, despite the excellent characterization that pervades the materials discussed in this chapter, it should be noted that with the widespread introduction of mass spectrometric techniques that can analyze such macromolecules, the structural perfection assumed in many depictions of dendrimers has been shown to be highly idealized. Indeed, spectrometric analysis of many samples has revealed that imperfections and defects are, in fact, very common.

Synthetic Metal-Containing Polymers. Ian Manners

ISBN: 3-527-29463-5

8.2
Metallodendrimers with Metals in the Core

Representative examples of dendrimers with metal-containing cores include the materials **8.1–8.6**, which were reported in the mid- to late 1990s. For example, first- (**8.1**), second- (**8.2**), third- (**8.3**), and fourth- (**8.4**) generation zinc porphyrin dendrimers (M = Zn) have been prepared by a convergent synthesis approach [18, 19]. Although the electrochemical and photophysical nature of the metalloporphyrin core was found to be preserved in the resultant materials, the rate of interfacial electron transfer was found to be reduced due to the separation of the electroactive centers from the electrode surface. Second- (**8.5**) and third-generation (**8.6**)

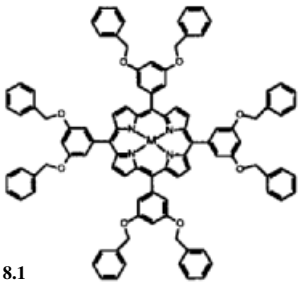

8.1

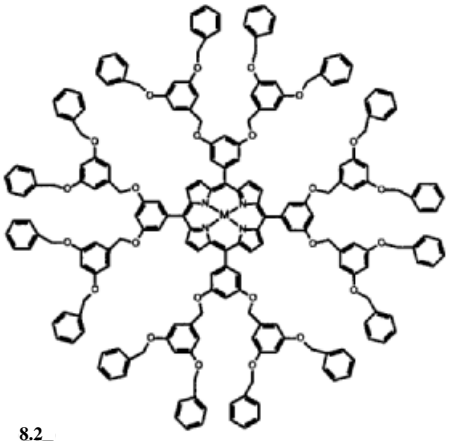

8.2

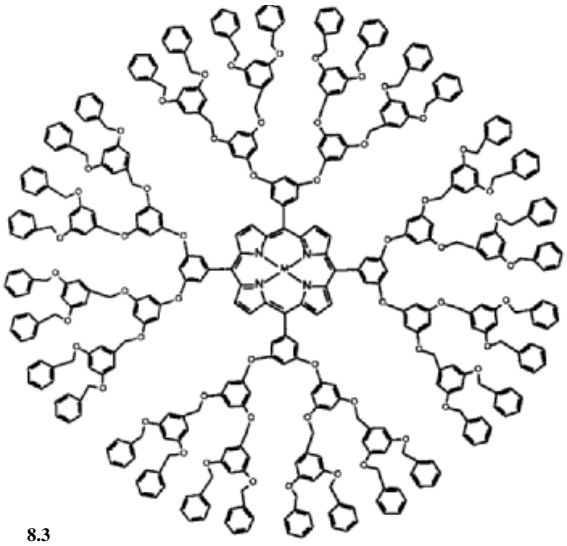

8.3

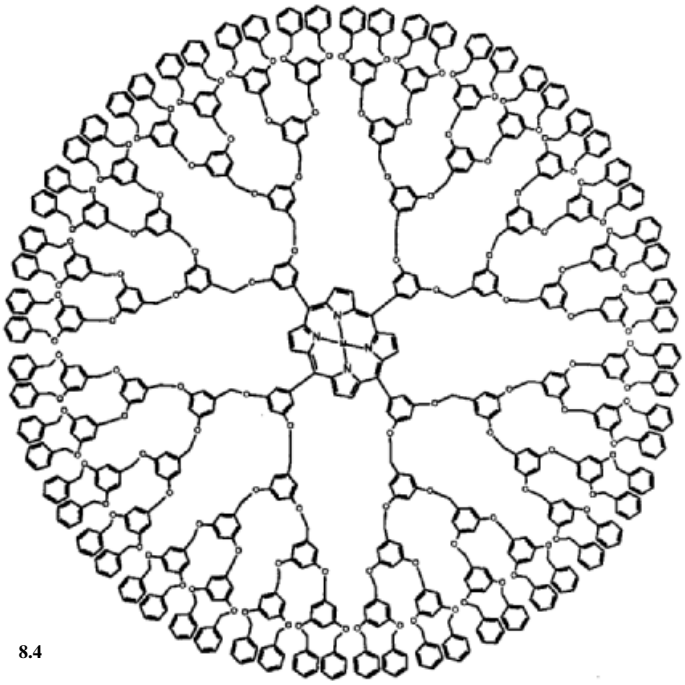

8.4

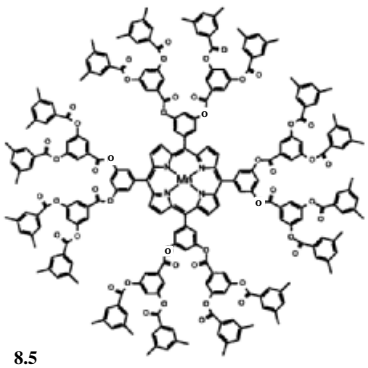

8.5

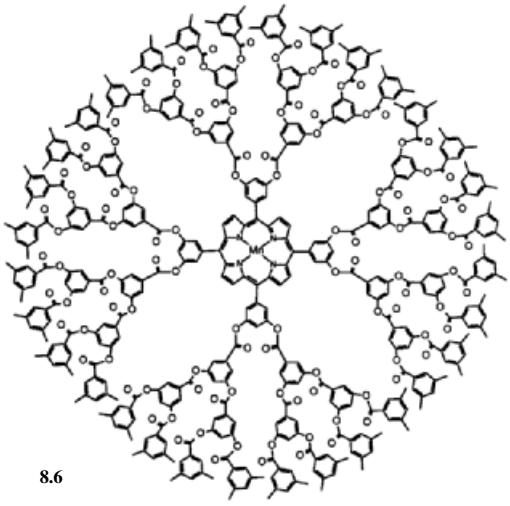

8.6

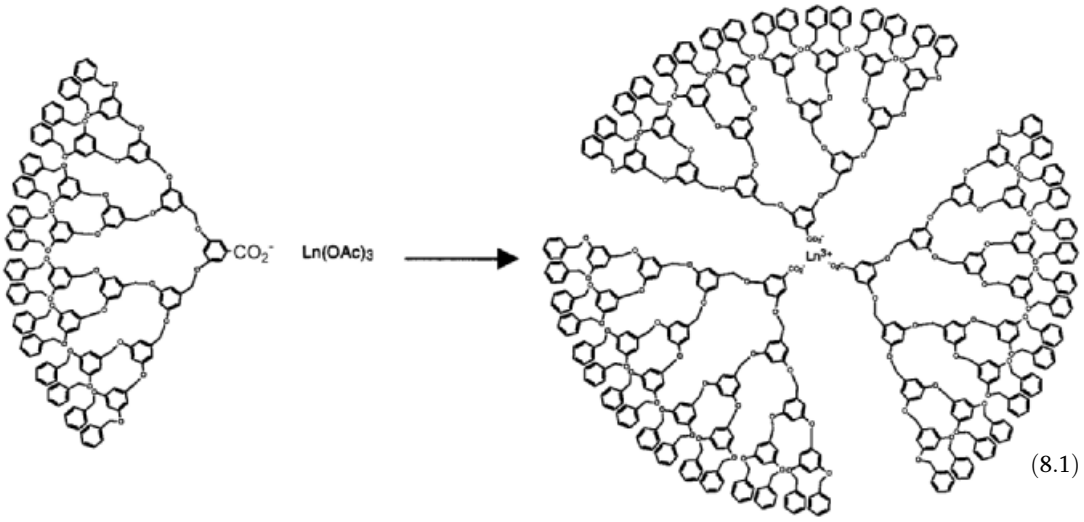

(8.1)

8.7 Ln = Er, Eu, Tb

Mn-containing dendrimers have been prepared and explored as selective oxidation catalysts [20, 21]. Improved regioselectivity was observed with various alkene substrates compared to that achieved with the non-dendronized metalloporphyrin.

Lanthanide-containing dendrimers such as **8.7** have been prepared by a convergent approach that uses polybenzyl ether dendrons and carboxylate anion coordination to the central Er^{3+}, Tb^{3+} or Eu^{3+} cations (Eq. 8.1) [22]. The luminescence of these metallodendrimers has been investigated and was found to be enhanced by both antenna effects involving the polybenzyl ether framework and site-isolation effects that hinder self-quenching processes.

Novel metallodendrimers **8.8** with a redox-active Fe_4S_4 cluster at the core have been prepared by a thiolate exchange reaction that involves the treatment of the dianion $[Fe_4S_4(S\text{-}^tBu)_4]^{2-}$ with four equivalents of thiol-terminated dendrons [23–28]. The molecular weights of these interesting materials were characterized by vapor-pressure osmometry. Studies of encapsulated electroactive moieties are of importance in order to understand biological electron transfer. Metallodendrimers of type **8.8** bear an intriguing resemblance to metalloproteins and this has led to significant effort aimed at obtaining a detailed understanding of their properties. These cluster-core dendrimers show an increasingly negative reduction potential for the one-electron reduction of the Fe_4S_4 unit as the number of dendrimer generations is increased. In addition, at the same time, the rate of electron transfer is found to decrease. The results are understandable in terms of the known sensitivity of the redox couple to the electronic nature of the thiolate substituents and the "insulating effect" of an increased number of generations of dendritic ligation.

Conformational analyses by means of a quench dynamics technique have been performed on the Fe_4S_4-core metallodendrimers of type **8.8**, which possess a relatively flexible structure, as well as on analogous materials with more rigid dendritic arms that contain acetylenic linkers between the aryl groups. The Fe_4S_4 cluster core was found to be centrally located and, thus, more efficiently encapsulated in the case of the low-energy conformers of the more rigid structure (Fig. 8.1a). In contrast, the cluster moiety was found to be substantially offset from the center in the low-energy conformers of the flexible metallodendrimer **8.8** (see Fig. 8.1b) [28]. Interestingly, measurements of the relative electron-transfer rates to the redox-active Fe_4S_4 cores in the dendrimers showed that for dendrimers of the same radius of gyration, the rate for the more rigid structure is significantly faster.

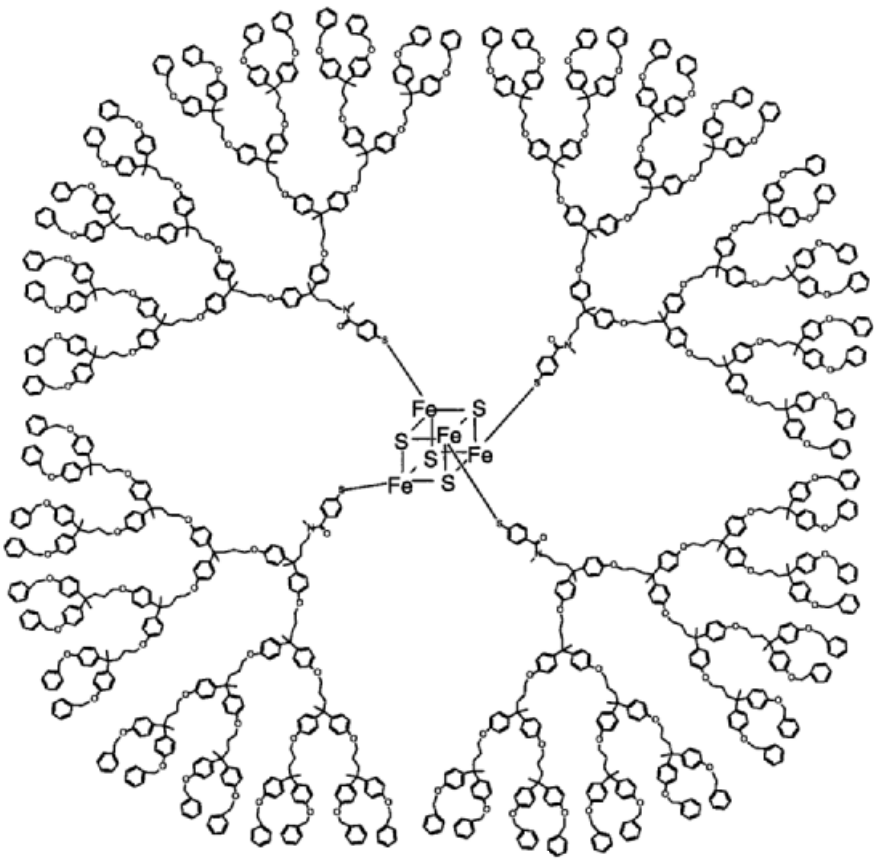

8.8

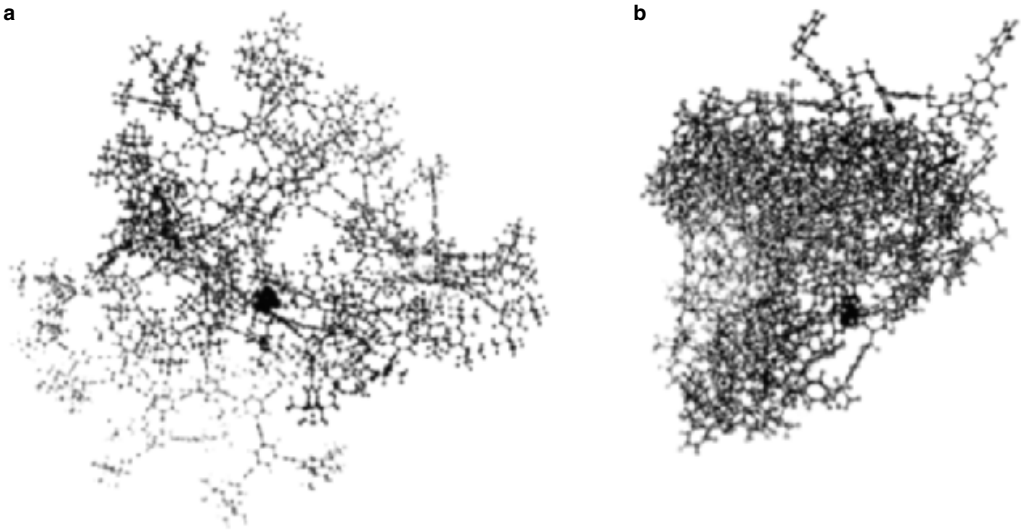

Fig. 8.1 Ball-and-stick models of the lowest-energy conformers for models of 4th generation Fe_4S_4-core dendrimers with **(a)** rigid and **(b)** more flexible arms. The core is the small dark region. (Reproduced from [28])

Another interesting approach to the synthesis of metal-cluster core dendrimers involves the displacement of the acetonitrile ligand from the rhenium cluster dication $[Re_6Se_6(NCMe)_6]^{2+}$ with pyridyl-functionalized dendrons. The resultant structures **8.9** possess a hexanuclear cluster core and exhibit electronic transitions that are very dependent on the structure of the dendrons [29].

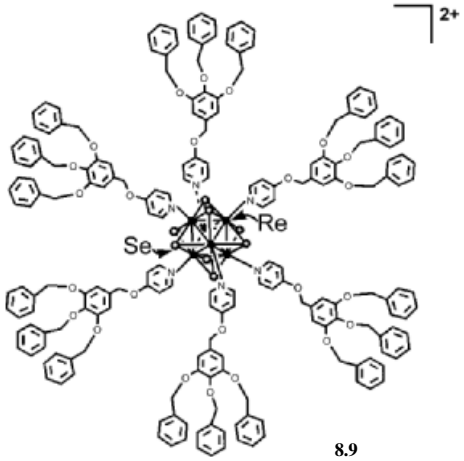

8.9

8.3
Metallodendrimers with Metals at the Surface

A wide range of dendrimers containing metal centers at the periphery have been reported. Ni-containing dendrimers **8.10** up to the second generation have been synthesized (Eq. 8.2) and have been shown to function as homogeneous catalysts for the Kharasch addition of perhalogenated alkanes across the C=C double bond of alkenes [30–32]. Metallodendrimers **8.10** were found to be less active than a monomeric analogue; however, a potential advantage of the dendritic catalyst is that it can be easily separated from the products, which offers the possibility of recycling.

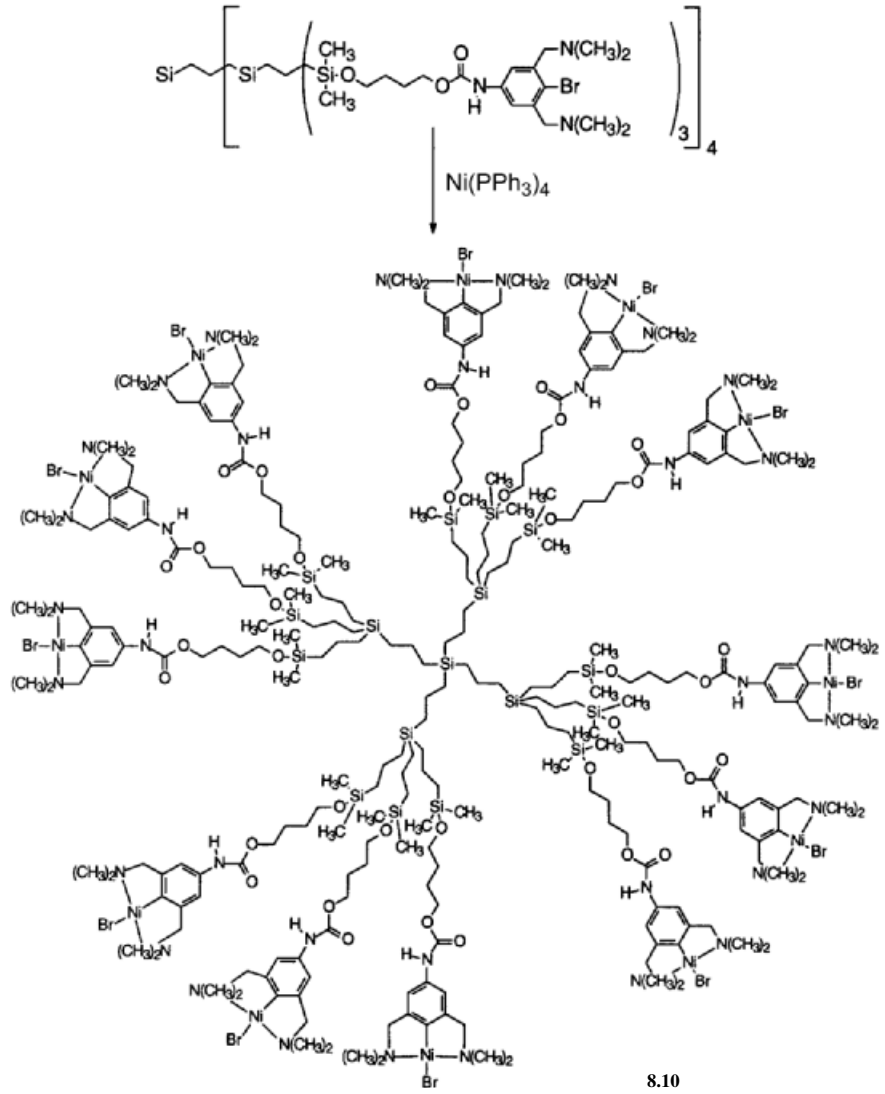

(8.2)

8.10

In another interesting application, members of a series of analogous platinum dendrimers have been found to function as useful sensors for SO_2 [33, 34]. For example, coordination of SO_2 to dendrimer **8.11** leads to the derivative **8.12**, a process that gives rise to an easily monitored color change from colorless to bright orange (Eq. 8.3). The coordination is reversible and repeated SO_2 adsorption/desorption cycles are shown for metallodendrimer **8.11** in Fig. 8.2. The sensing is selective for SO_2 and the sensors show promising resistance to acids and water.

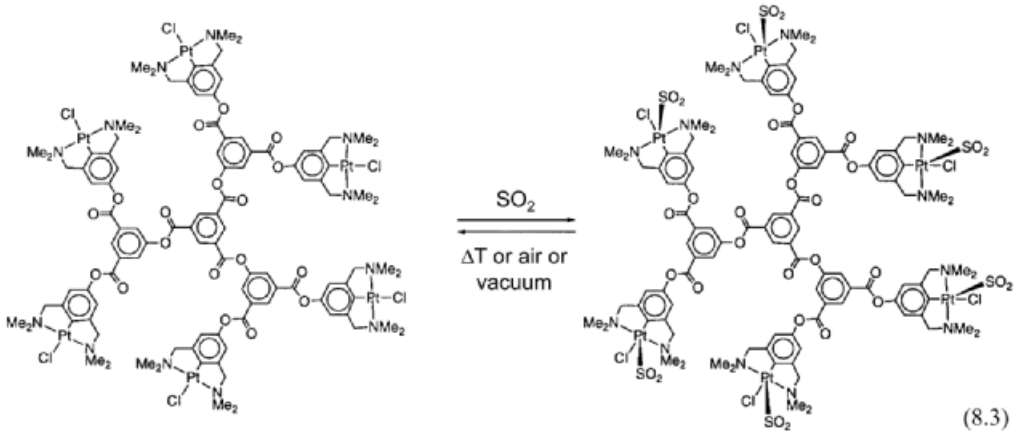

colorless

8.11

orange

8.12

(8.3)

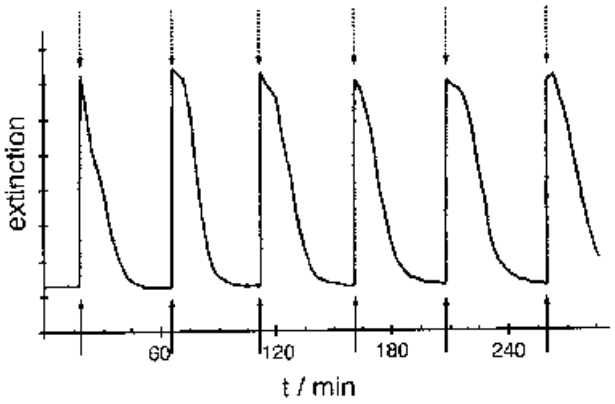

Fig. 8.2 Repeated SO_2 adsorption and desorption cycles with platinum metallodendrimers **8.11**. The arrows mark saturation of the solution with SO_2 (solid) and with air (dashed). (Reproduced from [33])

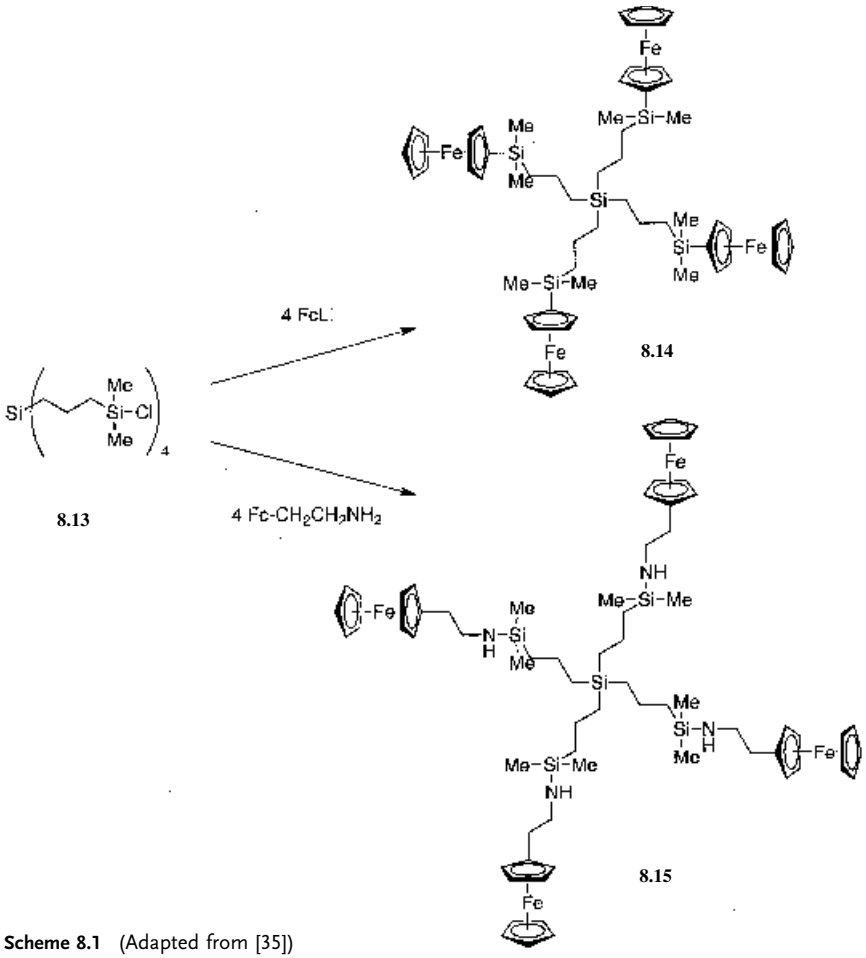

Scheme 8.1 (Adapted from [35])

Metallodendrimers bearing peripheral ferrocene groups have been prepared by means of a variety of different methodologies [35, 36]. For example, using tetraallylsilane as the initiator core, novel silane dendrimers (e.g. **8.13**) possessing reactive Si–Cl end groups, were constructed. The reaction with lithioferrocene or *β*-aminoethylferrocene afforded the corresponding tetra-ferrocenyl dendrimers **8.14** and **8.15**, which represented the first examples of well-defined and well-characterized, redox-active macromolecules of this type (Scheme 8.1) [35].

A similar synthetic approach has also been used to synthesize the corresponding octa-ferrocenyl derivatives [35]. A series of remarkable ferrocenyl dendritic macromolecules based on flexible poly(propyleneimine) dendrimer cores containing 4, 8, 16, 32 or 64 peripheral ferrocenyl moieties has been prepared by condensation reactions of ferrocenoyl chloride with the first-, second-, third-, fourth-, and fifth-generation diaminobutane-based poly(propyleneimine) dendrimers functiona-

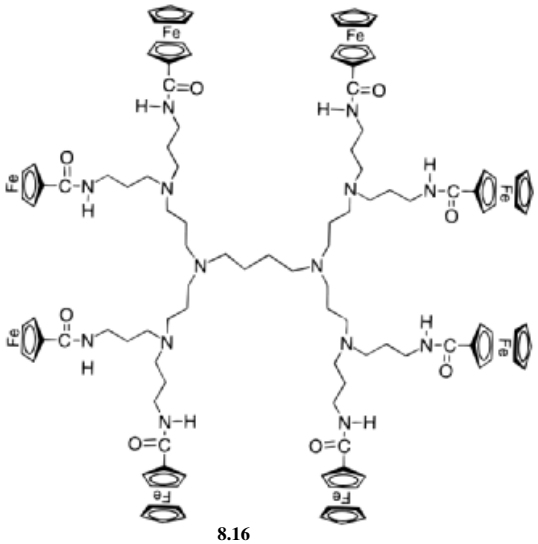

8.16

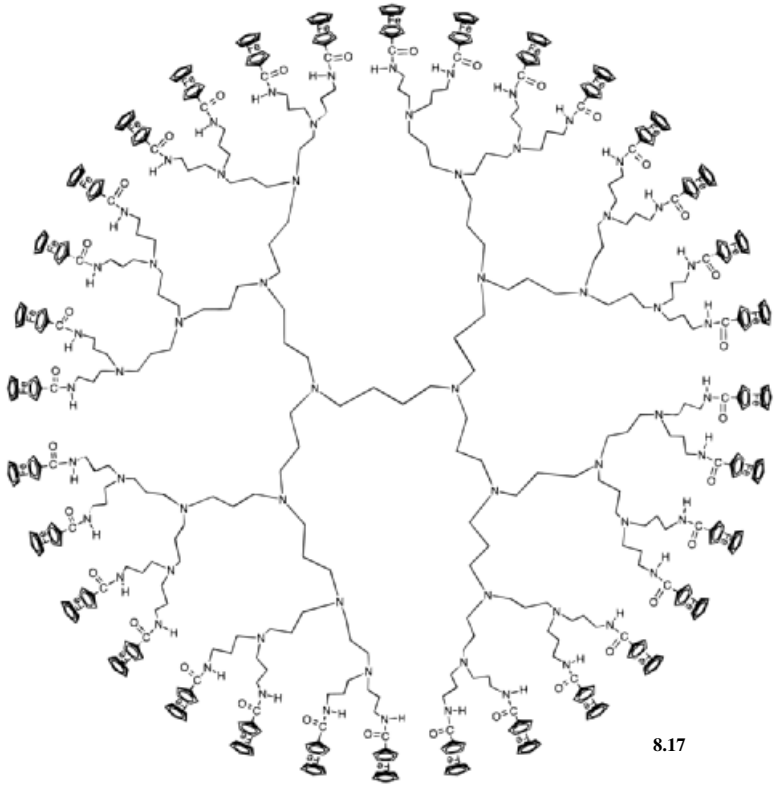

8.17

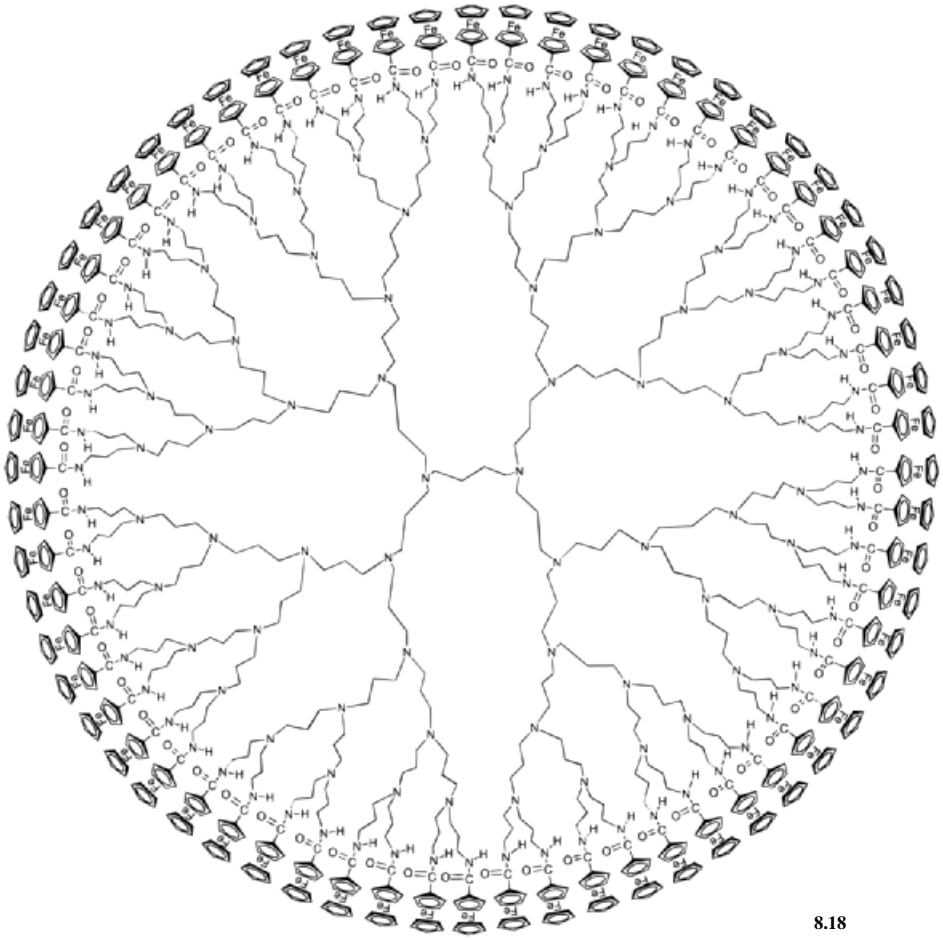

8.18

lized with terminal NH_2 groups [36]. Examples with 8, 32, and 64 ferrocene units are illustrated as **8.16–8.18**, respectively.

Cyclic voltammetric studies of these metallodendrimers showed one reversible oxidation wave, characteristic of independent, non-interacting redox centers. Also, the use of these materials for the modification of electrode surfaces was explored [37–39]. The researchers found that platinum, glass, and carbon-disk electrodes modified by electrodeposited films of these dendrimers are extremely durable and reproducible, with no detected loss of electroactivity even after their use in different electrolyte solutions or after standing for long periods in air. Studies on the thermodynamics and kinetics of adsorption of these redox-active dendrimers onto Pt electrodes by means of electrochemical and electrochemical quartz crystal microbalance techniques were conducted. These showed the adsorption processes to be activation-controlled rather than diffusion-controlled, and to be dependent on

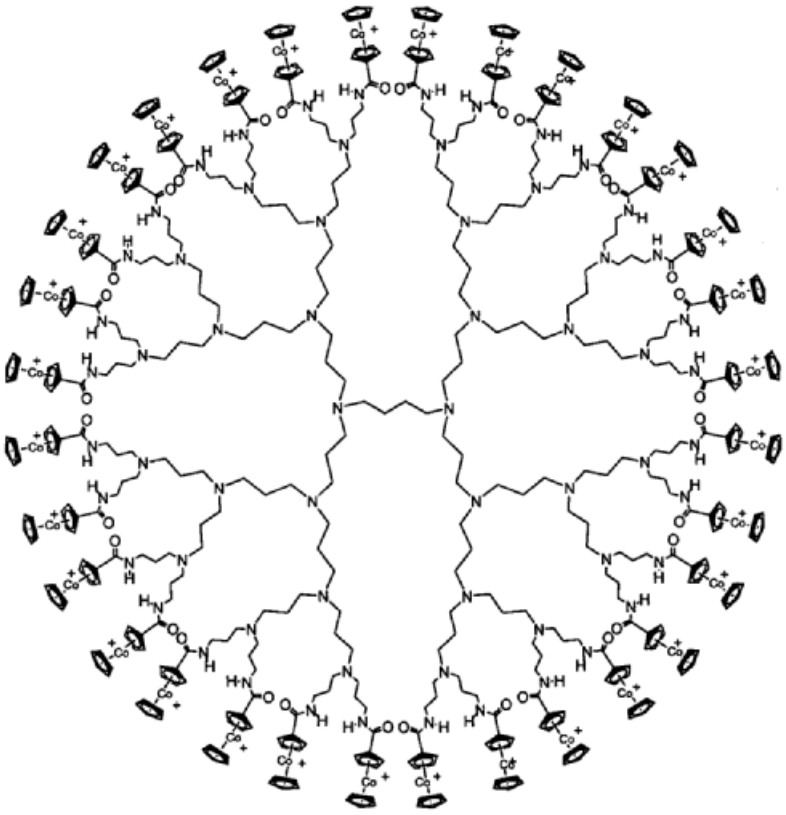

8.19

the nature of the dendrimer but not the concentration. The adsorption free energies were found to decrease in the order **8.18** > **8.17** > **8.16** [39]. Dendrimers of the type **8.16**–**8.18** and the cobaltocenium analogue **8.19** have also been explored as guest systems for inclusion complexation by cyclodextrin (*β*-CD) hosts [40–42].

Amido-ferrocene dendrimers containing 3, 9, and 18 ferrocene moieties (**8.20**–**8.22**) have been prepared by the reaction of ferrocenoyl chloride with the corresponding poly-NH_2 dendrimers. These materials were found to rapidly and reversibly bind small inorganic anions such as $[H_2PO_4]^-$, $[HSO_4]^-$, Cl^-, Br^-, and $[NO_3]^-$, as monitored by cyclic voltammetry. A dendritic effect was demonstrated; the sensing and recognition of the anions was found to improve as the number of generations was increased [43]. Analogous dendritic effects have also been observed for amidoferrocenyl dendrimers constructed by means of hydrogen bonding [44].

A convergent synthesis of dendrimers **8.23** and **8.24**, which possess interacting ferrocenyl units, by means of hydrosilylation reactions of the Si–H polyfunctionalized cores, has been described [45]. Cyclic voltammograms of these dendrimers exhibit two distinct oxidation waves separated by 0.19 and ca. 0.16 V for **8.23** (see Fig. 8.3) and **8.24**, respectively. This electrochemical behavior is consistent with

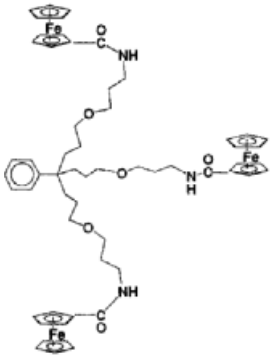

8.20

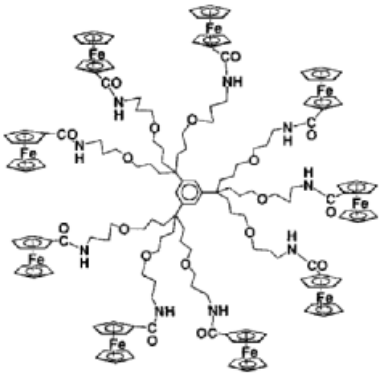

8.21

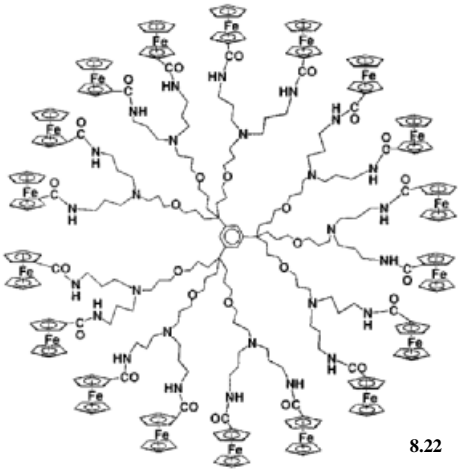

8.22

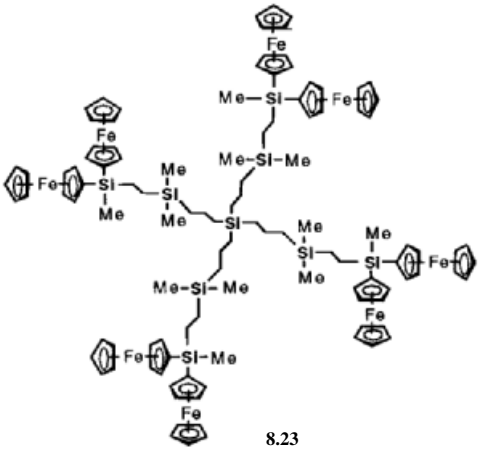

8.23

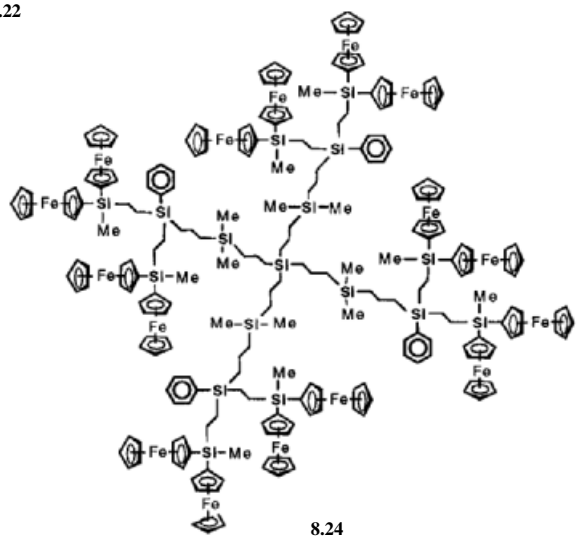

8.24

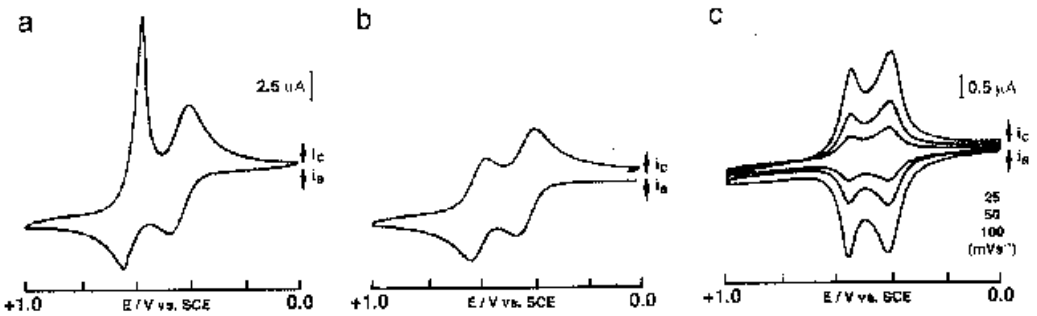

Fig. 8.3 Cyclic voltammograms for ferrocene dendrimer **8.23** in **(a)** CH_2Cl_2, **(b)** CH_2Cl_2/MeCN (5 : 1), and **(c)** as a film on a Pt electrode; supporting electrolyte: 0.1 M $[Bu_4N][PF_6]$; scan rate: 100 mV s^{-1}. (Reproduced from [45a])

significant communication between two ferrocenyl moieties linked together by a bridging Si atom. Similar cyclic voltammetric behavior is observed for linear oligomeric and polymeric analogues (see Chapter 3, Section 3.3.6.3).

Another interesting class of ferrocene dendrimers (**8.25**) possesses electrochemical properties that can be tuned by *N*-methylation or protonation of the nitrogen sites. For example, a shift in E° of 0.10–0.20 V for the ferrocene groups is effected on protonation of the adjacent nitrogen centers [46].

Ferrocene dendrimers are also of interest for reasons other than their redox activity. For example, metallodendrimer **8.26** possesses planar chiral ferrocene units that make the bidentate phosphine ligation sites of potential interest for applications in asymmetric catalysis. Indeed, asymmetric hydrogenations of dimethyl itaconate catalyzed by Rh complexes of **8.26** showed impressive enantiomeric excess values of 98% [47].

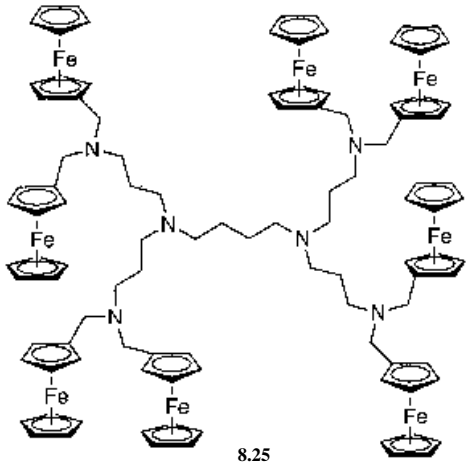

8.25

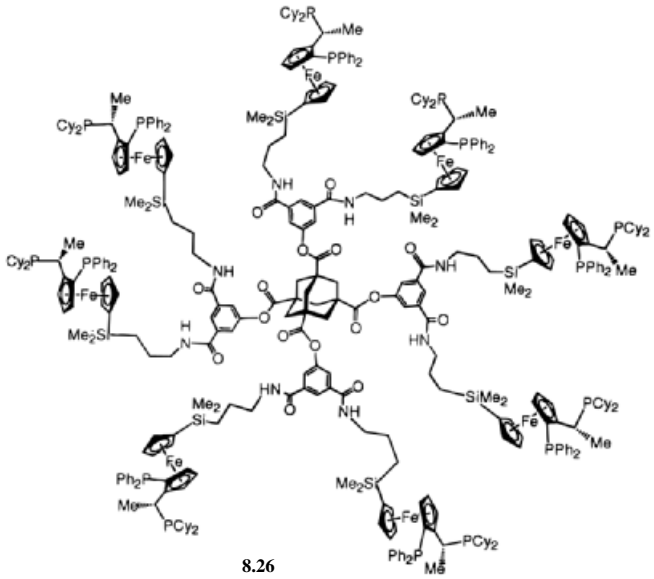

8.26

Dendrimers attached to silica with Rh complexes at the surface have been used as recyclable regioselective hydroformylation catalysts for styrene and vinyl acetate using a 1:1 CO/H_2 gas mixture [48]. The dendrimers were constructed by means of a divergent growth strategy that started with aminopropyl silica. The catalytic activity was found to improve as the steric congestion around the catalytic sites was alleviated by extension of the chain lengths of each generation. Thus, dendrimer **8.28** ($Rh=RhL_x$) was found to be more active and recyclable than the corresponding material **8.27** ($Rh=RhL_x$) with shorter linkers. The silica-supported catalysts were easily recovered by means of microporous filtration techniques.

Representative examples of other metallodendrimers with metal atoms at the surface are the ruthenium materials **8.29** [49–51] and the organometallic dendrimers **8.30** [52], possessing peripheral cobalt clusters, which were prepared by treatment of an alkyne-functionalized dendrimer precursor with $Co_2(CO)_8$ (Eq. 8.4). Versatile phosphorus-containing dendrimers with a variety of surface metal-containing centers (**8.31**) have also been prepared by a divergent approach, and catalytic applications for these materials have been demonstrated [53–55]. Metallodendrimers **8.32** bearing surface terpyridine groups have been linked together by ions such as Fe^{2+} on highly oriented graphite surfaces. Molecular resolution for 2-D-ordered films of the ca. 5 nm metallodendrimer structures was achieved using scanning tunneling microscopy (Fig. 8.4) [56]. In addition, reversible oxidation of the metal ions was demonstrated (Fig. 8.5). Dendrimers with 16 Au_2Ru_6 carbonyl clusters on the periphery have also been prepared and have been successfully imaged by high-resolution TEM [57].

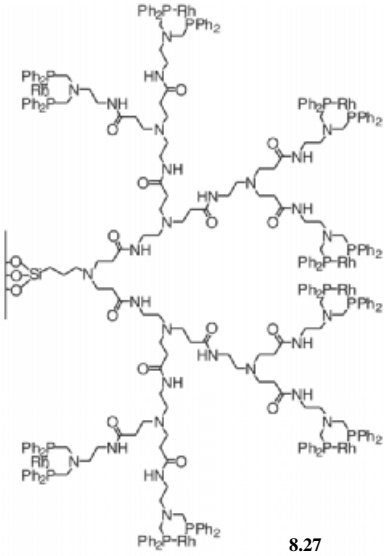

8.27

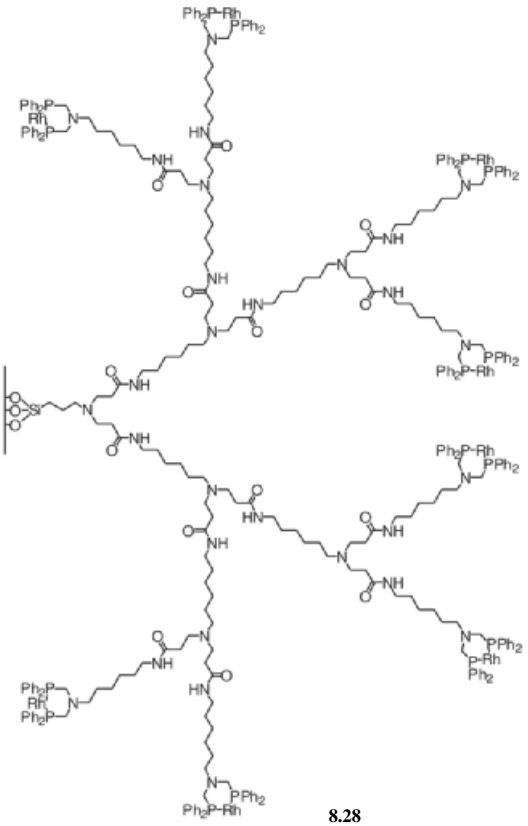

8.28

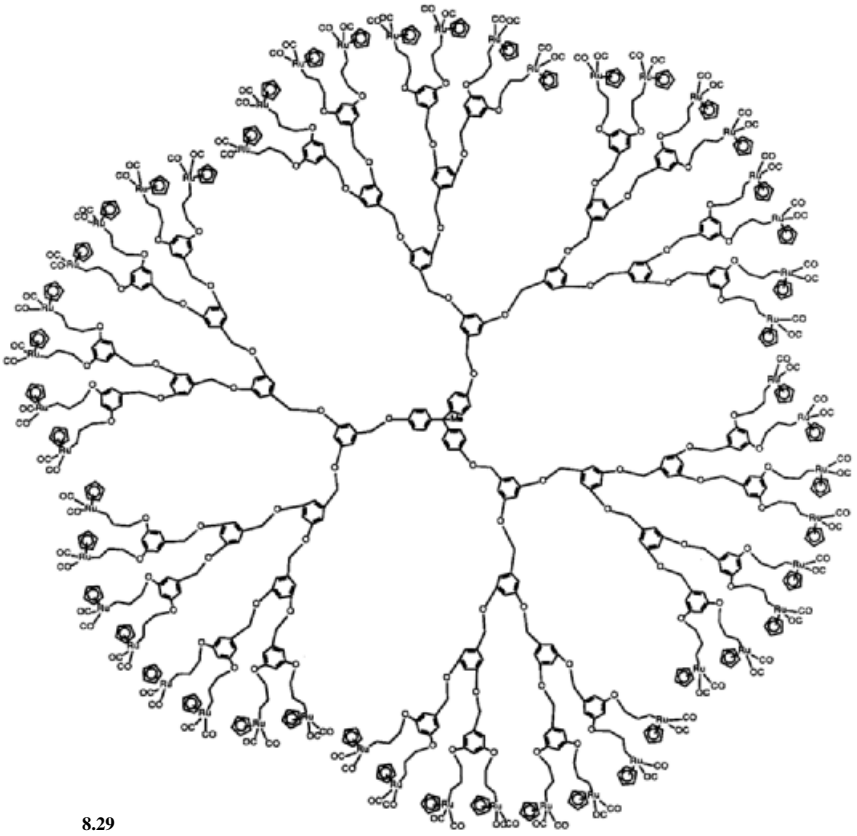

8.29

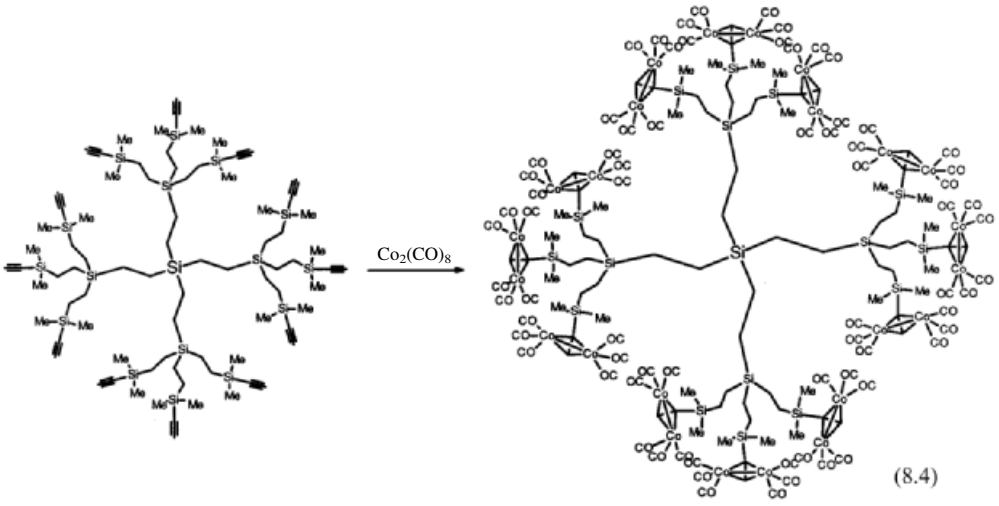

(8.4)

8.30

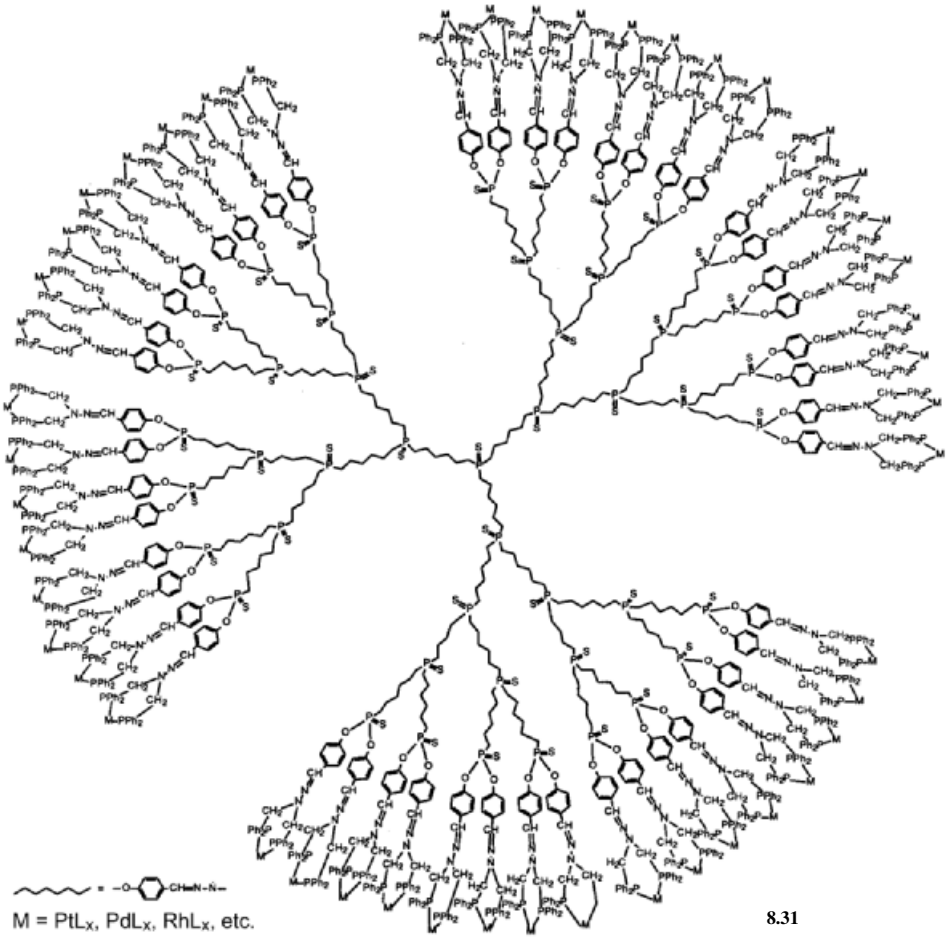

8.31

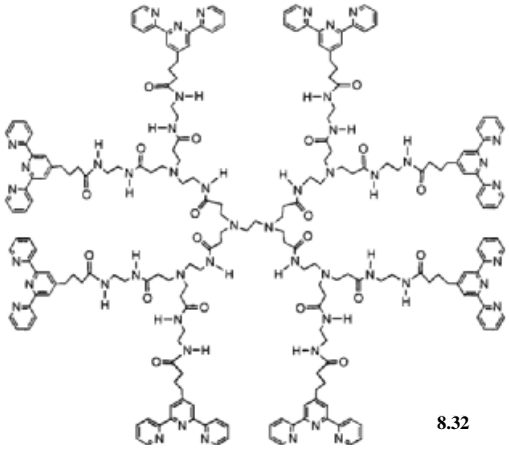

8.32

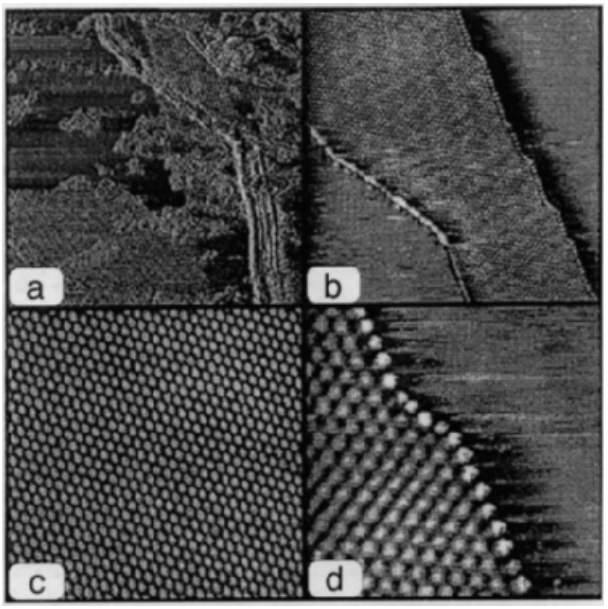

Fig. 8.4 Unfiltered STM images of **8.32** · $FeSO_4$ on highly oriented graphite: **(a)** 550×550 nm image, **(b)** 200×200 nm image, **(c)** 304×304 nm image, **(d)** 69×69 nm image. (Reproduced from [56])

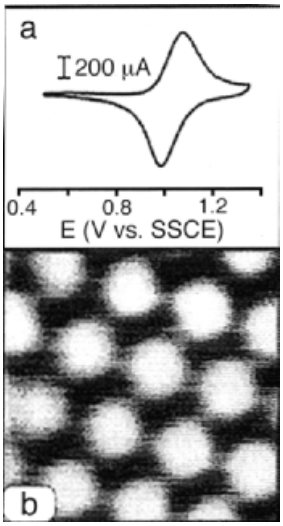

Fig. 8.5 **(a)** Cyclic voltammogram at 50 m Vs^{-1} of **8.32** · $FeSO_4$ on a modified highly oriented graphite electrode in MeCN/0.1 M $[Bu_4N][ClO_4]$; **(b)** high-resolution (26×26 nm) unfiltered STM image of **8.32** · Fe^{2+} on highly oriented graphite. (Reproduced from [56])

8.4
Metallodendrimers with Metals at Interior Sites

Metallodendrimers may also have metal-containing units placed within the interior of the structure in addition to, or instead of, in the core and at the periphery. Metal polypyridyl complexes have been particularly popular for the construction of metallodendrimers as a result of their ease of functionalization and the corresponding utilization of standard synthetic organic transformations. One of the first metallodendritic materials reported was the species **8.33** containing a trifunctional core [58–60]. Both homo- and heterometallic branching centers containing Ru or Os have been prepared (Eq. 8.5) and the luminescence, energy-transfer, and redox properties of these interesting materials have been explored in detail [61–69]. Electrochemical studies show that the redox steps appear to be essentially ligand-localized and the arrays can be regarded as ordered assemblies of weakly interacting metal-containing units. However, very fast energy transfer between nearby units was detected, and applications as light-harvesting materials have been proposed.

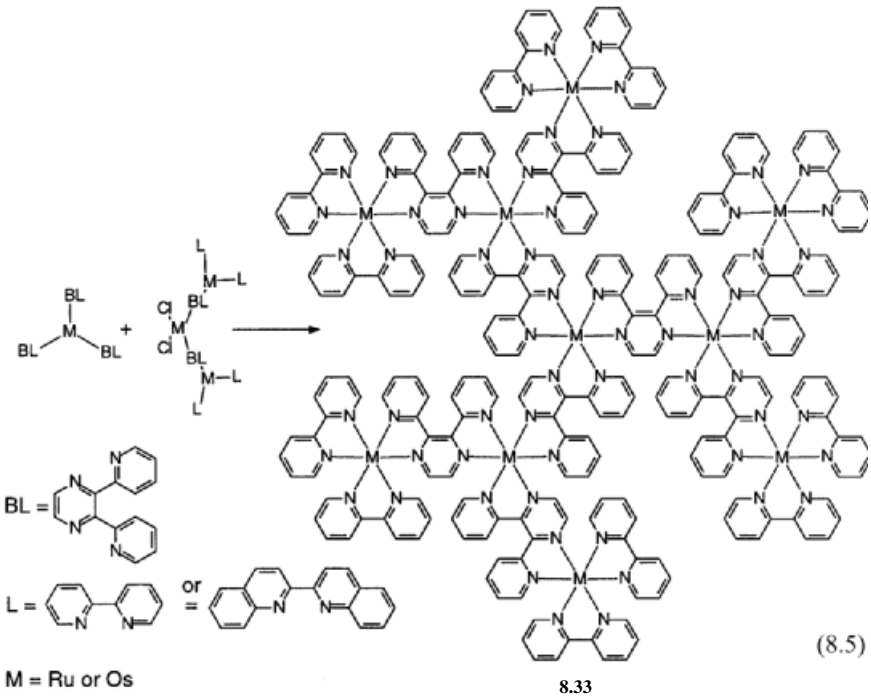

(8.5)

8.33

An interesting variant on metal polypyridyl-type metallodendrimers is the material **8.34**, which was prepared by a convergent synthetic approach (Scheme 8.2) [70]. A further example is the dendrimer **8.35**, which possesses 18 ruthenium centers [71].

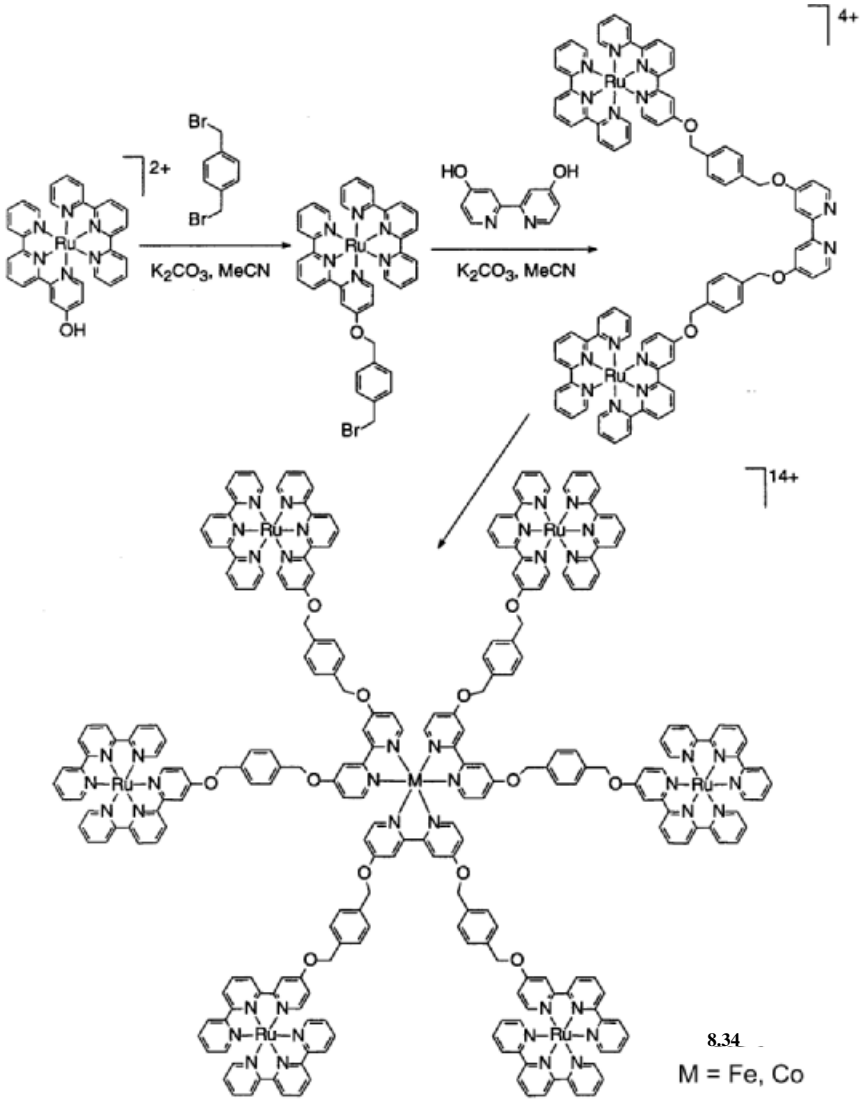

8.34

Scheme 8.2 (Adapted from [70])

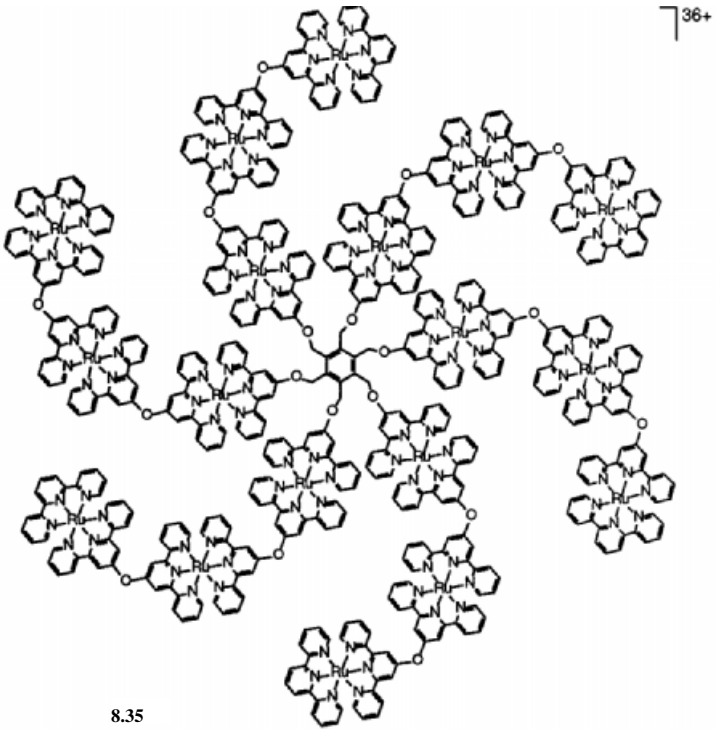

8.35

Lock-and-key metallodendrimer assemblies **8.36** have been prepared. The creative synthetic approach is outlined in Scheme 8.3; the "bisdendrimer" **8.36** was prepared from two independently constructed dendrons [72].

As a final example of a metal polypyridyl-type dendrimer, species **8.37** contains metal-containing units only as connectors and not in the core or on the surface. This material was prepared by a combined divergent-convergent approach [73].

A variety of other metal-containing building blocks have been used to create dendritic architecture with metals at interior sites. Porphyrins possess many of the advantages of polypyridyl complexes in terms of facile synthetic derivatization, and these have been used to construct a range of remarkable structures. For example, linear, four-directional complexes **8.38** have been prepared by means of metal-catalyzed coupling methodologies [74–76]. In addition, "windmill-like" light-harvesting porphyrin arrays **8.39** have been prepared [77, 78].

Ferrocene units have also proved popular for the construction of dendrimers with metal atoms throughout the structure. An example of the materials prepared is provided by the polyferrocene dendrimer **8.40**, which was synthesized by means of a hydrosilylation approach (Eq. 8.6) [79]. Cyclic voltammetric studies of **8.40** showed that the central and surrounding ferrocene units are oxidized reversibly, but at different potentials. Cyclopentadienyliron arene cations also provide broad

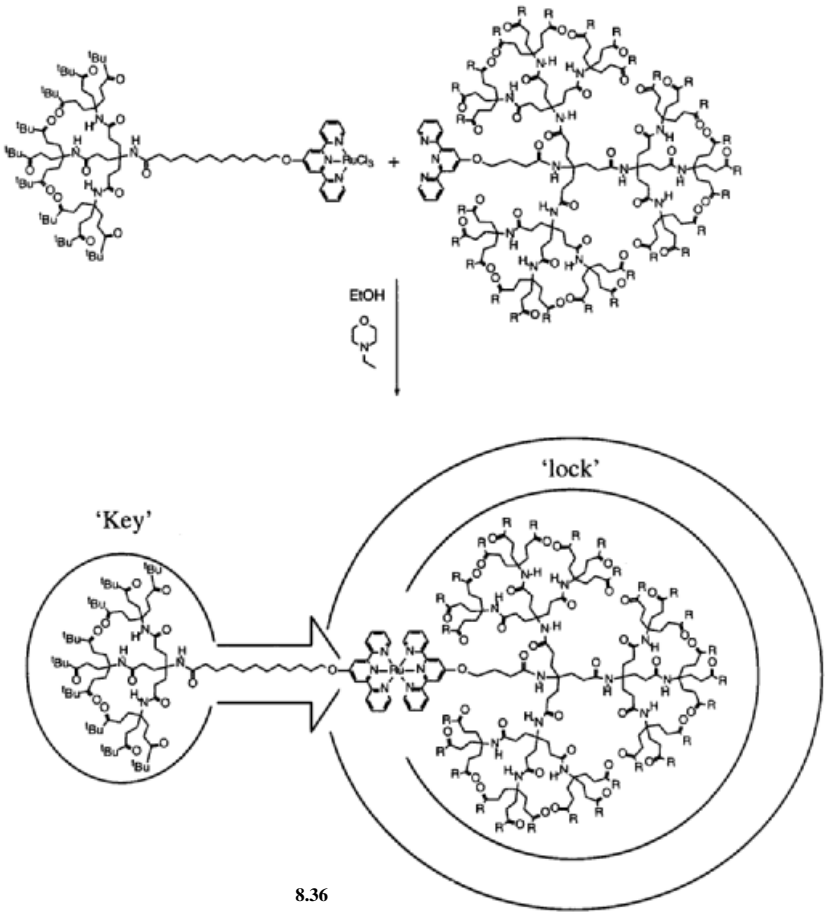

8.36

Scheme 8.3 (Adapted from [72])

possibilities as cores for dendrimer construction, and dendrimers with electrocatalytic functions have been reported [80, 81].

A variety of other strategies have been used to create metallodendritic architecture with metal-containing units in the interiors. Combinations of coordination chemistry and hydrogen bonding have allowed the synthesis of remarkable "rosette"-type structures such as **8.41** (Eq. 8.7) [82, 83]. Oxidative addition chemistry involving Pd^{II} and Pt^{II} centers and C–Br bonds has allowed the convergent synthesis of novel metallodendrimers **8.42** (Eq. 8.8) [84–89]. Metallodendrimers with $[Re_6Se_8]^{2+}$ units in the core and at the periphery have been prepared [90]. In another interesting development, Cu^{2+} ions were coordinated to polyamidoamine dendrimers, and subsequent reduction with aqueous hydrazine produced dendrimer-stabilized metal colloids [91–93].

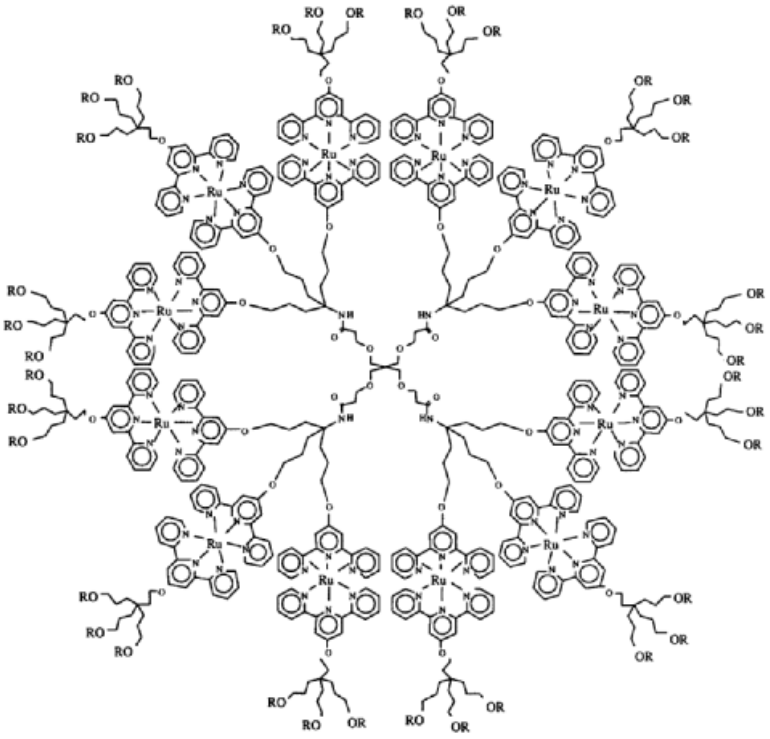

8.37
R = benzyl

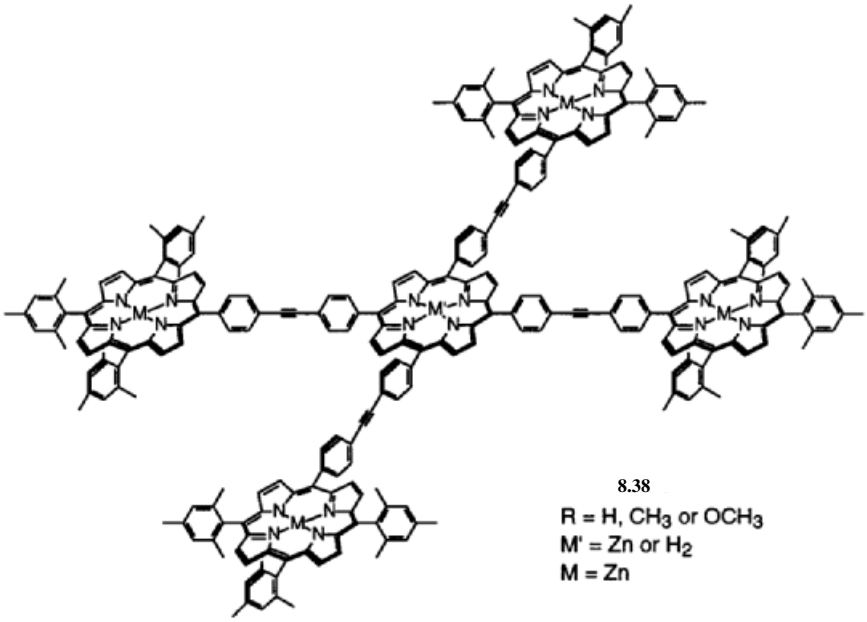

8.38
R = H, CH_3 or OCH_3
M' = Zn or H_2
M = Zn

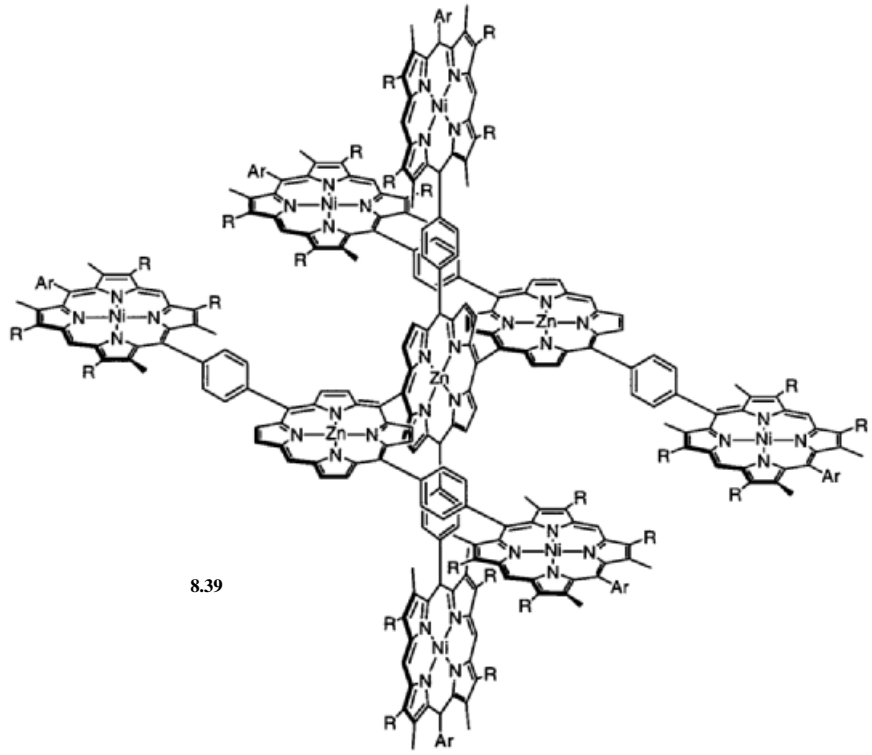

8.39

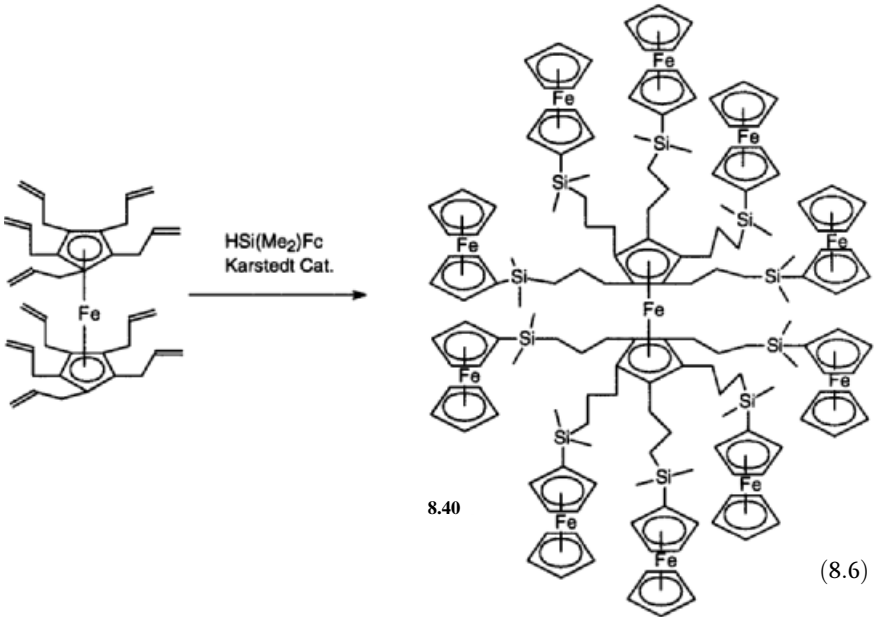

8.40

(8.6)

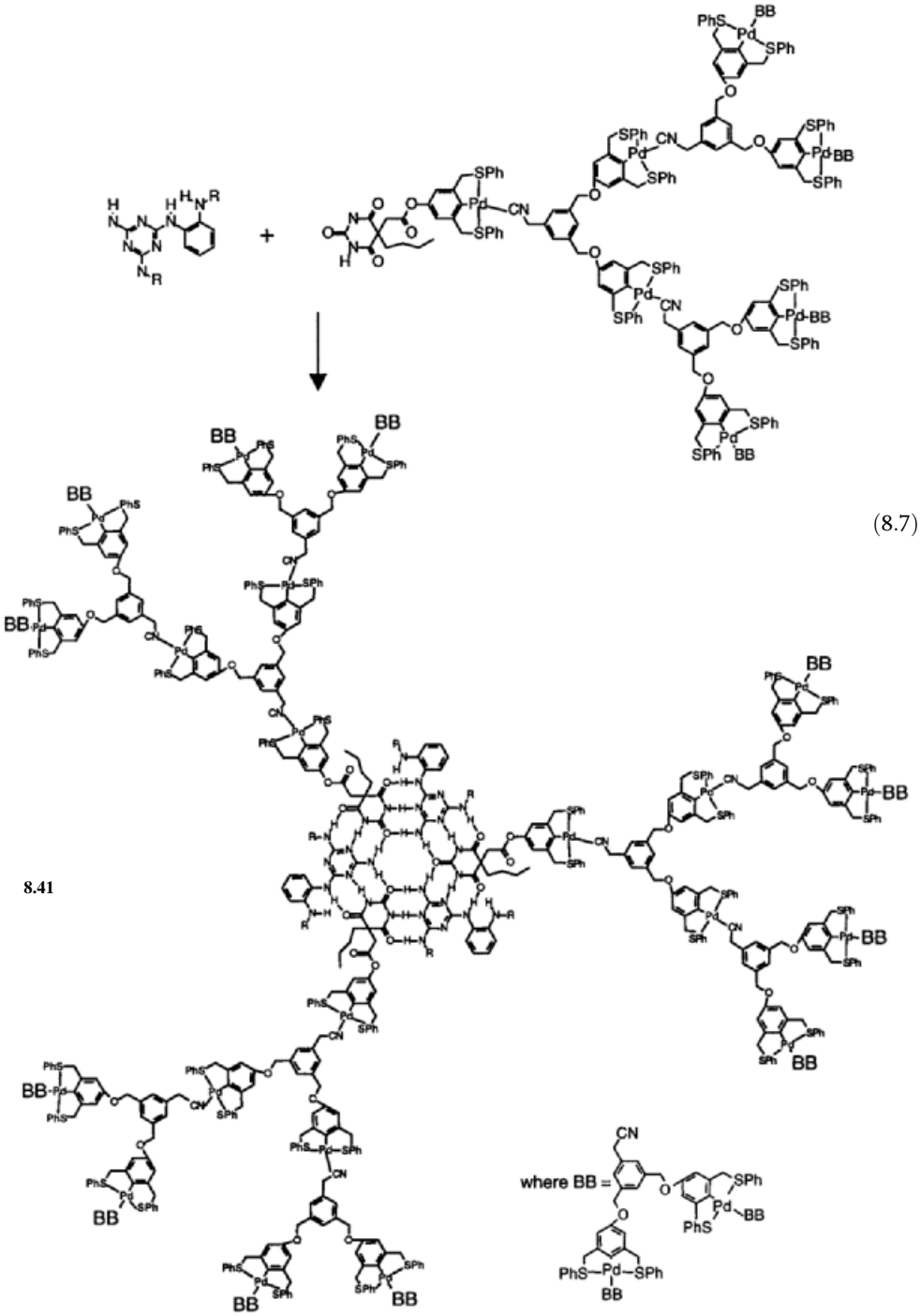

(8.7)

8.41

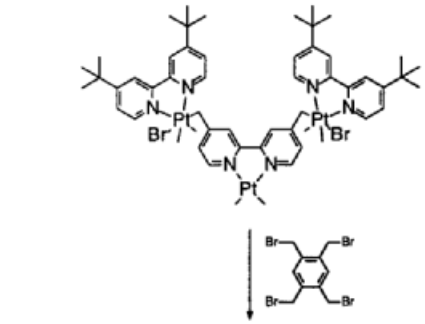

(8.8)

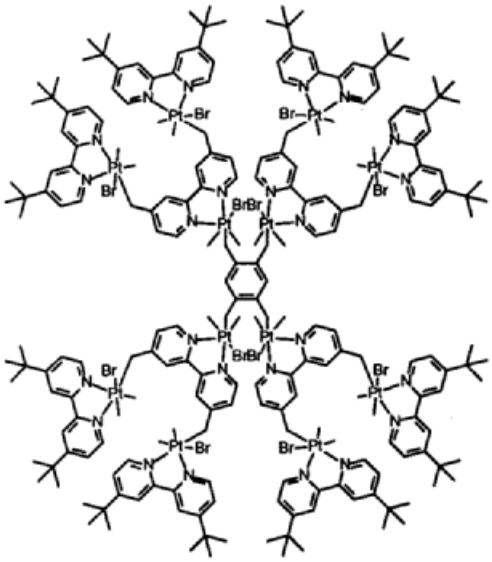

8.42

Platinum polyynes represent one of the most interesting and well-studied classes of linear metallopolymers (Chapter 5, Section 5.2). Dendritic analogues of these materials have been prepared by a variety of methodologies [94–96]. One example is the nonametallic dendrimer **8.43**, which was prepared by a convergent route as illustrated in Eq. 8.9 [94]. Dendrimers based on ruthenium polyyne architectures have also been prepared, and promising nonlinear optical properties have been identified [97, 98].

First-generation Ru_6 dendrimers **8.44** have been prepared, and the incorporation of functional groups allowed the fabrication of crosslinked films. Electrochemical studies showed that for each Ru_2 unit two one-electron oxidations are detected, with a very large redox coupling ($\Delta E_{1/2} \approx 0.55$ V). Materials **8.44** are of considerable interest, as one-electron oxidation of each Ru_2 unit leads to mixed-valence

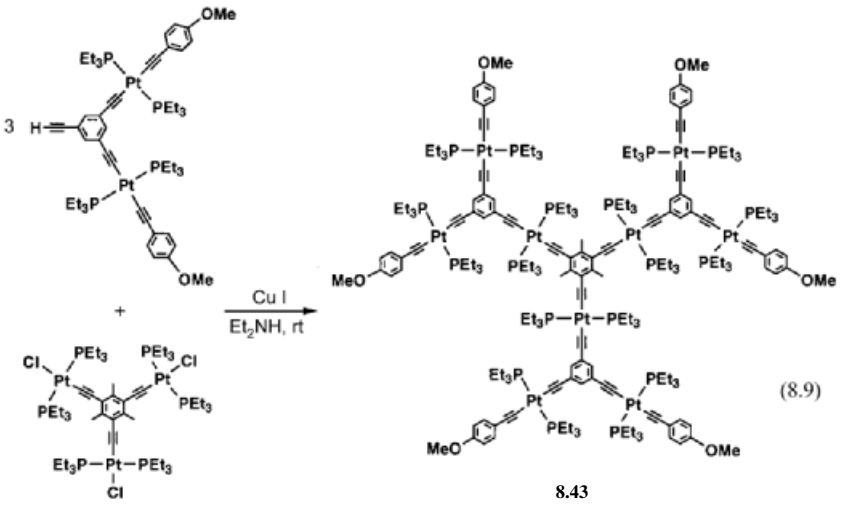

8.43

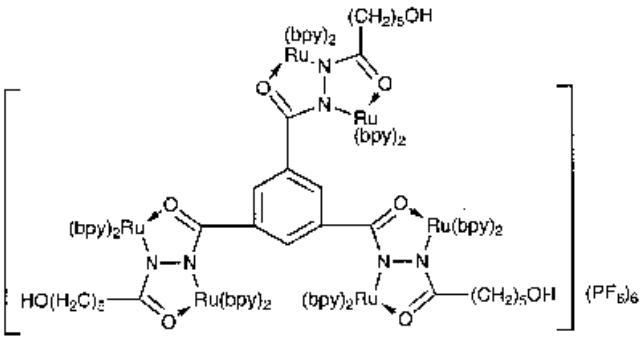

8.44

Ru^{II}-Ru^{III} species that display intense intervalence charge-transfer bands at 1550 nm, close to the telecommunication wavelength of 1.5 μm (Fig. 8.6). Cross-linked films can be used in variable optical attenuator devices, and stability over 18,000 switching cycles was demonstrated with a response time of ca. 2 s (see Fig. 8.7) [99, 100].

Finally, incorporation of entities such as fullerenes into dendritic structures in combination with metal centers has begun to be explored as a method for the preparation of a range of exciting materials [101, 102]. For example, remarkable dendrimers such as **8.45** with a C_{60} core and 8 ferrocene units throughout the structure have been prepared by a convergent synthetic approach. Dendrimer **8.45** proved to be readily soluble in organic solvents, showed good thermal stability, and displayed a liquid-crystalline smectic A phase at ambient temperature, which was identified by polarizing microscopy. The clearing temperature was found to be 157 °C [102].

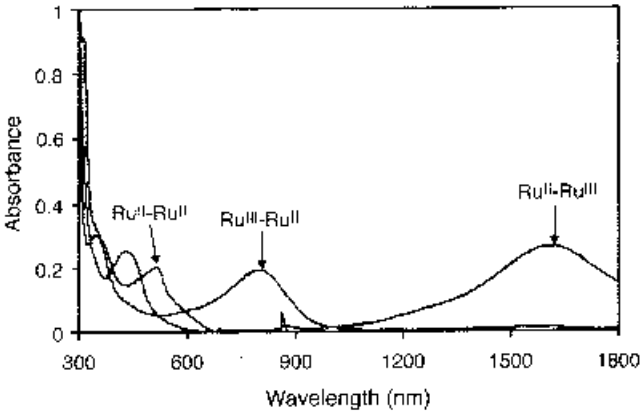

Fig. 8.6 UV/vis/NIR spectra for hexametallic dendrimer **8.44** in Ru^{II}-Ru^{II}, Ru^{III}-Ru^{III}, and Ru^{II}-Ru^{III} states. The latter state shows a NIR absorption at 1550 nm for the intervalence electron transfer. (Adapted from [100])

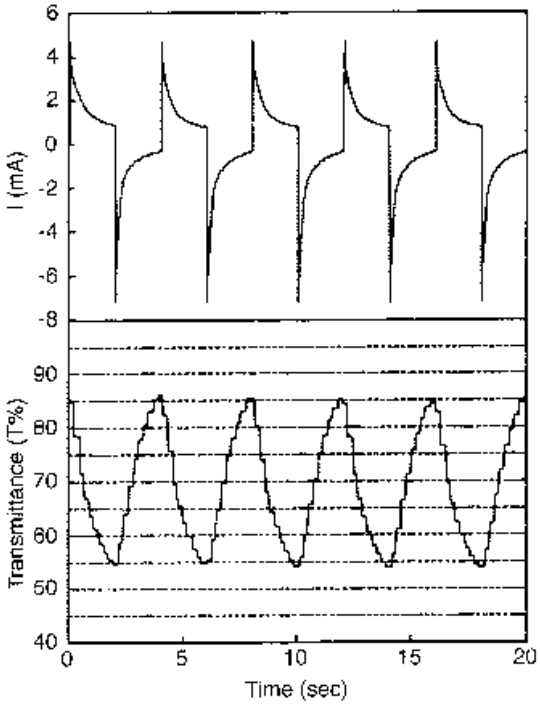

Fig. 8.7 Variation of current (top) and transmittance (bottom) as a function of time for a variable optical attenuator device that uses crosslinked films of dendrimer **8.44** for 5 switches (step time 2 s). (Adapted from [100])

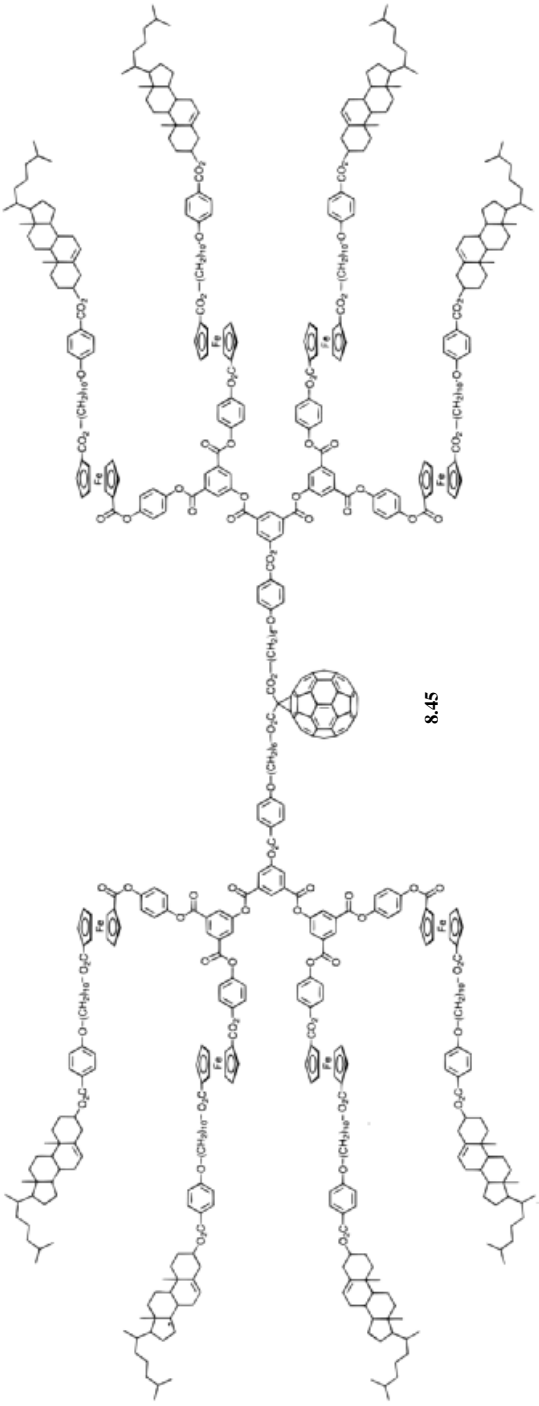

8.45

8.5 References

1 (a) G. R. Newkome, C. N. Moorefield, F. Vögtle, *Dendritic Molecules: Concepts, Syntheses, Perspectives,* VCH, Weinheim, **1996**; (b) G. R. Newkome, C. N. Moorefield, F. Vögtle, *Dendrimers and Dendrons: Concepts, Syntheses, Applications,* Wiley-VCH, Weinheim, **2001**.

2 E. Buhleier, W. Wehner, F. Vögtle, *Synthesis* **1978**, 155.

3 D. A. Tomalia, H. Baker, J. Dewald, M. Hall, G. Kallos, S. Martin, J. Roeck, J. Ryder, P. Smith, *Polym. J. (Tokyo)* **1985**, *17*, 117.

4 D. A. Tomalia, A. M. Naylor, W. A. Goddard III, *Angew. Chem. Int. Ed. Engl.* **1990**, *29*, 138.

5 D. A. Tomalia, *Sci. Am.* **1995**, *May*, 62.

6 A. D. Schlüter, J. P. Rabe, *Angew. Chem. Int. Ed.* **2000**, *39*, 864.

7 M. Fischer, F. Vögtle, *Angew. Chem. Int. Ed.* **1999**, *38*, 884.

8 (a) A. W. Bosman, H. M. Janssen, E. W. Meijer, *Chem. Rev.* **1999**, *99*, 1665; (b) J.-P. Majoral, A.-M. Caminade, *Chem. Rev.* **1999**, *99*, 845.

9 T. M. Miller, T. X. Neenan, *Chem. Mater.* **1990**, *2*, 346.

10 T. M. Miller, T. X. Neenan, R. Zayas, H. E. Bair, *J. Am. Chem. Soc.* **1992**, *114*, 1018.

11 C. Hawker, J. M. J. Fréchet, *J. Chem. Soc., Chem. Commun.* **1990**, 1010.

12 C. J. Hawker, J. M. J. Fréchet, *J. Am. Chem. Soc.* **1990**, *112*, 7638.

13 G. R. Newkome, E. He, C. N. Moorefield, *Chem. Rev.* **1999**, *99*, 1689.

14 D. Astruc, F. Chardac, *Chem. Rev.* **2001**, *101*, 2991.

15 M. A. Hearshaw, J. R. Moss, *Chem. Commun.* **1999**, 1.

16 I. Cuadrado, M. Morán, C. M. Casado, B. Alonso, J. Losada, *Coord. Chem. Rev.* **1999**, *193–195*, 395.

17 C. Gorman, *Adv. Mater.* **1998**, *10*, 295.

18 K. W. Pollak, J. W. Leon, J. M. J. Fréchet, *Am. Chem. Soc. Div. Polym. Mater. Sci. Eng.* **1995**, *73*, 333.

19 K. W. Pollak, J. W. Leon, J. M. J. Fréchet, M. Maskus, H. D. Abruña, *Chem. Mater.* **1998**, *10*, 30.

20 P. Bhyrappa, J. K. Young, J. S. Moore, K. S. Suslick, *J. Am. Chem. Soc.* **1996**, *118*, 5708.

21 P. Bhyrappa, J. K. Young, J. S. Moore, K. S. Suslick, *J. Mol. Catal. A: Chem.* **1996**, *113*, 109.

22 M. Kawa, J. M. J. Fréchet, *Chem. Mater.* **1998**, *10*, 286.

23 C. B. Gorman, B. L. Parkhurst, W. Y. Su, K.-Y. Chen, *J. Am. Chem. Soc.* **1997**, *119*, 1141.

24 K.-Y. Chen, C. B. Gorman, *J. Org. Chem.* **1996**, *61*, 9229.

25 C. B. Gorman, *Adv. Mater.* **1997**, *9*, 1117.

26 C. B. Gorman, J. C. Smith, M. W. Hager, B. L. Parkhurst, H. Sierzputowska-Gracz, C. A. Haney, *J. Am. Chem. Soc.* **1999**, *121*, 9958.

27 C. B. Gorman, J. C. Smith, *J. Am. Chem. Soc.* **2000**, *122*, 9342.

28 C. B. Gorman, J. C. Smith, *Acc. Chem. Res.* **2001**, *34*, 60.

29 R. Wang, Z. Zheng, *J. Am. Chem. Soc.* **1999**, *121*, 3549.

30 J. W. J. Knapen, A. W. van der Made, J. C. de Wilde, P. W. N. M. van Leeuwen, P. Wijkens, D. M. Grove, G. van Koten, *Nature* **1994**, *372*, 659.

31 G. van Koten, D. M. Grove, *Am. Chem. Soc. Div. Polym. Mater. Sci. Eng.* **1995**, *73*, 228.

32 R. A. Gossage, L. A. de Kuil, G. van Koten, *Acc. Chem. Res.* **1998**, *31*, 423.

33 M. Albrecht, G. van Koten, *Adv. Mater.* **1999**, *11*, 171.

34 M. Albrecht, R. A. Gossage, M. Lutz, A. L. Spek, G. van Koten, *Chem. Eur. J.* **2000**, *6*, 1431.

35 B. Alonso, I. Cuadrado, M. Moran, J. Losada, *J. Chem. Soc., Chem. Commun.* **1994**, 2575.

36 I. Cuadrado, M. Moran, C. M. Casado, B. Alonso, F. Lobete, B. Garcia, M. Ibisate, J. Losada, *Organometallics* **1996**, *15*, 5278.

37 B. Alonso, M. Moran, C. M. Casado, F. Lobette, J. Losada, I. Cuadrado, *Chem. Mater.* **1995**, *7*, 1440.

38 J. Losada, I. Cuadrado, M. Moran, C.M. Casado, B. Alonso, M. Barranco, *Anal. Chim. Acta* **1997**, *338*, 191.

39 K. Takada, D.J. Diaz, H.D. Abruna, I. Cuadrado, C. Casado, B. Alonso, M. Moran, J. Losada, *J. Am. Chem. Soc.* **1997**, *119*, 10763.

40 B. Gonzalez, C.M. Casado, B. Alonso, I. Cuadrado, M. Moran, Y. Wang, A.E. Kaifer, *Chem. Commun.* **1998**, 2569.

41 R. Castro, I. Cuadrado, B. Alonso, C.M. Casado, M. Moran, A.E. Kaifer, *J. Am. Chem. Soc.* **1997**, *119*, 5760.

42 A.E. Kaifer, *Acc. Chem. Res.* **1999**, *32*, 62.

43 C. Valerio, J.-L. Fillaut, J. Ruiz, J. Guittard, J.-C. Blais, D. Astruc, *J. Am. Chem. Soc.* **1997**, *119*, 2588.

44 M.-C. Daniel, J. Ruiz, D. Astruc, *J. Am. Chem. Soc.* **2003**, *125*, 1150.

45 (a) I. Cuadrado, C.M. Casado, B. Alonso, M. Moran, J. Losada, V. Belsky, *J. Am. Chem. Soc.* **1997**, *119*, 7613; (b) B. Alonso, B. González, B. García, E. Ramírez-Oliva, M. Zamora, C.M. Casado, I. Cuadrado, *J. Organomet. Chem.* **2001**, *637–639*, 642.

46 J. Alvarez, T. Ren, A.E. Kaifer, *Organometallics* **2001**, *20*, 3543.

47 C. Köllner, B. Pugin, A. Togni, *J. Am. Chem. Soc.* **1998**, *120*, 10274.

48 S.C. Bourque, F. Maltais, W.-J. Xiao, O. Tardif, H. Alper, P. Arya, L.E. Manzer, *J. Am. Chem. Soc.* **1999**, *121*, 3035.

49 Y.-H. Liao, J.R. Moss, *J. Chem. Soc., Chem. Commun.* **1993**, 1774.

50 Y.-H. Liao, J.R. Moss, *Organometallics* **1995**, *14*, 2130.

51 Y.-H. Liao, J.R. Moss, *Organometallics* **1996**, *15*, 4307.

52 D. Seyferth, T. Kugita, A.L. Rheingold, G.P.A. Yap, *Organometallics* **1995**, *14*, 5362.

53 M. Bardaji, M. Kustos, A.-M. Caminade, J.-P. Majoral, B. Chaudret, *Organometallics* **1997**, *16*, 403.

54 M. Bardaji, A.-M. Caminade, J.-P. Majoral, B. Chaudret, *Organometallics* **1997**, *16*, 3489.

55 M. Slany, M. Bardaji, A.-M. Caminade, B. Chaudret, J.-P. Majoral, *Inorg. Chem.* **1997**, *36*, 1939.

56 D.J. Díaz, G.D. Storrier, S. Bernhard, K. Takada, H.D. Abruña, *Langmuir* **1999**, *15*, 7351.

57 N. Feeder, J. Geng, P.G. Goh, B.F.G. Johnson, C.M. Martin, D.S. Shephard, W. Zhou, *Angew. Chem. Int. Ed.* **2000**, *39*, 1661.

58 G. Denti, S. Serroni, S. Campagna, V. Ricevuto, V. Balzani, *Inorg. Chim. Acta* **1991**, *182*, 127.

59 S. Campagna, G. Denti, L. Sabatino, S. Serroni, M. Ciano, A. Juris, V. Balzani, *Inorg. Chem.* **1992**, *31*, 2982.

60 G. Denti, S. Campagna, S. Serroni, M. Ciano, V. Balzani, *J. Am. Chem. Soc.* **1992**, *114*, 2944.

61 S. Campagna, G. Denti, L. Sabatino, S. Serroni, M. Ciano, V. Balzani, *J. Chem. Soc., Chem. Commun.* **1989**, 1500.

62 S. Campagna, G. Denti, S. Serroni, M. Ciano, V. Balzani, *Inorg. Chem.* **1991**, *30*, 3728.

63 P. Belser, A. von Zelewsky, M. Frank, C. Seel, F. Vögtle, L. De Cola, F. Bartigeletti, V. Balzani, *J. Am. Chem. Soc.* **1993**, *115*, 4076.

64 S. Roffia, M. Marcaccio, C. Paradisi, F. Paolucci, V. Balzani, G. Denti, S. Serroni, S. Campagna, *Inorg. Chem.* **1993**, *32*, 3003.

65 A. Juris, V. Balzani, S. Campagna, G. Denti, S. Serroni, G. Frei, H.U. Gudel, *Inorg. Chem.* **1994**, *33*, 1491.

66 V. Balzani, S. Campagna, G. Denti, A. Juris, S. Serroni, M. Venturi, *Acc. Chem. Res.* **1998**, *31*, 26.

67 S. Campagna, G. Denti, S. Serroni, A. Juris, M. Venturi, V. Ricevuto, V. Balzani, *Chem. Eur. J.* **1995**, *1*, 211.

68 S. Serroni, A. Juris, M. Venturi, S. Campagna, I.R. Resino, G. Denti, A. Credi, V. Balzani, *J. Mater. Chem.* **1997**, *7*, 1227.

69 J.-P. Sauvage, J.-P. Collin, J.-C. Chambron, S. Guillerez, C. Coudret, V. Balzani, F. Barigelletti, L. De Cola, L. Flamigni, *Chem. Rev.* **1994**, *94*, 993.

70 E.C. Constable, P. Harverson, M. Oberholzer, *Chem. Commun.* **1996**, 1821.

71 E.C. Constable, P. Harverson, *Inorg. Chim. Acta* **1996**, *252*, 9.

72 G.R. Newkome, R. Güther, C.N. Moorefield, F. Cardullo, L. Eche-

goyen, E. Pérez-Cordero, H. Luftmann, *Angew. Chem. Int. Ed. Engl.* **1995**, *34*, 2023.
73 G.R. Newkome, F. Cardullo, E.C. Constable, C.N. Moorefield, A.M.W.C. Thompson, *J. Chem. Soc., Chem. Commun.* **1993**, 925.
74 S. Prathapan, T.E. Johnson, J.S. Lindsey, *J. Am. Chem. Soc.* **1993**, *115*, 7519.
75 M.D. Benites, T.E. Johnson, S. Weghorn, L. Yu, P.D. Rao, J.R. Diers, S.I. Yang, C. Kirmaier, D.F. Bocian, D. Holten, J.S. Lindsey, *J. Mater. Chem.* **2002**, *12*, 65.
76 D. Holten, D.F. Bocian, J.S. Lindsey, *Acc. Chem. Res.* **2002**, *35*, 57.
77 A. Nakano, A. Osuka, I. Yamazaki, T. Yamazaki, Y. Nishimura, *Angew. Chem. Int. Ed.* **1998**, *37*, 3023.
78 N. Aratani, A. Osuka, *Macromol. Rapid Commun.* **2001**, *22*, 725.
79 P. Jutzi, C. Batz, B. Neumann, H.-G. Stammler, *Angew. Chem. Int. Ed. Engl.* **1996**, *35*, 2118.
80 (a) F. Moulines, L. Djakovitch, R. Boese, B. Gloaguen, W. Theil, J.-L. Fillaut, M.-H. Delville, D. Astruc, *Angew. Chem. Int. Ed. Engl.* **1993**, *32*, 1075; (b) V. Marvaud, D. Astruc, *Chem. Commun.* **1997**, 773.
81 S. Rigaut, M.-H. Delville, D. Astruc, *J. Am. Chem. Soc.* **1997**, *119*, 11132.
82 W.T.S. Huck, R. Hulst, P. Timmerman, F.C.J.M. van Veggel, D.N. Reinhoudt, *Angew. Chem. Int. Ed. Engl.* **1997**, *36*, 1006.
83 H.J. van Manen, F.C.J.M. van Veggel, D.N. Reinhoudt, *Top. Curr. Chem.* **2001**, *217*, 121.
84 S. Achar, R.J. Puddephatt, *Angew. Chem. Int. Ed. Engl.* **1994**, *33*, 847.
85 S. Achar, J.J. Vittal, R.J. Puddephatt, *Organometallics* **1996**, *15*, 43.
86 S. Achar, R.J. Puddephatt, *J. Chem. Soc., Chem. Commun.* **1994**, 1895.
87 S. Achar, R.J. Puddephatt, *Organometallics* **1995**, *14*, 1681.
88 G.-X. Liu, R.J. Puddephatt, *Inorg. Chim. Acta* **1996**, *251*, 319.
89 G.-X. Liu, R.J. Puddephatt, *Organometallics* **1996**, *15*, 5257.
90 B.K. Roland, C. Carter, Z. Zheng, *J. Am. Chem. Soc.* **2002**, *124*, 6234.
91 M. Zhao, L. Sun, R.M. Crooks, *J. Am. Chem. Soc.* **1998**, *120*, 4877.
92 L. Balogh, D.A. Tomalia, *J. Am. Chem. Soc.* **1998**, *120*, 7355.
93 M. Zhao, R.M. Crooks, *Angew. Chem. Int. Ed.* **1999**, *38*, 364.
94 K. Onitsuka, M. Fujimoto, N. Ohshiro, S. Takahashi, *Angew. Chem. Int. Ed.* **1999**, *38*, 689.
95 K. Onitsuka, H. Kitajima, M. Fujimoto, A. Iuchi, F. Takei, S. Takahashi, *Chem. Commun.* **2002**, 2576.
96 K. Onitsuka, A. Iuchi, M. Fujimoto, S. Takahashi, *Chem. Commun.* **2001**, 741.
97 A.M. McDonagh, M.G. Humphrey, M. Samoc, B. Luther-Davies, *Organometallics* **1999**, *18*, 5195.
98 S.K. Hurst, M.P. Cifuentes, M.G. Humphrey, *Organometallics* **2002**, *21*, 2353.
99 Y.H. Qi, P. Desjardins, X.S. Meng, Z.Y. Wang, *Opt. Mater.* **2003**, *21*, 255.
100 Y.H. Qi, P. Desjardins, Z.Y. Wang, *J. Opt. A: Pure Appl. Opt.* **2002**, *4*, S 273.
101 R. Deschenaux, E. Serrano, A.-M. Levelut, *Chem. Commun.* **1997**, 1577.
102 B. Dardel, R. Deschenaux, M. Even, E. Serrano, *Macromolecules* **1999**, *32*, 5193.

Subject Index

a

acyclic diene metathesis (ADMET) polymerization 176
acyclic diyne metathesis (ADIMET) polymerization 143
alkyne metal polymers 149–150
amorphous polymers 5
arene metal polymers 87, 147–149, 175
atom abstraction-induced ring-opening polymerization of chalcogenido-bridged metallocenophanes 117–118
aurophilic bonding 22

b

block copolymers 11–14
– micellization 11–13
– microphase separation 11–13
– with metals in the main chain 108–116
– – uses in nanolithography 111–114
– with pendant metal-containing groups 62–67
– – use in the formation of semiconductor and metal nanoclusters 64
– – uses in nanolithography 65

c

Carothers' theory of step-growth polycondensations 30
chain entanglement 9
– weight-average critical entanglement chain length 9
chain-growth polymerization 28
– chain-transfer 28
– initiation 28
– propagation 28
– termination 28
cluster polymers 196–198
– dendrimers 242, 253
cobaltocenium polymers 132–134
conjugated metallopolymers 153, 172–174, 182–189, 199–200, 203, 210, 212, 215
– conductivity 215, 226
– coordination polymers 203–236
– as fluorescent sensors for metal ions 215
– as photoconducting materials 171–172, 212
– as photorefractive materials 210–211
– polymetallocyclopentadienes 172–174
– polystannanes 181–189
– supramolecular materials 199–200
coordination polymers (main-chain coordination polymers) 203–233
– based on DNA (*see* metallized DNA)
– based on phthalocyanine ligands and related macrocycles 226–227
– based on Schiff-base ligands 221–226
– ferrocene coordination polymers 231
– lanthanide (*see* lanthanide coordination polymers) 223–224
– via ring-opening polymerization 232–233
copolymers 11
– block copolymers 11–14
– random copolymers 11
crystalline polymers (*see* semicrystalline polymers) 5–7
cyclobutadiene cobalt polymers 142–146
– liquid crystalline properties 142–146
– synthesis 142–146
cyclopentadienyl manganese polymers 54, 146–147

d

dendrimers 14
– cluster polymers 242, 253
– liquid crystalline polymers 264
– metallodendrimers 23, 237–266

Synthetic Metal-Containing Polymers.
Ian Manners

ISBN 3-527-29463-5

– rigid-rod transition metal acetylide polymers 263–264
DNA
– metallized 229–231
– i.e. -and polymer with pendant polypyridyl complexes 59
– – use in a DNA base-pair mismatch detection system 59–60

e
electrically conducting polymers 14–16
– delocalization mechanism 14
– redox conduction or hopping mechanism 15
electropolymerization 161–162, 212, 215, 225–226, 228–229

f
face-to-face multidecker polymetallocenes 118–121
ferrocene-containing
– arylidene polyesters 130
– copolyesters 131
ferrocene-coordination polymers 231

h
hierarchical
– order 21
– structures 21
hydride-proton bonding 22
hyperbranched polymers 14

l
lanthanide coordination polymers 223–224
liquid-crystalline polymers 8
– cyclobutadiene cobalt polymers 142–146
– dendrimers 264
– lyotropic 8
– main-chain 8
– nematic 8
– polysiloxanes with ferrocene side groups 51–52
– redox-induced nematic to smectic transition 46
– rigid-rod transition metal acetylide polymers 166
– side-chain 8
– – with side-chain ferrocene groups 46
– smectic 8
– thermotropic 8

m
magnetic materials 19
metallized DNA 229–231
metallocene-containing polyethers 132
metallodendrimers 23, 237–266
– catalytic applications 243, 250–252
– with metals
– – in the core 238–242
– – at interior sites 256–266
– – at the surface 243–255
– sensor applications 244, 248
– variable optical attenuator devices and non-linear optical properties 263–265
metalloenzymes 20
metalloinitiators 23, 220–221
metallomesogens 22
metallopolymers
– conjugated 153, 172–174, 181–189, 199–200, 203, 210, 212, 215
– main-chain, containing π-coordinated metals and long spacer groups 129–150
– with metal-carbon σ-bonds in the main chain 153–176
– rigid-rod transition metal acetylide polymers 23, 154–172, 264
metallo-supramolecular polymers 199–200, 203–233
molecular weight distributions (*see* polymer molecular weights) 3–5

n
NLO materials 131, 170–171

o
oligomers 9–10

p
phosphinated polystyrene 25, 62
poly(ferrocenylene perselenide)s 118
poly(ferrocenylene persulfide)s 117
poly(ferrocenylene vinylene) 80
polyaniline 15
polyborazylene 2
polycarbosilane 18
– with metallocene side groups 50–53
polycobaltocyclopentadiene 145, 172–174
polycondensation 29–32
– Carothers' theory of step-growth polycondensations 30
– influence
– – of conversion on molecular weight 30–32
– – of reaction stoichiometry on molecular weight 30–32

polycyclodiborazane 2
poly(ethynylferrocene) 45
poly(ethynylruthenocene) 45
polyferrocenes
– with hexasilane spacers 140
– with thiophene spacers 140–141
polyferrocenylboranes 85
polyferrocenylene 23–24, 73–78
– band structure 75–76
– conductivity of 74
– persulfide 24, 117
– redox properties 77–78
polyferrocenylethylene 86, 108
polyferrocenylgermanes 84
– properties of 106–107
– synthesis
– – by thermal ring-opening polymerization 84
– – by transition metal-catalyzed ring-opening polymerization 89
polyferrocenylphenylphosphines 79, 84, 88
polyferrocenylphosphines 34, 79, 84, 88, 91
– block copolymers 34, 115
– early work on 79
– synthesis by thermal ring-opening polymerization 84–85
polyferrocenylphosphinesulfides 85, 107
polyferrocenylsilanes 24, 33–34, 91–112
– applications in nanolithography 111–114
– block copolymers 34, 108–116
– – applications in nanolithography 111–114
– – self-assembly 109–115
– – – in block-selective solvents 109–112
– – – in the solid state 112–115
– – synthesis of 108–109
– charge dissipative properties 99
– conductivity of 98
– conformational properties 93–96
– conversion to nanostructured magnetic ceramics 101
– early work on 79
– electrochromic properties 98
– fabrication of 93–94
– – variable refractive index sensors 106
– gels 100
– metal-metal interactions in 96–100
– microspheres 103–105
– morphology 93–96
– non-linear optical materials 106
– patterned by soft lithography 102–103
– random copolymers 86–87
– redox properties 96–100
– solution properties 92–93
– synthesis
– – by living anionic ring-opening polymerization 87–89
– – by thermal ring-opening polymerization 82–85
– – by transition metal-catalyzed ring-opening polymerization 89–90
– thermal transitions 92–96
– water-soluble materials and layer-by-layer assembly applications 105–106
polyferrocenylstannanes 33, 85, 107
– synthesis by cationic ring-opening polymerization 91
polyferrocenylsulfides 85, 107
polygermanes 19, 181
polymer
– containing clusters (*see* cluster polymers) 196–198
– containing main-chain
– – cobaltocenium units 132–134
– – metal-metal bonds 181–200
– – – photosensitivity 189–190
– – – polystannane 181–189
– – – Pt-Pt interactions 199–200
– – Pt-Pt covalent bonds 191–192
– main-chain coordination polymers (*see* coordination polymers) 203–233
– molecular weights 3–5
– – gel-permeation chromatography (GPC) 4
– – number-average molecular weight 4
– – polydispersity index (PDI) 4
– – size-exclusion chromatography (SEC) 4
– – weight-average molecular weight 4
– with pendant polypyridyl complexes 55–60
– – application as phosphorescent oxygen sensors 57
– – fabrication
– – – of emitting diodes from 56
– – – of glucose sensors from 58
– – – of self-oscillating gels from 58
– – use in a DNA base-pair mismatch detection system 59
– with skeletal metallocyclopentadiene units 172–174
– solubility 10–11
– – entropy of dissolution (ΔS_{diss}) 10
– – influence of crystallinity on 10
– – water-soluble hydroformylation catalysts 61

polymerization
– acyclic diene metathesis (ADMET) 176
– acyclic diyne metathesis (ADIMET) 143
– addition 28–29
– chain-growth 28
– electropolymerization 161–162, 212, 215, 225–226, 228–229
– ring-opening (ROP) process 33–34, 72, 82–116, 232–233
– ring-opening metathesis polymerization (ROMP) process 33, 44, 116–117
– step-growth 28
– synthesis by radical polymerization 40
polymer-supported catalysts 60–62
polymethacrylates with ferrocene side groups 43
polymetallayne (*see* rigid-rod transition metal acetylide polymers) 23, 154–172
polymetallocenes
– face-to-face multidecker 118–121
– main-chain with short spacer groups 71–121
– with long conjugated spacer groups 138–142
– with long insulating spacer groups 129–138
– – with organic spacers 129–134
– – with organosilicon spacers 135–137
– – with siloxane spacers 137
polymetallorotaxanes 215–216
polynickelocene 119
polynorbornenes with ferrocene side groups, ROMP 44
polyoxothiazenes 2, 32
polypeptides with ferrocene side groups 47
poly(phenylene vinylene) 203
polyphosphazenes 2, 25, 32
– with metallocene side groups 25, 49
polypyridyl coordination polymers 204–221
– as fluorescent sensors for metal ions 215
– homopolymers
– – with octahedral metals 204–212
– – with tetrahedral metals 213–216
– light emitting layer-by-layer assemblies 207
– photorefractive materials 210
– stars and block copolymers 216–221
polypyrrole 15
– with pendant ferrocene groups 45–46
polyruthenocenylene 77–78
polyruthenocenylethylene 86
polysilanes 2, 19
– with metallocene side groups 50–53
– random copolymers with polyferrocenylsilanes 86, 140
polysiloxanes 1
– with metallocene side groups 50–53
polystannanes 24, 182–189
– band structure of 186–188
– properties 184–188
– synthesis 184–186
– oligostannanes 182–183
polystyrene, phosphinated 25–26
poly(styrene chromiumtricarbonyl) 55
– copolymers of 55
polythionylphosphazenes 2
– with pendant ruthenium phenanthroline complexes for oxygen sensing application 57
polythiophene 15, 203
– with pendant ferrocene groups 45–46
polytitanoxane 81–82
poly(vinyl carbazole) 16
poly(vinyl cymantrene) 25, 54
poly(vinyl ferrocene) 23, 39–43
– block copolymers of 40–41
– fabrication of diodes from 43
– redox properties, conductivity 41–42
– thermal transitions of 41
poly(vinyl osmocene) 48
poly(vinyl ruthenocene) 47–48
poly(vinyl cyclopentadienylchromiumdicarbonylnitrosyl) 55
poly(vinyl cyclopentadienyliridiumdicarbonyl) 55
poly(vinyl cyclopentadienyltungstentricarbonylmethyl) 55
polyzirconacyclopentadienes 174
preceramic polymers (precursors to ceramics) 18, 101–105
precursors to ceramics (*see* preceramic polymers)

r

random copolymers 11
rigid-rod transition metal acetylide polymers 23, 154–172
– dendrimers 264
– electrical and photoconductive properties 171–172
– fabrication of photocells from 172
– lyotropic liquid crystallinity 166–167
– non-linear optical properties 170–171
– optical properties 167–170
– photoluminescence 169–170
– solution properties 165–166

– structural and theoretical studies 162–164
– synthesis of 154–162
– thermal properties of 165
ring-opening
– metathesis polymerization (ROMP) 33, 63
– – of metallocenophanes 116–117
– – of polynorbornenes with ferrocene side groups 44
– polymerization (ROP) 33–34, 72, 82–116, 232–233
– – coordination polymers via ROP 232–233
– – of strained metallocenophanes 82–116

s

semicrystalline polymers (crystalline polymers) 5–7
– influence of crystallinity on polymer properties 6
– rate of polymer crystallization 7
spin-orbit coupling 20
step-growth polymerization 28
stereoregular polymers 6
– atactic polymers 5
– isotactic polymers 6
– syndiotactic polymers 6
stimuli responsive gels
– based on polyferrocenylsilanes 100–101
– based on Ru bipyridyl polymers 57–58
supramolecular chemistry 21

t

thermal transitions 6–8
– clearing temperature 8
– crystallization transition (T_c) 7
– glass transition (T_g) 7
– melting temperature (T_m) 6
– – to give a mesophase (T_{1c}) 8

z

zirconocene silsesquioxane polymers 137–138